UNIVERSIDADE ESTADUAL PAULISTA
"JÚLIO DE MESQUITA FILHO"
Câmpus de São José do Rio Preto

**SUNGIL FERREIRA**

# Development of semi-continuous processes for production of ginger oil (*Zingiber officinale* Roscoe) microcapsules by complex coacervation: atomization and membrane emulsification

**São José do Rio Preto**

**2021**

SUNGIL FERREIRA

# Development of semi-continuous processes for production of ginger oil (*Zingiber officinale* Roscoe) microcapsules by complex coacervation: atomization and membrane emulsification

Tese apresentada como parte dos requisitos para obtenção do título de Doutor em Engenharia e Ciência de Alimentos, junto ao Programa de Pós-Graduação em Engenharia e Ciência de Alimentos, do Instituto de Biociências, Letras e Ciências Exatas da Universidade Estadual Paulista "Júlio de Mesquita Filho", Câmpus de São José do Rio Preto.

Financiadora/Financial support: FAPESP – Proc. 2015/23290-0 e 2018/16976-0

Orientadora/Supervisor: Profª. Drª. Vania Regina Nicoletti

São José do Rio Preto

2021

F383d

Ferreira, Sungil

Development of semi-continuous processes for production of ginger oil (Zingiber officinale Roscoe) microcapsules by complex coacervation: atomization and membrane emulsification / Sungil Ferreira. -- São José do Rio Preto, 2021

187 p. : il., tabs., fotos

Tese (doutorado) - Universidade Estadual Paulista (Unesp), Instituto de Biociências Letras e Ciências Exatas, São José do Rio Preto

Orientadora: Vania Regina Nicoletti

1. Microencapsulação. 2. Atomização. 3. Engenharia de processos. 4. Membranas (Tecnologia). 5. Físico-química orgânica. I. Título.

Sistema de geração automática de fichas catalográficas da Unesp. Biblioteca do Instituto de Biociências Letras e Ciências Exatas, São José do Rio Preto. Dados fornecidos pelo autor(a).

Essa ficha não pode ser modificada.

SUNGIL FERREIRA

# Development of semi-continuous processes for production of ginger oil (*Zingiber officinale* Roscoe) microcapsules by complex coacervation: atomization and membrane emulsification

Tese apresentada como parte dos requisitos para obtenção do título de Doutor em Engenharia e Ciência de Alimentos, junto ao Programa de Pós-Graduação em Engenharia e Ciência de Alimentos, do Instituto de Biociências, Letras e Ciências Exatas da Universidade Estadual Paulista "Júlio de Mesquita Filho", Câmpus de São José do Rio Preto.

Financiadora/Financial support: FAPESP – Proc. 2015/23290-0 e 2018/16976-0

Comissão Examinadora/Examining Board

Profª. Drª. Vania Regina Nicoletti
UNESP – Câmpus de São José do Rio Preto
Orientador

Profª. Drª. Márcia Regina de Moura Aouada
UNESP – Câmpus de Ilha Solteira

Profª. Drª. Miriam Dupas Hubinger
UNICAMP – Universidade Estadual de Campinas

Prof. Dr. Gustavo Nakamura Alves Vieira
UNESP – Câmpus de Araraquara

Profª. Drª. Ana Sílvia Prata
UNICAMP – Universidade Estadual de Campinas

São José do Rio Preto
4 de dezembro de 2020

To my parents, João and Geni, and to my grandma, Ana Maria (*in memoriam*), whom gave me the opportunity to study even when the conditions were adverse.

## ACKNOWLEDGMENT

I thank God, in all its manifestations, for gifting me good health, guiding my path and giving me the opportunity to become a better person every day.

I thank my beloved wife, Adiella Abelseth, for supporting and encouraging me in achieving this goal.

I thank my family for all the support throughout my academic studies.

I thank my supervisor, Prof. Dr. Vânia Regina Nicoletti, for trusting me since my undergraduate research and for embarking with me on this "Doctorate without master's" epic journey. For the patience, guidance and friendship that will surely be for all my life.

I thank Prof. Dr. Augusto Agostinho Neto (*in memoriam*) for opening the doors of my academic life.

I thank Prof. Dr. Cassia Roberta Malacrida Mayer for the support and guidance during the beginning of my research career.

I thank Dr. Marijana Dragosavac for supervision and support at the University of Loughborough in the United Kingdom.

I thank professors Drs. Vanildo Luiz Del Bianchi, João Cláudio Thoméo, Marília Gonçalves Cattelan and Iasnaia Maria de Carvalho Tavares for suggestions and corrections after the qualification exam.

I thank professors Drs. Miriam Dupas Hubinger, Ana Sílvia Prata, Márcia Regina de Moura Aouada, Gustavo Nakamura Alves Vieira, Gustavo César Dacanal, Larissa Consoli and Paulo Marfil for accepting the invitation to participate in the examination board and to contribute in this thesis.

I thank all and every colleague that I've had the chance to share the laboratory, knowledge and a brief but important part of my life, in Brazil and in the United Kingdom (Poliana, Gabriela Piovani, Thais Benatti, Diana, Harvey, Larissa, Natalia, Caroline, Miriam, João Vitor, Yuri, Gisandro, Tiago, Elisa, Caroline Fuzetti, Adilson, Andreas, Cristyana, Marianny, Bruna, Paulo, Isabella, Vitor, Tais, Giulliana, Caroline, Nathalie, Nayla, Kivia, Michele, Marilia, Aline, Francisco, Izabella, Diego, Salomé, Claudia).

I thank all my friends from my undergraduate studies (Physics and Food Engineering), ballroom dance group, cheerleading teams (T-Birds – UBC in Canada, Psicoliders and Black Rivers All Stars in Brazil and Loughborough Cheerleading in the United Kingdom), Athletics UNESP Rio Preto, Table tennis team and all extra actives for keeping me "mentally heathy" during my academic path.

I thank all faculty and technicians from the Department of Food Engineering and Technology department for all support and knowledge shared.

I thank all my teachers and professors for laying the stepping stones that have guided my path to where I am today.

I thank all of the people of Sao Paulo and Brazil, because our taxes have allowed me go through school, from preschool to PhD.

I thank the São Paulo Research Foundation - FAPESP for the financial support through the research scholarships grant numbers 2015/23290-0 and 2018/16976-0.

I thank the National Council for Scientific and Technological Development - CNPq (grant number 305355/2016-3) for its financial support.

I thank the "Central Analítica de Química" of the Federal University of Maranhão (UFMA) for support on FTIR analysis.

I thank the University of Loughborough, the faculty and the technicians for support on studies in the Chemical Engineering department.

I thank the Micropore Technologies Ltd for providing the equipment for studies using metal membranes.

“How can we know the divine nature of the invisible God? One way to fathom His deity is by observing the universe which He created.”

Sun Myung Moon (1996, p. 30)

## RESUMO

Coacervação complexa é uma técnica de microencapsulação versátil com capacidade de encapsular e proteger compostos hidrofóbicos e hidrofílicos. Além disso, é capaz de proteger os ativos encapsulados de diferentes condições adversas como luz, oxigênio e baixo pH durante a digestão. Contudo, devido à sua própria natureza, a técnica apresenta algumas limitações que a impedem de ser aplicada em grande escala ou em processos que não sejam em batelada. Este trabalho propõe algumas alternativas com o intuito de facilitar a aplicação da técnica de coacervação complexa em maior escala. No processo tradicional de coacervação complexa as soluções poliméricas são misturadas e em seguida o pH é ajustado para promover interação e subsequente coacervação. Foi desenvolvida uma nova configuração em que a coacervação complexa é induzida pela atomização do material de recheio emulsificado em uma solução de proteína sobre a solução de polissacarídeo; neste caso em particular, emulsão de óleo de gengibre em gelatina sobre solução aquosa de goma arábica. A coacervação complexa por atomização, além de ser um método promissor para produção de cápsulas, abre a possibilidade de prever o tamanho final das mesmas em função das condições de atomização ou de números adimensionais representativos. Um importante gargalo no processo de coacervação complexa a ser considerado é a cura das cápsulas. Tradicionalmente, a cura é realizada em batelada em um processo de resfriamento lento. Neste trabalho propõe-se o uso de um trocador de calor tubular com bombeamento e temperatura controlados para realizar a cura das cápsulas em processo contínuo. Assim o tempo demandado na etapa de cura diminuiu consideravelmente, abrindo novas oportunidades para aumento de escala e realização do processo de coacervação como um todo de forma semi-contínua. Também foi avaliado o uso de membranas metálicas para formação das emulsões a serem utilizadas durante o processo de coacervação complexa, além da utilização desta mesma configuração de membranas para indução da coacervação complexa, como um novo método. Isso é importante porque já existem sistemas para utilização de membranas em escala industrial e em processo contínuo, os quais podem ser eventualmente adaptados para realização do processo de coacervação complexa em modo contínuo. As cápsulas formadas por atomização foram iguais ou melhores que as cápsulas produzidas pelo método tradicional, considerando tamanho, morfologia e propriedades de encapsulação. A cura das cápsulas no trocador de calor se mostrou factível, com resultados promissores, e assim a coacervação complexa em processo semi-contínuo foi viabilizada.



**Palavras–chave:** Coacervação complexa. Atomização. Números adimensionais. Membranas metálicas. Processo semi-contínuo. Trocador de calor.

**ABSTRACT**

Complex coacervation is a versatile microencapsulation technique capable of encapsulating and protecting hydrophobic and hydrophilic compounds. In addition, it is able to protect encapsulated core materials from different adverse conditions such as light, oxygen and low pH during digestion. However, due to its very nature, the technique has some limitations that prevent it from being applied on a large scale or in non-batch processes. This work proposes a few alternatives in order to facilitate the application of the complex coacervation technique on a larger scale. In the traditional complex coacervation process, polymeric solutions are mixed and then the pH is adjusted to promote interaction and subsequent coacervation. A new configuration has been developed in which complex coacervation is induced by the atomization of the emulsified core material in a protein solution over the polysaccharide solution; in this particular case, ginger oil emulsion in gelatin over aqueous solution of gum Arabic. Complex coacervation by atomization, in addition to being a promising method for producing capsules, opens up the possibility of predicting their final size depending on atomization conditions or representative dimensionless numbers. An important bottleneck in the complex coacervation process to be considered is the cure of the capsules. Traditionally, curing is carried out in batches in a slow cooling process. In this work it is proposed to use a tubular heat exchanger with controlled pumping and temperature to cure the capsules in a continuous process. Thus, the time required in the curing stage has decreased considerably, opening up new opportunities to increase the scale and carry out the coacervation process as a whole in a semi-continuous manner. The use of metallic membranes for the formation of emulsions to be used during the complex coacervation process was also evaluated, in addition to the use of this same configuration of membranes to induce complex coacervation, as a new method. This is important because there are already systems for using membranes on an industrial scale and in a continuous process, which can eventually be adapted to carry out the complex coacervation process in a continuous mode. The capsules formed by atomization were equal to or better than the capsules produced by the traditional method, considering size, morphology and encapsulation properties. The cure of the capsules in the heat exchanger proved feasible, with promising results, and thus the complex coacervation in a semi-continuous process was made possible.

**Keywords:** Complex coacervation. Atomization. Dimensionless numbers. Metal membranes. Semi-continuous process. Heat exchanger.

## LIST OF FIGURES

**CHAPTER 5**



**CHAPTER 6**

**CHAPTER 7**

f). The symbols represent coacervation shear stress of (●) 1.1 Pa, (■) 5.8 Pa, and (▲) 12.6 Pa.

Figure 7.9. Encapsulation yield, encapsulation efficiency, and oil at the surface of microcapsules versus shear stress for capsules produced for emulsions with 4 % (w/w) gelatin (a, c, and e) and with 10 % (w/w) of gelatin (b, d, and f). The symbols represent injection rates of (●) 3 mL/min, (■) 5 mL/min, and (▲) 10 mL/min for membrane complex coacervation and (♦) atomization complex coacervation.

## LIST OF TABLES

**SUMMARY**

# CHAPTER 1 – INTRODUCTION AND OBJECTIVES

## 1.1 Introduction

Complex coacervation results from the interaction of oppositely charged polymers that, due to solvent repulsion, form complexes that tends to precipitate. Thus, two phases are formed, one of which contains the precipitated coacervate and is called "rich in polymer", whereas the other, in which the solvent remains, is called "poor in polymer" (DICKINSON, 2003; STRAUSS; GIBSON, 2004). Complex coacervation has been successfully used for microencapsulation of essential oils and flavours, which have extensive application in food, agricultural, textile and pharmaceutical industries. The technique is very versatile and is suitable for protection of these compounds against degradation, to prevent loss of volatiles, besides allowing modulated release and increased stability of the encapsulated material (XIAO et al., 2014a). On the other hand, the complex coacervation technique presents some limitations: sometimes the method does not produce individualized particles, interfering in the granulometry of the produced powder and in the release properties (BURGESS; PONSART, 1998; ERATTE et al., 2018; TIMILSENA et al., 2019). Yet, there are some difficulties related to the use of complex coacervation in industrial scale because of its high operational costs – which are associated to the requirement of manipulating large volumes of water in diluted solutions, besides that few studies have been carried out evaluating possibilities of its application in continuous operation processes (XIAO et al., 2014a).

A possible process configuration to carry out complex coacervation as a continuous process is based on atomization. By atomizing the gelatin/ginger oil emulsion over a vessel containing gum Arabic solution, complex coacervation between the biopolymers takes place on the surface of the emulsion droplets that are formed during the atomization step, as it flows through the gum Arabic solution. Thus, studying the atomization step and atomized droplet formation is crucial in order to obtain efficient oil encapsulation. The atomization process can be described by the dimensionless numbers Weber (*We*) and Ohnesorge (*Oh*). *We* number correlates the inertial and surface tension components of the resultant force during atomization, whereas *Oh* relates the viscous forces to the surface tension forces in the liquid. According to Varga et al. (2003), different ranges of *We* correspond to different patterns of liquid atomization: bag-type breakup of the liquid occurs at $12 < We < 80$, atomization by air-shear breakup occurs at $80 < We < 350$, and catastrophic breakup at $We > 350$. In addition, when $Oh \leq 0.1$, it is possible to assume that only *We* affects the atomization process, whereas for $0.1 < Oh < 1$ the system is in the transition regime, in which both *We* and *Oh* exert influence (GUILDENBECHER; LÓPEZ-RIVERA; SOJKA, 2009). The effects of atomization in the

functionality of particles produced by a number of encapsulation processes have been investigated by different approaches, mainly because it represents a flexible and economical choice to transform liquid materials into particles. Jiang et al. (2013) presented a study for enzyme encapsulation process in which the complex coacervation and drying processes are combined into a single step, using a novel three-fluid nozzle for atomization. Kašpar et al. (2013) produced chitosan microparticles crosslinked by sodium tripolyphosphate by spray drying, using a three-fluid nozzle. Chen et al. (2006) studied acetaminophen particles produced with chitosan and hydroxypropyl-methylcellulose using solid dispersions formed by a 4-fluid nozzle spray dryer, evaluating their sustained release and morphological characteristics.

On the other hand, the use of membranes for emulsification and formation of microcapsules in the process of encapsulation by complex coacervation is presented as a solid alternative for continuous microencapsulation, and this system can be scaled up for industrial scale (CONSOLI; HUBINGER; DRAGOSAVAC, 2020; PENG; WILLIAMS, 1998; ZAWALA; SZCZEPANOWICZ; WARSZYNSKI, 2015). The use of membranes has been shown to be efficient in the formation of stable emulsions that present desirable characteristics to be subsequently microencapsulated by complex coacervation (DRAGOSAVAC et al., 2008).

The emulsification method for subsequent encapsulation by complex coacervation is an important task to be considered. Many of the properties of the emulsions, such as stability, volume fraction of the dispersed phase, droplets' size distribution and average particle diameter, are determined by both the formulation and the homogenization method (SCHUBERT; AX; BEHREND, 2003). Conventional emulsifying devices such as rotor and stator type systems, high-pressure homogenizers and ultrasonic homogenizers provide limited flexibility in terms of controlling the average particle size and the size distribution. Membrane emulsification has received attention precisely because of its ability to produce particles or droplets with low size dispersion (DRAGOSAVAC et al., 2008; KOSVINTSEV et al., 2005). It should also be considered that traditional homogenization methods can degrade filling materials due to the instability of these compounds when subjected to the high shear rates employed (SANTOS et al., 2015a).

Considering that membrane emulsification happens drop by drop, it is possible to predict the diameter of the emulsion droplets by applying balance of capillary and drag forces (KOSVINTSEV et al., 2005). The membrane emulsification process developed in this research project was carried out using a dispersion cell (*DC*), in which the dispersed phase is forced through the membrane pores in a constant flow forming droplets. As the droplets are being formed they are involved by the continuous phase, whereas the shear stress applied by the stirrer

separates the newly formed emulsion droplets from the metallic surface. That is why membrane emulsification is considered a drop by drop technique (DRAGOSAVAC et al., 2012).

Ginger (*Zingiber officinale* Roscoe) has been used by humankind for more than 2000 years as a condiment or spice. In addition, ancient peoples knew their ability to stimulate digestion in a natural way. It was found that the phenolic compounds present in ginger stimulate production and release of gastric juices, bile, intestinal fluids among others (PLATEL; SRINIVASAN, 2000). The phenolic compounds with antioxidant capacity present in ginger extract are basically 6-Gingerol, 6-shogaol, 8-gingerol and 10-gingerol (EL-GHORAB et al., 2010; SCHWERTNER; RIOS, 2007). Taking into account that phenolic compounds can be susceptible to thermal degradation, by light, or by oxygen action, the use of microencapsulation by complex coacervation is a viable solution for its protection.

In summary, this thesis proposes the development and comparative evaluation of two methods for microencapsulation of ginger oil in a semi-continuous process by complex coacervation and an alternative to induce the cure of the capsules. In the first method of coacervation proposed, emulsions of ginger oil in gelatine were atomized over gum Arabic solutions for complex coacervation. In the second proposal, the emulsion was forced through a membrane, forming emulsion droplets dispersed in the gum Arabic solution in which coacervation occurred. A tubular heat exchanger was used to induce the cure of the capsules in a continuous mode.

## 1.2 General objective

The general objective of this project was the development and the comparative evaluation of two process configurations to induce complex coacervation, for microencapsulation of ginger oil in gelatin and gum Arabic matrices. Both of these new methods has potential for scale up and to be carried at least in semi-continuous operation regime. One of the techniques was based on the atomization of the gelatin/ginger oil emulsion over the gum Arabic solution. The other method involves the flow of the emulsion through a metal membrane with a predetermined pore diameter and pore distance, with the subsequent dispersion of the micelles in the gum Arabic solution in a dispersion cell. The use of a tubular heat exchanger to achieve the cure of the capsules was evaluated in order to allow scale up of the complex coacervation process.

## 1.3 Specific objectives and thesis organization

The present chapter (Chapter 1), present the justification and contextualization of the main concepts used in this thesis. The Chapter 2 contains the literature review with the basic concepts used throughout the thesis.

Chapter 3 presents and describes complex coacervation assisted by a two-fluid nozzle, studying the influence of polymer ratio and emulsion concentration in the capsule formation and morphology. The atomization equations were written in terms of dimensionless numbers. The influence of gelatin concentration in the emulsion on the capsules' size, size distribution, encapsulation parameters and the formation of chemical interactions expected for complex coacervation was investigated and compared with coacervation by batch stirring.

In Chapter 4, the influence of atomization process conditions during complex coacervation was evaluated: the process of atomization (shear rate, shear stress, theoretical capsule size) was described in terms of process conditions and dimensionless numbers (Weber and Ohnesorge). A model to determine the coacervated capsule size based on atomization equation and experimental capsule size was proposed and the influence of coacervation shear rate, shear stress, Weber and Ohnesorge numbers on encapsulation parameters was examined.

Chapter 5 presents and describes an alternative method to carry out the curing step of the capsules, bringing complex coacervation from a batch to a semi-continuous process: the influence of curing flow rate and temperature on capsules' size, morphology and encapsulation parameters was studied. Release assays in simulated gastric conditions were done to evaluate the capsules' resistance to those conditions in retaining the encapsulated oil.

In Chapter 6, the production of emulsions of gelatin and ginger oil by membrane emulsification was studied to be used in complex coacervation by atomization and batch stirring. Membranes parameters were correlated to droplet size and size distribution in function of emulsification conditions. Emulsification conditions were optimized to produce emulsion droplets with determined size and low size distribution. The influence of emulsification shear stress in the capsules' size and morphology in coacervation by atomization and batch stirring was evaluated. In addition, was studied the influence of membrane emulsification parameters, coacervation method and its process conditions on encapsulation parameters.

In Chapter 7, the feasibility of inducing complex coacervation utilizing a metal membrane setup was evaluated: coacervation conditions were determined in function of polymer ratio and coacervation pH, the influence of process conditions during complex coacervation assisted by metal membranes on capsule size, capsule morphology and encapsulation parameters was described and compared to atomization and batch stirring.

The main results are summarized and discussed in Chapter 8. The general conclusion of the thesis is presented in Chapter 9 and suggestions for future studies are presented in Chapter 10.

# CHAPTER 2 – LITERATURE REVIEW

## 2.1 Microencapsulation

The term "microencapsulation" was introduced by Green and Schleicher (1956), when the authors registered the patent for capsules that could be used in industries for copying documents, in which these capsules were able to store and release ink (PAULO; SANTOS, 2017). Over time, different methodologies have been developed and improved in order to protect a material, which can be called "core", encapsulated material or capsule core, using a wall material, "wall", carrier agent or encapsulating agent (CARVALHO; ESTEVINHO; SANTOS, 2016; DESAI; PARK, 2005). In general, microencapsulation can be defined as a process in which a membrane involves small particles forming systems of micrometric dimensions of solid, liquid or gas, giving rise to microcapsules: with a single core; or microspheres: which present a matrix structure with several nuclei. In the literature it is observed that these terms are sometimes presented as synonyms (HERRERO-VANRELL et al., 2014; JACKSON; LEE, 1991).

Based on industrial applications of microencapsulation, approximately 68% of them are in the pharmaceutical industry, 13% in the food industry, 8% in the cosmetics industry and the remaining 11% are divided between the areas of biomedicine, agriculture, textiles and electronics (PAULO; SANTOS, 2017). As a rule, the goal is to apply microencapsulation technology as a means to protect the encapsulated agent from different adverse conditions in the environment, such as light, moisture, oxygen and interactions with other compounds, stabilizing the product, thus increasing the life of the encapsulated material (CASANOVA; SANTOS, 2016; ZUANON; MALACRIDA; TELIS, 2013).

Furthermore, not only the potential of protection should be considered, as mentioned above, but also the phenomenon of controlled release of the encapsulated material, triggered off by physical or chemical phenomena, as well as the thickness of the capsule wall can be manipulated to alter the permeability and the stability of the material (LAM; GAMBARI, 2014; MÜLLER; RADTKE; WISSING, 2002). In addition, microencapsulation can be applied to mask the unpleasant properties (odour, taste, low pH, visual aspect) of numerous substances (GOUIN, 2004), may convert liquid materials into solid capsules or granular powders, which facilitates processing and eliminates the waste of time in product lines or cleaning operations (FAVARO-TRINDADE; PINHO, 2008; REBELLO, 2009). It is possible to change the properties of microcapsules to provide specific applications of ingredients as to their composition, solubility, release mechanism, particle size and shape, in addition to improving

the nutritional properties of products and enhancing the bioavailability of active compounds, when these are microencapsulated (DESAI; PARK, 2005; ENDO et al., 2007).

The microencapsulation process basically involves the following steps: formation of an emulsion or suspension of the encapsulating agent and the active material, formation of the microcapsule itself, followed by evaporation of the solvent with consequent drying and resulting in the dry product, when desired (JACKSON; LEE, 1991; SHAHIDI; HAN, 1993). The encapsulating materials used in microencapsulation represent a variety of compounds that include carbohydrates (gums, starch, dextrin, sugar, corn syrup, celluloses, among others), lipids (waxes, oils, mono and diglycerols) and proteins (gluten, gelatin, albumin, milk and soy proteins) (CORRÊA-FILHO; MOLDÃO-MARTINS; ALVES, 2019; JAFARI et al., 2008).

There are several microencapsulation techniques used commercially, divided into three main groups: physical methods (atomization, lyophilisation/freeze drying, extrusion, cocrystallization), chemical (interfacial polymerization, in situ polymerization, molecular inclusion) and physical-chemical (coacervation, inclusion in liposomes) (JYOTHI et al., 2010; SHAHIDI; HAN, 1993). The choice of the method depends on a number of factors, including: desired particle size, physical and chemical properties of the core and wall material, application of the final product, desired release mechanisms, production scale and cost (ALEMZADEH et al., 2020; JAFARI et al., 2008). The use of different techniques will result in microcapsules with particular characteristics (FANG; BHANDARI, 2010). The choice of the microencapsulation method is directly related to the nature of the material to be encapsulated, the wall material used, as well as the intended application to the final product (AUGUSTIN; HEMAR, 2009).

According to Arshady (1993), the critical issues of microencapsulation processes are: the correct ratio between the encapsulating material and the core, the edibility of the food containing the encapsulated ingredient, the correct choice of the microcapsule wall material (its physical-chemical characteristics, solubility, crystallinity, film forming capacity and barrier properties), the desired size of the microcapsule, the sensitivity of the encapsulated material, the cost of operation, the applicability for food products and the mechanism for releasing the active material. However, in practice, generally the decisive criteria in the choice of the encapsulation methods is the operational cost and the encapsulating material.

## 2.2 Emulsification

An emulsion is composed of two immiscible liquids (usually oil and water), with one of the liquids dispersed in the other in the form of small spherical drops. The substance or solution

that makes up the drops is called the dispersed phase, while the one that makes up the medium is called the continuous phase. The emulsion formation process consists of mixing two immiscible liquids through a homogenization step (MCCLEMENTS, 2005). Important properties of an emulsion are its stability, droplet size and size distribution.

The destabilization of an emulsion can be related to four main phenomena: flocculation, creaming, coalescence, and phase separation. Flocculation can be defined as the reversible aggregation of the droplets of the internal phase. Chronologically, it is the first phase of the change in the stability of an emulsion, followed by creaming or sedimentation, which consists of the aggregation of flakes previously originated that become a layer arranged on the surface or bottom of the emulsion, respectively. Because it is easy to measure, creaming is the most used index as a stability factor, and the lower the creaming, the more stable the emulsion is (FERREIRA; MALACRIDA; TELIS, 2016; PERRECHIL; CUNHA, 2010). Coalescence is a process of approximating droplets, during which they unite to form larger droplets, being irreversible and culminating in the total separation of phases. Flocculation and coalescence differ from each other by the fact that in flocculation the interfacial droplet film remains intact, whereas in coalescence this film is broken (DICKINSON, 2003; LACHMAN, LIEBERMAN, KANIG, 2001; WILLIAMS; PHILLIPS, 2009).

All emulsions are thermodynamically unstable and tend to break down over time, resulting in two separated liquid phases. However, there is a distinction between thermodynamic stability and kinetic stability, the first indicating whether the process may or may not occur, while the second informs the rate at which the process will occur (MCCLEMENTS, 2005). Information on kinetic stability is important for the development of products that have desirable properties for a sufficiently long period of time. Thus, to produce kinetically stable emulsions, it is necessary to add emulsifiers and/or stabilizers (DICKINSON, 2003; WILLIAMS; PHILLIPS, 2009).

In microencapsulation by complex coacervation it is important that the stability of the emulsion is assured throughout processing time, from the end of the homogenization process to the beginning of the coacervation process (BUTSTRAEN; SALAÜN, 2014). The emulsification method for subsequent encapsulation by complex coacervation is an important task to be considered, as the emulsion properties such as stability and droplets' size distribution are determined by both the formulation and the homogenization method (VLADISAVLJEVIĆ; SCHUBERT, 2003). Conventional emulsifying devices such as rotor and stator type systems and high-pressure homogenizers provide limited flexibility in terms of controlling the average particle size and the size distribution having a high energy input (DRAGOSAVAC et al., 2008).

It should also be considered that traditional homogenization methods can degrade filling materials due to the instability of these compounds when subjected to the high shear rates employed (SANTOS et al., 2015).

### *2.2.1 Ultrasound emulsification*

The method of emulsification by ultrasound is well known and can be used in the production of nano emulsions and/or nano particles, based on the phenomenon of cavitation (ANTON et al., 2007). It is considered to be a high energy consumption technique, in which energy is applied to the system by means of piezoelectric quartz probes that respond to the variation of the electric voltage, by expanding and contracting as a result of this variation (CANSELIER et al., 2002).

Emulsification by sonication is believed to occur by two possible mechanisms. One of them results from interfacial waves generated by ultrasound between the lipophilic and hydrophilic phases, which eventually become very unstable and collapse, causing the lipophilic phase to form small drops within the hydrophilic phase. A second mechanism is based on acoustic cavitation: application of low sound frequencies leads to formation of microbubbles that collapse quickly, generating high shear rates and local turbulence, thus resulting in homogenization (CANSELIER et al., 2002; FERREIRA et al., 2019).

Results presented by Ferreira, Malacrida, Telis (2016), Gaikwad and Pandit (2008) and Canselier et al. (2002) show that it is possible to obtain oil in water (O/W) emulsions by sonification with an average particle diameter between 1 and 4 μm with low dispersion of droplet sizes. Thus, the use of this technique in the formation of emulsions for microencapsulation by complex coacervation is indicated, both for the formation of stable emulsions and for obtaining small size drops.

### *2.2.2 Membrane emulsification*

Membrane emulsification can be carried out by different types of membranes such as glass, ceramic or metal membranes (HANCOCKS; SPYROPOULOS; NORTON, 2016). One important difference in membrane composition lays on the tortuosity of each individual channel. In ceramic membranes there are tortuous paths where the dispersed phase has to go through, whereas in metal membranes the path is a cylindrical channel, with no tortuosity (EGIDI et al., 2008; GIJSBERTSEN-ABRAHAMSE; VAN DER PADT; BOOM, 2004; VLADISAVLJEVIĆ; SCHUBERT, 2003). The results of the differences in the membrane nature is a lower backpressure of the system and lower shear on the dispersed phase going

through the pores in metal membranes (HANCOCKS; SPYROPOULOS; NORTON, 2016). In addition, metal membrane emulsification has received attention precisely because of its ability to produce particles or droplets with lower size dispersion in addition to be a system that allow scale up for industrial applications (DRAGOSAVAC et al., 2008; HOLDICH et al., 2020; KOSVINTSEV et al., 2005; ZAWALA; SZCZEPANOWICZ; WARSZYNSKI, 2015). The use of membranes has been shown to be efficient in the formation of stable emulsions that present desirable characteristics to be subsequently microencapsulated by complex coacervation (PIACENTINI et al., 2013).

Considering that membrane emulsification happens drop by drop as the droplets are being formed, they are involved by the continuous phase, whereas the shear stress applied by the stirrer detaches the newly formed droplets from the metallic surface (EGIDI et al., 2008). In addition, it is possible to predict or engineer the size of the emulsion droplets by a balance of capillary and drag forces during droplet formation (KOSVINTSEV et al., 2005). A handful of recent works studied the application of membrane emulsification, such as production of eco-friendly emulsions (SANTOS et al., 2015), production of food grade emulsions with different membrane compositions and morphologies (HANCOCKS; SPYROPOULOS; NORTON, 2016), comparison of azimuthal and axial oscillation microfiltration for non-Newtonian fluids (HOLDICH et al., 2018), preparation of micro and nano emulsions (VLADISAVLJEVIĆ, 2019) and the use of annular crossflow membrane using a single-pass (HOLDICH et al., 2020).

## 2.3 Complex coacervation

### *2.3.1 Microencapsulation by complex coacervation*

The first reference to the application of coacervation with potential for use in microencapsulation dates from the late 1920s, when gelatin spheres were obtained by coacervation (DE JONG BUNGENBERG; KRUYT, 1929). The term "coacervation" comes from the study of colloid chemistry, where there is phase separation by association of one or more polymers, and this separation can occur due to changes in ionic strength, temperature, pH or medium solubility (TIMILSENA et al., 2017b). Thus, microencapsulation by coacervation is a physical-chemical phenomenon in which spontaneous separation of colloidal liquid phases occurs where a target material is encapsulated in the process (KAUSHIK et al., 2015). It can be described as: a) formation of three phases, in which a liquid phase acts as a vehicle, one phase of the material to be encapsulated, and a third phase of the wall material. The colloid-rich liquid phase separates from a macromolecular solution as a result of reduction in solubility by chemical or physical means, such as changing the temperature and pH; b) the colloid-rich phase

remains in a dispersed state and presents itself as amorphous droplets, which is called coacervate. These droplets coalesce, forming a clarified liquid layer and another colloid-rich phase, known as coacervate, which is deposited around the droplets of the active material in a continuous coating to form the capsule wall; c) solidification of the wall material and insulation of the capsules (ERATTE et al., 2018; LIU; CHAPEL; SCHATZ, 2017; SILVA et al., 2012; XIAO et al., 2014a). In the case of simple coacervation there is the action of only one polymer, while in complex coacervation there must be an interaction between at least two polymers (XIAO et al., 2014a).

Complex coacervation using the gelatin-gum Arabic system is the most studied and the process is conducted as shown in Figure 2.1: the core material is emulsified or suspended in one of the two solutions (usually in gelatin) and the other solution is then added, thus forming a system with three phases. With a gradual decrease in pH up to 3.8 - 4.5, gelatin acquires positive charges, which interact with the negative charges of gum Arabic, forming coacervates that deposit around the droplets of the hydrophobic nucleus (MARFIL et al., 2018). To ensure greater integrity of the cover, the formation of cross-links of the material with a crosslinking agent can subsequently be carried out (PRATA et al., 2008; ZUANON; MALACRIDA; TELIS, 2013).

Coacervated microcapsules can be dried to extend their shelf life and to make their use in dehydrated products viable. For this, drying methods such as freeze drying, oven drying, solvent removal and drying in ambient conditions can be used. A problem with these methods is that most of them do not allow individualized particles to be obtained, interfering with the size of the final product and the release properties of the filling (ERATTE et al., 2014; XIAO et al., 2014b).

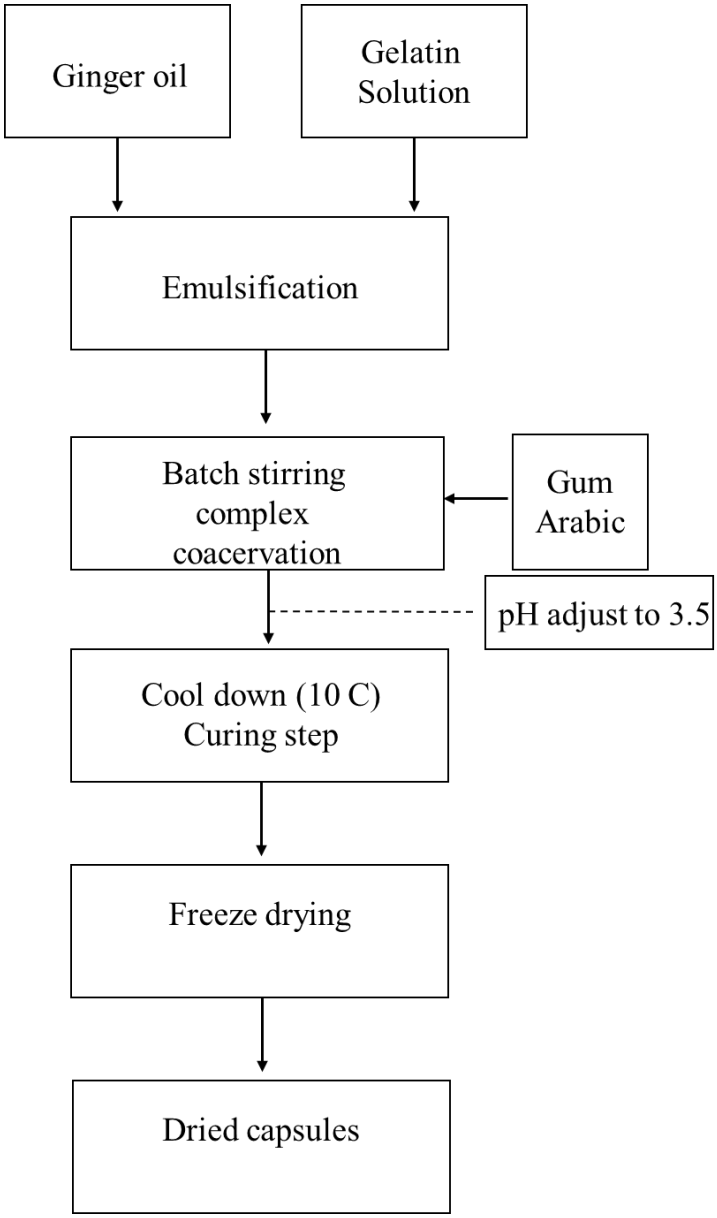


Figure 2.1. Block diagram of the traditional method of complex coacervation by batch stirring.

Among the main advantages of the use of complex coacervation for microencapsulation are: micrometric capsules which is a positive factor, considering it has the potential to promote retention encapsulated material; less aggressive process conditions and variety of biopolymers that are candidates for possible encapsulating materials, such as gelatin, albumin, gum Arabic, cellulose, alginate, caseinate, carrageenan, pectin, among others; possibility of high efficiency and retention in the encapsulation of core ranging from 60 to 90%; low oil migration to the capsule surface (KAUSHIK et al., 2015; KRALOVEC et al., 2012; SCHMITT et al., 1998). On the other hand, some disadvantages can be mentioned: with the technology currently available, the technique can be applied in a batch process, which is time consuming and tends to decrease the yield of encapsulated material; the stability of the coacervate complexes is directly linked

to the pH, ionic strength and temperature ranges responsible for their formation, as it is a reversible process; the need, in most cases, for the particle cross linking process, either by physical action or by chemical agents, which are often not suitable for use in food due to their toxicity; attention should be given to the origin of the protein used, taking into account consumers' food options and allergens to certain proteins; possible occurrence of Maillard reaction in the processing of the final product that can degrade both the capsule and the encapsulated material (CONSOLI; HUBINGER; DRAGOSAVAC, 2020; KAUSHIK et al., 2015; XIAO et al., 2014a).

Studies have shown that there is a correlation between the complex coacervation pH and the polymer ratio (LI et al., 2018; LV et al., 2014; MA et al., 2019). In order to provide a successful delivery of the encapsulated oil in intestine conditions the capsules would have to endure gastric conditions. Few studies have shown that the use of lower coacervation pH values provides better protection against gastric conditions of the capsule and its core, and a better release of the core on the intestine (HUANG et al., 2017a, 2017b).

### *2.3.2 Gelatin and gum Arabic*

Gelatin is one most used proteins applied both in microencapsulation and in complex coacervation, due to its low cost, good emulsifying properties, appropriate flavour/sensorial profile and, being a protein, it has a net charge depending of the medium pH (HECKERT BASTOS et al., 2020; KARIM; BHAT, 2008). Gelatin is a derivative of collagen, which is included among the proteins used for food encapsulation due to its ability to form a film and stable gel at temperatures below 40 ºC, provided that its concentration is at least 1 g of gelatin / 100 g of solution (MARFIL et al., 2018). This polymer is structured in the form of a triple helix composed of a repeating chain of amino acids, whose composition depends on the source from which it is extracted. In general, the three amino acids present in the greatest amount in gelatin molecules are glycine, proline and hydroxyproline (FERREIRA; MALACRIDA; TELIS, 2016; GILSENAN; ROSS-MURPHY, 2000; GOSAL; ROSS-MURPHY, 2000).

Like other proteins, gelatin has an amphoteric character, in which the groups of amino acids present may be positively or negatively charged depending on the pH of the medium. If the pH is below the gelatin isoelectric point (Ip), it will tend to have a positive resultant surface charge, while if the pH is above the gelatin Ip, it will tend to have a negative resultant surface charge. Also, gelatin can be divided into two types, depending on the type of hydrolysis suffered in the extraction process. For gelatin called "type A", the extraction takes place by acid hydrolysis, and its Ip will be in alkaline pH ranges between 7.0 to 9.5. On the other hand, for

"type B" gelatin, alkaline type hydrolysis occurs and, therefore, the Ip will be at acidic pHs, between 4.5 to 5.5 (MARFIL et al., 2018; PRATA et al., 2008).

Gum Arabic is a gum extracted from two species of acacia: Acacia *senegal* and Acacia *seyal*. It has fractions with different chemical structures: the main fraction consists of polysaccharide chains (ZUANON; MALACRIDA; TELIS, 2013); a protein fraction - about 2% of the gum - is covalently linked to the carbohydrate and plays a crucial role in determining the emulsifying and stabilizing properties of gum Arabic (DIVISION et al., 2013). It is a carbohydrate vastly used in complex coacervation, presenting low viscosity, mild flavour, protection against volatile oxidation (COMUNIAN et al., 2016; OSMAN et al., 1993; RAY et al., 1995). It has fractions with different chemical structures and about 70% of it consists of polysaccharide chains of a highly branched arrangement of galactose, arabinose, rhamnose, and glucuronic acid with little or no nitrogenous material between them.

From the standpoint of the process proposed in this work, gum Arabic has some essential characteristics, namely: having structural characteristics that allow it to be adsorbed on lipophilic surfaces, in addition to presenting high solubility, low viscosity in solution and Newtonian behaviour in concentrations below 35%. It is negatively charged above pH 2.2 and, at pH less than 2.2, the dissociation of carboxyl groups is suppressed (DIVISION et al., 2013; MARFIL et al., 2018).

### *2.3.3 Effect of process parameters on complex coacervation*

Providing mathematical descriptions of microencapsulation processes by complex coacervation is an important step towards the development of a continuous process, considering the reproducibility of results and paving the way for scale up (JEGAT; TAVERDET, 2000; LEMETTER; MEEUSE; ZUIDAM, 2009).

In studies of the application of hydrodynamic models for microencapsulation by complex coacervation, it has been shown that the agitation of solutions in complex coacervation can be correlated with the size of the particles formed, and the agitation parameters can be determined by the physical parameters of the fluids involved and the power that is exerted in the system (DOBETTI; PANTALEO, 2002; LEMOS; MARIANO MARFIL; NICOLETTI, 2017). In the last decades, studies have been carried out to describe complex coacervation by means of the process parameters involved in this phenomenon. This approach is essential when seeking to increase the scale of production, especially when it is hoped that this technique can be applied on an industrial scale. According to Jegat and Taverdet (2000), there is a need for

quantitative description of the variables involved in complex coacervation, thus facilitating the reproducibility of the results and scaling up. Before these studies with a quantitative focus, what was observed in the literature was an empirical approach to scale up for complex coacervation, in which the conclusions obtained were based more on trial and error than on a systematic process to describe the phenomenon, which could allow the reproducibility of the results obtained (ACH et al., 2015).

A limited number of previous works described quantitative process variables for complex coacervation. Lemetter, Meeuse, Zuidam (2009) conducted a careful study in order to control the capsules morphology produced by complex coacervation. The authors sought to: identify which were the main parameters involved in the quality of the obtained capsules and, thus, to understand how these parameters influence the formation of the capsules, in order to develop a pilot plant for the production of microcapsules that was reliable and reproducible. Their results showed that the initial size of the emulsion drop plays a major role in the dimensions of the coacervate capsule, and the size of the emulsion drops can be controlled by the stirring speed, and other factors. Additionally, it was shown that for the formation of individualized particles it is necessary that the number of Reynolds is greater than 15000. Also, there is a strong dependence on the morphological characteristics of the capsules obtained in function of the conditions of time and temperature in the stage of cooling the solution for cure of the capsules. Ma, Zhao, Wang and Sun (2019) investigated the influence of polymer concentration, polymer ratio, core to polymer ratio, stirring speed and coacervation pH on morphology and oxidative stability of lipid capsules formed by complex coacervation. Lemos, Marfil, and Nicoletti (2017) evaluated the effects of stirring speed on gelatin-sodium alginate complex coacervation by batch stirring. Dobetti and Pantaleo (2002) studied the influence of hydrodynamic conditions on the morphology and size of capsules for encapsulation of water-soluble drugs in cellulose acetate phthalate. All these studies showed a correlation between the stirring speed and physical properties of the fluids with the size and morphology of the produced microcapsules in batch stirring complex coacervation.

Another way to increase production scale with a focus on industrial applicability is to carry out complex coacervation in continuous process. By using agitators that operate in a continuous regime, it is possible to agitate and promote coacervation, being possible to control the flow rate of the solutions, as well as the agitation rate. With the application of this technique, Chapeau et al. (2017) managed to increase the scale of capsule production by complex coacervation, from laboratory scale to bench scale.

Thus, there is a strong tendency and need to seek to describe the complex coacervation process in a quantitative way, based mainly on the physical parameters of the different solutions used, agitation parameters, time, temperature, cooling rate, among others, opening path to solid and reliable scaling-up processes.

## 2.4 Atomization

Dual-fluid atomization nozzle operates by transferring the momentum between a high-speed gas stream and a liquid stream. The dynamic air pressure thus breaks the liquid jet into filaments and droplets (GUILDENBECHER; LÓPEZ-RIVERA; SOJKA, 2009). The properties of the liquids that have greater influence on the atomization process are: density, surface tension and viscosity. Other factors also affect the characteristics of the resulting spray, mainly the gas velocity, liquid velocity, gas/liquid mass and velocity ratios, pressure, and atomizer geometry (OMER; ASHGRIZ, 2011).

The surface tension is an important parameter in atomization, which represents the force that resists to the increase of the surface area. The higher the surface tension, the greater the difficulty of the liquid to disintegrate in drops (DUBE, 2000). Like the surface tension, the viscosity of the fluid exerts resistance to the disintegration of the liquid in drops. Newtonian liquids do not show variation in viscosity with shear rate, whereas non-Newtonian fluids show a strong dependence on viscosity with shear rate (BAYVEL et al., 2019a; STEFFE; PH; PRESS, 1994; STEFFE; DAUBERT, 2006; WOOD, 1995). Density is the physical property that has less influence on the droplet formation process. This occurs for two reasons: the first is that the fluids commonly used for atomization have densities close to each other, which makes it difficult to compare this property between them; the second is that when two fluids of very different densities are used for testing purposes, the other properties, such as viscosity and surface tension, also vary widely, which undermines the individual analysis of density (BAYVEL et al., 2019b).

An effective way to describe the atomization process is the use of dimensionless numbers Weber ($We = \frac{\rho_g (V_g - V_l)^2 D_l}{\sigma}$) and Ohnesorge ($Oh = \frac{\mu_l}{\sqrt{\sigma D_l \rho_l}}$), in which $V_g$ is the atomizing air velocity; $V_l$ is the emulsion velocity; $\rho_g$ is the density of the atomizing air; $D_l$ is the diameter of the discharge orifice of the nozzle; σ is the emulsion surface tension; $\mu_l$ is the emulsion viscosity and $\rho_l$ the emulsion density. *Oh* number relates the viscous forces to the surface tension forces in the solution, whereas *We* correlates the inertial and surface tensional

components of the resultant force during atomization. In general, high Ohnesorge values indicate a low tendency to atomize the system (GUILDENBECHER; LÓPEZ-RIVERA; SOJKA, 2009). According to Cao et al. (2007), in studies of droplet formation the Weber and Ohnesorge numbers are crucial parameters of the atomization process. When $Oh \leq 0.1$, it is assumed that only *We* interferes on the atomization process, and for $0.1 < Oh < 1$ both *We* and *Oh* will affect atomization (GUILDENBECHER; LÓPEZ-RIVERA; SOJKA, 2009). In addition, different ranges of *We* results in different regimes of atomization: at $12 < We < 80$ a bag-type liquid's breakup occurs, at $80 < We < 350$ an air-shear breakup occurs, and at $We > 350$, a catastrophic liquid's breakup will be present (VARGA; LASHERAS; HOPFINGER, 2003).

A study by Filková, Huang and Mujumdar (2014) presented a hydrodynamic model with the purpose of predicting the size of the liquid droplets during the atomization process. It will be used as reference in an attempt to predict the capsules size after complex coacervation. A similar approach was adopted by Thybo et al. (2008), to estimate the size of atomized droplets for spray-dryer scale up. The influence of atomization parameters on distinct microencapsulation processes has been studied by different approaches, mainly because it represents a flexible and economical technology to transform liquid solutions into solid particles/capsules. Ferreira et al. (2019) evaluated the influence of atomization parameters on microencapsulation of turmeric oleoresin by spray drying, using gelatin and maltodextrin as wall material. Zuanon et al. (2019) reported that higher values of atomization airflow generated smaller liquid droplets, potentializing the spray drying/encapsulation process. Moser, Ferreira and Nicoletti (2019) encapsulating buriti oil in chickpea protein-pectin matrix by spray drying, studied the influence of airflow on the carotenoid retention and process yield. Jiang et al. (2013) combined complex coacervation and drying into one step using a novel three-fluid nozzle to encapsulate α-amylase. Kašpar, Jakubec and Štěpánek (2013), using a three-fluid nozzle, produced crosslinked chitosan particles by spray drying. Chen et al. (2006) explored the release behaviour and morphology of particles produced using acetaminophen, chitosan and hydroxypropyl-methylcellulose formed by a 4-fluid nozzle spray dryer. Also using a 4-fluid nozzle, Ozeki et al. (2005) produced microparticles of water-insoluble and water-soluble drugs, and doing so, improved water solubility of the particles. In those studies, important advances in the mathematical description of the atomization as a method to improve the encapsulation were done. Also, new encapsulation additives and techniques were presented as alternatives to improve encapsulation by atomization, independently of the method used. This is important because atomization is an easily scalable technique, what makes it cost effective.

## 2.5 Ginger oil

Ginger (*Zingiber officinale*) is known worldwide and used as a spice or condiment around the world. For centuries, it has been an important ingredient for Chinese, Japanese, and Indian medicine. It is used in the treatment of diseases in the respiratory mucous membranes, rheumatism, nervous diseases, gingivitis, toothache, asthma, constipation, stroke and diabetes (TAPSELL et al., 2006). Other studies have been carried out to understand specific aspects of the action of ginger compounds, such as anti-inflammatory action or even in the prevention of cancer (GRZANNA; LINDMARK; FRONDOZA, 2005).

Fresh ginger contains about 85-95% water and may be susceptible to microbial, chemical and biochemical deterioration. Thus, dehydration of ginger or extraction of oils and/or oleoresins are good alternatives to avoid any type of deterioration. Different processes can be applied, including microencapsulation, to further promote the viability of the compounds present in ginger. Among the applications of dry or microencapsulated ginger can be mentioned the manufacture of ginger spices, use in medicine and cosmetics as well as foods with ginger flavour, such as soft drinks and sweets (AN et al., 2016; FERNANDES et al., 2016; SCHWERTNER; RIOS, 2007).

The spicy taste of fresh ginger is mainly due to gingerols, which are a homologous series of phenolic compounds. Among these compounds, the one that presents itself in greater quantity is 6-gingerol, although smaller amounts of gingerols with different chain lengths may be present. Studies with these phenolic compounds have shown analgesic, antipyretic, cardiological effects, inhibiting spontaneous motor activity and prostaglandin biosynthesis and preventing certain types of cancer (SHOJI et al., 1982; SHUKLA; SINGH, 2007). In addition, 6-gingerol has shown antioxidant and anti-inflammatory properties in other studies (GRZANNA; LINDMARK; FRONDOZA, 2005). However, when dehydrated or stored for long periods, 6-gingerol can be oxidized to 6-shogaol, and this compound is not found in fresh ginger extract (SCHWERTNER; RIOS, 2007).

Studies have achieved good results in encapsulation of ginger oleoresin by spray drying using gum Arabic, maltodextrin and inulin, reaching oil retention ranging from 48.0 to 93.0%. Furthermore, the use of ultrasound for the emulsification process was studied, and this method generated smaller particles when compared to conventional mechanical agitation, such as ultraturrax for example (FERNANDES et al., 2016). In addition, recent works studied the microencapsulation of ginger oil by spray drying (MAULIDNA et al., 2020), by electrostatic interaction (BAN et al., 2020), and by complex coacervation between gelatin and sodium alginate (WANG et al., 2016). This shows that there is a growing interest on the encapsulation

of ginger hydrophobic compounds, protecting them from oxidation during processing and storage.

# CHAPTER 3 - MICROENCAPSULATION OF GINGER OIL BY COMPLEX COACERVATION USING ATOMIZATION: EFFECTS OF POLYMER RATIO AND WALL MATERIAL CONCENTRATION

Sungil Ferreira[1], Vania Regina Nicoletti[1]

[1]São Paulo State University (UNESP), Department of Food Engineering and Technology, São Jose do Rio Preto – SP, 15054-000, Brazil

Published in Journal of Food Engineering, Volume 291, February 2021, 110214.

https://doi.org/10.1016/j.jfoodeng.2020.110214

Abstract

The objective of this work was to investigate the feasibility of inducing complex coacervation by atomizing an emulsion of gelatin/ginger oil over a gum Arabic solution, which would be a first step towards continuous process configuration. The influence of gelatin:gum Arabic ratio was investigated regarding capsule formation by atomization. In addition, the effects of emulsion concentration on coacervation by atomization and by batch stirring were studied. Gelatin:gum Arabic ratio strongly affected the capsule formation. The gelatin concentration affected the size of capsules for both methods, whereas the increase of gelatin concentration did not affect encapsulation parameters for atomized capsules. The diameter of microcapsules varied from 57 to 85 μm, encapsulation efficiency varied between 89.74 and 98.7%, and encapsulation yield ranged from 21 to 88%, with the atomization process resulting in higher encapsulation yield. The results indicated that microcapsules produced by atomization were comparable with capsules produced by batch stirring.

Keywords: encapsulation, ginger oil, complex coacervation, atomization, Weber number, Ohnesorge number.

## 3.1. Introduction

The pungent flavour of fresh ginger is mainly due to gingerols, and these compounds may be susceptible to degradation caused by harsh conditions during production and storage, decreasing their functional properties (DUGASANI et al., 2010). Thus, different processes, including microencapsulation, can be applied to promote further viability of the compounds present in ginger (FERNANDES et al., 2016). Dried ginger or microencapsulated ginger oil can be applied in the manufacturing of ginger spices, in pharmaceuticals and cosmetics, as well as in ginger-flavoured foods, such as soft drinks and sweets (SCHWERTNER; RIOS, 2007). Recent works investigated microencapsulation of ginger oil by spray drying (MAULIDNA et al., 2020), microencapsulation by electrostatic interaction (BAN et al., 2020) and by complex coacervation between gelatin and sodium alginate (WANG et al., 2016).

Complex coacervation has been successfully used for microencapsulation of oils and flavours, with extensive application in the food, agricultural, textile and pharmaceutical industries (MARTINS et al., 2014). Complex coacervation is usually carried out in batch configuration, and few studies have been carried out aiming its application in continuous regime. The reason is that sometimes the method does not allow the production of individual microcapsules, affecting the granulometry of the powder produced and the releasing properties of the core material, in addition to the fact that, traditionally, batch process is carried out using very diluted solutions (BURGESS; PONSART, 1998; ERATTE et al., 2018). The technique is very versatile and is suitable for protection of compounds against degradation, to prevent loss of volatiles, in addition to allowing for modulated release and increased stability of the encapsulated material (XIAO et al., 2014a). Complex coacervation results from the interaction of oppositely charged colloidal polymers, which under certain conditions form complexes that tend to precipitate due to solvent repulsion. As a consequence, two phases are formed, one of which contains the precipitated coacervate and is called "rich in polymer", whereas the other, in which the solvent remains, is called "poor in polymer" (KAUSHIK et al., 2015; STRAUSS; GIBSON, 2004). Some important points must be considered in the coacervation process, including the ratio between the polymeric compounds, the charge density, ionic strength, pH of the solutions, stability, and solubility of the complexes formed (RUTZ et al., 2017).

The well-known pair of biopolymers gelatin and gum Arabic is often used for studies on complex coacervation as a reference system, taking into account that their performance is predictable and they provide proper spherical-shaped microcapsules by the traditional process of complex coacervation carried out in batch stirring (MARFIL et al., 2018; PIACENTINI et

al., 2013; PRATA et al., 2008; SHADDEL et al., 2018; ZUANON; MALACRIDA; TELIS, 2013).

There is a need for quantitative description of the variables involved in complex coacervation, thus facilitating reproducibility of results and allowing for scale up (JEGAT; TAVERDET, 2000). In previous studies, application of hydrodynamic models for microencapsulation by complex coacervation has shown that the stirring speed and the physical parameters of the fluids involved in the process can be correlated with the size of the resulting microcapsules (DOBETTI; PANTALEO, 2002; LEMETTER; MEEUSE; ZUIDAM, 2009; LEMOS; MARIANO MARFIL; NICOLETTI, 2017). In addition, description of the complex coacervation process by non-dimensional numbers is an important step towards scale up and, ultimately, to allow for development of a continuous process (JEGAT; TAVERDET, 2000).

A possible process configuration to carry out complex coacervation as a continuous process is based on atomization. By atomizing the gelatin/ginger oil emulsion over a vessel containing gum Arabic solution, complex coacervation between the biopolymers takes place on the surface of the emulsion droplets that are formed during the atomization step, as it flows through the gum Arabic solution. In this sense, studying the atomization step and atomized droplet formation is crucial in order to obtain efficient oil encapsulation. The atomization process can be described by the non-dimensional numbers Weber (*We*) and Ohnesorge (*Oh*). *We* number correlates the inertial and surface tensional components of the resultant force during atomization, whereas *Oh* relates the viscous forces with the surface tension forces in the liquid. According to Varga et al. (2003), different ranges of *We* correspond to different patterns of liquid atomization: bag-type breakup of the liquid occurs at $12 < We < 80$, atomization by air-shear breakup occurs at $80 < We < 350$, and catastrophic breakup at $We > 350$. In addition, when $Oh \leq 0.1$, it is possible to assume that only *We* affects the atomization process, whereas for $0.1 < Oh < 1$ the system is in the transition regime, in which both *We* and *Oh* exert influence (GUILDENBECHER; LÓPEZ-RIVERA; SOJKA, 2009). The effects of atomization in the functionality of particles produced by a number of encapsulation processes have been investigated by different approaches, mainly because it represents a flexible and economical choice to transform liquid materials into particles. Jiang et al. (2013) presented a study for enzyme encapsulation process in which the complex coacervation and drying processes are combined into a single step, using a novel three-fluid nozzle for atomization. Kašpar et al. (2013) produced chitosan microparticles crosslinked by tri-polyphosphate by spray drying, using a three-fluid nozzle. Chen et al. (2006) studied acetaminophen particles produced with

chitosan and hydroxypropyl-methylcellulose using solid dispersions formed by a 4-fluid nozzle spray dryer, evaluating their sustained release and morphological characteristics.

In this context, the aim of this work was to first investigate the influence of gelatin:gum Arabic ratio on the formation of microcapsules by complex coacervation induced using a two-fluid atomization nozzle. Once a proper ratio between the polymers was established, we evaluated the effects of gelatin concentration in the emulsion on the atomization and coacervation processes. The size of wet microcapsules, infrared spectrum, and encapsulation performance parameters were evaluated and compared with complex coacervation carried out by batch stirring. In addition, a study of the atomization process using hydrodynamic models was applied, and the results were correlated with the microencapsulation performance.

## 3.2 Material and methods

### *3.2.1 Material*

Cold pressed ginger oil (Gran Oils, São Paulo, Brazil) was used as microencapsulated core material. Type B gelatin, 240 bloom (Gelita, Mococa, Brazil) and gum Arabic (Dinâmica, Campinas, Brazil) were used as wall material. Glacial acetic acid (Dinâmica, Campinas, Brazil) was used for pH adjustment. Hydrochloric acid 4 N (Dinâmica, Campinas, Brazil) was used to digest the capsules to release the encapsulated oil. Hexane (Dinâmica, Campinas, Brazil) was used as organic solvent for oil extraction.

### *3.2.2 Preparation of ginger oil/gelatin emulsions and gum Arabic solution*

Oil-in-water emulsions were prepared by dispersing ginger oil in aqueous gelatin solution. The mass ratio of oil:gelatin was maintained as 1:1 in all assays and concentration of gelatin in the aqueous solution ranged from 1 to 10 g of gelatin/100 g. Primary emulsification was performed using high shear homogenizer Ultra Turrax T-25 (IKA, Germany) at 15,000 rpm for 2 min, followed by secondary homogenization by ultrasound (Sonic Ruptor 4000 ultrasonic probe, Omni International, USA) at frequency of 20 kHz for 3 minutes with nominal power of 210 W.

The aqueous solution of gum Arabic (1 g/100 g) was prepared by adding the polymer to preheated (50 °C) deionized water and by magnetic stirring until complete dissolution. The concentration of gum Arabic in the solution was the same in all the assays.

*3.2.3 Ginger oil/gelatin emulsion and gum Arabic solution characterization*

Surface tension measurements of the ginger oil/gelatin emulsion and gum Arabic solution, were done using an Attension Sigma 701 tensiometer (Biolin Scientific, Sweden) by the Wilhelm plate method using a platinum plate. Density of the solutions was determined using a densimeter Attension Sigma 701 (Biolin Scientific, Sweden) with glass sphere probe. Rheological behaviour was evaluated through flow curves determined in a rheometer AR2000ex (TA Instruments, USA), equipped with Peltier system for temperature adjustment (35 $^{o}$C) and cone and plate geometry. The emulsion stability was evaluated using transparent, graduated, plastic tubes, centrifuged at 50×g (model Z 326 K, Hermle, Germany) for 5 minutes. The tubes were observed in order to detect the appearance of a cream layer or free oil on the upper part of the emulsion, but there was no evidence of creaming or phase separation after centrifugation (FERREIRA et al., 2016).

*3.2.4 Complex coacervation in batch stirring*

For complex coacervation in batch stirring, the ginger oil/gelatin emulsion (22 to 200 mL) (50 ± 1 °C) was added to the gum Arabic solution (380 mL) (50 ± 1 °C) in a 1 L beaker, and the mixture was kept under magnetic stirring (approximately 300 rpm). The pH (3.5 ± 0.1) was adjusted using glacial acetic acid and the system was immersed in an ice bath, maintaining agitation for slow cooling until 10 ± 1 °C. After 24 hours, the sedimented particles were transferred to aluminium trays and frozen in ultra-freezer (Liobrás, FV 500, Brazil) at -40 °C and freeze-dried (Liobrás, L101, Brazil) at less than 500 μmHg for 72 hours. The dried samples were ground, packed in aluminium foil for light protection and stored in a desiccator with silica gel for further analysis.

*3.2.5 Complex coacervation by atomization*

For complex coacervation by atomization, the ginger oil/gelatin emulsion was atomized over the aqueous solution of gum Arabic using a dual fluid atomizer nozzle (0.7 mm diameter, Labmaq, Brazil), with controlled air and emulsion flowrates. The pH of the emulsion and of gum Arabic solution were adjusted to 3.5 using glacial acetic acid (> 96%), before atomization. The atomization conditions and additional operational parameters were determined based on the results of exploratory assays, and are summarized in Table 3.1. The nozzle was positioned at a fixed height of 0.2 m above the vessel containing gum Arabic solution as described in Figure 3.1. Air flowrate was controlled using a rotameter FT074-02-

CA-VN (Omega, Stamford, USA). After all the emulsion was atomized, the system was immersed in an ice bath until reaching 10 ± 1 °C and then stored at 5 ± 1 °C in refrigerator.

Table 3.1. Physical properties of atomization air, dimensions of the atomization nozzle and operational parameters of atomization.

| | |
|---|---|
| **Characteristics of the two fluid nozzle** | |
| Diameter of emulsion outlet ($D_l$) - (mm) | 0.7 |
| Internal diameter of air outlet ($D_{int}$) - (mm) | 1.90 |
| External diameter of air outlet ($D_{ext}$) - (mm) | 2.80 |
| **Physical properties of the atomization air (25 °C)** | |
| Density ($\rho_g$) - (kg $m^{-3}$) | 1.23 |
| Viscosity ($\mu_g$) - (µPa s) | 18 |
| **Atomization process parameters** | |
| Atomization air volumetric flow rate ($Q_g$) - $10^{-04}$ ($m^3$ $s^{-1}$) | 3.60 |
| Emulsion volumetric flow rate ($Q_l$) - $10^{-07}$ ($m^3$ $s^{-1}$) | 2.45 |

To determine the influence of the ratio between the polymers (gelatin:gum Arabic) on the complex coacervation process, the emulsion previously prepared, as described in section 3.2.1, was atomized over the gum Arabic solution. Concentrations of the gelatin/ginger oil emulsion and of the gum Arabic solution were fixed at 1 g of polymer/100 g and the gelatin:gum Arabic mass ratio was varied (in the range of 1:0.5 to 1:10) by keeping the volume of atomized emulsion constant and increasing the volume of gum Arabic solution for each assay.

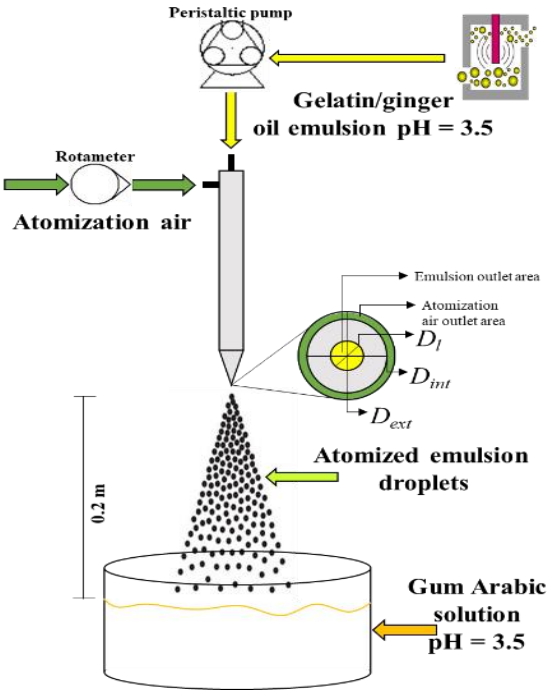


Figure 3.1. Schematic diagram of the complex coacervation process by atomization.

*3.2.6 Characterization of wet microcapsules*

Density of the wet microcapsules formed by complex coacervation was determined in a densimeter DMA™ 4500 M (Anton Paar, Austria). After coacervation, the suspension containing the microcapsules was stored at 5 °C for 24 hours to allow particles to settle and approximately 2 mL of the precipitate were collected using a Pasteur pipette. The density determination was done at 10 ºC. The total solids of the supernatant were determined by gravimetry in oven at 105 ºC.

The microstructure of wet microcapsules was evaluated using an optical microscope (CX31-III, Olympus, Japan) coupled with a video camera (SIS-SC30). The samples were conditioned on glass slides without dilution. The scanned images were analysed by Image Pro Plus 6.0 software (Media Cybernetics Inc., USA) for measurement of microcapsule diameter. The reported diameter is the mean calculated after measurement of 300 microcapsules per treatment.

*3.2.7 Characterization of dried microcapsules*

After complex coacervation the microcapsules were freeze-dried as described in item 3.2.3 and subjected to analysis as follows. Encapsulation efficiency (*EE*) and encapsulation yield (*EY*) were calculated based on the oil content initially present in the emulsion (*OI*), the oil present on the surface of the microcapsules (*OS*), and in the total oil present in the microcapsules (*OT*). To determine *OS*, 100 mg of microcapsules and 10 mL of hexane were placed in a capped test tube and shaken for one minute. The organic phase was filtered and transferred to Petri dishes. The solvent was evaporated at room temperature in a hood and then kept at 60 °C until maintaining a constant weight. To determine *OT*, 100 mg of microcapsules were dispersed in 20 mL of 4 N hydrochloric acid solution and shaken for 1 hour at 35 °C for dissolution of the wall material. Then, 13 mL of hexane were added and stirred for 10 hours at 25 °C, forming a two-phase system. The non-organic and organic phases were separated by centrifugation (model Z 326 K, Hermle, Germany) at 10000×g for 30 minutes and the organic phase containing hexane and oil was transferred to Petri dishes. The solvent was evaporated at room temperature in a hood and then at 60 °C until maintaining a constant weight. The *EE* and *EY* were calculated by Equations 3.1 and 3.2 (TONON; GROSSO; HUBINGER, 2011; WANG; ADHIKARI; BARROW, 2014), respectively.

$$EE(\%) = \frac{OT - OS}{OT} \times 100 \quad (3.1)$$

$$EY(\%) = \frac{OT}{OI} \times 100 \quad (3.2)$$

Fourier transform infrared spectroscopy (FTIR) was performed on a Prestige-21 IR spectrometer (Shimadzu, Japan). The analysis was performed using potassium bromide tablets from 400 to 4000 cm $^{-1}$ with a resolution of 8 cm$^{-1}$.

The morphology of the dried microcapsules was analysed by SEM microscope (FEI, USA), with spot 4.0 and 25 kV. Microcapsules were deposited on carbon tape and metallized with a thin gold layer of 5 nm. The images were obtained with topography detector to visualize the surface morphology of the samples.

*3.2.8 Mathematical description of the atomization process*

The atomization process was evaluated through the Weber (Equation 3.3) and Ohnesorge (Equation 3.4) non-dimensional numbers, and the theoretical Sauter diameter, $D_{3,2}$, (Equation 3.5) of the emulsion droplets after being atomized in the pneumatic nozzle and before getting in contact with the gum Arabic solution (FILKOVÁ; HUANG; MUJUMDAR, 2014).

$$We = \frac{\rho_g (V_g - V_l)^2 D_l}{\sigma} \tag{3.3}$$

$$Oh = \frac{\mu_l}{\sqrt{\sigma D_l \rho_l}} \tag{3.4}$$

$$D_{3,2} = \frac{535 \times 10^3 \sqrt{\sigma}}{(V_g - V_l)\sqrt{\rho_l}} + 597 \times 10^3 \frac{Q_l}{Q_g} \left(\frac{\mu_l}{\sqrt{\sigma \rho_l}}\right)^{0.45} \tag{3.5}$$

In which $Q_l$ and $Q_g$ are the volumetric flowrates of liquid and air, respectively; $V_g$ is the atomizing air velocity; $V_l$ is the emulsion velocity; $\rho_g$ is the density of the atomizing air; $D_l$ is the diameter of the discharge orifice of the nozzle; σ is the emulsion surface tension; $\mu_l$ is the emulsion viscosity and $\rho_l$ the emulsion density.

*3.2.9 Statistical analysis*

All the assays were performed in triplicate. The results of the analytical determinations are expressed in arithmetic average (*AV*) submitted to analysis of variance (ANOVA) and comparison of means by Tukey test with probability level at 5% ($p \leq 0.05$), using statistical software Minitab 17 (MINITAB, State College - PA, USA). The uniformity of the data (size distribution) was presented as variation coefficient [VC=(SD/AV)*100], in which *SD* stands for standard deviation.

### 3.3 Results and discussion

*3.3.1 Characterization of ginger oil/gelatin emulsion and gum Arabic solution*

The emulsions produced were stable during the whole atomization process. No phase separation and no creaming were observed for all formulations. This is important because it assured that the flocculation or coalescence of the oil droplets prior to complex coacervation will not affect the encapsulation parameters.

As presented in Table 3.2, the density of the ginger oil/gelatin emulsion ranged from 997 to 1058 kg/m$^3$, being directly proportional to gelatin/ginger oil concentration, as the proportion between oil and gelatin in the emulsion was fixed at 1:1 for all emulsions. The apparent viscosity was also proportional to gelatin concentration, varying from 0.0013 to 0.0483 Pa·s, with the determination coefficients, $R^2$, of the rheological models being higher than 0.995. The samples with 6 and 10 g of gelatin/100 g of emulsion presented rheological behaviour of Bingham fluids. The samples with less gelatin concentration behaved like Newtonian fluids. Considering that the main difference between a Newtonian and Bingham fluid lays on an initial shear stress prior to flowing that is observed in Bingham fluids, the difference on the rheological behaviour should not have effects on the atomization of the emulsion, which occurs at high shear rates (STEFFE; PH; PRESS, 1994). The surface tension varied from 39 to 53 *m*N/m, which is a range similar to those observed in other investigations involving atomization of gelatin solutions (PITT et al., 1996). In a work measuring atomized droplets of Newtonian and non-Newtonian fluids, Mansour and Chigier (1995) reported surface tensions of 73 *m*N/m. Thybo et al. (2008) investigating the scale up of spray dryers, used solutions with surface tension varying from 23 to 72 *m*N/m. Studying the relationship between surfactant structure and surface tension in gelatin solutions, Pitt et al. (1996) presented surface tension values varying from 23 to 60 *m*N/m.

Table 3.2. Physical-chemical properties of the gelatin/ginger oil emulsions and gum Arabic aqueous solution.

| **Liquid Phase** | **Polymer concentration (g/100g)** | **Density[1] (*k*g/m)** | **Surface Tension[2] (*m*N/m)** | **Apparent Viscosity (Pa·s)** | **Rheological model`s best fit/$R^2$** |
|---|---|---|---|---|---|
| Ginger oil/GE emulsion | 1 | 997.0±0.7$^{cd}$ | 45.4±0.2$^{c}$ | 0.0016 | Newtonian/0.998 |
| | 2 | 999.3±1.1$^{cd}$ | 49.7±0.3$^{b}$ | 0.0025 | Newtonian/0.999 |
| | 4 | 1005.0±2.0$^{bc}$ | 49.2±0.3$^{b}$ | 0.0054 | Newtonian/0.999 |
| | 6 | 1008.7±2.4$^{b}$ | 48.8±0.2$^{b}$ | 0.0116 | Bingham/0.999 |
| | 10 | 1058.0±4.7$^{a}$ | 52.4±0.5$^{a}$ | 0.0483 | Bingham/0.999 |
| Gum Arabic solution | 1 | 994.3±1.6$^{d}$ | 39.6±1.1$^{d}$ | 0.0013 | Power law/0.995 |

[1]Mean values ± standard error (n = 3); [2]Mean values ± standard error (n = 10); *Different letters in superscript in each column indicate significant differences (Tukey test, $p < 0.05$).

*3.3.2 Influence of polymer ratio on complex coacervation by atomization*

The ratio of gelatin:gum Arabic was fundamental to formation of regular shaped microcapsules in the complex coacervation carried out by atomization. Based on the results obtained varying the gelatin:gum Arabic ratios from 1:0.5 to 1:10 (Table 3.3), it was possible to classify the treatments into three main groups with distinct characteristics. Despite all the groups ending up in phase separation, they resulted in particles with different morphology, as shown by the typical images of each group presented in Table 3.3.

Group I, with ratios 1:0.5, 1:1 and 1:1.2 (gelatin:gum Arabic) resulted in particles with non-spherical conformation, contrary to what would be expected to complex coacervation. The particles in group I had undefined steric conformation, in which there were some regions around the particles resembling a membrane, incipiently exhibiting the shape expected in microcapsules formed by complex coacervation. This suggests that the formulations in this group might be lacking gum Arabic, which would be necessary to fully attend the thermodynamic requirements for complex coacervation. In previous studies of complex coacervation by batch stirring (LV et al., 2014; MARFIL et al., 2018; SHADDEL et al., 2018; ZUANON; MALACRIDA; TELIS, 2013) using the pair gelatin and gum Arabic, have shown that the optimum ratio between the polymers was 1:1, for pH around 4.5.

Group II encompasses the assays carried out with ratios 1:1.5, 1:1.8, 1:2, and 1:3 (gelatin:gum Arabic), which resulted in spherical microcapsules as expected in complex coacervation. The range of polymer ratios used in group II seems to meet the kinetic and thermodynamic criteria for both phase separation and complex coacervation. Li et al. (2018) in a study of complex coacervation using fish gelatin and gum Arabic also found the ratio of 1:2 (gelatin:gum Arabic) as the optimum coacervation condition at pH 3.5, the same condition used in this work.

Finally, in group III, the ratios 1:4, 1:5, 1:7, and 1:10 (gelatin:gum Arabic) resulted in phase separation but there was no capsule formation, although the particle morphology was different from the observed in group I. Particles in group III had a flake-like morphology, with no tendency to form large aggregates and appearing to be less dense than those observed in group I, with lesser amount of polymer deposited on the particle surface. A possible explanation for this result might be that, after part of the gum Arabic had been used for complex coacervation with gelatin, the excess gum Arabic begins the process of enclosing the individual

particles previously formed, destabilizing the system and resulting in particles with an undefined morphology.

Thus, it is possible to say that the ratio between the polymers used for complex coacervation have great interference on the capsule formation. All samples in group 2 presented spherical morphology, however the ratio 1:1.8 (gelatin:gum Arabic) presented more individualized capsules, with less aggregation, which was possible to observe by examining various images of the different treatments (images not shown). The optimum ratio of gelatin:gum Arabic showed to be between 1:1.5 to 1:3 and the optimum ratio chosen for the next steps was 1:1.8, based on the lower degree of microcapsule aggregation. For ratios under 1:1.5 (Group I) there is a lack of polymer to form the capsule membrane and to produce spherical particles. On the other hand, for ratios above 1:3 (Group III), the excess of polymers destabilizes the capsule structure.

Table 3.3. Effects of the polymer ratio (gelatin:arabic gum) on capsule formation and morphology produced using complex coacervation by atomization. Ratios of polymers are classified in groups in function of the particle/capsule morphology in each group.

| Group | Gelatin:gum Arabic | Description | Morphology* |
|---|---|---|---|
| I | 1:0.5<br>1:1<br>1:1.2 | No capsule formation. Tendency to form large aggregates. | 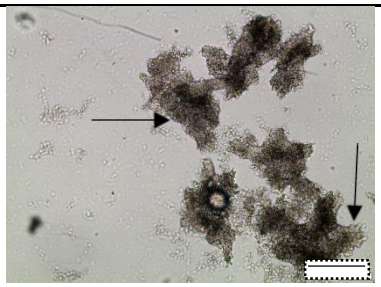 |
| II | 1:1.5<br>1:1.8<br>1:2<br>1:3 | Microcapsule formation with defined spherical morphology. | 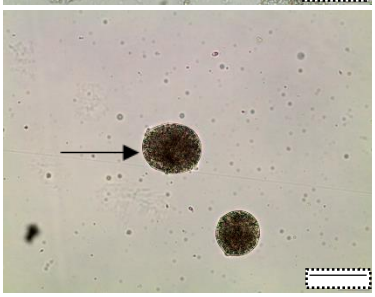 |
| III | 1:4<br>1:5<br>1:7<br>1:10 | No capsule formation. Formation of particles with flake-like morphology. | 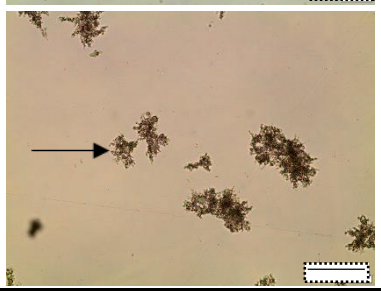 |

*Scale bars correspond to 100 µm

There are some other important characteristics of the proposed atomization process that must be considered and could help explain the differences in the most suitable ratio between gelatin and gum Arabic to achieve complex coacervation in comparison with the conventional batch stirring configuration. Firstly, in order to allow for adoption of a continuous regime processing in future studies, it was necessary to acidify the oil/gelatin emulsion and the gum Arabic solution before their contact, which occurs when the atomized emulsion droplets sink in the gum Arabic solution vessel. This early acidification step may lead to formation of intrapolymer complexes, mainly in gelatin, before the effective contact between the protein and the polysaccharide. The acidification kinetics, in turn, may affect the size and morphology of aggregates and coacervates due to different rates in intra/interpolymer complexation (GIRARD et al., 2004). In addition, in order to keep the viscosity of the liquid phases unaltered in all the assays, changes in the ratio gelatin:gum Arabic were made by increasing the amount of gum Arabic solution in the vessel (see item 2.4), instead of increasing the concentration of gum Arabic in the solution, which was kept fixed at 1 g of gum Arabic/100 g of solution. This strategy may have affected the fluid dynamic of the atomized emulsion droplets after submerging in the gum solution. Taking into account that complex coacervation is supposed to be a nucleation and growth type process (SANCHEZ; MEKHLOUFI; RENARD, 2006), the kinetic constraints of the process could explain the results presented in Table 3.3. Our hypothesis is that the early acidification of the gelatin could result in partial unfolding of the protein structure, exposing charged groups that could readily interact with other charged molecules in the vicinity. When the previously acidified emulsion is atomized over a small volume of gum Arabic solution, the possibility of gelatin-gelatin interactions between oppositely charged patches, in the same polymer-type molecules, may result in particle aggregation as observed in group I treatments (DE VRIES, 2004). On the other hand, the small flake-like particles observed in group III might be a result from the high dispersion of atomized emulsion droplets over a large volume of gum Arabic solution, which would hinder the growth of coacervate nuclei, as there were not enough gelatin molecules in the particle surface to interact with the gum Arabic available in solution. Thus, the range of gelatin:gum Arabic ratios included in group II seems to represent the most favourable balance between the operational parameters to achieve individual and spherical microcapsules by complex coacervation by atomization.

Several studies have shown a direct correlation between polymer ratio and complex coacervation pH (LI et al., 2018; LV et al., 2014; MA et al., 2019). Considering future applications of the capsules on investigation of targeted release in intestine conditions, the pH

for this study was 3.5. The capsules would have to endure gastric conditions, and studies have shown that the use of lower coacervation pH values potentialize gastric protection of the capsule, the core and intestine core release (HUANG et al., 2017b, 2017a).

*3.3.3 Characterization of wet microcapsules produced by atomization and batch stirring*

This section discusses the effects of variation in the concentration of gelatin in the emulsion (1 to 10 g of gelatin/ 100 g of emulsion) during complex coacervation induced by atomization, keeping the ratio gelatin:gum Arabic fixed at 1:1.8, and the results are compared with batch stirring coacervation. All the conditions investigated resulted in formation of microcapsules for both processing strategies, atomization and batch stirring (Figure 3.2). This is an indication that the ratio between the polymers may play a more important role on capsule formation than the emulsion concentration. Another important is that we assayed emulsions with gelatin concentration up to 10 g of gelatin/100 g of emulsion, with successful particle formation in both methods tested, atomization and batch stirring. This is an important achievement in order to increase the yield of microcapsules with less intensive use of water in the process.

The mean diameter of the capsules produced by the atomization method varied from 57 to 85 μm and, except for the most concentrated emulsion, they were slightly smaller than those of batch stirring (Table 3.4). The capsule size obtained is in agreement with the results of Alvim and Grosso (2010) whom obtained capsules of paprika oil by complex coacervation using gelatin and gum Arabic with diameters around of 52 μm. The variation coefficient (*VC*) for atomized particles ranged from 21 to 31 %. In the case of the most concentrated emulsions, the variation coefficient indicates that the atomization method produced particles with a wider size distribution than batch stirring. Nevertheless, it is important to highlight that all the assayed conditions produced microcapsules smaller than 100 μm, which is important for further application in food formulation in order to avoid a grainy mouthfeel (SHAHIDI; HAN, 1993; WYNN; PARIKH, 2013). The precipitate bulk density of capsules was higher for the atomization process, indicating that those capsules would have a higher sedimentation velocity than capsules produced by batch stirring. The precipitate bulk density for the atomization method varied from 1009 to 1022 $kg/m^3$, and a higher density may be an important factor considering that particle separation is done by sedimentation.

The capsules formed by batch stirring complex coacervation presented mean diameters ranging from 63 to 79 μm (Table 3.4). Different studies report different ranges of microcapsule size produced by batch stirring complex coacervation, such as 61 to 144 μm

(ROCHA-SELMI; FAVARO-TRINDADE; GROSSO, 2013), 97 to 690 μm (MARFIL et al., 2018), and 46 to 53 μm (ZUANON; MALACRIDA; TELIS, 2013). This indicates that the coacervation parameters have strong influence on the overall size of microcapsules. The *VC* of the microcapsules produced by batch stirring ranged from 19 to 26%, indicating uniformity of the capsules regarding their mean diameter (MORELLI; HOLDICH; DRAGOSAVAC, 2017). The precipitate bulk density of capsules produced by batch stirring was smaller varying from 1003 to 1014 kg/m$^3$ (Table 3.4).

The total solids in the supernatant solution after the complex coacervation process for both methods varied from 0.13 to 0.22%. The total solids in the supernatant solution increased with the increasing concentration of the ginger oil/gelatin emulsion. Nevertheless, all the values were similar and very low for both processes, which is an indication that the method applied to carry out the complex coacervation did not affect the effectiveness of the phase separation.

The microcapsules produced by both methods presented regular and mostly spherical morphology (Figure 3.2). For samples with lower gelatin concentration the capsules were closer together, whereas with increasing polymer concentration in the emulsion the capsules presented a more defined boundary. Also, the capsules produced by atomization seemed more individualized than the capsules produced by batch stirring. The authors believe that this could happen due to the nature of the droplet formation process: in atomization the droplets are individually formed in the nozzle, thus resulting in more separated capsules. In addition, as discussed in section 3.2, the early acidification of the gelatin/ginger oil emulsion that is necessary for coacervation by atomization, may promote the interaction between the positively charged gelatin amine groups with the gum Arabic's negatively charged carboxyl groups, resulting in capsules further apart. Otherwise, there were no major differences between the capsules produced by batch stirring and by atomization, and the microcapsules also had similar morphology to those presented in different studies of complex coacervation (ALVIM; GROSSO, 2010; LI et al., 2018; LV et al., 2014; SHADDEL et al., 2018; ZUANON; MALACRIDA; TELIS, 2013).

It is important to remark that this work is an initial step towards the development of a continuous process for complex coacervation, and future works should be carried out to optimize the atomization conditions in order to decrease the size distribution or even engineer the particle sizes. The sample 2GE/3.6GA in both coacervation methods produced the smallest microcapsules. In addition, except for the treatment 1GE/1.8GA, all the samples presented significantly different sizes between the processes, indicating that the process configuration may be a variable to be considered when engineering the size of microcapsules.

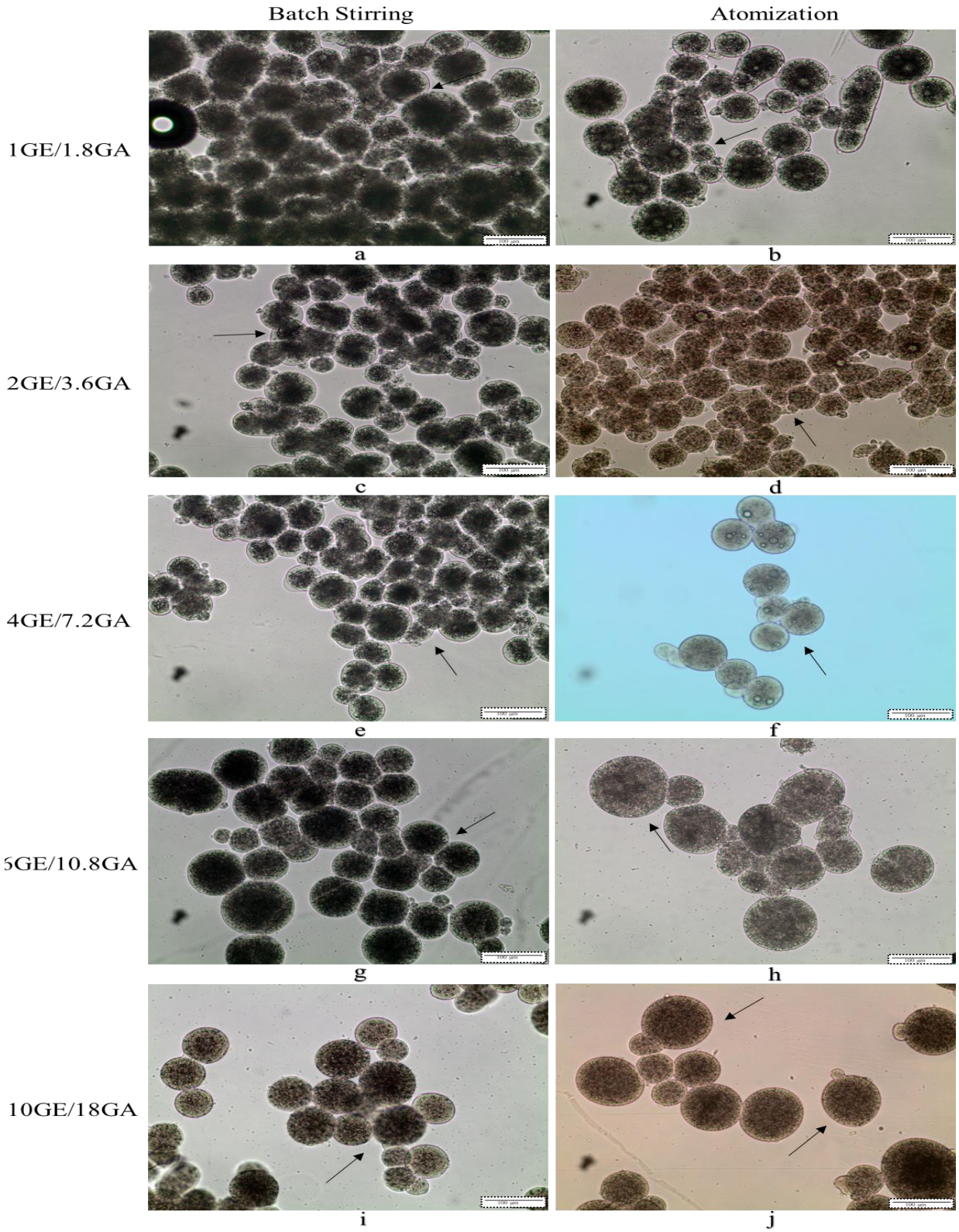


Figure 3.2. Optical microscopy morphology of wet microcapsules produced by atomization and batch stirring, keeping constant ratios of ginger oil:gelatin (1:1) and gelatin:gum Arabic (1:1.8), and using different concentrations of gelatin in the emulsion: (a), (b) 1 wt%; (c), (d) 2 wt%; (e), (f) 4 wt%; (g), (h) 6 wt%; (i), (j) 10 wt%. Scale bars correspond to 100 µm.

Table 3.4. Physicochemical properties of wet microcapsules produced by atomization and batch stirring. keeping constant ratios of ginger oil:gelatin (1:1) and gelatin:gum Arabic (1:1.8). and using different concentrations of gelatin in the emulsion.

| Sample code | Gelatin concentration | Ginger oil | Gum Arabic | Batch stirring | | | | Atomization | | | |
|---|---|---|---|---|---|---|---|---|---|---|---|
| | | | | Mean diameter[1] | VC | Total solids in supernatant[2] | Precipitate bulk density[2] | Mean diameter[1] | VC | Total solids in supernatant[2] | Precipitate bulk density[2] |
| | (g 100g$^{-1}$) | (g 100g$^{-1}$) | (g 100g$^{-1}$) | (µm) | (%) | (%) | (kg m$^{-3}$) | (µm) | (%) | (%) | (kg m$^{-3}$) |
| 1GE/1.8GA | 1 | 1 | 1.8 | 79.4$^{b}$ | 22.3 | 0.13±0.01 | 1003.6±0.24 | 77.3$^{bc}$ | 21.6 | 0.13±0.01 | 1009.8±0.4 |
| 2GE/3.6GA | 2 | 2 | 3.6 | 63.7$^{d}$ | 20.8 | 0.15±0.00 | 1010.6±0.68 | 57.1$^{e}$ | 20.1 | 0.15±0.01 | 1019.2±0.3 |
| 4GE/7.2GA | 4 | 4 | 7.2 | 74.9$^{c}$ | 25.4 | 0.18±0.00 | 1007.1±0.13 | 64.9$^{d}$ | 21.0 | 0.18±0.00 | 1015.0±0.6 |
| 6GE/10.8GA | 6 | 6 | 10.8 | 79.7$^{b}$ | 19.0 | 0.20±0.00 | 1012.7±0.32 | 61.90$^{d}$ | 31.0 | 0.19±0.00 | 1017.6±0.6 |
| 10GE/18GA | 10 | 10 | 18 | 79.5$^{b}$ | 24.4 | 0.22±0.00 | 1013.9±0.11 | 84.8$^{a}$ | 29.2 | 0.22±0.00 | 1022.1±0.1 |

[1]Mean values ± standard error (n = 300); [2]Mean values ± standard error (n = 3); [*]Different letters in superscript indicate significant differences (Tukey test. $p < 0.05$)

*3.3.4 Mathematical description of the atomization process and complex coacervation by atomization*

The possibility of engineering the size of the produced microcapsules with basis on the selection of the atomization parameters is a relevant task, thus in this section we discuss the possible correlations between the size distribution of the produced microcapsules and the operational conditions of the atomization process.

First, we will consider prediction of the emulsion droplet sizes leaving the atomization nozzle, given by Equation 3.5. According to this model, if the atomizing air velocity ($V_g$ = 106.6 m/s) is much greater than the emulsion velocity ($V_l$ = 0.64 m/s), the term $(V_g - V_l)$ becomes approximately equal to $V_g$. The Reynolds number for the atomization air stream is calculated as $Re_g=\rho_g V_g b_g/\mu_g$, in which $b_g$ is the air-layer thickness, given by $b_g=(D_{ext}-D_{int})/2$, with $D_{ex}$ and $D_{int}$ being the external and internal diameters of the air outlet channel, and $\mu_g$ is the atomization air viscosity. Upon rearranging Equation 3.5 using Equations 3.3 and 3.4, it is possible to estimate the Sauter mean diameter of the emulsion droplets produced by atomization in function of non-dimensional numbers (Equation 3.6), with the maximum difference between the estimated Sauter diameters using Equations 3.5 and 3.6 being smaller than 0.5%.

$$D'_{3,2} = 5.35 \times 10^5 \left(\frac{D_l^{\frac{3}{2}}\mu_g}{b_g\mu_l}\right)\left(\frac{OhRe_g}{We}\right) + 5.97 \times 10^5 \frac{Q_l}{Q_g}\left(Oh\sqrt{D_l}\right)^{0.45} \quad (3.6)$$

When analysing the Sauter mean diameter of the emulsion droplets in the atomization process and the experimental mean diameter of the microcapsules after complex coacervation (Figure 3.3), it is possible to observe that both had similar correlations with the treatments applied. The $D'_{3,2}$ and the experimental mean diameter values have a similar behaviour, except for the highest *We* number and lowest *Oh* number (1GE/1.8GA; *Oh* = 0.009). This demonstrates that the emulsion droplet sizes formed in the atomization nozzle affects the final diameter of the complex coacervated microcapsules. Considering that the atomization conditions (described mainly by the *We* number) were constant in all the assays, the emulsion formulation was the main factor causing the divergence of the trends between the experimental data and predictions of the hydrodynamic model. The *Oh* number is directly dependent on the properties of the liquid atomized, being directly correlated with the viscosity of the liquid (ALISEDA et al., 2008). Thus, hydrodynamic models such as Equations 3.5 or 3.6 may not be suitable to describe atomization process of emulsions with lower viscosity or lower *Oh* number. Nevertheless, a model expressed in function of non-dimensional numbers (Equation 3.6), that is able to predict the size of microcapsules, is an important result for future applications on scale up of the process.

The Weber number varied from 183 to 212, meaning that the emulsion droplets were formed by shear breakup of the air on the liquid interface (GUILDENBECHER; LÓPEZ-RIVERA; SOJKA, 2009). The variation of *We* values were due to changes in the formulation and not in the atomization parameters. Based on the results presented so far, it is possible to say that the hydrodynamic model (Equation 3.6) could be used to predict the final diameter of capsules when atomizing emulsions with $Oh > 0.01$. This hypothesis and the influence of the *We* number will be further studied in a future paper.

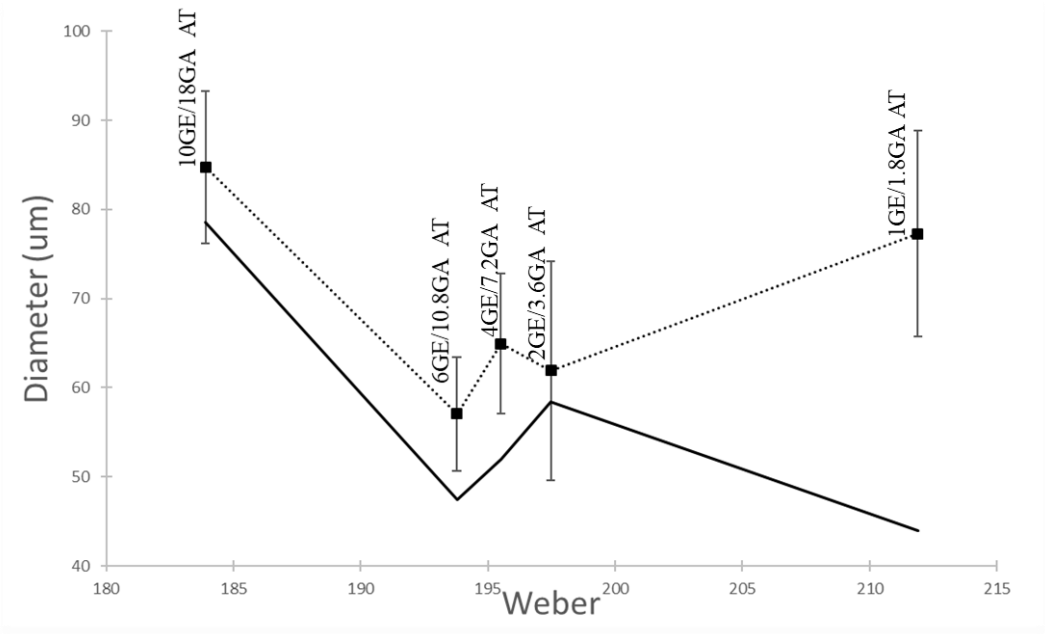


Figure 3.3. Experimental mean diameter (■) of wet microcapsules produced by atomization keeping constant ratios of ginger oil:gelatin (1:1) and gelatin:gum Arabic (1:1.8), with different concentrations of gelatin in the emulsion, and predicted Sauter mean diameter by Equation 3.6 (▬) in function of Weber number.

*3.3.5 Characterization of dried microcapsules produced by atomization and batch stirring*

Fourier transform infrared spectroscopy (FTIR) is a valuable technique to investigate the occurrence of chemical interactions or bonds between compounds, such as those expected in complex coacervation (LEMOS; MARIANO MARFIL; NICOLETTI, 2017; SANTOS et al., 2015b). The FTIR spectra of pure gelatin shows a peak of amide A around 3580 $s^{-1}$ and the same peak is not observed in the spectra of the capsules (Figure 3.4). Amide A has its band between 2300 and 3600 $s^{-1}$ (ANVARI; CHUNG, 2016), which leads to the conclusion that gelatine's amide A portion may be in part responsible for the interaction with the gum Arabic. The gum Arabic spectra presented the characteristic bond of –OH around 3350 $s^{-1}$ and the

stretching of -$COO^-$ at 1617 $s^{-1}$ (Figure 3.4). The peaks for amide B (3000 to 3100 $s^{-1}$) can be observed in pure gelatin and in lower intensity in all capsules around 3010 $s^{-1}$, indicating an interaction in this region (WANG et al., 2016). Amide I peak can be seen in around 1650 $s^{-1}$. This result is in accordance with Anvari and Chung (2016) that reported Amide I bond at 1630 $s^{-1}$ and Muyonga et al. (2004) that reported it between 1600 and 1700 $s^{-1}$. Amide II bonds can be seen around 1550 $s^{-1}$ and there is a decrease of this band on the capsules when compared to pure gelatin, which indicates that an interaction might be occurring between such functional groups in the molecules of gelatin and gum Arabic (GARCÍA-SALDAÑA et al., 2016; MUYONGA; COLE; DUODU, 2004). The spectra for the microcapsules presented a peak at 1450 $cm^{-1}$, which is indicative of successful electrostatic interaction between the amine group of gelatin with the free carboxylic from gum Arabic (SHADDEL et al., 2018). In general, the spectra of the microcapsules were similar, being possible to state that the capsules produced by atomization have a chemical signature similar to those produced by batch stirring, which is considered as the standard method for complex coacervation.

The morphology of the freeze-dried capsules was investigated by scanning electron microscopy. Within each coacervation method - atomization and batch stirring - there were no apparent differences detected in the micrographs. Therefore, in order to allow comparison between both treatments, the micrographs obtained for the sample 4GE/7.2GA, produced by batch stirring (Figure 3.5) and by atomization (Figure 3.6) are presented. The microcapsules produced by atomization seemed to be less aggregated, which was also observed in the dried powder. The microcapsules produced by batch stirring have a smooth surface (Figure 3.5c) whereas the microcapsules produced by atomization have bubbles or globules under the surface of the capsules (Figure 3.6c). The authors attribute these structures to oil droplets close to the capsule surface, trapped within the matrix. When the emulsion goes through the nozzle, it suffers shear forces caused by the atomization air, which may change the emulsion microstructure, creating a more heterogeneous distribution of the oil droplets inside the atomized particle. In addition, no porosity was observed on the SEM images, indicating high encapsulation efficiency of the core material (JIANG et al., 2013). The fact that there were not major differences between the capsules produced by the different methods, except for the small globules under the surface, is positive, confirming that complex coacervation by atomization generates capsules with similar morphology to those obtained by the traditional method of batch stirring complex coacervation.

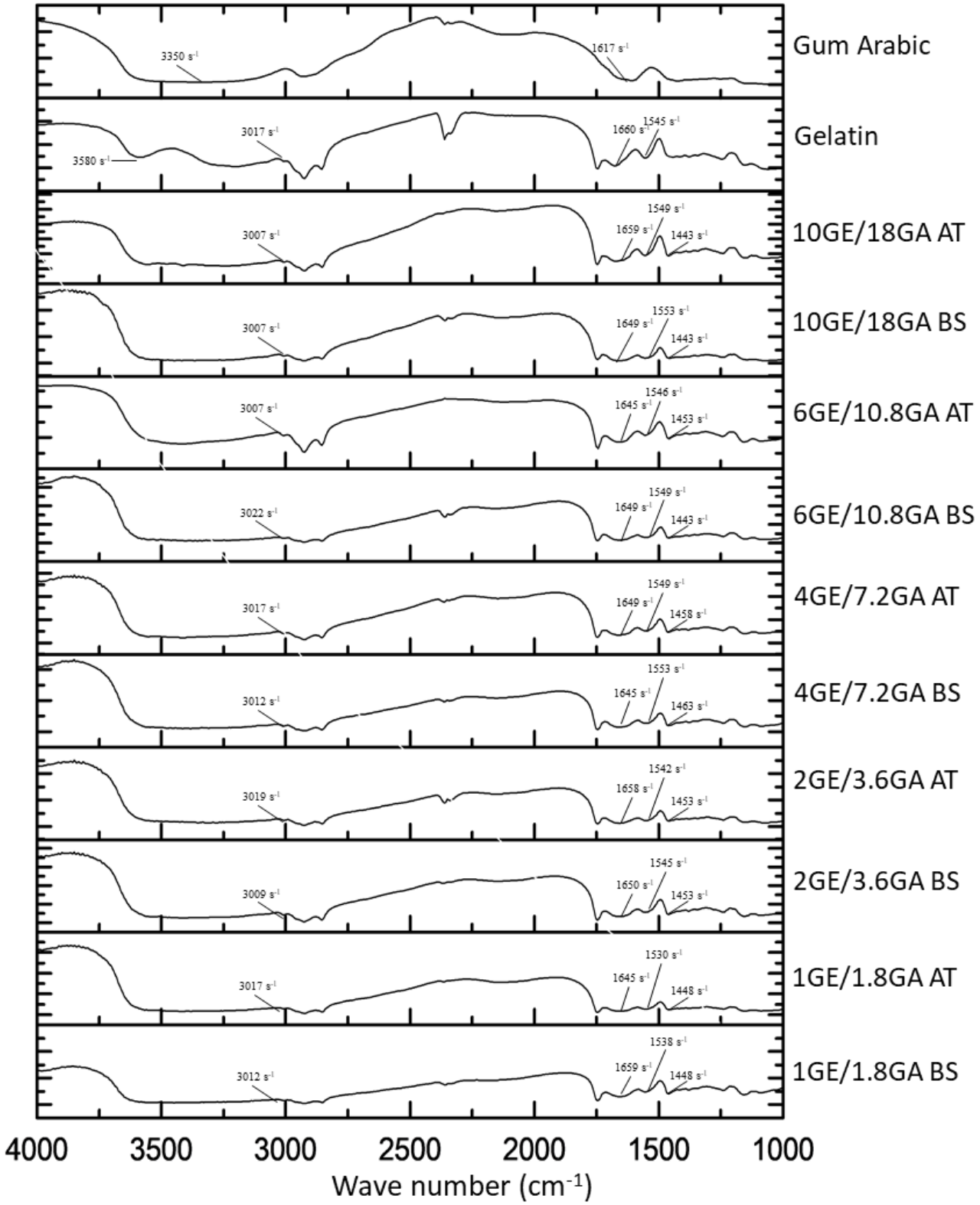


Figure 3.4. Infrared spectra of wall materials and microcapsules produced by atomization (AT) and batch stirring (BS) keeping constant ratios of ginger oil:gelatin (1:1) and gelatin:gum Arabic (1:1.8), with different concentrations of gelatin in the emulsion.

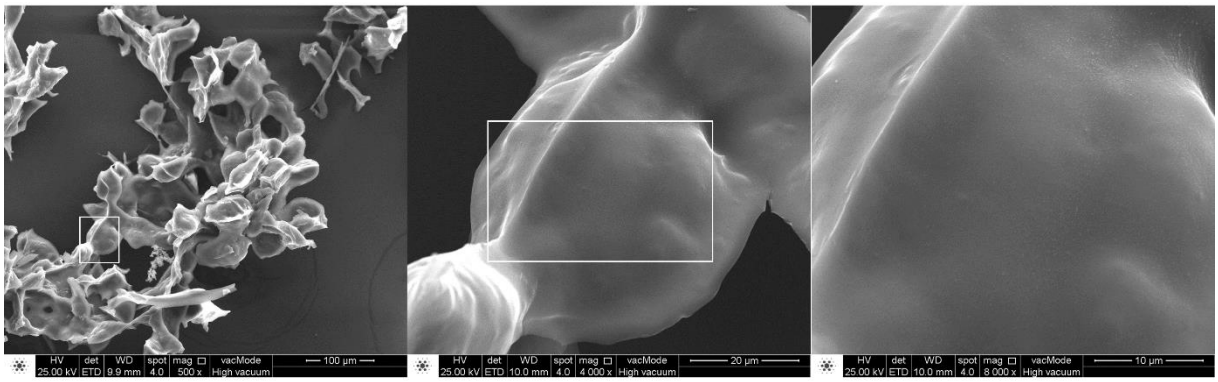


a b c

Figure 3.5. Scanning electron micrographs showing morphology of the capsules produced by batch stirring complex coacervation of sample 4GE/7.2GA at magnifications of: (a) 500×; (b) 4000×; (c) 8000×.

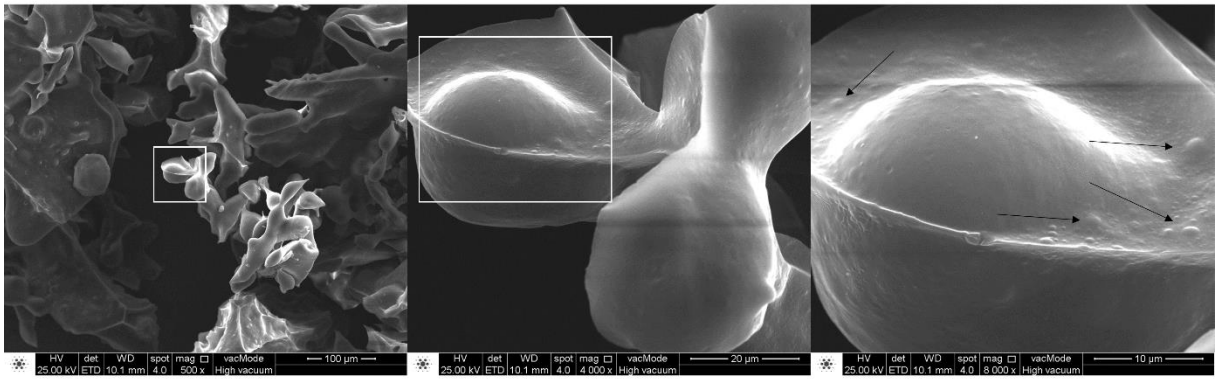


a b c

Figure 3.6. Scanning electron micrographs showing morphology of the microcapsules produced by atomization complex coacervation of sample 4GE/7.2GA at magnifications of: (a) 500×; (b) 4000×; (c) 8000×

The encapsulation efficiency (*EE*) and encapsulation yield (*EY*) are presented in Table 3.5 and should be taken into consideration in order to determine the efficiency of the microencapsulation process (ERATTE et al., 2014). For all the formulation tested along with method of complex coacervation, the values of *EE* varied from 89.7 to 98.7% (Table 3.5). Alvim and Grosso (2010) obtained similar results while studying the application of crosslinking agents in microencapsulation by complex coacervation. Zuanon et al. (2013) reported an *EE* in the range of 49.4 to 72.5%, while microencapsulating turmeric oleoresin with gelatin and gum Arabic. Moser et al. (2019) obtained an *EE* of 82 to 91% in a study about the influence of spray drying parameters on the microencapsulation of buriti oil by chickpea protein/pectin electrostatic interaction. The high values of *EE* obtained for complex coacervation by atomization in the present study, are evidence of its potential for microencapsulation. The *EY* for microcapsules produced by batch stirring ranged from 21.5 to 64.6% (Table 3.5), and the

sample 1GE/1.8GA showed the highest encapsulation yield for this method. Wang et al. (2016) studied the influence of pH, mass ratio, polymer concentration and core to wall material ratio, on batch stirring complex coacervation of gelatin and sodium alginate to encapsulate ginger oil, and reported *EY* varying from 40 to 70%. On the other hand, the *EY* of microcapsules produced by atomization varied from 67.3 to 88.7%, being significantly higher than those produced by batch stirring with the same formulation, with the exception of samples with lower gelatin concentration (1GE/1.8GA and 2GE/3.6GA) that presented no significant difference. This indicates that emulsion with gelatin concentration higher than 2 % (w/w) endure better the shear forces during the atomization step, entrapping the oil and resulting in higher *EY*. The higher *EY* observed for atomized microcapsules may be due to the spray process, by which the emulsion droplets come in contact with the gum Arabic solution in a spherical shape previously defined by the atomization process. Thus, it is expected that the adsorption of gum Arabic around the droplet of atomized emulsion may start faster than in batch stirring, which would prevent oil leaking from the stabilizing protein layer and ensuring high encapsulation yield properties. Various values of *EY* have been reported using ginger oil and spray drying: Ban et al. (2020) reported *EY* values of 55 to 89%, Ferreira et al. (2019) reported *EY* values of 3 to 77% and Maulidna et al. (2020) obtained *EY* values from 60 to 72%. Therefore, it could be inferred that the combination of high encapsulation efficiency with the superior encapsulation yield in microcapsules produced by atomization, is a promising result.

We correlated *EY* with the experimental mean diameter for microcapsules produced by both methods (Figure 3.7) and observed that the encapsulation yield for capsules produced by batch stirring tends to decrease with the increase in mean diameter. The relationship between capsule size and *EY* can be attributed to the total surface area of the system, that increases with decreasing capsule size, thus promoting higher *EY* (ZUANON et al., 2019). The same correlation was observed for the capsules produced by atomization, although with a much lower effect. This may be related to the shear forces that the emulsion goes through during the atomization process, which causes a second homogenization at the atomization nozzle, counterbalancing the effect of the total surface area, providing high values of *EY* even for larger capsules.

Table 3.5. Encapsulation efficiency (*EE*), encapsulation yield (*EY*), and water content of dried microcapsules produced by atomization and batch stirring complex coacervation.

| Sample code | Batch stirring | | | Atomization | | |
|---|---|---|---|---|---|---|
| | EE[1] (%) | EY[1] (%) | Water content[1] (g/100 g, wb) | EE[1] (%) | EY[1] (%) | Water content[1] (g/100 g, wb) |
| 1GE/1.8GA | 94.4±1.4$^{abc}$ | 64.6±9.8$^{\alpha\beta}$ | 2.20±0.01 | 94.3±0.5$^{abc}$ | 80.9±1.6$^{\alpha\beta}$ | 2.13±0.00 |
| 2GE/3.6GA | 93.5±1.7$^{abc}$ | 55.2±7.9$^{\beta\varphi}$ | 3.00±0.03 | 91.5±0.8$^{bc}$ | 83.3±2.5$^{\alpha\beta}$ | 2.71±0.01 |
| 4GE/7.2GA | 89.7±1.2$^{c}$ | 31.2±5.3$^{\varphi\varepsilon}$ | 1.61±0.00 | 96.1±0.0$^{abc}$ | 78.1±2.9$^{\alpha\beta}$ | 2.65±0.01 |
| 6GE/10.8GA | 94.2±2.2$^{abc}$ | 21.5±4.4$^{\varepsilon}$ | 2.51±0.01 | 97.3±0.1$^{ab}$ | 88.7±0.7$^{\alpha}$ | 2.92±0.02 |
| 10GE/18GA | 95.5±2.0$^{abc}$ | 27.2±6.9$^{\varphi\varepsilon}$ | 3.00±0.02 | 98.7±0.1$^{a}$ | 67.3±4.2$^{\alpha\beta}$ | 3.15±0.02 |

[1]Mean values ± standard error (n = 3); [*]Different letters (*EE*) or symbols (*EY*) in superscript indicate significant differences (Tukey test, $p < 0.05$); wb: wet basis

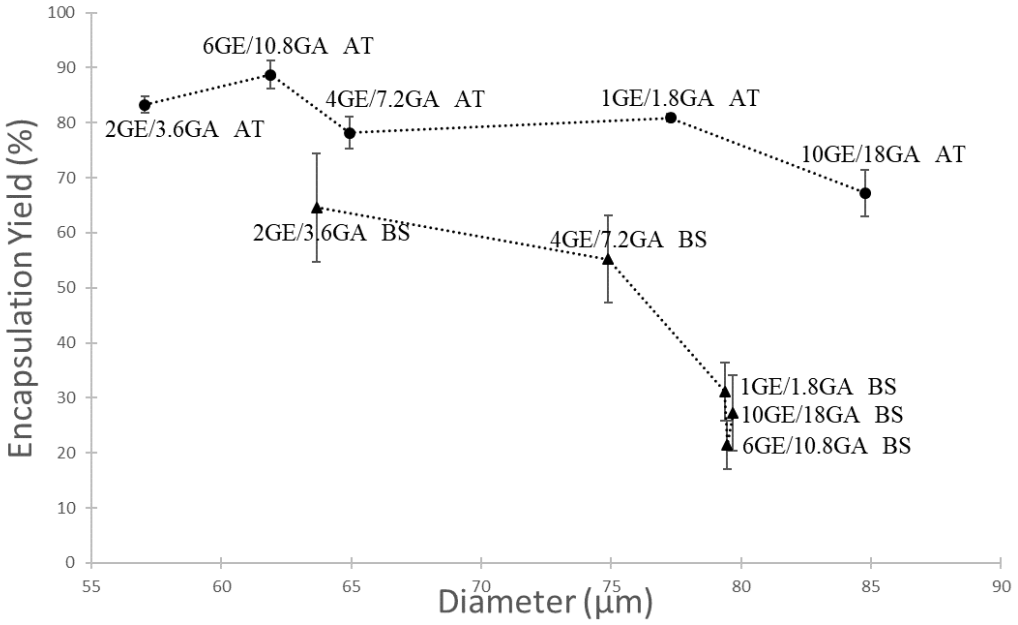


Figure 3.7. Encapsulation yield (*EY*) of the dried capsules produced by atomization (●) and batch stirring (▲), in function of the experimental mean diameter of wet microcapsules.

### 3.4. Conclusions

We proposed a process configuration that demonstrated to be feasible for producing microcapsules of ginger oil by complex coacervation in gelatin/gum Arabic by atomization, representing an initial step towards the development of a process that can be performed in a continuous regime. The ratio between the polymers used for complex coacervation had a strong influence on the formation and morphology of microcapsules by atomization. The increase of gelatin concentration on the atomization process, did not affect the encapsulation parameters.

FTIR and SEM analyses revealed that microcapsules produced by batch stirring and by atomization had similar morphology and chemical signature. As it was expected for the complex coacervation technique, encapsulation efficiency was higher than 89% with no differences between samples coacervated by batch stirring and by atomization. On the other hand, the microcapsules produced by atomization presented significantly ($p < 0.05$) higher encapsulation yield than batch stirring. The final diameter of the microcapsules could be well correlated with an empirical hydrodynamic model to predict the Sauter mean diameter of atomized emulsion droplets for Ohnesorge numbers higher than 0.01. Hence the use of atomization for complex coacervation showed potential for microencapsulation of ginger oil, representing a step forward towards complex coacervation in continuous process.

**Acknowledgements**

The authors thank: The Central for analytical chemistry from the Federal University of Maranhão – UFMA, for supporting with FTIR analysis; Dr. Marijana Dragosavac from the Chemical Engineering department of the Loughborough University – UK, for proof reading the article, Adiella Abelseth for proof reading with a focus on the English language of the article and Isabella Serpa Villas Boas for assistance during the experiments.

This work was supported by the São Paulo Research Foundation - FAPESP (grant numbers 2015/23290-0 and 2018/16976-0) and National Council for Scientific and Technological Development - CNPq (grant number 479822/2009-3).

| Symbol | Definition |
|---|---|
| $We$ | Weber number |
| $Oh$ | Ohnesorge number |
| $D_l$ | Diameter of emulsion outlet |
| $D_{int}$ | Internal diameter of air outlet |
| $D_{ext}$ | External diameter of air outlet |
| $D_{32}$ | Sauter mean diameter - Equation 3.5 |
| $D`_{32}$ | Sauter mean diameter in function of atomization non dimensional numbers - Equation 3.6 |
| $V_g$ | Atomization air`s velocity |
| $V_l$ | Emulsion`s velocity |
| $Q_g$ | Atomization air volumetric flow rate |
| $Q_l$ | Emulsion volumetric flow rate |
| $\mu_l$ | Emulsion`s apparent viscosity |
| $\mu_g$ | Atomization air`s viscosity |
| $\rho_g$ | Atomization air`s density |
| $\sigma$ | Emulsion's surface tension |
| $\rho_l$ | Emulsion`s density |
| $Re_g$ | Atomization air`s Reynolds number |
| $b_g$ | Atomization air layer thickness |
| $EE$ | Encapsulation Efficiency |
| $EY$ | Encapsulation yield |
| $OS$ | Capsule surface`s oil |
| $OT$ | Capsule total oil |

# CHAPTER 4 - COMPLEX COACERVATION ASSISTED BY A TWO-FLUID NOZZLE FOR MICROENCAPSULATION OF GINGER OIL: EFFECT OF ATOMIZATION PARAMETERS

Sungil Ferreira[1]*, Vania Regina Nicoletti[1]

[1]São Paulo State University (UNESP), Department of Food Engineering and Technology, São Jose do Rio Preto – SP, 15054-000, Brazil

Published in the Food Research International, Volume 138, Part B, 109828.

https://doi.org/10.1016/j.foodres.2020.109828

Abstract

This study investigates the influence of the atomization parameters on complex coacervation by atomization, and is following a preceding study that presented the technique and investigated the effects of formulation. Complex coacervated capsules were produced by atomization, using emulsions with 1 and 6 %(w/w) of gelatin and ginger oil atomized over a 1 %(w/w) solution of gum Arabic, at constant polymer ratio of 1:2 (gelatin:gum Arabic) at pH 3.5. The air velocity at the nozzle varied from 72 to 168 m/s and the emulsion velocity at the nozzle varied from 0.4 to 0.6 m/s, maintaining the air to liquid velocity ratio at 170, 220 and 270. The mean diameter of the microcapsules produced varied from 52 to 75 μm and no crosslinking agents were used. The influence of atomization numbers Weber (*We*) and Ohnesorge (*Oh*), shear rate and shear stress on the encapsulation performance was carried out and a proposed model was able to predict the final size of the microcapsules produced at $We \geq 180$ and $Oh = 0.063$. Encapsulation efficiency varied from 9 to 95 %, and encapsulation yield varied from 50 to 99 %. Finally, optimum conditions based on size prediction and microencapsulation parameters were proposed.

Keywords: Weber number, Ohnesorge number, particle size, encapsulation efficiency, encapsulation yield, gelatin, gum Arabic.

## 4.1. Introduction

Microencapsulation is an innovative technique that is intended to help tackle the increasing demand on value added products for food and pharmaceutical industries (PAULO; SANTOS, 2017). These industries have a growing interest in techniques to produce functional products with nutritional quality, safety, and improved shelf-life that can offer health benefits (CORRÊA-FILHO; MOLDÃO-MARTINS; ALVES, 2019). One of the core materials of interest to be microencapsulated is ginger oil, in which microencapsulation can be applied to increase the stability of its antioxidant and antimicrobial compounds (FERNANDES et al., 2016).

Microencapsulation by complex coacervation is an elegant solution to protect materials that are sensitive to high temperatures and to encapsulate hydrophobic substances, while providing high values of encapsulation efficiency (ALVIM; GROSSO, 2010; HECKERT BASTOS et al., 2020). During complex coacervation, ionic interactions between oppositely charged polymers cause aggregation of the polymer molecules and phase separation. If the core material chosen to be encapsulated is hydrophobic, an emulsion may be formed with one or both of the encapsulating polymers (TIMILSENA et al., 2019; ZUANON; MALACRIDA; TELIS, 2013). Gelatin and gum Arabic are among the most used pair for complex coacervation, mainly due to their, emulsifying properties, electrochemical compatibly and because they are able to form spherical shaped coacervated capsules (PRATA et al., 2008). Once the complex coacervated capsules are formed, they tend to behave like the hydrogels that they originated from, with size varying from 30 to 500 μm, depending on the formulation and complex coacervation conditions (GONÇALVES et al., 2018; KRALOVEC et al., 2012).

Providing mathematical descriptions of microencapsulation processes by complex coacervation is an important step towards the development of a continuous process, considering the reproducibility of results and paving the way for scale up (JEGAT; TAVERDET, 2000; LEMETTER; MEEUSE; ZUIDAM, 2009). A limited number of previous works described quantitative process variables for complex coacervation. Ma et al. (2019) investigated the influence of polymer concentration, polymer ratio, core to polymer ratio, stirring speed and coacervation pH on morphology and oxidative stability of lipid capsules formed by complex coacervation. Lemos, Marfil, and Nicoletti (2017) evaluated the effects of stirring speed on gelatin-sodium alginate complex coacervation by batch stirring. Dobetti and Pantaleo (2002) studied the influence of hydrodynamic conditions on the morphology and size of capsules for encapsulation of water-soluble drugs in cellulose acetate phthalate. All these studies showed a

correlation between the stirring speed and the fluids' physical properties with the size and morphology of the produced microcapsules.

One novel approach to induce complex coacervation is using a two-fluid nozzle (FERREIRA; NICOLETTI, 2021). By atomizing an oil-in-water emulsion stabilized by gelatin over a vessel containing aqueous gum Arabic solution, both solutions with pH below gelatin pI, complex coacervation between the polymers occurs, encapsulating the oil droplets. One important characteristic of this coacervation design is that it allows operation as a continuous process. In this configuration, formation of the back bone of the final microcapsules resides on the atomization process, by which the emulsion droplets are individually formed due to the shear forces exerted by the atomization air on the emulsion when using a two-fluid nozzle (KEMP et al., 2013; MANSOUR; CHIGIER, 1995). Complex coacervation occurs as the emulsion droplets flow through the gum Arabic solution, and that is the reason why understanding the quantitative and qualitative effects of the atomization process on microcapsules' size and on the encapsulation parameters is crucial to improving the overall process performance.

The influence of atomization parameters on distinct microencapsulation processes has been studied by different approaches, mainly due to it representing a flexible and economical technology to transform liquid solutions into solid particles/capsules. Ferreira et al. (2019) evaluated the influence of atomization parameters on microencapsulation of turmeric oleoresin by spray drying, using gelatin and maltodextrin as wall material. Zuanon et al. (2019) reported that higher values of atomization airflow generated smaller liquid droplets, potentializing the drying/encapsulation process. Moser, Ferreira and Nicoletti (2019) encapsulated buriti oil in chickpea protein-pectin matrix by spray drying and studied the influence of airflow on the carotenoid retention and process yield. Jiang et al. (2013) combined complex coacervation and drying into one step using a novel three-fluid nozzle to encapsulate α-amylase. Kašpar, Jakubec and Štěpánek (2013), using a three-fluid nozzle, produced crosslinked chitosan particles by spray drying. Chen et al. (2006) explored the release behaviour and morphology of particles produced using acetaminophen, chitosan and hydroxypropyl-methylcellulose formed by a 4-fluid nozzle spray dryer. Also using a 4-fluid nozzle, Ozeki et al. (2005) produced microparticles of water-insoluble and water-soluble drugs, and doing so, improved water solubility of the particles.

An effective way to describe the atomization process is the use of non-dimensional numbers Weber (*We*) and Ohnesorge (*Oh*). *Oh* number relates the viscous forces with the surface tension forces in the solution, whereas *We* correlates the inertial and surface tensional

components of the resultant force during atomization. When $Oh \leq 0.1$, it is assumed that only *We* interferes on the atomization process, and for $0.1 < Oh < 1$ both *We* and *Oh* will affect the atomization process (GUILDENBECHER; LÓPEZ-RIVERA; SOJKA, 2009). In addition, different ranges of *We* results in different regimes of atomization: at $12 < We < 80$ a bag-type liquid's breakup occurs, at $80 < We < 350$ an air-shear breakup occurs, and at $We > 350$, a catastrophic liquid's breakup will be present (VARGA; LASHERAS; HOPFINGER, 2003). In a former study (FERREIRA; NICOLETTI, 2021), our group rewrote a hydrodynamic model presented by Filková, Huang and Mujumdar (2014) in terms of *We* and *Oh*, with the purpose of predicting the size of microcapsules formed by complex coacervation by atomization, using a two-fluid nozzle. A similar approach was adopted by Thybo et al. (2008), to estimate the size of atomized droplets for spray-dryer scale up.

The aim of this work was to study the influence of atomization parameters (air and liquid flow) and emulsion formulation, both expressed as different values of *We* and *Oh* numbers, on the size and encapsulation performance of microcapsules produced by complex coacervation using a two-fluid nozzle. A mathematical description of the atomization and encapsulation process was proposed in function of *We*, shear rate and shear stress at the nozzle. Finally, a mathematical model was proposed to predict the size of the microcapsules after coacervation, in function of the atomization parameters. This study complements a previous work (FERREIRA; NICOLETTI, 2021), in which the effect of polymer ratio and emulsion concentration was evaluated.

## 4.2. Material and methods

### *4.2.1 Materials*

Cold pressed ginger oil (Gran Oils, São Paulo, Brazil) was microencapsulated using type B gelatin, 240 bloom (Gelita, Mococa, Brazil) and gum Arabic (Dinâmica, Campinas, Brazil) as wall materials. The analytical-grade reactants glacial acetic acid (Dinâmica, Campinas, Brazil), hydrochloric acid (Dinâmica, Campinas, Brazil), and hexane (Dinâmica, Campinas, Brazil) were used in the production and analyses of microcapsules.

### *4.2.2 Preparation of ginger oil emulsion and gum Arabic solution*

Before atomization, ginger oil was dispersed in aqueous gelatin solution at mass ratio oil:gelatin of 1:1, forming primary O/W emulsions. Emulsions containing 1 and 6 g gelatin/100 g of emulsion were tested. Emulsification was performed by high-shear homogenization in Ultra Turrax T-25 (IKA, Germany) at 15000 rpm for 2 min, followed by ultrasound

homogenization using Sonic Ruptor 4000 ultrasonic probe (Omni International, USA) at 20 kHz and nominal power of 210 *W* continuously for 3 minutes.

The solution of gum Arabic (1 g/100 g) was prepared by gum addition to preheated deionized water (50 °C) under magnetic stirring until complete dissolution.

*4.2.3 Complex coacervation by atomization*

Complex coacervation by atomization was achieved following the procedure previously described by Ferreira and Nicoletti (2021). The ginger oil/gelatin emulsion was atomised over the aqueous solution of gum Arabic, both solutions with pH previously adjusted to 3.5, using a two-fluid nozzle (0.7 *mm* diameter, Labmaq, Brazil), with controlled airflow and emulsion feed flow adjusted to conditions described in item 2.6. The nozzle dimensions and atomization air physical properties are presented in Table 4.1.

Table 4.1. Physical properties of atomization air and dimensions of the atomization nozzle.

| **Characteristics of the two fluids nozzle** | |
|---|---|
| Diameter of emulsion outlet ($D_l$) - (m) | $7.00\times10^{-04}$ |
| Internal diameter of air outlet ($D_{int}$) - (m) | $1.90\times10^{-03}$ |
| External diameter of air outlet ($D_{ext}$) - (m) | $2.80\times10^{-03}$ |
| Emulsion outlet area - ($m^2$) | $3.85\times10^{-07}$ |
| Atomization air outlet area - ($m^2$) | $3.32\times10^{-06}$ |
| **Physical properties of the atomization air (25 ºC)** | |
| Density ($\rho_g$) - ($kg/m^3$) | 1.23 |
| Viscosity ($\mu_g$) - (Pa s) | $1.80\times10^{-05}$ |

The nozzle was initially positioned at a fixed height of 0.2 m above the vessel containing gum Arabic solution. Airflow was controlled using a rotameter FT074-02-CA-VN (Omega, Stamford, USA) as described in Figure 4.1. At the end of the complex coacervation process the system was immersed in ice bath until attaining (10 ± 1) °C. After 24 hours, the particles were transferred to aluminium trays and frozen in ultra-freezer (Liobrás, FV 500, Brazil) at -40 °C and freeze-dried (Liobrás, L101, Brazil) for 72 hours. The samples were then ground, packed in aluminium foil for light protection and stored in desiccator with silica gel for further testing.

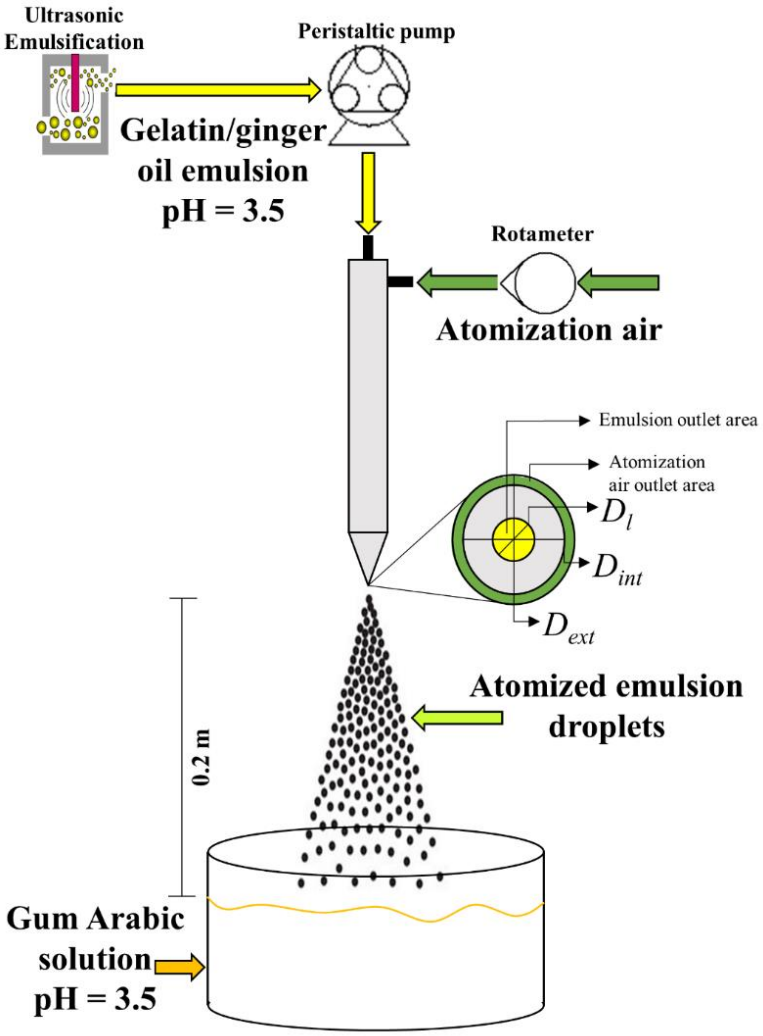


Figure 4.1. Design for atomization of the gelatin/ginger oil emulsion over the gum Arabic solution for microencapsulation by complex coacervation.

*4.2.4 Optical microscopy analysis*

The microstructure and size of wet capsules were evaluated in optical microscope (CX31-III, Olympus, Japan) coupled with a video camera (SIS-SC30). Samples were deposited over glass slides without dilution. The scanned images (2048×1532 pixels, 4×-optical magnification) were analysed by Image Pro Plus 6.0 software (Media Cybernetics Inc., USA) using the three-point circle function for measuring the size of each individual capsule, taking the average diameter of 500 microcapsules per sample (*d*).

*4.2.5 Microencapsulation performance*

Microencapsulation parameters were determined as described by Tonon, Grosso and Hubinger (2011) and by Wang, Adhikari and Barrow (2014) with modifications. Encapsulation efficiency (*EE*) and encapsulation yield (*EY*) were determined in freeze-dried microcapsules, based on the oil content initially present in the emulsion (*OI*), oil present on the surface of microcapsules (*OS*), and total oil present in the microcapsules (*OT*). To determine *OS*, 100 mg of microcapsules and 10 mL of hexane were added to a capped test tube and shaken for one minute. The organic phase was filtered, transferred to Petri dishes, and the solvent was evaporated first at room temperature in a hood, and finally in an oven at 60 °C until constant weight. To determine *OT*, 100 mg of microcapsules were dispersed in 20 mL of 4N hydrochloric acid solution and shaken for 1 hour at 35 °C for dissolution of the wall material. Then, 13 mL of hexane were added and stirred for 10 hours at 25 °C, forming a two-phase system. The non-organic and organic phases were separated by centrifuging (model Z 326 K, Hermle, Germany) at 10000×g for 30 minutes and the organic phase was transferred to Petri dishes. The solvent was evaporated first at room temperature in a hood and finally in an oven at 60 °C, until constant weight (FERREIRA; NICOLETTI, 2021). The *EE* and *EY* were calculated by Equations 4.1 and 4.2, respectively.

$$EE(\%) = \frac{OT - OS}{OT} \times 100 \quad (4.1)$$

$$EY(\%) = \frac{OT}{OI} \times 100 \quad (4.2)$$

*4.2.6 Mathematical description of the atomization process*

The atomization process was described by means of non-dimensional numbers: Weber (*We*, Equation 4.3), Ohnesorge (*Oh*, Equation 4.4), Reynolds number for atomization air ($Re_g$, Equation 4.5), and Emulsion's Reynolds number at the nozzle ($Re_n$, Equation 4.6). Equation 4.7 (FERREIRA; NICOLETTI, 2021) is a hydrodynamic model to predict the size of atomized emulsion droplets ($D'_{3,2}$) after leaving the nozzle in function of atomization non-dimensional numbers , whereas Equation 4.8 describes the velocity of the emulsion waves ($V_w$) leaving the nozzle (FILKOVÁ; HUANG; MUJUMDAR, 2014; GUILDENBECHER; LÓPEZ-RIVERA; SOJKA, 2009; VARGA; LASHERAS; HOPFINGER, 2003).

$$We = \frac{\rho_g (V_g - V_l)^2 D_l}{\sigma} \quad (4.3)$$

$$Oh = \frac{\mu_l}{\sqrt{\sigma D_l \rho_l}} \quad (4.4)$$

$$Re_g = \frac{\rho_g V_g b_g}{\mu_g} \quad (4.5)$$

$$Re_n = \frac{\rho_l V_w l_w}{\mu_l} \quad (4.6)$$

$$D'_{3,2} = 5.35 \times 10^5 \left(\frac{D_l^{3/2} \mu_g}{b_g \mu_l}\right)\left(\frac{OhRe_g}{We}\right) + 5.97 \times 10^5 \frac{Q_l}{Q_g}\left(Oh\sqrt{D_l}\right)^{0.45} \quad (4.7)$$

$$V_w = \left(\frac{\sqrt{\rho_l} V_l + \sqrt{\rho_g} V_g}{\sqrt{\rho_l} + \sqrt{\rho_g}}\right) \quad (4.8)$$

In which $Q_l$ and $Q_g$ are the volumetric flows of emulsion and air, respectively; $V_g$ is the atomization air velocity; $V_l$ is the emulsion velocity; $\rho_g$ is the density of atomization air; $D_l$ is the diameter of the nozzle's discharge orifice; $\sigma$ is the emulsion surface tension; $\mu_l$ is the emulsion apparent viscosity; $\rho_l$ is the emulsion density; the parameter $b_g$ is the thickness of the air layer, being equal to 0.45 mm; $\mu_g$ is the atomization air viscosity; $l_w = \frac{2\,C\,b_g\sqrt{\rho_l}}{\rho_g\sqrt{Re_g}}$ is the emulsion wavelength caused by the atomization air leaving the nozzle; $C$ is a constant (1.2) inherent to the coaxial two-fluid nozzle (MARMOTTANT; VILLERMAUX, 2002; VARGA; LASHERAS; HOPFINGER, 2003).

The atomization parameters (Table 4.2) were defined based on the equipment available in the facility and in order to guarantee that air velocity was much greater than emulsion velocity, making sure that the process would occur at the high-speed air stream regime (VARGA et al., 2003). The air and emulsion velocity were calculated using the information in Tables 4.1 and 4.2 and knowing that $V = Q/A$, where $V$ is the velocity, $Q$ the volumetric flow and $A$ flowing area, for atomization air and emulsion both at the nozzle (MUNSON et al., 2013).

Table 4.2. Atomization conditions for complex coacervation assays.

| Sample Code* | Emulsion composition | *Oh* | Atomization condition | | | |
|---|---|---|---|---|---|---|
| | | | **Emulsion flow (*ml/min*)** | **Air flow ($m^3/s$) $\times 10^4$** | $V_g/V_l$ | *We* |
| G1-AC1 | Gelatin:oil ratio 1:1 1 g gelatin/100 g | 0.009 | 9.8 | 2.36 | 170 | 94 |
| G1-AC2 | | | 8.8 | 2.75 | 220 | 129 |
| G1-AC3 | | | 8.2 | 3.15 | 270 | 168 |
| G1-AC4 | | | 14.7 | 3.54 | 170 | 212 |
| G1-AC5 | | | 12.6 | 3.93 | 220 | 262 |
| G1-AC6 | | | 11.3 | 4.33 | 270 | 318 |
| G1-AC7 | | | 19.6 | 4.72 | 170 | 377 |
| G1-AC8 | | | 16.4 | 5.11 | 220 | 443 |
| G1-AC9 | | | 14.4 | 5.51 | 270 | 515 |
| G6-AC1 | Gelatin:oil ratio 1:1 6 g gelatin/100 g | 0.063 | 9.8 | 2.36 | 170 | 88 |
| G6-AC2 | | | 8.8 | 2.75 | 220 | 120 |
| G6-AC3 | | | 8.2 | 3.15 | 270 | 157 |
| G6-AC4 | | | 14.7 | 3.54 | 170 | 197 |
| G6-AC5 | | | 12.6 | 3.93 | 220 | 244 |
| G6-AC6 | | | 11.3 | 4.33 | 270 | 296 |
| G6-AC7 | | | 19.6 | 4.72 | 170 | 351 |
| G6-AC8 | | | 16.4 | 5.11 | 220 | 413 |
| G6-AC9 | | | 14.4 | 5.51 | 270 | 480 |

*The number following letter G indicate gelatin concentration and the number following letters AC refers to atomization condition

*4.2.7 Statistical analysis*

All the tests were performed in repetition in order to guarantee robust results. For the microencapsulation parameters the assays were performed in triplicate. The results of analytical determinations are expressed in arithmetic average (*AV*) submitted to analysis of variance (ANOVA) and comparison of means by Tukey test with probability level at 5% ($p \leq 0.05$), using statistical software Minitab 17 (MINITAB, State College - PA, USA) (FERREIRA; MALACRIDA; TELIS, 2016). The uniformity of data (size distribution) was evaluated through the coefficient of variation [$CV = (SD/AV)*100$], in which *SD* stands for standard deviation (MORELLI; HOLDICH; DRAGOSAVAC, 2017). The model to predict final diameter of microcapsules as a function of atomization parameters was determined by non-linear regression using Gauss-Newton algorithm, with 200 maximum iterations, tolerance of 0.00001 and significance level of 95% (GRATTON; LAWLESS; NICHOLS, 2007; MANSOURKHAKI; HAGHIRI; BERANGI, 2018).

## 4.3. Results and discussion

### *4.3.1 Effects of atomization conditions on the size of wet microcapsules*

The major goal of this work was investigating the effect of atomization parameters on the size distribution and microencapsulation performance, as expressed by encapsulation efficiency and encapsulation yield in the complex-coacervated microcapsules. The size and size distribution of microcapsules is of great relevance, as it affects one of the major functional properties of this type of system, which is the release profile of the encapsulated material (CANAPLE; REHOR; HUNKELER, 2002; YOUSEFDOOST et al., 2019). In general, the proposed process was able to produce microcapsules with diameters smaller than 100 μm when measured in the wet state, i.e., measured by optical microscopy before freeze drying (Table 4.3). Different studies present a broad range of capsule size formed by batch stirring complex coacervation: 132 to 490 μm on the microencapsulation of buriti oil using gelatin/sodium alginate complex at different stirring speeds (LEMOS; MARFIL; NICOLETTI, 2017); 97 to 689 μm in microencapsulation of palm oil using gelatin/gum Arabic as wall material (MARFIL et al., 2018); and 35 to 80 μm in encapsulation of black raspberry anthocyanin using gelatin/gum Arabic (SHADDEL et al., 2018).

When the atomized ginger oil emulsion contained 1%(w/w) of gelatin, the average diameter (*d*) of wet capsules varied from 52 to 75 μm with *CV* ranging from 17 to 35%, whereas the capsules produced using ginger oil emulsions containing 6%(w/w) of gelatin presented average diameter between 57 and 67 μm with *CV* in the range of 19 to 25%. This indicates that the emulsion with higher gelatin concentration resulted in capsules with smaller size dispersion. In previous studies, Morelli, Holdich and Dragosavac (2017) produced wet capsules with a *CV* of 17% under optimum conditions for cell microencapsulation using membrane emulsification, which is considered a suitable process to produce particles with low polydispersity. Thus, it is possible to conclude that the technique proposed in this study is promising to allow particle engineering with convenient size properties. Values of *CV* between 15 and 30% are considered indicative of medium size dispersion and a controlled process (BROWN; BROWN, 1998). In general, the size distributions of wet capsules produced with 6%(w/w) of gelatin (Figure 4.2b) were narrower and more similar than those with 1%(w/w) of gelatin (Figure 4.2a). This corroborates with the *CV* values presented in Table 4.3, and indicates that the atomization parameters had lower influence on the wet particle size resulting from atomization of emulsions with higher gelatin concentration and, as a consequence, higher *Oh* number (BONDAREVA et al., 2019; KEMP et al., 2013). It is important to highlight that all the atomization conditions

applied, for emulsion containing both gelatin contents, 1 and 6 %(w/w) of gelatin/ginger oil, produced capsules with spherical shape (Figures 4.3 and 4.4), showing that the tested variations on *Oh* and *We* did not affect the morphology of the complex-coacervated microcapsules produced by atomization.

Table 4.3. Experimental average diameter (*d*) and respective coefficient of variation (*CV*) for wet microcapsules, and encapsulation efficiency (*EE*) and encapsulation yield (*EY*) for freeze dried microcapsules.

| Sample Code | Wet capsules | | Freeze dried capsules | | |
|---|---|---|---|---|---|
| | ***d*[1]*** (um) | ***CV*** (%) | ***EE*[2]*** (%) | ***EY*[2]*** (%) | **Water content (%, wet basis)[2]*** |
| G1-AC1 | $61.5^{cd}$ | 28.9 | $74.4 \pm 5.5^{cd}$ | $96.4 \pm 2.2^{a}$ | $1.4 \pm 0.2^{bcdef}$ |
| G1-AC2 | $75.0^{a}$ | 35.5 | $65.2 \pm 2.8^{de}$ | $89.6 \pm 2.5^{a}$ | $1.3 \pm 0.1^{def}$ |
| G1-AC3 | $73.7^{a}$ | 26.1 | $78.4 \pm 1.8^{bcd}$ | $97.9 \pm 0.2^{a}$ | $1.9 \pm 0.2^{abcdef}$ |
| G1-AC4 | $71.5^{a}$ | 20.4 | $53.3 \pm 2.0^{efg}$ | $95.8 \pm 0.5^{a}$ | $1.6 \pm 0.2^{abcdef}$ |
| G1-AC5 | $73.1^{a}$ | 17.6 | $63.5 \pm 2.1^{de}$ | $90.5 \pm 3.0^{a}$ | $0.5 \pm 0.0^{ef}$ |
| G1-AC6 | $65.7^{b}$ | 17.8 | $57.6 \pm 0.1^{ef}$ | $89.7 \pm 2.6^{a}$ | $0.3 \pm 0.1^{f}$ |
| G1-AC7 | $73.6^{a}$ | 25.9 | $44.1 \pm 0.3^{fg}$ | $93.8 \pm 4.6^{a}$ | $0.2 \pm 0.0^{f}$ |
| G1-AC8 | $58.0^{ef}$ | 20.7 | $39.4 \pm 2.4^{g}$ | $99.0 \pm 0.1^{a}$ | $0.2 \pm 0.0^{f}$ |
| G1-AC9 | $52.5^{g}$ | 19.8 | $9.4 \pm 5.9^{h}$ | $97.6 \pm 1.2^{a}$ | $0.1 \pm 0.0^{f}$ |
| G6-AC1 | $67.1^{b}$ | 23.6 | $95.2 \pm 1.4^{a}$ | $93.2 \pm 4.9^{a}$ | $3.6 \pm 0.8^{ab}$ |
| G6-AC2 | $66.7^{b}$ | 24.1 | $95.2 \pm 1.3^{a}$ | $97.8 \pm 0.4^{a}$ | $1.3 \pm 0.5^{cdef}$ |
| G6-AC3 | $65.6^{b}$ | 25.2 | $95.6 \pm 0.8^{a}$ | $96.8 \pm 2.0^{a}$ | $2.6 \pm 0.8^{abcde}$ |
| G6-AC4 | $64.8^{bc}$ | 21.1 | $89.9 \pm 0.8^{ab}$ | $99.1 \pm 0.1^{a}$ | $2.9 \pm 0.9^{abcd}$ |
| G6-AC5 | $61.9^{cd}$ | 21.5 | $94.0 \pm 1.6^{a}$ | $91.3 \pm 4.4^{a}$ | $1.3 \pm 0.2^{def}$ |
| G6-AC6 | $60.8^{de}$ | 20.0 | $88.3 \pm 0.7^{abc}$ | $53.4 \pm 5.1^{b}$ | $3.5 \pm 0.4^{abc}$ |
| G6-AC7 | $66.4^{b}$ | 21.5 | $84.4 \pm 1.2^{abc}$ | $50.9 \pm 6.3^{b}$ | $3.0 \pm 0.1^{abcd}$ |
| G6-AC8 | $61.9^{cd}$ | 21.3 | $84.6 \pm 4.9^{abc}$ | $59.1 \pm 9.9^{b}$ | $3.7 \pm 0.2^{a}$ |
| G6-AC9 | $57.3^{f}$ | 19.7 | $86.3 \pm 1.4^{abc}$ | $51.5 \pm 1.6^{b}$ | $2.7 \pm 0.1^{abcde}$ |

[1]Mean values (n = 500); [2]Mean values ± standard error (n = 3); *Different letters in superscript in each column indicate significant differences (Tukey test, $p < 0.05$)

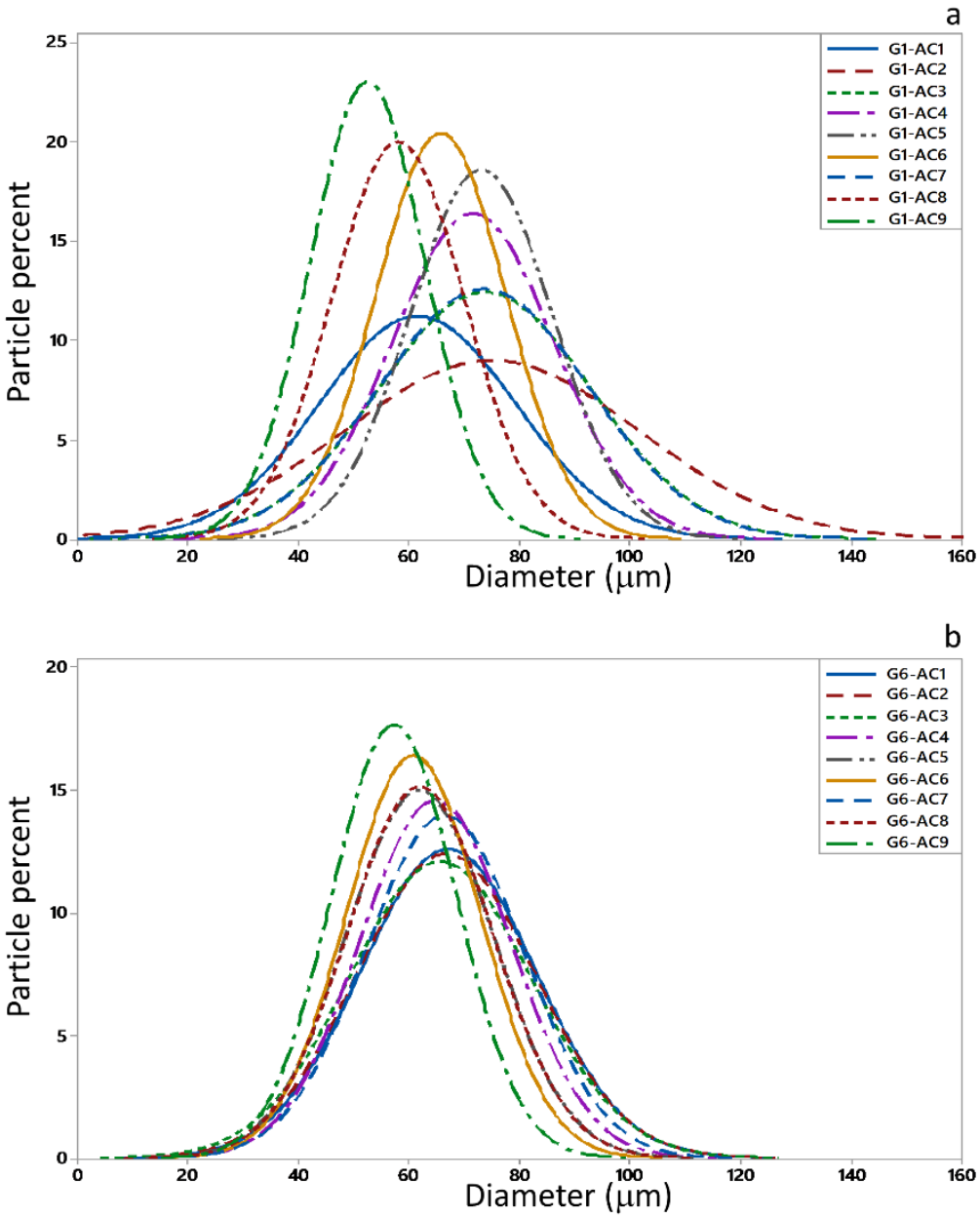


Figure 4.2. Size distribution of wet microcapsules produced with emulsions containing (a) 1%(w/w) of gelatin and (b) 6%(w/w) of gelatin.

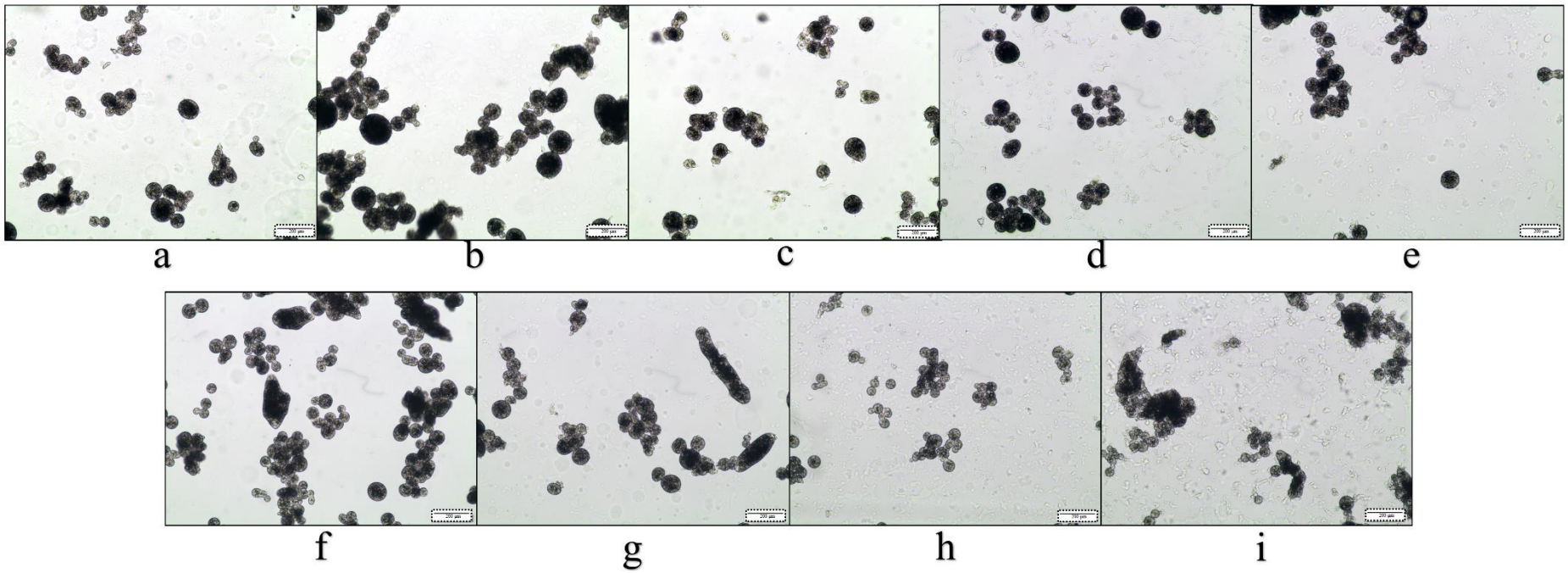


Figure 4.3. Morphology of wet complex-coacervated microcapsules produced by different atomization conditions of emulsion containing 1 %(w/w) of gelatin: (a) G1-AC1, (b) G1-AC2, (c) G1-AC3, (d) G1-AC4, (e) G1-AC5, (f) G1-AC6, (g) G1-AC7, (h) G1-AC8, (i) G1-AC9. Lower bar indicates 200 µm.

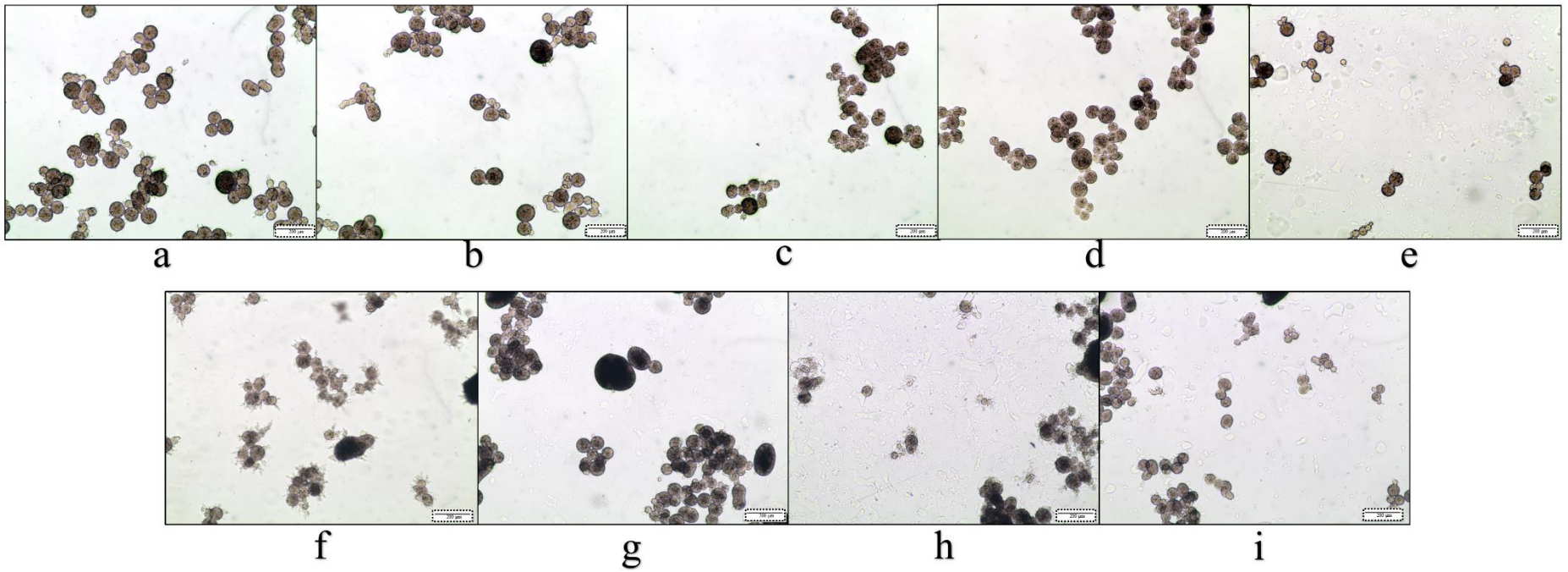


Figure 4.4. Morphology of wet complex-coacervated microcapsules produced by different atomization conditions of emulsion containing 6 %(w/w) of gelatin: (a) G6-AC1, (b) G6-AC2, (c) G6-AC3, (d) G6-AC4, (e) G6-AC5, (f) G6-AC6, (g) G6-AC7, (h) G6-AC8, (i) G6-AC9. Lower bar indicates 200 μm.

The ratio between the velocities of the atomization air and emulsion ($V_g/V_l$) had influence on the wet capsule diameter (Table 4.3). For atomization conditions (explained in Table 4.2) AC7, AC8 and AC9, the increase on $V_g/V_l$ values decreased significantly the capsule diameter, for both formulations (Table 4.3). Considering that *We* > 350 was observed for these atomization conditions, it is possible to say that when the atomization process occurs on catastrophic regime (VARGA; LASHERAS; HOPFINGER, 2003), the increase $V_g/V_l$ significantly decreases the size of the capsules formed. In a study of atomization of xanthan gum solution, the same trend was observed, in which increasing $V_g/V_l$ decreased the size of the droplets formed, and the droplet size ranged from 50 to 130 μm for $25 < V_g/V_l < 252$ (MANSOUR; CHIGIER, 1995).

The atomization process in a two-fluid nozzle is caused by shear forces that occurs at the interface between sprayed liquid and surrounding atomizing air, which emerges at high velocity from the annulus (KEMP *et al.*, 2016). The air velocity, $V_g$, is much higher than the liquid velocity, $V_l$, in such a way that the transfer of kinetic energy and the resulting shear stress at the gas-liquid interface cause break up of liquid into droplets (KEMP et al., 2013; VARGA; LASHERAS; HOPFINGER, 2003). Thus, atomization performance and the resulting particle sizes are affected by the rheology of the atomized liquid and by the atomization conditions, which will determine the applied shear rate.

The values of density ($\rho_l$) ,viscosity ($\mu_l$) and superficial tension ($\sigma$) of the emulsion were determined in a previous study and were used for the determination of the non-dimensional numbers (FERREIRA; NICOLETTI, 2021). For emulsions with 1 g of gelatin/100 g, $\rho_l$ = 997.0 kg/m$^3$ and $\sigma$ = 45.4 *m*N/m. For emulsions with 6 g of gelatin/100 g, $\rho_l$ = 1008.7 kg/m$^3$ and $\sigma$ = 48.8 *m*N/m. The rheological behaviour, determined previously of emulsions containing 1 g of gelatin/100 g follow the Newtonian model (Equation 4.9), with $\mu_l$ = 0.0016 Pa·s, and those with 6 g of gelatin/100 g of emulsion can be described by the Bingham model (Equation 4.10), with $\tau_0$ = 0.0057 Pa and $\mu_l$ = 0.0116 Pa·s (FERREIRA; NICOLETTI, 2021). The shear rate experienced by the liquid in a two-fluid atomization nozzle can be calculated by Equation 4.11 (ALISEDA et al., 2008).

$$\tau_{Newton} = \mu_l \dot{\gamma} \tag{4.9}$$

$$\tau_{Bingham} = \tau_0 + \mu_l \dot{\gamma} \tag{4.10}$$

$$\dot{\gamma}_{real} = \frac{V_{wav}}{l_{wav}} \tag{4.11}$$

The shear rate and *We* number do not depend on the rheological properties of the fluid (STEFFE; PH; PRESS, 1994) and, as can be seen in Figure 4.5a, a linear relationship exists

between these variables. This is of interest, considering that the expression to calculate *We* is simpler and requires less parameters than are necessary to calculate shear rate using Equation 4.11, being both independent of the atomized liquid's viscosity. A linear regression of shear rate versus *We* (Equation 4.12) resulted in determination coefficient, $R^2$, of 0.99.

$$\dot{\gamma}_{model} = 25.3\, We + 2247.3 \quad (4.12)$$

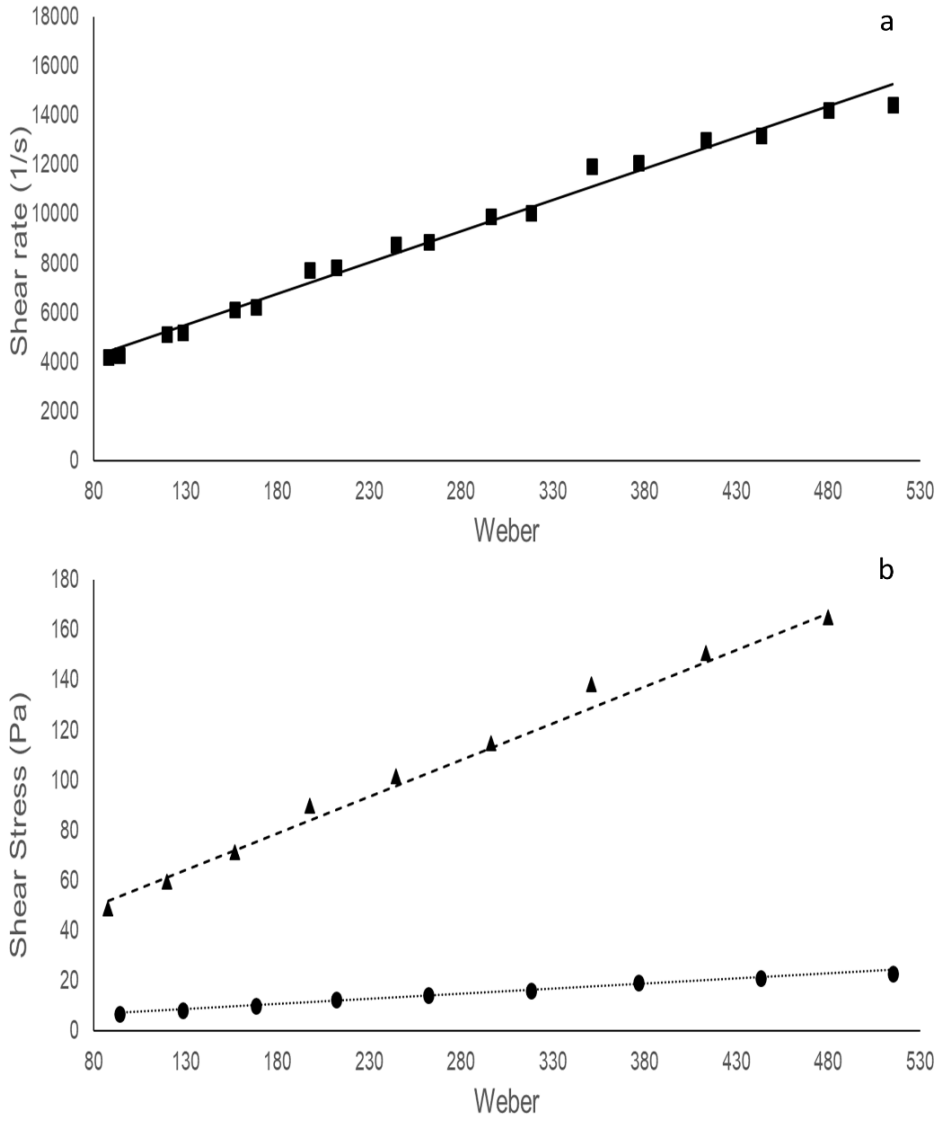


Figure 4.5. Shear rate (a) and shear stress (b) versus Weber number for atomization of ginger oil/gelatin emulsions: (■) real shear rate (Equation 4.11); (—) Equation 4.12; (●) real shear stress (Equation 4.15) for 1% (w/w) of gelatin; (···) Equation 4.13; (▲) real shear stress (Equation 4.16) for 6 % (w/w) of gelatin; (---) Equation 4.14.

The shear rate ($\dot{\gamma}$) varied from 4220 to 14500 $s^{-1}$ (Figure 4.5a). In general, proteins can sustain shear stress values up to $10^5$ $s^{-1}$ without affecting its structural amino acids' chain, and usual spray drying processes have shear rates varying from $10^4$ to $10^5$ $s^{-1}$ (AMERI; MAA,

2006). Moser, Ferreira and Nicoletti (2019) reported $\dot{\gamma}$ ranging from $1.6\times10^3$ to $1.7\times10^3$ $s^{-1}$ while microencapsulating buriti oil in chickpea protein-pectin matrix. In a study of atomization of xanthan gum solution, Mansour and Chigier (1995) presented values of droplet sizes varying from 50 to 130 μm for $\dot{\gamma}$ between 786 and 9754 $s^{-1}$. Considering that the emulsifying agent used throughout this study was gelatin, it is possible to say that the highest shear forces applied during the atomization process are on the lower range of usual spray drying processes, and thus, no mechanical denaturation of the proteins should occur (AMERI; MAA, 2006).

When the atomized liquid is an emulsion, it is important to know the magnitudes of shear stress ($\tau$) it will undergo, as this knowledge helps predict if the emulsion will endure the stress applied in the nozzle, which on its turn may affect the size, morphology and functionality of microcapsules (Ferreira et al., 2016). In such a way, shear stress was also correlated with *We*. Equation 4.12 was combined with Equation 4.9 resulting in Equation 4.13 which represents a model of shear stress for Newtonian fluids ($\tau_{mn}$). Equation 4.12 was also combined with Equation 4.10 resulting in Equation 4.14 which gives a model of shear stress for Bingham fluids ($\tau_{mb}$). In addition, the real shear stress was calculated combining Equations 4.9 and 4.11, and Equations 4.10 and 4.11, which resulted in Equations 4.15 for Newtonian fluids, and 4.16 for Bingham fluids, respectively. The results of both approaches for calculating shear stress at the atomization nozzle, in function of Weber number, are presented in Figure 4.5b.

$$\tau_{mn} = \mu_l(25.3\,We + 2247.3) \tag{4.13}$$

$$\tau_{mb} = \tau_0 + \mu_l(25.3\,We + 2247.3) \tag{4.14}$$

$$\tau_{rn} = \frac{V_{wav}}{l_{wav}}\,\mu_l \tag{4.15}$$

$$\tau_{rb} = \tau_0 + \mu_l\frac{V_{wav}}{l_{wav}} \tag{4.16}$$

The shear stress applied at the atomization nozzle had different effects on the average diameter of the microcapsules produced with distinct gelatin contents in the emulsion (Figure 4.6). For samples produced with 1%(w/w) of gelatin, *d* remained between 60 and 75 μm for shear stress increasing from 6 to 20 Pa, then drastically dropped below 60 μm for further increase in $\tau$. On the other hand, for samples produced with 6%(w/w) of gelatin, *d* remained between 60 and 67 μm up to $\tau = 151\ Pa$, then decreasing to its lowest value (57.2 μm) at higher shear stress.

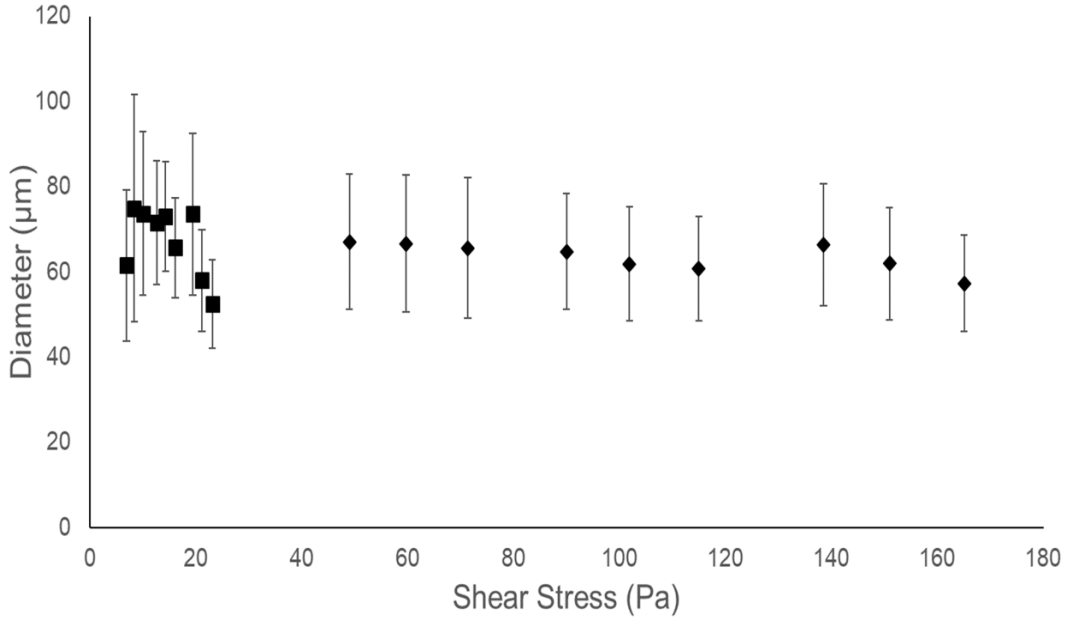


Figure 4.6. Experimental average diameter of wet complex-coacervated microcapsules produced with 1%(w/w) (■) and 6%(w/w) (♦) of gelatin in function of the real shear stress at the nozzle calculated by Equations 4.15 and 4.16.

The average diameter of the wet complex-coacervated microcapsules were also correlated with Weber number by applying a non-linear regression using Gauss-Newton algorithm, which resulted in Equation 4.17. The regression was applied for both emulsion formulations, independently. Ferreira and Nicoletti (2021) showed that a hydrodynamic model was able to predict the diameter of coacervated wet microcapsules produced by atomization at $Oh > 0.01$. Taking into account that atomization of the emulsion containing 6 %(w/w) of gelatin resulted in $Oh = 0.063$, it was expected to obtain a good correlation for this emulsion, but not necessarily for the more diluted emulsion that contained only 1 %(w/w) of gelatin, for which $Oh = 0.009$.

$$D'_{3,2cc} = a\left(\frac{D_l^{3/2}\mu_g}{b_g\mu_l}\right)\left(\frac{OhRe_g}{We^n}\right) + b\frac{Q_l}{Q_g}\left(Oh\sqrt{D_l}\right)^{0.45} \quad (4.17)$$

In which $a = 58415$, $b = 300000$, and $n = 0.52$.

As it can be seen in Figure 4.7, $D'_{3,2}$ calculated by Equation 4.7 presented a similar trend to the experimental diameters obtained, especially for the formulation with 6 %(w/w) of gelatin. Doing so, Equation 4.7 was used as the starting function for fitting the experimental data of wet capsules and performing the nonlinear regression.

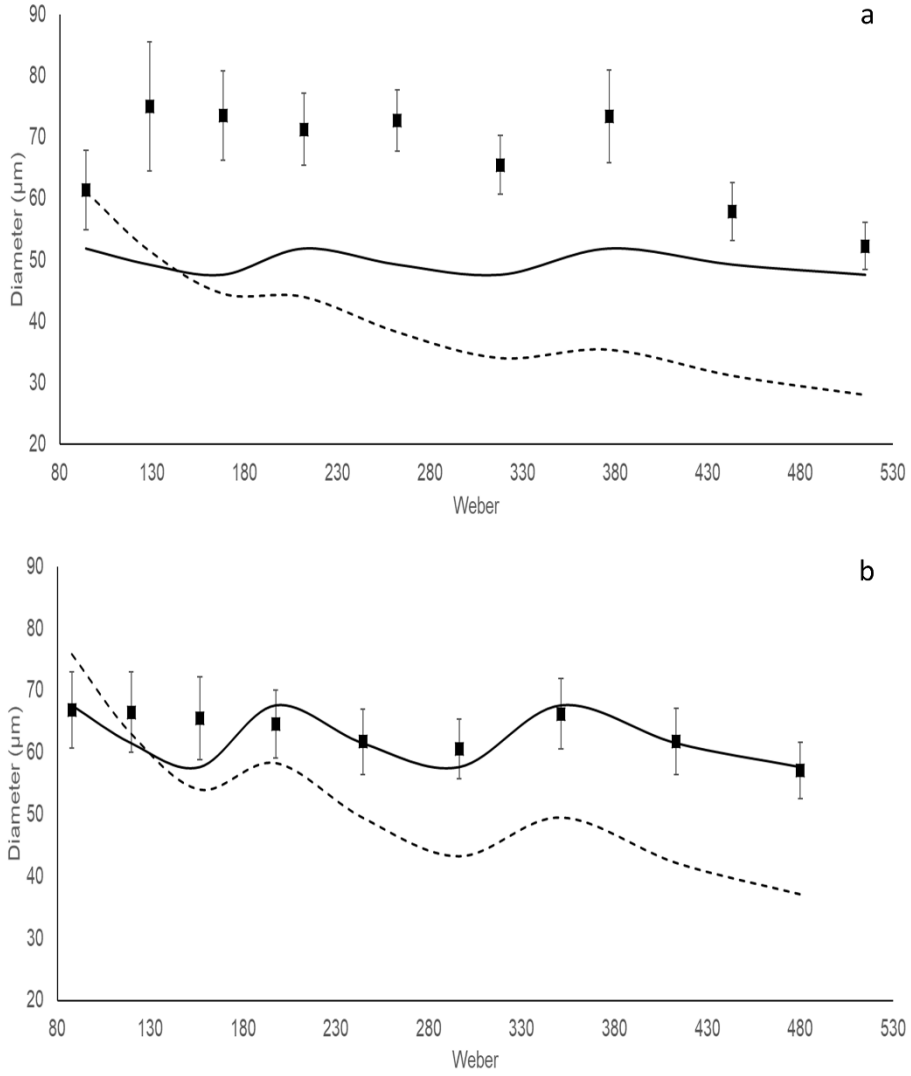


Figure 4.7. Experimental diameter (■) for coacervated microcapsules produced with (a) 1 %(w/w) gelatin and (b) 6 %(w/w) gelatin in function of *We* number; (---) $D'_{3,2}$ (Equation 4.7); (—) $D'_{3,2CC}$ (Equation 4.17).

The model $D'_{3,2CC}$ (Equation 4.17) obtained did not fit the data for samples with 1 %(w/w) gelatin (Figure 4.7a). This result was expected, as these samples had $Oh < 0.01$, and as observed by Ferreira and Nicoletti (2021), models such Equation 4.7 were not able to predict the final diameter of the capsules in this condition, which could be attributed to the low viscosity of the sample. For samples containing 6 %(w/w) gelatin, two situations appeared (Figure 4.7b). For $We < 180$, Equation 4.17 did not fit properly the experimental data, whereas for $We \geq 180$ the model fit the data with 95 % of confidence, evidencing an increase in the correlation with increasing values of *We*. Varga et al., (2003) stated that liquid bag-type breakup occurs at $12 < We < 80$, and atomization by air-shear breakup occurs for $80 < We < 350$. Based on this

information, prediction of wet microcapsule size begins to be more representative when the emulsion droplets are at the mid region of air-shear breakup regime.

Table 4.4. Statistical parameters of the lack-of-fit of the non-linear regression to obtain Equation 4.17, for samples with 6 % (w/w) of gelatin.

| **Lack of fit** | | | | | | |
|---|---|---|---|---|---|---|
| Source | | DF | SS | MS | F | P |
| Error | | 15 | 47.8884 | 3.19256 | | |
| | Lack of fit | 3 | 20.8622 | 6.95405 | 3.09 | 0.068 |
| | Pure error | 12 | 27.0263 | 2.25219 | | |
| Summary | | | | | | |
| Interactions | 6 | | | | | |
| Final SSE | 47.8884 | | | | | |
| DFE | 15 | | | | | |
| MSE | 3.19256 | | | | | |
| S | 1.78677 | | | | | |

Table 4.4 presents the results of the lack-of-fit test obtained during the non-linear regression to obtain Equation 4.17. The standard deviation of the fitted values, $S$ = 1.80 (μm) for $We \geq 180$, is considered a good result for predicting particle sizes in the domain of particle engineering, and the lack-of-fit was not significant for the model at the level of 95% ($p > 0.05$). In addition, the distribution of residues is close to a normal distribution (Figures 4.8a, 4.8c), the residual values are randomly distributed with constant variance (Figure 4.8b), and are independent from each other (Figure 4.8d). Therefore, it is possible to say that Equation 4.17 appropriately predicted the final diameter of wet capsules with 6 %(w/w) of gelatin produced by complex coacervation by atomization for $We \geq 180$. Nevertheless, Equation 4.17 was not able to predict the final diameter of capsules with 1 %(w/w) of gelatin.

In studies for determination of semi-empirical models for atomization droplets, a similar approach was done for several fluids, with different rheological behaviours and nozzle characteristics also resulting in a good fit between the experimental and modelled values, with coefficient of correlation varying from 0.933 to 0.972 (MANSOUR; CHIGIER, 1995) and from 0.961 to 0.994 (THYBO et al., 2008).

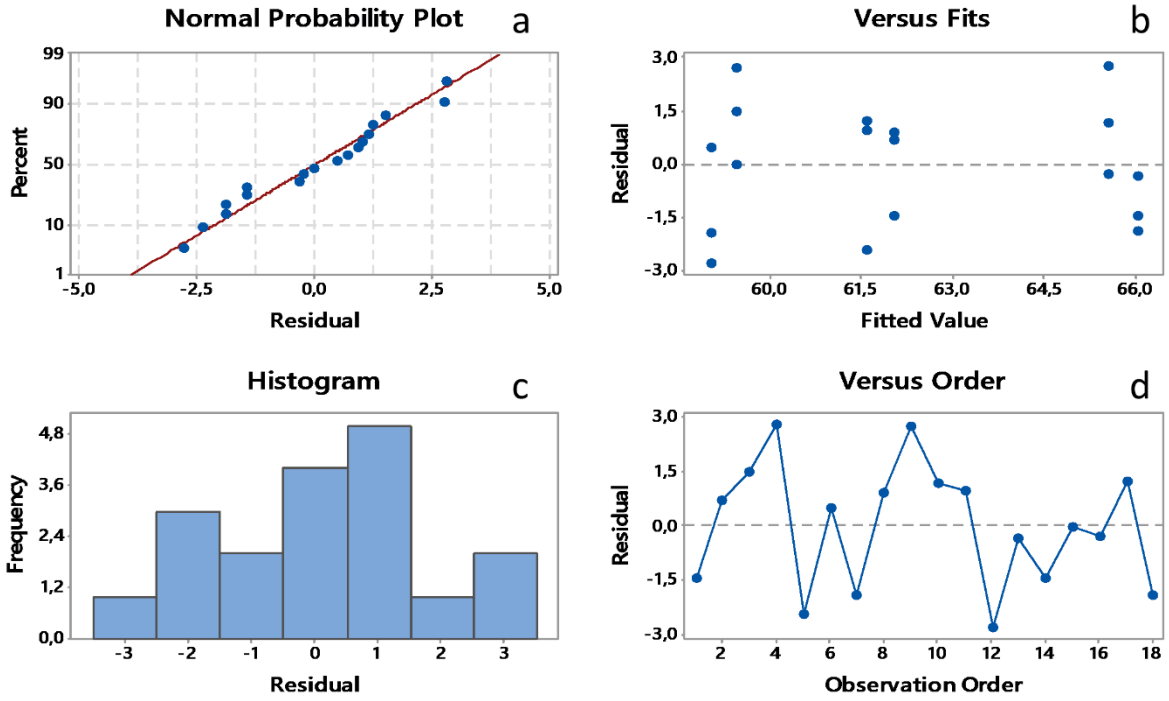


Figure 4.8. Residue plots of the non-linear regression of the model - Equation 4.17, for samples with 6 %(w/w) of gelatin.

*4.3.2 Encapsulation efficiency and encapsulation yield in freeze dried microcapsules*

The technique of microencapsulation by complex coacervation is known to produce capsules with high encapsulation efficiency (TIMILSENA et al., 2019). In addition to high encapsulation efficiency, i.e., to have most of the encapsulated material inside the capsule, rather than on its surface, it is important to retain most of the initial mass of encapsulated material throughout the microencapsulation process (OZKAN et al., 2019). In this work, the values of *EE* varied from 9 to 78% for freeze-dried capsules produced by atomization of emulsions containing 1 %(w/w) gelatin, and from 84 to 95% for capsules produced with 6 %(w/w) gelatin in the atomized emulsion (Table 4.3). The high *EE* obtained when using the more concentrated emulsions are comparable to values reported for complex coacervation carried out by batch stirring using gelatin and Arabic gum as wall materials, with (ALVIM; GROSSO, 2010) and without (COMUNIAN et al., 2016; MARFIL et al., 2018; QV; ZENG; JIANG, 2011) crosslinking agents. A study of encapsulation of β-carotene by complex coacervation using a blend of casein and gum guar with genipin as crosslinking agent resulted in *EE* varying from 57 to 65 % (THAKUR et al., 2017). In addition, lower values of *We* and $\dot{\gamma}$ , as showed in Figure 4.5a and Table 4.2, tend to provide higher values of *EE* (Table 4.3). Lemos et al. (2017) reported values of 80% of *EE* for shear rate values from 90 to 306 $s^{-1}$ in encapsulation of buriti oil by complex coacervation. Even though the shear rates used in this

study were significantly higher (4220 to 14500 $s^{-1}$), the *EE* are comparable. The *EY* values ranged from 89 to 99% for samples produced from emulsions containing 1 %(w/w) gelatin, and between 50 and 99% for samples produced by atomization of emulsions containing 6 %(w/w) gelatin. A similar range of *EY* (50 -90 %) was reported in a study of β-carotene by complex coacervation using casein/gum tragacanth as wall material with genipin as crosslinking agent (JAIN et al., 2016). In a study comparing combinations of gelatin, chitosan and gum Arabic in complex coacervation by batch stirring, capsules with gelatin and gum Arabic had an *EY* of 90 % (GONÇALVES et al., 2018). Studying the microencapsulation of anchovy oil using one and two-steps batch stirring complex coacervation using gelatin and sodium hexametaphosphate as shell materials, Wang et al. (2019) achieved 95% of encapsulation yield with the use of crosslinking agents.

As it was already mentioned, the shear rate applied at the atomization nozzle - which can be represented by Weber number (Figure 4.5a) - is critical for the stability of emulsions and for encapsulation performance, thus *EE* and *EY* were represented in function of the *We* (Figure 4.9). For microcapsules produced by atomization of emulsions containing 1 %(w/w) gelatin, encapsulation yield was not affected by the increase in Weber number (Figure 4.9a). For *We* > 250, however, there was an increase in *OS* and, as a consequence, a decrease in *EE*. This suggests that, despite samples produced from the lesser concentrated emulsion being able to carry most of the oil in all atomization conditions applied, a part of it may be moved to the surface of the capsules at high values of *We*. The increase in Weber values implies a higher influence of the inertial forces during the atomization process over the surface tension forces, and this higher stress on the emulsion may cause it to lose stability, releasing the oil from the inner droplets and increasing the values of *OS*. It is important to note that one of the main reasons to microencapsulate a certain core material is to protect it against harsh conditions (e.g. light or oxygen oxidation), keeping the core inside the capsule (GONÇALVES et al., 2018). Moser et al., (2019) studying the encapsulation of buriti oil by spray drying in chickpea protein-pectin matrix and the influence of non-dimensional numbers during the atomization process, reported values of *EE* between 81 and 92%, for *We* > 420. Microencapsulation by spray drying and by complex coacervation are quite different in their nature, and because of this, the atomization process interferes in different mechanisms, which may explain the distinct behaviour of *EE* in function of *We* in both works. The microcapsules produced with emulsions containing 6 %(w/w) gelatin showed a different trend (Figure 4.9b). In this case, *OS* did not change with increasing *We* and, as a result, *EE* did not change as well, remaining higher than 89%. In microencapsulation of tuna oil using whey protein isolate and gum Arabic, Eratte,

Wang et al. (2014) reported values of 11.4 % of *OS* and 72.9 % for *EE* for capsules dried in a freeze drier. On the other hand, *EY* decreased significantly from a plateau around 90% to another plateau around 50% for *We* > 250. This indicates that for *We* > 250, part of the encapsulated core was not carried inside nor outside of the capsules during the encapsulation process. This may be directly related with the emulsion's structure, whether it is able or not to keep its stability when receiving the shear forces on the atomization process. Also, this may be related with the transition of the atomization regime from air-shear breakup to catastrophic breakup, where the morphology of the droplet changes due to the shear stress caused on the liquid by the atomization air (ALISEDA et al., 2008; GUILDENBECHER; LÓPEZ-RIVERA; SOJKA, 2009; VARGA; LASHERAS; HOPFINGER, 2003). Finally, the water content (Table 4.3) in microcapsules produced from emulsions containing 1 %(w/w) gelatin (0.1 to 1.9%) tended to be lower than in capsules produced with emulsions containing 6 %(w/w) gelatin (1.3 to 3.6%), which may be explained by the high hygroscopicity of the gelatin (FERREIRA; MALACRIDA; TELIS, 2016).

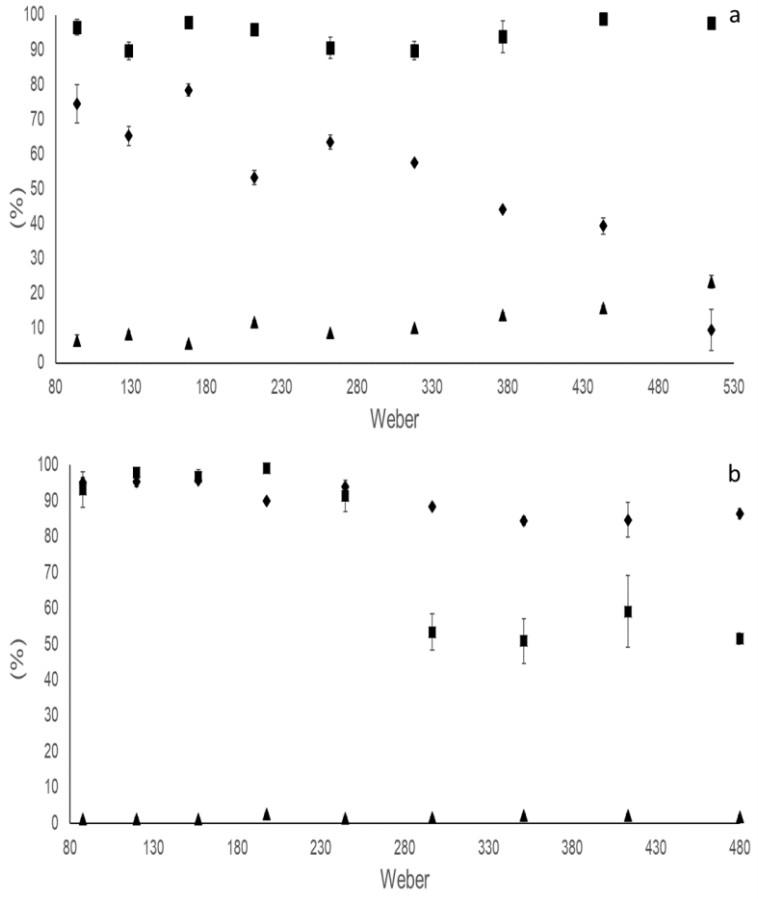


Figure 4.9. Encapsulation yield (■), encapsulation efficiency (♦), and oil at the surface of microcapsules (▲) versus Weber number for emulsions produced with (a) 1 %(w/w) of gelatin (*Oh* = 0.009), and (b) 6 %(w/w) of gelatin (*Oh* = 0.063).

## 4.4. Conclusions

It was possible to determine a model to predict the final diameter of the complex coacervated capsules produced by atomization. The conditions for which the model was able to predict the diameter of the microcapsules were $Oh = 0.063$ and $We \geq 180$. A model for the shear rate at the atomization nozzle was proposed in function of the Weber number. The atomization parameters did not affect the morphology of the capsules produced.

The encapsulation efficiency and encapsulation yield were affected differently by the shear stress and Weber number, depending on the *Oh* value of the emulsion atomized. For capsules produced with 1 %(w/w) of gelatin the encapsulation efficiency with increasing of *We*. Capsules produced with 6 %(w/w) of gelatin were affected more on their encapsulation yield. From the results, two possible scenarios might be considered regarding the optimum conditions to produce complex-coacervated microcapsules by atomization: the first one considers the size prediction as the main factor and, in this case, $We \geq 180$ and $Oh > 0.01$ are mostly indicated; in the second scenario, when trying to maximize *EE* and *EY*, $We < 250$ and $Oh > 0.01$ would be most indicated. Taking both factors into consideration, size prediction and microencapsulation parameters, $180 < We < 250$ and $Oh > 0.01$ would be considered as optimum conditions.

This investigation on complex coacervation carried out by atomization presented a comprehensive study of how the atomization parameters may affect the size of the ginger oil capsules produced, and its encapsulation parameters, for complex coacervation with gelatin and Arabic gum as wall material.

**Acknowledgements**

The authors thank: Dr. Marijana Dragosavac from the Chemical Engineering department of the Loughborough University – UK, for proof reading the article, Adiella Abelseth for proof reading with a focus on the English language of the article and Isabella Serpa Villas Boas for assistance during the experiments. This work was supported by the São Paulo Research Foundation - FAPESP (grant numbers 2015/23290-0 and 2018/16976-0) and National Council for Scientific and Technological Development - CNPq (grant number 479822/2009-3).

| Symbol | Definition |
|---|---|
| $EE$ | Encapsulation Efficiency - Equation 4.1 |
| $EY$ | Encapsulation yield - Equation 4.2 |
| $OS$ | Capsule surface`s oil |
| $OT$ | Capsule total oil |
| $OI$ | Emulsion initial oil content |
| $We$ | Weber number - Equation 4.3 |
| $Oh$ | Ohnesorge number - Equation 4.4 |
| $Re_g$ | Atomization air`s Reynolds number - Equation 4.5 |
| $Re_n$ | Emulsion's Reynolds number - Equation 4.6 |
| $D`_{32}$ | Sauter mean diameter in function of atomization non dimensional numbers - Equation 4.7 |
| $V_w$ | Velocity of the emulsion waves leaving the nozzle - Equation 4.8 |
| $\tau_{Newton}$ | Newtonian shear stress - Equation 4.9 |
| $\tau_{Bingham}$ | Bingham shear stress - Equation 4.10 |
| $\gamma_{real}$ | Emulsion's real shear rate at the nozzle - Equation 4.11 |
| $\gamma_{model}$ | Model of emulsion's shear rate at the atomization nozzle in function of *We* - Equation 4.12 |
| $\tau_{mn}$ | Shear Stress model for Newton fluids - Equation 4.13 |
| $\tau_{mb}$ | Shear Stress model for Bingham fluids - Equation 4.14 |
| $\tau_{rn}$ | Shear Stress real for Newtonian fluids - Equation 4.15 |
| $\tau_{rb}$ | Shear Stress real for Bingham fluids - Equation 4.16 |
| $D'_{3,2cc}$ | Model to predict diameter of the complex coacervated capsules produced by atomization - Equation 4.17 |
| $D_l$ | Diameter of emulsion outlet |
| $D_{int}$ | Internal diameter of air outlet |
| $D_{ext}$ | External diameter of air outlet |
| $d$ | Capsule experimental average diameter |
| $V_g$ | Atomization air`s velocity |
| $V_l$ | Emulsion`s velocity |
| $Q_g$ | Atomization air volumetric flow rate |
| $Q_l$ | Emulsion volumetric flow rate |
| $\mu l$ | Emulsion`s apparent viscosity |
| $\mu_g$ | Atomization air`s viscosity |
| $\rho_g$ | Atomization air`s density |
| $\sigma$ | Emulsion's surface tension |
| $\rho_l$ | Emulsion`s density |
| $b_g$ | Atomization air layer thickness |

# CHAPTER 5 - USE OF A TUBULAR HEAT EXCHANGER TO ACHIEVE COMPLEX COACERVATION IN A SEMI-CONTINUOUS PROCESS: EFFECTS OF CAPSULES CURING TEMPERATURE AND SHEAR RATE

Sungil Ferreira[1]*, Vania Regina Nicoletti[1]

[1]São Paulo State University (UNESP), Department of Food Engineering and Technology, São Jose do Rio Preto – SP, 15054-000, Brazil

Abstract

The main objective of this study was to convert the cure of the capsules produced by complex coacervation in a continuous process. To achieve this, a tubular heat exchanger operating in continuous mode was used. The complex coacervation step was induced by atomization and compared with the traditional batch stirring method. The influence of curing step was evaluated by varying the tubular heat exchanges curing flow rate (2.4, 5.3 and 8.3 mL/s) and the curing temperature (8, 10 and 11.5 $^{o}$C), immediately after the coacervation step. One important result reported in this study is the reduction in total time to cure the capsules, that varied from 2.7 to 9.4 minutes, without affecting the capsules morphology, size and encapsulation parameters. The capsules size varied from 22 to 36 µm, the encapsulation yield ranged from 66 to 93 % and the maximum oil released during simulated gastric conditions was less than 14 %. This indicates that this new configuration to carry out complex coacervation in a semi-continuous process is effective in producing proper capsules and it opens important possibilities to scale up the process, making it cheaper, faster and more efficient.

Keywords: Microencapsulation, scale up, cooling rate, atomization, process optimization, simulated gastric conditions

## 5.1. Introduction

There is constant growing interest in studying microencapsulation by complex coacervation for industrial applications (TANG; SCHER; JEOH, 2020; ZHOU et al., 2020). Complex coacervation is a versatile technique that allows encapsulation of core materials of different natures (e.g. hydrophobic, hydrophilic, cells) by using single or double emulsions (COSTA et al., 2020; FRAJ et al., 2021; ZHAO et al., 2020). Briefly, the formation of complex coacervated capsules happens due to an electrostatic interaction between two polymers (a protein and a polysaccharide) with opposite electric net change, followed by the solvent repulsion (VEIS, 2011; ZHOU et al., 2020).

This work is the third part of a series of studies with the objective to present new configurations to induce complex coacervation. In the first two parts, atomization was applied, evaluating the influence of formulation and atomization conditions (FERREIRA; NICOLETTI, 2020, 2021). The process was described in function of dimensionless numbers and studies of particle engineering and mathematical modelling were done. In these studies, the authors focused in production of coacervated capsules that can be used either in their wet or dried state. There is a growing demand of new alternatives to scale up complex coacervation. In this scenario, atomization is one approach that has been studied, considering its low operating cost and scale up possibility. Jiang et al. (2013) described the use of a three-fluid nozzle to encapsulate α-amilase by complex coacervation. Another approach was described by Tang et al. (2020), in which the coacervation during spray drying was achieved by using highly volatile solvents that, when evaporating would lead to pH adjustment, inducing the coacervation.

To thermodynamically promote the encounter between the polymers and to ensure that all binding sites are available, the coacervation step occurs at high temperatures, around 50 $^{o}$C (KAYITMAZER, 2017; LV et al., 2014). When this happens under proper conditions, phase separation and capsule formation is observed. With the capsules formed, the system must be cooled to induce the capsules' cure and hardening. Along the curing step, gelatin solidifies and the interaction with the polysaccharide increases, enhancing the mechanical and chemical resistance of the capsules (DA SILVA SOARES et al., 2019; FUNAMI et al., 2007). Nevertheless, the curing step is a known bottle neck of the whole coacervation process. There are no studies evaluating the influence of the curing step on the formation of the capsules and on their properties. Usually, complex coacervation uses slow cooling rates to allow the cure of the capsules (LAMPRECHT; SCHÄFER; LEHR, 2000; LEMETTER; MEEUSE; ZUIDAM, 2009; LEMOS; MARIANO MARFIL; NICOLETTI, 2017; RODRIGUES DA CRUZ et al., 2019; XIAO et al., 2016). If the system is cooled too fast the capsules may lose their

conformation and release the encapsulated material. Traditionally, the curing step is done by cooling the system (capsules + supernatant/solvent) in a jacketed vessel. What the authors propose in this study is to perform the curing of the capsules in continuous process, by using a tubular heat exchanger with controlled flow rate and temperature. Since the coacervation step is done in batch mode, the whole complex coacervation process would be considered a semi-continuous process.

Therefore, the main objective of this study is to introduce, evaluate and describe the use of a tubular heat exchanger to promote the cooling and curing of complex coacervation capsules in a continuous mode. By doing so, it is expected to achieve a significant decrease of the curing time, to carry out the complex coacervation process (coacervation step + curing step) in a semi-continuous configuration, and to facilitate the scale up of the coacervation process. The influence of the coacervation step (atomization or batch stirring) and of curing conditions (flow rate and temperature) on capsules' morphology, size, size distribution, encapsulation parameters and resistance to simulated gastric conditions was evaluated.

## 5.2. Material and methods

### *5.2.1 Materials*

Cold pressed ginger oil (Gran Oils, Brazil) was used as core material. The wall material applied to achieve complex coacervation was type B gelatin, 240 bloom (Gelita, Brazil) and gum Arabic (Dinâmica, Brazil). Glacial Acetic Acid (Dinâmica, Brazil), Hydrochloric acid (Dinâmica, Brazil) and hexane (Dinâmica, Brazil), all analytical-grade, were used during production and analyses of microcapsules. Pepsin with proteolytic activity of 1:10000 was used during simulated gastric fluid assays (Dinâmica, Brazil).

### *5.2.2 Preparation of gelatin/ginger oil emulsion and gum Arabic solution*

To form the primary O/W emulsion, ginger oil was dispersed in aqueous gelatin solution at mass ratio oil:gelatin of 1:1. Emulsions containing 6 g gelatin/100 g of solution were tested, based on previous results (FERREIRA; NICOLETTI, 2020, FERREIRA; NICOLETTI, 2021). Emulsification was performed at 15000 rpm for 2 min in Ultra Turrax T-25 (IKA, Germany) homogenizer, followed by ultrasound homogenization at 20 kHz and nominal power of 210 W continuously for 3 minutes, using Sonic Ruptor 4000 ultrasonic probe (Omni International, USA) (FERREIRA et al., 2019; FERREIRA; MALACRIDA; TELIS, 2016). The 1371.5 g of solution of gum Arabic (1 g/100 g), per sample, was prepared by gum addition to preheated deionized water (50 °C) under magnetic stirring until complete dissolution.

The gelatin/ginger oil emulsion and the gum Arabic solution had their pH adjusted to 3.5 using glacial acetic acid prior to the complex coacervation induction.

*5.2.3 Complex coacervation in semi-continuous process by atomization and batch stirring*

The approach proposed in this study configures a semi-continuous process to achieve complex coacervation, as the process itself is divided in two main steps or unit operations. The first step was the induction of complex coacervation by mixing of the ginger oil/gelatin emulsion with the gum Arabic solution. The second step to transform the curing step of the complex coacervation process into a continuous one, using a tubular heat exchanger with controlled temperature and flow rate. The schematic drawing of the system employed is shown in Figure 5.1 and the results related to the characteristics of the particles obtained comparing complex coacervation step done by atomization and compared with the traditional method of batch stirring. For each treatment 100 g of emulsion and 1371.5 g of gum Arabic solution were used.

Complex coacervation in batch stirring was carried out as described by Marfil et al, (2018) and Ferreira and Nicoletti (2021), with the difference that the pH of the solutions was adjusted prior to the coacervation step. The gelatin/ginger oil emulsion (50 ± 1 °C) was added to the gum Arabic solution (50 ± 1 °C) in a 2 L beaker. The mixture was kept under stirring (approximately 300 rpm) while it was being pumped through the tubular heat exchanger to promote the cure of the capsules.

Complex coacervation by atomization was induced following the method described by Ferreira and Nicoletti (2020) and Ferreira and Nicoletti (2021). The gelatin/ginger oil emulsion was atomized the solution of gum Arabic. Atomization was promoted using a two-fluid nozzle (Labmaq, Brazil) with 0.7 mm diameter of emulsion outlet, 1.2 and 1.6 mm internal diameter and external diameter of air outlet, respectively. The emulsion flow rate was $2.11\times10^{-7}$ $m^3/s$, controlled using a peristaltic pump LDP-201-3 (MS Tecnopon, Brazil). The atomization air flow rate was $3.93\times10^{-4}$ $m^3/s$, controlled using a rotameter FT074-02-CA-VN (Omega, USA). The nozzle was positioned at 0.2 m above the level of gum Arabic solution kept under heating (50 $^oC$) (Figure 5.2). Once all ginger oil emulsion was atomized, the solution was pumped through a heat exchanger to promote the cure/cooling of the capsules.

The cure of the capsules was achieved using a heat exchanger (Figure 5.1). The suspension containing the capsules was pumped through a copper pipe folded as a coil, with 3.05 mm of internal diameter and 4.5 m of length. The copper pipe was installed inside a PVC pipe of 0.65 m in length and 0.14 m of diameter, closed in both sides, with four openings being

two for inlet and outlet of the coolant fluid and two for inlet and outlet of the suspension containing the capsules. A peristaltic pump BP 600/1 (Milan, Brazil) was used to pump the capsule suspension throughout the heat exchanger, with flow rates varying from 2.4 to 8.3 mL/s. A thermostatic bath TE-2005 (Tecnal, Brazil) was used to control the temperate and to cool the water that flowed inside the PVC shell, acting as the coolant fluid, with temperature that was assumed constant throughout the process. Assays were carried out with coolant temperature set on the thermostatic bath varying from 8 to 11.5 °C. The cooling rate (CR) was calculated correlating the temperature difference between the inlet and outlet capsules mixtures (△T) with the residence time (t) of the mixtures inside the heat exchanger [CR=△T/t].

The shear rate ($\dot{\gamma}$) during the curing step was considered as the maximum shear rate and it was determined using Equation 5.1 (STEFFE; DAUBERT, 2006).

$$\dot{\gamma} = \frac{4Q}{\pi r^3} \tag{5.1}$$

In which *Q* is the volumetric flow rate and *r* being the radius of the internal pipe.

After the cooling/hardening step, images of the wet capsules were collected to further analysis, as described in section 5.2.4. The precipitated capsules were transferred to aluminium trays and frozen in ultra-freezer FV 500 (Liobras, Brazil) at -40 °C and dried in a freeze drier L101 (Liobras, Brazil) for 72 hours. The samples were then ground, packed in aluminium foil for light protection and stored in desiccator with silica gel for further testing.

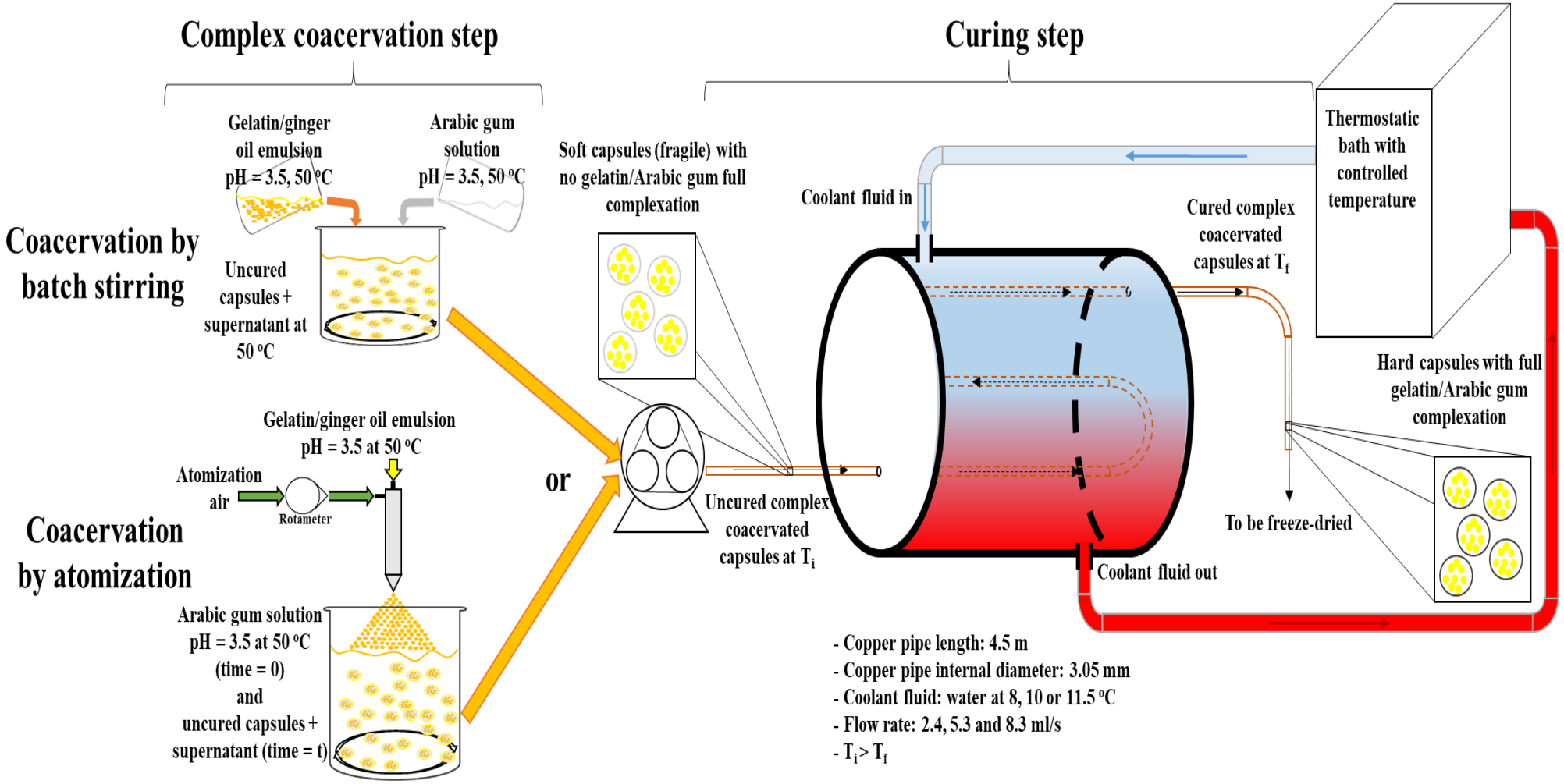


Figure 5.1. Schematic design of the heat exchanger used to cure the complex coacervated capsules, produced by batch stirring and atomization, in semi-continuous configuration.

*5.2.4 Characterization of wet capsules*

The microstructure of wet capsules was evaluated in optical microscope (CX31-III, Olympus, Japan) coupled with a video camera (SIS-SC30). Samples were deposited over glass slides without sample dilution. The scanned images were analysed by Image Pro Plus 6.0 software (Media Cybernetics Inc., USA) for measurement of particle diameter, taking the average diameter of 600 microcapsules, in triplicate, per sample. The wet microcapsules bulk density was determined in a densimeter DMA™ 4500 M (Anton Paar, Austria) at 10 ºC after complete phase separation, measuring only the precipitated, in triplicate.

*5.2.5 Microencapsulation performance*

Encapsulation parameters were determined following methods described by Tonon, Grosso and Hubinger (2011) and by Wang, Adhikari and Barrow (2014) with modifications. Encapsulation efficiency (*EE*) and encapsulation yield (*EY*) were determined in dried capsules, considering the oil initially added in the emulsion (*OI*), the oil at the surface of capsules (*OS*) and the total oil present in the capsules (*OT*) after freeze drying. To determine *OS*, 100 mg of capsules and 10 mL of hexane were shaken for one minute. The mixture was filtered and the hexane was evaporated at room temperature in a hood, then in an oven at 60 °C. To determine *OT*, 100 mg of dried capsules were added to 20 mL of 4N hydrochloric acid solution (pH = 0.8) and shaken for 1 hour at 35 °C. Then, 13 mL of hexane were added and the mixture shaken for 10 hours at 35 °C, forming a two-phase system, which was separated by centrifuging (model Z 326 K, Hermle, Germany) at 10000×g for 30 minutes. The organic phase (hexane + ginger oil) was transferred to Petri dishes and the hexane was evaporated at room temperature in a hood followed, then in an oven at 60 °C. The *EE* and *EY* were calculated by Equations 5.2 and 5.3, respectively.

$$EE(\%) = \frac{OT - OS}{OT} \times 100 \quad (5.2)$$

$$EY(\%) = \frac{OT}{OI} \times 100 \quad (5.3)$$

*5.2.6 Encapsulated ginger oil release in simulated gastric conditions*

The release of ginger oil from the capsules in simulated gastric conditions was evaluated as described by da Silva Soares et al. (2019), Rutz et al. (2017), and Timilsena et al. (2017) with adaptations. A simulated gastric fluid (SGF) was prepared by adding 2 g of NaCl and 3.2 g of pepsin (1:10000) CAS 9001-75-6 into a 1 L volumetric flask with 500 mL of distilled water and shaken until complete solid dissolution. Then 7 mL of HCl 36% (v/v) was added to the

volumetric flask and the volume completed to 1 L with distilled water, being the pH of the SGF 1.2. To perform the release assays, 200 mg of dried capsules were added to 20 mL of SGF at 37 $^{o}$C and incubated for time periods varying from 0 to 120 minutes in a flask shaker at 37 $^{o}$C. After the incubation period, 10 mL of hexane were added, the mixture was agitated and centrifuged in a Z 326 K centrifuge (Hermle, Germany) at 10000×g for 5 minutes. The organic phase (hexane + ginger oil) was transferred to Petri dishes and the hexane was evaporated at room temperature in a hood, then in an oven at 60 °C to determine the amount of ginger oil released considering the total encapsulated.

*5.2.7 Statistical analysis*

All the tests were performed at least in triplicate. The results of analytical determinations are expressed in arithmetic average (*AV*) submitted to analysis of variance (ANOVA) and comparison of means by Tukey test with probability level at 5% ($p \leq 0.05$), using statistical software Minitab 17 (MINITAB, State College - PA, USA). The uniformity of data (size distribution) was evaluated through the coefficient of variation [$CV = (SD/AV)*100$], in which *SD* stands for standard deviation.

**5.3. Results and discussion.**

*5.3.1 Complex coacervation as a semi-continuous process*

Complex coacervation to produce the ginger oil capsules was carried out using emulsions with 6 % w/w of gelatin/ginger oil and gum Arabic solution (1% w/w). Previous work (FERREIRA; NICOLETTI, 2020, 2021) showed that this formulation provides high values of both encapsulation efficiency (*EE*) and encapsulation yield (*EY*). Complex coacervation was performed successfully, comparing atomization with batch stirring. In complex coacervation by atomization there is a relationship between the emulsion droplets, which have the influence of the atomization conditions, formed on the two fluid nozzle and the coacervated capsules coacervated after the contact of the droplet emulsion with the gum Arabic solution. The same effect is not present for capsules produced by batch stirring (FERREIRA; NICOLETTI, 2021). For conciseness and since all the capsules after complex coacervation step had the same spherical multinuclear morphology for both atomization and batch stirring, it will not be further discussed in this study. Right after the ginger oil/gelatin emulsion and gum Arabic solution were mixed in complex coacervation by batch stirring, or all the emulsion was atomized in complex coacervation by atomization, the cooling step took place in the heat

exchanger. To accomplish the cure/hardening of the capsules the concept of a tubular heat exchanger described in section 2.3.3 and Figure 5.1. The cooling rate varied from 1.7 to 9.2 $^{o}$C/s (Table 5.1). When coacervation was induced by atomization the cooling rates were smaller, what is explained considering that, despite the gelatin/ginger oil emulsion and gum Arabic were both at 50 $^{o}$C before the coacervation step, atomization air exerts a cooling effect on the mixture containing the soft capsules and the supernatant solution.

Two main parameters were varied independently in the curing step, the curing flow rate (2.4, 5.3, and 8.3 mL/s), and the coolant temperature (8.0, 10.0, and 11.5 $^{o}$C) that will be referred as curing temperature, whereas the dependent responses studied were the turbulence or shear rate inside the internal tube and the average particle size, size distribution, encapsulation performance and capsule resistance to gastric conditions. Pumping the capsule suspension through the heat exchanger potentializes the convection heat transfer coefficient inside of the internal pipe, what does not happen when curing is done in a jacketed vessel. In addition, the shear forces during the process may help decrease the size of the capsules. One important process parameter that was considerably improved was the curing time. The curing time ranged from 162 to 562 s (2.7 to 9.4 min) resulting in formation of spherical capsules in all the conditions applied. The total curing time, i.e. the residence time, is a function of the curing flow rate, since the total heat exchanger area and length of the internal tube was not changed throughout the assays. This is a relevant result, as it demonstrates that it is possible to produce intact and spherical microcapsules by cooling the suspension in a tube with small diameter, thus enlarging the heat transfer area and accelerating the process, which was achieved in times much smaller than it would be feasible using a jacketed vessel and takes hours to be completed. The laboratory scale method to cure the capsules after complex coacervation is by using an jacketed vessel or an ice bath, in a way that the cooling process is slow, which can reach up to hours to cool around 1 litre of solution (LAMPRECHT; SCHÄFER; LEHR, 2000; LEMETTER; MEEUSE; ZUIDAM, 2009; LEMOS; MARIANO MARFIL; NICOLETTI, 2017; RODRIGUES DA CRUZ et al., 2019; XIAO et al., 2016). In previous studies of complex coacervation by atomization in laboratorial scale, the cooling time varied from 30 to 60 minutes, depending of the final volume of the previous (FERREIRA; NICOLETTI, 2020, 2021). Evaluating the laboratorial method of curing the capsules, from a heat transfer efficiency point of view, it is possible to say that the process has potential for further improvement. Since usually there is no agitation of the coolant fluid, the convective heat transfer coefficient has the tendency to assume small values. This contributes to a larger thermal boundary layer, decreasing the overall heat transfer (INCROPERA et al., 2013). The same is true to the mixture

of supernatant and coacervated capsules being cooled. In general, the agitation during the curing of the capsules in done using low stirring rates (ACH et al., 2015; BUTSTRAEN; SALAÜN, 2014; COMUNIAN et al., 2018; MARFIL et al., 2018). There are studies that evaluate the influence of stirring speed (DOBETTI; PANTALEO, 2002; JEGAT; TAVERDET, 2000; LEMOS; MARIANO MARFIL; NICOLETTI, 2017), however the cooling process is still carried out slowly.

In this sense, the possibility of carrying out complex coacervation in a semi-continuous process, without the necessity of jacketed tanks to cure the capsules and with substantial gains in process time are a significant advance. Thus, in the next sections the influence of the curing process conditions on capsules size, morphology, encapsulation performance and gastric stability, will be discussed providing a basis to the feasibility of this configuration for future applications.

*5.3.2 Influence of cooling parameters on wet capsules density, size and morphology*

The influence of process conditions over thermodynamic conditions on the determination of capsules size distribution can be further observed in Figure 5.2. The size distribution of capsules produced by batch stirring (Figure 5.2a, 5.2b and 5.2c) is significantly wider than for the capsules coacervated by atomization (Figure 5.2d, 5.2e and 5.2f). The capsules cured with flow rate of 8.3 mL/s presented the narrower size distribution, in which capsules coacervated by atomization reached its percentage peak of particle percent between 20 and 25 µm (Figure 5.2f). This shows the importance to take into consideration both parameters, capsules mean diameter and size distribution, when studying the influence of different parameters on capsules/particle size profile during encapsulation processes.

When considering the influence of curing temperature, the highest flow rate presented a slight tendency of increasing diameter with increase in curing temperature (Figures 5.2c and 5.2f). Capsules coacervated by batch stirring and cured in those conditions presented a significant increase in its size. It is important to point out that, to the best of our knowledge, this is the first time that a study evaluates the influence of the curing temperature on the complex coacervation process.

The morphology of the capsules produced could be divided in three main groups, which were directly correlated with the process conditions during the curing step, independently of the coacervation method (Figure 5.2). For flow rate of 2.4 mL/s, it is possible to see a high number of individually separated capsules. As the flow rate increased (5.3 mL/s) the capsules started to became less separated and finally at 8.3 mL/s the capsules could not be easily

identified separated, forming clusters of capsules. In addition, the tendency to form clusters increased with the increase of the curing temperature in the heat exchanger. The process of curing or hardening of the capsules is linked with the change of the gelatin structure, as the capsule temperature decreases. For lower flow rates, the residence time of the capsules in the heat exchanger increases, allowing a more intense cooling effect. The residence time was 13 seconds for flow rate of 2.4 mL/s, 6 seconds for flow rate of 5.3 mL/s and 4 seconds for flow rate of 8.3 mL/s. On the other hand, at the same flow rate, as lower is the curing temperature in the heat exchanger, higher will be the cooling rate (Table 5.1). The results obtained corroborate with what would be expected considering the residence time of the capsules and cooling rate in the heat exchanger, i.e., higher cooling rates allow formation of more individual particles However, it was observed that there is a limit over which the increase in the cooling rate hampers formation of capsules. Preliminary assays (data not published) showed that for curing temperatures as low as 6 $^{o}$C (using the same heat exchanger) there was no capsule formation. The authors attributes that when the cooling rate is too high, the change on the gelatin structure during its gelation may happens too fast, in such a way that gelatin loses its ability to interact electrostactly between its triple helixes and with gum Arabic, destabilizing the capsules wall. In gelatin solution above 40 $^{o}$C each molecule assumes a random coil configuration of a single polypeptide chain (BUREY et al., 2009; FINER et al., 1975). As the system is cooled, there is a conformational transition to random coil-to-helix conformation. Burey et al. (2009) describes the gelation of gelatin in two main steps: “setting” where the network is formed due to the interaction between several regions of the triple helix and “ageing” where the strength of the gel is established to due to the mobility of the chains and the adjustment in function of temperature of hydrogen bonding inside the polypeptide chain. In this sense, if the change on temperature happens too fast, there is no strengthen of the initial interchains interaction, and proper gelation is not observed (FINER et al., 1975; JOHNSTON-BANKS, 1990; KASAPIS et al., 2003). Considering that the ageing step in gelatin gelation takes a long time, it would explain why the curing step after complex coacervation must be either slow or have a low cooling rate.

With regard to differences between both methods of complex coacervation, as the coacervation induced by atomization employed air at 25 $^{o}$C to break down the emulsion (initially at 50 $^{o}$C) to small droplets, the atomization air contributed to the cooling effect on the system prior to the heat exchanger. Thus, the variation between inlet and outlet temperature of samples coacervated by atomization was always smaller than for samples coacervated in batch stirring (Table 5.1). Samples coacervated in batch stirring entered the heat exchanger at 50 $^{o}$C, whereas samples coacervated by atomization entered the heat exchanger at 36 $^{o}$C. This caused

batch stirred samples with flow rate of 8.3 mL/s to present higher degrees of capsule agglomeration (clusters) than the atomized samples under the same curing conditions (Figure 5.2). In addition, the sample coacervated by batch stirring, with flow rate of 8.3 mL/s and curing temperature of 11.5 $^{o}$C exited the heat exchanger at 17 $^{o}$C, being the only one above 15 $^{o}$C (Table 5.1). It is known that when the curing process stops at temperatures above 14 $^{o}$C, capsule agglomeration is more likely to happen (LEMETTER; MEEUSE; ZUIDAM, 2009). In spite of capsules atomized and cured under the same conditions and exiting the heat exchanger at 15 $^{o}$C presented some degree of agglomeration, it was still possible to distinguish the individual capsules, what was not possible in the batch stirred capsules. Lemetter et al. (2009) reported similar morphology of aggregated capsules, which was attributed to the need of controlling both stirring speed and curing temperature.

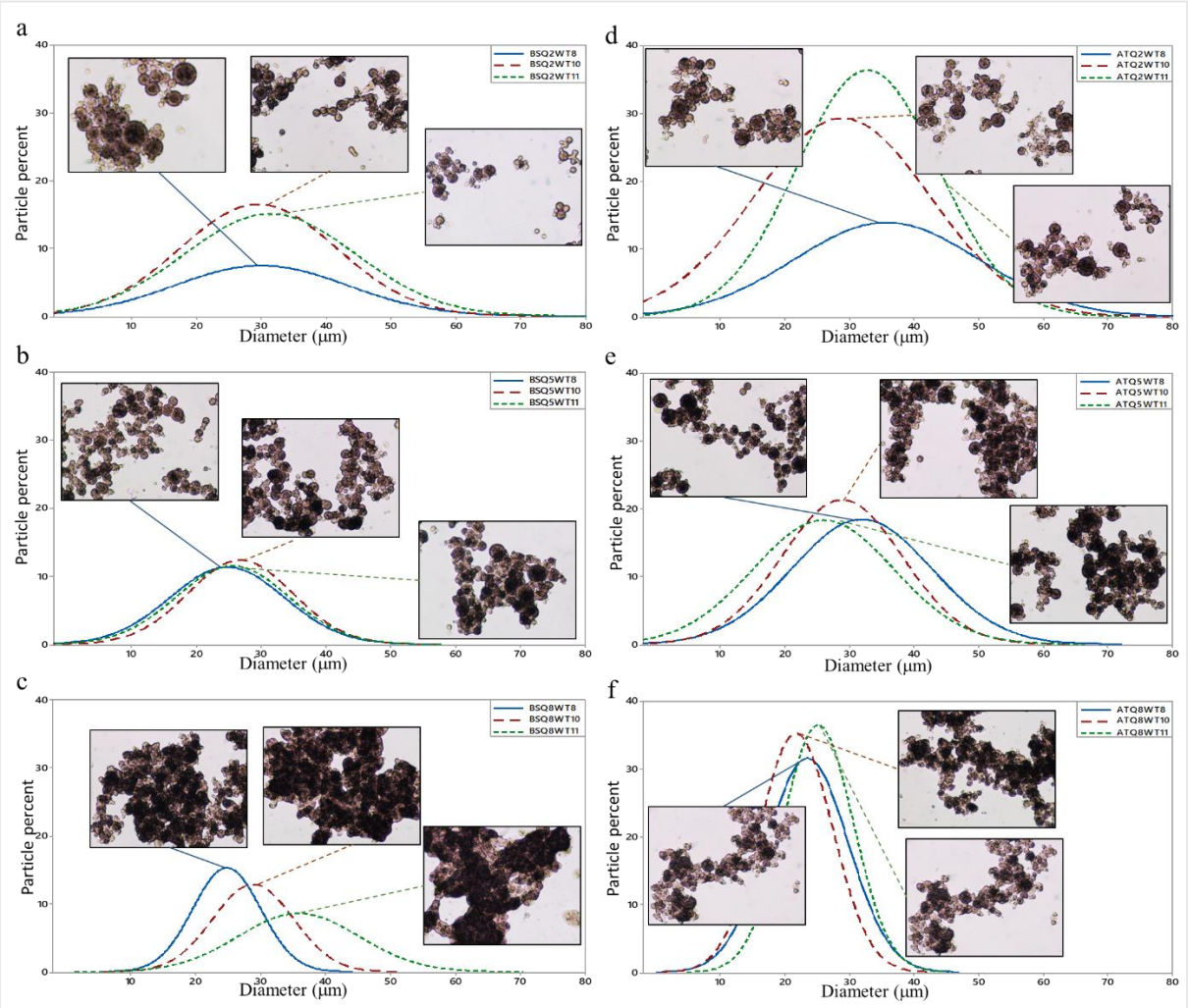


Figure 5.2. Size distribution and morphology of wet microcapsules coacervated by batch stirring (a, b and c) and atomization (c, d and e). Curing flow rate data are represented in separated graphs, being 2.4 mL/s (862 $s^{-1}$) (a and d), 5.3 mL/s (1904 $s^{-1}$) (b and e) and 8.3 mL/s (2981 $s^{-1}$) (c and f).

Table 5.1. Curing operational parameters and capsules size, size distribution, encapsulation parameters and maximum oil released in simulated gastric conditions.

| | | Heat exchanger conditions during cooling/hardening step | | | | | | Wet capsules | | Dried capsules | | |
|---|---|---|---|---|---|---|---|---|---|---|---|---|
| Sample Code | Complex coacervation method | Heat exchanger flow rate (ml/s) | Heat exchanger shear rate ($s^{-1}$) | Curing Temperature (°C) | Temperature variation[1] (°C) | Temperature after curing (°C) | Cooling rate (°C/s) | Capsule mean diameter[2] (µm) | Capsule bulk density[3] ($kg/m^3$) | EE[3] (%) | EY[3] (%) | Oil released after 120 min[3] (%) |
| BSQ2WT8 | | | | 8.0 | 40.0 | 10.0 | 2.9 | $30.0\pm10.7^{def}$ | $1013.2^{h}$ | $99.2\pm0.0^{a}$ | $89.2\pm0.0^{ab}$ | $11.0\pm1.4^{ab}$ |
| BSQ2WT10 | | 2.4 | 862 | 10.0 | 38.5 | 11.5 | 2.8 | $29.5\pm9.5^{def}$ | $1013.6^{g}$ | $99.1\pm0.1^{a}$ | $77.1\pm0.5^{cde}$ | $8.4\pm0.4^{bcd}$ |
| BSQ2WT11 | | | | 11.5 | 36.5 | 13.5 | 2.7 | $31.3\pm9.8^{bcd}$ | $1012.9^{i}$ | $98.9\pm0.3^{a}$ | $66.1\pm0.4^{e}$ | $14.0\pm2.1^{a}$ |
| BSQ5WT8 | | | | 8.0 | 38.5 | 11.5 | 6.2 | $24.8\pm6.3^{jk}$ | $1011.8^{j}$ | $99.0\pm0.0^{a}$ | $89.2\pm1.9^{ab}$ | $8.3\pm0.1^{bcde}$ |
| BSQ5WT10 | Batch stirring | 5.3 | 1904 | 10.0 | 38.0 | 12.0 | 6.1 | $26.8\pm6.2^{hi}$ | $1013.3^{h}$ | $99.2\pm0.1^{a}$ | $84.0\pm1.7^{abc}$ | $6.5\pm0.3^{cdef}$ |
| BSQ5WT11 | | | | 11.5 | 35.5 | 14.5 | 5.7 | $25.6\pm6.3^{ij}$ | $1011.6^{k}$ | $98.9\pm0.1^{a}$ | $71.4\pm3.5^{de}$ | $6.8\pm2.7^{cdef}$ |
| BSQ8WT8 | | | | 8.0 | 36.5 | 13.5 | 9.2 | $24.8\pm3.9^{jk}$ | $1013.6^{g}$ | $99.3\pm0.1^{a}$ | $87.4\pm1.6^{abc}$ | $10.8\pm0.3^{ab}$ |
| BSQ8WT10 | | 8.3 | 2981 | 10.0 | 35.0 | 15.0 | 8.8 | $28.8\pm4.8^{efg}$ | $1016.7^{a}$ | $99.4\pm0.1^{a}$ | $71.2\pm2.9^{de}$ | $5.3\pm0.5^{cdef}$ |
| BSQ8WT11 | | | | 11.5 | 33.0 | 17.0 | 8.3 | $35.9\pm7.0^{a}$ | $1014.2^{f}$ | $99.4\pm0.2^{a}$ | $91.8\pm6.7^{a}$ | $4.1\pm1.9^{f}$ |
| ATQ2WT8 | | | | 8.0 | 26.5 | 9.5 | 1.9 | $32.2\pm9.7^{bc}$ | $1016.2^{b}$ | $98.5\pm0.4^{a}$ | $78.4\pm2.1^{bcd}$ | $8.5\pm1.6^{bc}$ |
| ATQ2WT10 | | 2.4 | 862 | 10.0 | 25.0 | 11.0 | 1.8 | $30.6\pm9.5^{cde}$ | $1015.4^{d}$ | $98.2\pm1.0^{a}$ | $79.2\pm1.2^{bcd}$ | $5.6\pm0.1^{cdef}$ |
| ATQ2WT11 | | | | 11.5 | 23.0 | 13.0 | 1.7 | $33.1\pm8.5^{b}$ | $1014.9^{e}$ | $98.4\pm0.1^{a}$ | $93.5\pm6.4^{a}$ | $5.7\pm0.5^{cdef}$ |
| ATQ5WT8 | | | | 8.0 | 24.5 | 11.5 | 4.0 | $29.9\pm7.9^{def}$ | $1015.7^{c}$ | $99.4\pm0.2^{a}$ | $70.9\pm4.9^{de}$ | $8.6\pm2.0^{bc}$ |
| ATQ5WT10 | Atomization | 5.3 | 1904 | 10.0 | 24.0 | 12.0 | 3.9 | $28.4\pm7.2^{fgh}$ | $1014.7^{e}$ | $99.5\pm0.0^{a}$ | $76.8\pm2.5^{cde}$ | $4.6\pm0.0^{ef}$ |
| ATQ5WT11 | | | | 11.5 | 22.0 | 14.0 | 3.5 | $27.5\pm6.2^{ghi}$ | $1014.3^{f}$ | $99.7\pm0.0^{a}$ | $84.1\pm1.2^{abc}$ | $6.2\pm1.1^{cdef}$ |
| ATQ8WT8 | | | | 8.0 | 26.0 | 10.0 | 6.6 | $22.3\pm4.8^{l}$ | $1013.3^{h}$ | $97.8\pm0.7^{a}$ | $70.8\pm7.3^{de}$ | $3.6\pm0.1^{f}$ |
| ATQ8WT10 | | 8.3 | 2981 | 10.0 | 23.0 | 13.0 | 5.8 | $23.4\pm4.7^{kl}$ | $1014.8^{e}$ | $97.8\pm0.2^{a}$ | $86.2\pm5.2^{abc}$ | $3.2\pm0.2^{f}$ |
| ATQ8WT11 | | | | 11.5 | 21.0 | 15.0 | 5.3 | $25.6\pm4.6^{ij}$ | $1014.8^{e}$ | $98.1\pm1.2^{a}$ | $85.2\pm4.9^{abc}$ | $4.7\pm0.3^{def}$ |

[1]Difference of inlet and outlet temperature of the capsules on the heat exchanger; [2]Mean values ± standard error (n = 600); [3]Mean values ± standard error (n = 3); *The number after "Q" indicate heat exchanger flow rate, the number following "T" refers to heat exchanger (curing) temperature, "BS" stands for batch stirring and "AT" refers to atomization. *Different letters in superscript in each column indicate

The overall capsule diameters varied from 22.3 to 35.9 µm. For capsules produced by batch stirring the wet capsules' diameter varied from 24.8 to 35.9 µm and from 22.3 to 33.1 µm to capsules coacervated by atomization (Table 5.1). From a technological and sensory point of view, having particles or capsules with sizes smaller than 100 µm is highly desirable to avoid a "grainy" texture on the final product (LEE; LEE; DONOVAN, 2014). These results indicate that the use of a heat exchanger in a continuous mode instead of cooling in a jacketed vessel decreases the size of the capsules. In previous studies, in which complex coacervation was induced by atomization and curing the capsules was done in an cooled agitated vessel, the capsules size ranged from 57 to 85 µm (FERREIRA; NICOLETTI, 2021) and from 52 to 75 µm (FERREIRA; NICOLETTI, 2020). The smaller capsule size may be attributed to the higher shear forces, which decreases the size of the capsules in the beginning of the curing step, when temperature is not low enough to solidify the capsule wall. The capsules sizes obtained in this study are comparable to those reported in the literature using gelatin and gum Arabic: 61 to 144 µm in encapsulation of lycopene (ROCHA-SELMI; FAVARO-TRINDADE; GROSSO, 2013); 46 to 53 µm in encapsulation of turmeric oleoresin (ZUANON; MALACRIDA; TELIS, 2013), 38 to 58 µm (GUO; ZHAO, 2008) and 35 to 80 µm in encapsulation of blackberry anthocyanin (SHADDEL et al., 2018). In recent study where the complex coacervation and spray drying were combined in one step, Tang et al. (2020) reported capsules size from 13 to 18 µm. Hernández-Nava et al. (2020) obtained 21 to 94 µm in encapsulation of oregano oil using gelatin and chia mucilage by complex coacervation followed by spray drying.

The increase in shear rate caused by the increase in flow rate of the mixture containing the coacervated capsules had different effects on the capsules size for both coacervation methods (Figure 5.3). When capsules were produced by batch stirring, the increase in shear rate did not have a clear effect on the average size of the capsules (Figure 5.3a). This may be explained because at higher shear rates, although the system becomes more turbulent, which could contribute to decrease the size of the capsules, the residence time is too short to properly cool down the particles, allowing the capsules to agglomerate, thus increasing the overall size. When complex coacervation was induced by atomization, the increase in shear rate during the curing step caused the capsules size to decrease (Figure 5.3b). The difference on the relationship between capsules size and the shear rate applied can be attributed to the influence of the atomization air. Also, coacervation by batch stirring is a process driven mainly by thermodynamic forces, where those forces form the capsules and determine their size. On the other hand, coacervation by atomization has a contribution of the process conditions during atomization that forms base or foundation of the capsule when the emulsion is atomized in the

nozzle (FERREIRA; NICOLETTI, 2021). The increase of shear rate increases the energy applied on the system that decreases the size of the capsules. Since atomized capsules have already lower temperature at the beginning of the curing step the agglomeration is supressed, promoting the hardening of the capsules as expected. Some studies varying the shear forces in different ranges also reported that the increase in turbulence decreases the size of coacervated capsules (JEGAT; TAVERDET, 2000; LEMETTER; MEEUSE; ZUIDAM, 2009; LEMOS; MARIANO MARFIL; NICOLETTI, 2017).

A clear effect of the increasing shear rate was the decrease in the coefficient of variation (*CV*) of the capsules that ranged between 16 and 35 % (Figures 5.3b and 5.3d). This indicates an increase on the uniformity of the capsules sizes formed at higher values of shear rate. Having capsules with higher size uniformity is important mainly for targeted or controlled delivery of drugs, where is important to estimate, with the highest possible precision, the content of active core per capsules or per unit mass of capsules (MORELLI; HOLDICH; DRAGOSAVAC, 2017; PIACENTINI et al., 2013). Generally, *CV* values under 30 % are associated to samples with medium size distribution and under 15 % to low size distribution (BROWN; BROWN, 1998). Gomez-Estaca et al. (2016) reported *CV* of 30% in complex coacervation between gelatin and cashew gum, Morelli et al. (2017) obtained *CV* between 19 and 23 % in complex coacervation for cell encapsulation and Ferreira and Nicoletti (2020) obtained *CV* from 17 to 35 % in complex coacervation by atomization between gelatin and gum Arabic with cooling in an agitated vessel.

One important physical property, considering the separation of the capsules formed by complex coacervation, is the capsules density (Table 5.1). Capsules with higher density are of interest when separating these capsules from its supernatant solution by gravity/sedimentation (PAWAR; BOHIDAR, 2011). The overall density of the capsules coacervated by atomization (1013 to 1016 $kg/m^3$) was in the same range of the capsules coacervated in batch stirring (1011 to 1016 $kg/m^3$). After the curing step, the sedimentation of the capsules from the liquid supernatant took less than 5 minutes. In previous work, the capsules density increased from 1003 to 1022 $kg/m^3$ by increasing gelatin concentration (FERREIRA; NICOLETTI, 2021). In encapsulation of eugenol by complex coacervation using gelatin and sodium alginate Shinde and Nagarsenker (2011) reported dry capsule density of 1059 $kg/m^3$.

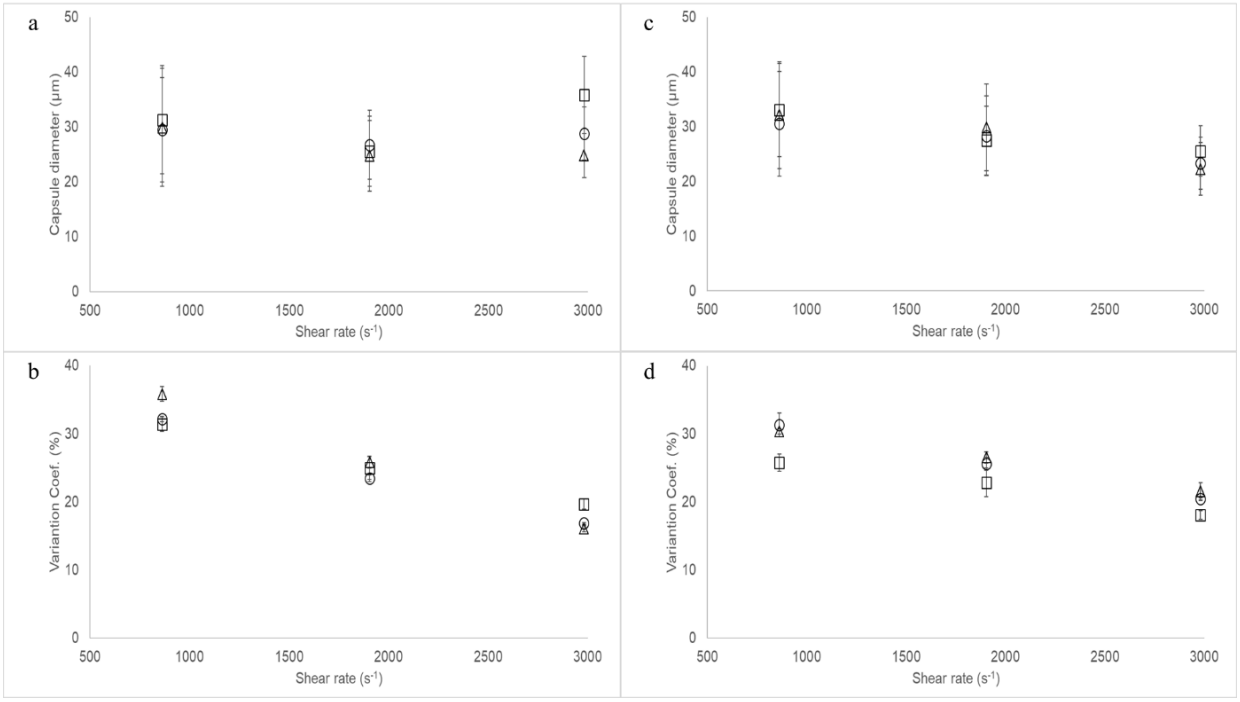


Figure 5.3. Experimental mean diameter and respective variation coefficient of wet microcapsules produced by batch stirring (a and b) and atomization (c and d) in function of shear rate during cooling. The symbols correspond to curing temperature of 8 ºC (△), 10 ºC (○) and 11.5 ºC (□).

*5.3.3 Influence of curing parameters on encapsulation performance of dried capsules*

The results previously discussed in sections 5.3.1 and 5.3.2 were obtained analysing wet capsules, right after the curing step. Encapsulation efficiency and yield were determined and will be discussed with regard to the freeze-dried capsules. The values of encapsulation efficiency (EE) were above 97 % for both coacervation methods and all curing conditions (Table 5.1). This is an important property when considering the capsule ability to protect the encapsulated core against harsh conditions after the production, instead of just transporting the core (COMUNIAN et al., 2013; ROJAS-MORENO et al., 2018). Complex coacervation is traditionally used and studied because, when carried out properly, produces capsules with high *EE* values (TIMILSENA et al., 2019; VEIS, 2011). The *EE* values obtained in this work are in accordance with previous results obtained for complex coacervation by atomization and batch stirring but cured in jacketed agitated vessel, in which different formulations caused *EE* to vary from 89 to 98% (FERREIRA; NICOLETTI, 2021), whereas the variation on the atomization conditions and emulsion concentration resulted in capsules with *EE* varying from 9 to 95 % (FERREIRA; NICOLETTI, 2020). Different values of *EE* were reported on literature: 82 % in encapsulation of pequi oil using gelatin and gum Arabic (DO NASCIMENTO et al., 2020); 57 to 65 % in encapsulation of β-carotene with casein and gum guar as wall material (THAKUR

et al., 2017) and 55 to 81 % in encapsulation of ginger oil by complex coacervation having as wall material whey protein isolate/gum Arabic and gum Arabic/chitosan (TAVARES; NOREÑA, 2020).

The overall encapsulation yield (*EY*), which represents the capsules capacity to transport the initial oil content throughout the process, varied from 66 to 93 % (Table 5.1). For capsules produced by batch stirring the *EY* ranged from 66 to 91 %. Capsules for which coacervation was induced by atomization presented slightly higher values of *EY*, which varied from 70 to 93 %. In general, the increase in the flow rate (shear rate) during cooling caused a slight decrease of *EY* (Table 5.1), with exception of sample *BSQ8T11* that will be further discussed in this section. The overall values of *EY* are in consonance with other studies of complex coacervation of ginger oil, which reported *EY* varying between 21 to 88 % (FERREIRA; NICOLETTI, 2021), 50 to 99 % (FERREIRA; NICOLETTI, 2020), 36 to 69 % (RIOS-MERA et al., 2019) and 40 to 70 % (WANG et al., 2016).

The influence of the curing temperature is presented in Figure 5.4. As a general trend, for capsules produced by batch stirring, the increase of curing temperature caused the *EY* to decrease significantly (Figure 5.4a). The only situation where there was significant increase of *EY* with increase of curing temperature was above 10 $^{o}$C for flow rate of 8.3 mL/s. On the other hand, for capsules produced by atomization, the increase of the curing temperature caused the *EY* value to increase (Figure 5.4b). These opposite behaviours between capsules produced by atomization and batch stirring may be attributed to the different procedures involved in capsule formation. Capsules coacervated in batch stirring are formed primarily by the electrostatic interaction and solvent repulsion that induces phase separation and capsule formation (ERATTE et al., 2018; TIMILSENA et al., 2019; VEIS, 2011). Since this is a slow process, when the capsules are submitted to low curing temperatures, often the gelatine/gum Arabic interactions are not completely formed and the occurrence of shear forces on the capsules allows the ginger oil (core) to leave the capsule, decreasing the *EY*. In parallel, the effects of process conditions on coacervated capsules induced by atomization may happen in two interconnected moments: first, the atomization air causes the droplet temperature to decrease and thus promotes some organization of the gelatin structure; second, as these atomized droplets with some structural organization get in contact with the gum Arabic solution, the process of coacervation (interaction) is potentialized, creating a mechanically stronger capsule in a shorter time. When these capsules undergo shear during the curing step, as the gelatin/gum Arabic interaction is already underway, lower curing temperatures causes the structure to contract and repulse the solvent faster than in proper conditions, causing the oil to be expelled from the capsules as well.

For higher curing temperature, the curing of the capsules is gentler, expelling less oil during the hardening process due to the influence of gelatin gelation, as discussed in section 5.3.2. A hypothesis is that, if higher curing temperature were applied for capsules produced by batch stirring, they could present similar behaviour to capsules produced by atomization. One indication of this can be observed for sample *BSQ8T11* (curing flow rate of 8.3 mL/s and curing temperature of 11.5 $^{o}$C coacervated in batch stirring), for which *EY* was among the highest (91.8 %). Since this sample had the shortest residence time (curing time) and highest curing temperature, the capsules would not be completely cured, forming clusters, as discussed in section 5.3.2 (Figure 5.2). The capacity of storing the oil in this case was attributed to the its possible entrapment inside the clustered structure, increasing the oil retention and *EY*.

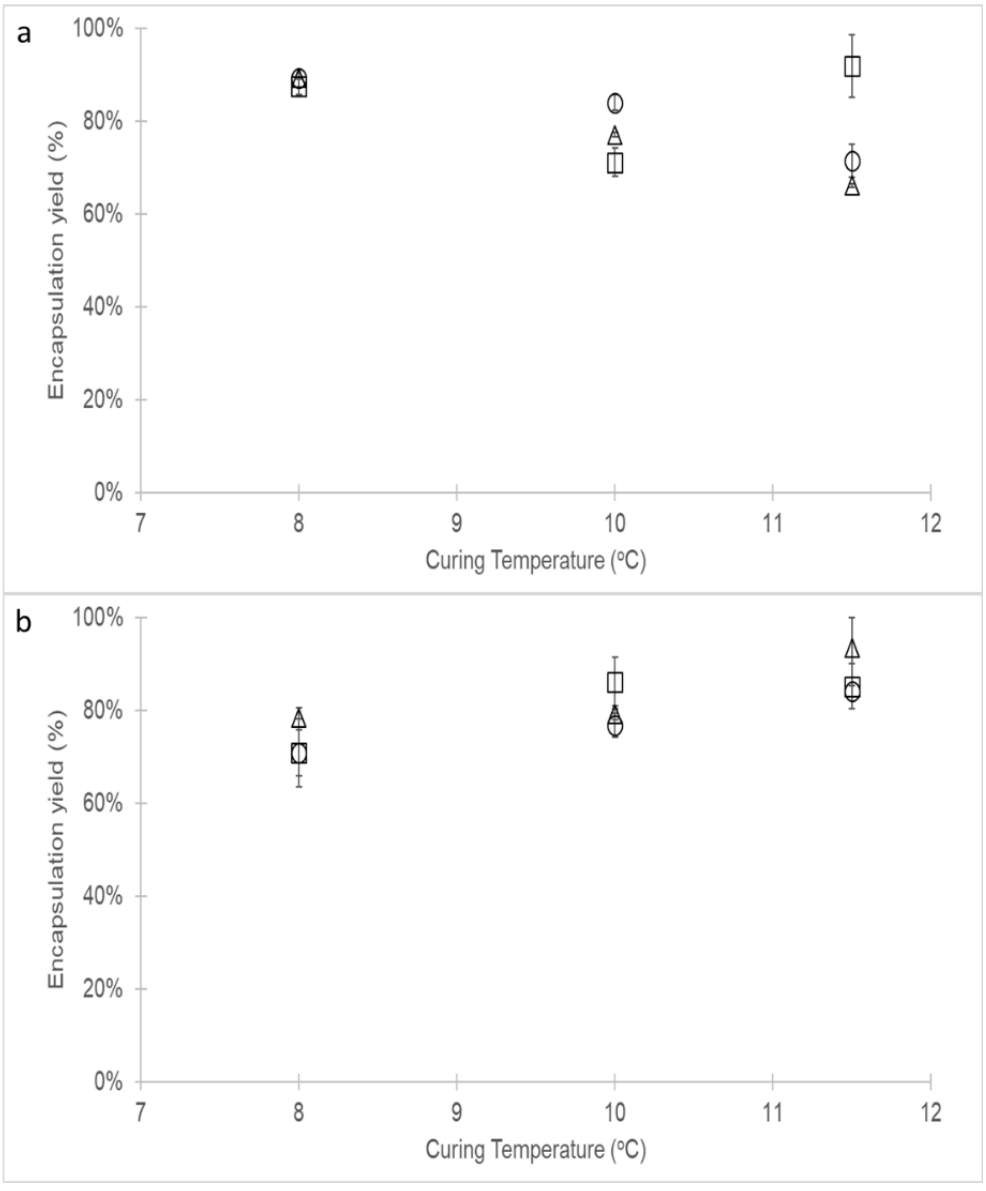


Figure 5.4. Encapsulation yield (*EY*) of the dried capsules produced by batch stirring (a) and atomization (b) in function of the curing temperature. The symbols correspond to curing flow rate (shear rate) of 2.4 mL/s (862 $s^{-1}$) (△), 5.3 mL/s (1904 $s^{-1}$) (○) and 8.3 mL/s (2981 $s^{-1}$) (□).

*5.3.4 Oil release under simulated gastric conditions*

The oil released (OR) in simulated gastric conditions was evaluated along 120 min for both complex coacervation methods and all curing conditions (Figure 5.5). Samples produced by atomization released less oil and had a lower oil release rate than capsules produced by batch stirring. In general, most of the oil was released between 0 and 60 minutes for batch stirred samples and between 0 and 30 minutes for atomized samples. The literature reports different times for the release of encapsulated core in gastric conditions, which can be attributed to different formulations, coacervation conditions, degree of interaction between the polymers and other reasons, but the reported times are of the same order of magnitude of those found in this work. Souza et al. (2019) reported release of core material around 45 minutes from complex coacervated capsules of gelatin and gum Arabic, whereas da Silva Soares et al. (2019) observed release of core material until 15 minutes from capsules produced by complex coacervation between sodium alginate and ovalbumin.

When considering the influence of the curing temperature on the OR profile of batch stirred samples, flow rate of 2.4 mL/s and curing temperature of 11.5 ºC produced capsules with the highest OR (Figure 5.5a). From 0 to 60 minutes higher curing temperature released more oil, what may indicate not proper curing of the capsules. For curing flow rate of 5.3 mL/s the curing temperature presented no influence, with OR until 60 minutes (Figure 5.5b). For curing flow rate of 8.3 mL/s the increase of curing temperature decreased the OR over time (Figure 5.5c). This means that the curing the temperature affects OR in an opposite way, depending of the curing flow rate. As discussed in section 5.3.3, this was attributed to formation of clusters of capsules, that sterically promotes retention of oil. Taking into consideration the influence of the curing flow rate, at 11.5 ºC and 2.4 mL/s OR is always increasing over time, but for higher flow rates OR increases overtime only until 60 minutes. The curing temperature affected differently the OR profile of atomized samples, mainly for flow rate of 2.4 mL/s where lower curing temperature caused higher OR overtime (Figure 5.5d). For atomized samples most of the oil was released until 30 minutes, except when curing temperature was 11.5 ºC when, independently of the curing flow rate, OR growth rate over time was constant. Flow rates of 5.3 and 8.3 mL/s presented similar OR profiles overtime independently of the curing temperature, being equal or smaller than 6% (Figure 5.5e and 5.5f). As the atomized capsules presented less formation of clusters there was less oil retention between agglomerated capsules.

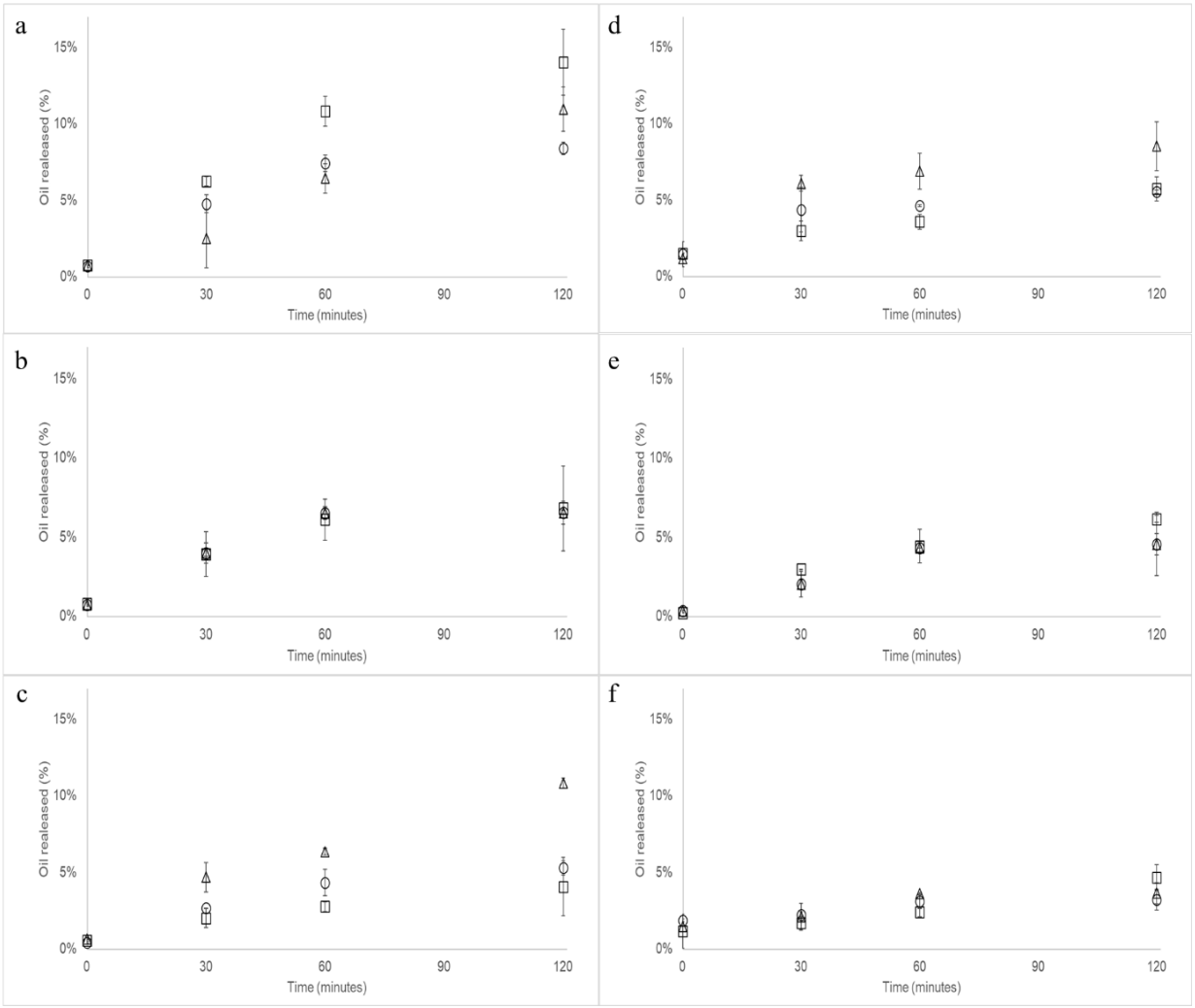


Figure 5.5. Oil released (*OR*) over time for several curing conditions for capsules coacervated by batch stirring (a, b and c) and atomization (c, d and e). Curing flow rate are represented in separated graphs, being 2.4 mL/s (862 $s^{-1}$) (a and d), 5.3 mL/s (1904 $s^{-1}$) (b and e) and 8.3 mL/s (2981 $s^{-1}$) (c and f) and the symbols correspond to curing temperature of 8 ºC (△), 10 ºC (○) and 11.5 ºC (□).

The maximum release attained after 120 minutes under gastric conditions, varied from 4 to 14 % for complex coacervation induced by batch stirring, and from 3 to 8 % for coacervation induced by atomization (Table 5.1). These results are equal or better than results of gastric stability of coacervated capsules reported in the literature. Souza et al. (2019) described lactase release of less than 20 % in complex coacervation between gelatin and gum Arabic. In complex coacervation between gelatin and gum Arabic with extra crosslinking by tannic acid, Zhang et al. (2011) presented core release of 46 %. In encapsulation of black pepper oil using lactoferrin and sodium alginate, Bastos et al. (2020) reported OR up to 24 %.

The low values of maximum OR in gastric conditions obtained in this work were expected, since the formulation was optimized by using a low pH (3.5) to induce complex coacervation (FERREIRA; NICOLETTI, 2021). Studies have shown that capsules produced by

complex coacervation at low pH tend to present higher gastric resistance (HUANG et al., 2017b, 2017a). The higher resistance to gastric conditions can be attributed to several factors. One is that when coacervation is induced at a lower pH, the gelatin surface conformation is organized in a way that can decrease its proteolysis by pepsin (FUNAMI et al., 2007). Since most of oil is released from the capsules by the proteolysis, with less active sites for the pepsin to act, less oil would be released (DA SILVA SOARES et al., 2019; DUPONT et al., 2018). A second explanation to higher gastric resistance is that for gelatin and gum Arabic, lower coacervation pH requires higher gum Arabic over gelatin ratio (FERREIRA; NICOLETTI, 2021; LI et al., 2018). Since pepsin does not hydrolyses the polysaccharide, higher concentrations of this polymer may shield the gelatin from proteolysis, thus decreasing the maximum OR (DA SILVA SOARES et al., 2019).

## 5.4. Conclusions

This work presented a novel method to carry out the cooling/curing step after complex coacervation. It opens new and promising doors to complex coacervation scale up and to carry out the process in continuous operation.

The curing process conditions (temperature and flow rate) had influence on capsule morphology, size and encapsulation parameters. Capsules for which coacervation was induced in batch stirring, with higher curing temperature and flow rate produced agglomerates or clusters of capsules that improved encapsulations parameters. The increase in shear rate (flow rate) decreased the size of atomized capsules. The encapsulation parameters obtained were satisfactory, with high encapsulation efficiency (> 97%) and high encapsulation yield, mainly for atomized capsules. The oil release in simulated gastric conditions assays was low (less than 15%), mainly for atomized capsules. This indicates that curing coacervated capsules using a heat exchange in a continuous step produces capsules resistant to gastric conditions.

The results presented in this study indicates that the use of a tubular heat exchanger to cool/cure the capsules after coacervation is a promising configuration to carry out encapsulation by complex coacervation. There are real opportunities to scale up the process of complex coacervation and to perform it in a semi-continuous configuration.

## Acknowledgements

The authors thank Adiella Abelseth for proof reading with a focus on the English language of the article.

This work was supported by the São Paulo Research Foundation - FAPESP (grant numbers 2015/23290-0 and 2018/16976-0) and National Council for Scientific and Technological Development - CNPq (grant number 305355/2016-3).

# CHAPTER 6 - METAL MEMBRANES FOR EMULSIFICATION APPLIED TO COMPLEX COACERVATION

Sungil Ferreira[12], Vania Regina Nicoletti[1], Marijana Dragosavac[2].

[1]São Paulo State University (UNESP), Department of Food Engineering and Technology, São Jose do Rio Preto – SP, 15054-000, Brazil

[2]Department of Chemical Engineering, Loughborough University, S Building, Loughborough, LE11 3TU, United Kingdom

Abstract

This study aimed to produce emulsion droplets using metal membranes to be used in complex coacervation in batch stirring and by a new method in which coacervation is induced using a two-fluid nozzle. Investigation on the optimum membrane morphology, dispersed phase injection rate and emulsification shear stress was carried out. Emulsions of gelatin and ginger oil (4 and 10 % w/w) were produced by membrane emulsification in a dispersion cell, with droplet sizes varying from 32 to 128 μm; gelatin concentration had great influence on droplet size and size distribution. Complex coacervation between gelatin and gum Arabic was carried out by atomization and batch stirring, and the size of the parent emulsion droplets, coacervation shear stress and emulsion formulation influenced the size of the capsules produced, which varied from 35 to 151 μm. Batch stirring complex coacervation produced single core capsules and atomization coacervation produced multicore capsules, both with spherical morphology. Encapsulation yield of dried capsules varied from 37 to 99% and encapsulation efficiency 5 to 66 %. Formulation had a greater effect on the encapsulation efficiency than on the encapsulation yield.

Keywords: particle size distribution, dispersion cell, membrane morphology, dimensionless numbers, low shear emulsification.

## 6.1. Introduction

The always growing application of ginger oil in several products in the food industry is mainly due to its pungent taste and characteristic odour, allied to functional properties such as antimicrobial and antioxidant activities (BAN et al., 2020; FERNANDES et al., 2016). The use of microencapsulation techniques for ginger oil is efficient, not only to increase protection of the functional compounds, but also may provide conditions to targeted delivery and controlled release of those compounds (KHODE; KATRE, 2019; MAULIDNA et al., 2020). A few methods of microencapsulation of ginger oil are reported in the literature, such as: spray drying (MAULIDNA et al., 2020), electrostatic interaction (BAN et al., 2020), and complex coacervation between gelatin and sodium alginate (WANG et al., 2016). The literature describes several techniques of microencapsulation of lipophilic compounds, in which the goal is to increase the oil bioavailability, to promote protection against degradation by physically shielding the oil using biopolymers to reduce contact between oxidizing agents (CORRÊA-FILHO; MOLDÃO-MARTINS; ALVES, 2019; RUTZ et al., 2017). The main techniques of microencapsulation for oil protection and application are spray or freeze drying of stable emulsions, ionic gelation followed or not by protein layering, and complex coacervation (GONÇALVES; ESTEVINHO; ROCHA, 2016; KANDANSAMY; SOMASUNDARAM, 2012; PAULO; SANTOS, 2017). Complex coacervation is a technique known to be effective for microencapsulation of oils and applications in food, pharmaceutical and agricultural industries, providing high values of encapsulation efficiency (ALEMZADEH et al., 2020; MARTINS et al., 2014).

Complex coacervation is carried by three independent steps: emulsification, coacervation, and shell formation (HECKERT BASTOS et al., 2020). The emulsification method for subsequent encapsulation by complex coacervation is an important task to be considered, taking into account that many of the properties of the emulsions, such as stability, volume fraction of the dispersed phase, droplets' size distribution and average particle diameter, are determined by both the formulation and the homogenization method (VLADISAVLJEVIĆ; SCHUBERT, 2003). Conventional emulsifying devices such as rotor and stator type systems, high-pressure homogenizers and ultrasonic homogenizers provide limited flexibility in terms of controlling the average particle size and the size distribution having a high energy input (DRAGOSAVAC et al., 2008). It should also be considered that traditional homogenization methods can degrade filling materials due to the instability of these compounds when subjected to the high shear rates employed (SANTOS et al., 2015). Membrane emulsification can be carried out by different types of membranes such as glass, ceramic or metal membranes

(HANCOCKS; SPYROPOULOS; NORTON, 2016). The one important difference on membranes composition lays on the tortuosity of each individual channel. In ceramic membranes there are tortuous paths where the dispersed phase has to go through, whereas in metal membranes the path is a cylindrical channel, with no tortuosity (CONSOLI; HUBINGER; DRAGOSAVAC, 2020; EGIDI et al., 2008; GIJSBERTSEN-ABRAHAMSE; VAN DER PADT; BOOM, 2004; VLADISAVLJEVIĆ; SCHUBERT, 2003). The results of the differences in the membrane natures is a lower backpressure of the system and lower shear on the dispersed phase going through the pores for metal membranes (HANCOCKS; SPYROPOULOS; NORTON, 2016). In addition, metal membrane emulsification has received attention precisely because of its ability to produce particles or droplets with low size dispersion in addition to be a system that can be scaled up for industrial scale (DRAGOSAVAC et al., 2008; HOLDICH et al., 2020; KOSVINTSEV et al., 2005; ZAWALA; SZCZEPANOWICZ; WARSZYNSKI, 2015).

The use of membranes has been shown to be efficient in the formation of stable emulsions that present desirable characteristics to be subsequently microencapsulated by complex coacervation (PIACENTINI et al., 2013). Considering that membrane emulsification happens drop by drop, as the droplets are being formed they are involved by the continuous phase, whereas the shear stress applied by the stirrer detaches the newly formed droplets from the metallic surface (EGIDI et al., 2008). In addition, it is possible to predict or engineer the size of the emulsion droplets by a balance of capillary and drag forces during the droplet formation (KOSVINTSEV et al., 2005). A handful of recent works studied the application of membrane emulsification, such as production of eco-friendly emulsions (SANTOS et al., 2015), production of food grade emulsions with different membrane compositions and morphologies (HANCOCKS; SPYROPOULOS; NORTON, 2016), comparison of azimuthal and axial oscillation microfiltration for non-Newtonian fluids (HOLDICH et al., 2018), preparation of micro and nano emulsions (VLADISAVLJEVIĆ, 2019) and the use of annular crossflow membrane using a single-pass (HOLDICH et al., 2020).

Complex coacervation is a result of the interaction polymers oppositely charged that, due to solvent repulsion, precipitate due to the solvent repulsion (KAUSHIK et al., 2015). Traditionally complex coacervation is carried out in batch stirring, where the polymers are mixed together and the coacervation is induced by pH adjustment “in loco” in order to promote electrostatic interaction. There are a few alternatives to induce complex coacervation, one of them is using atomization nozzles, were the solutions have pH adjusted beforehand. In previous works the induction of complex coacervation by atomizing the oil emulsified in gelatin over a

gum Arabic solution was studied (FERREIRA; NICOLETTI, 2020, 2021). Another approach is to induce complex coacervation using a three-fluid nozzle, in which the coacervation, shell formation and drying happens in a single step (JIANG et al., 2013). A few studies were done on membrane emulsification followed by batch stirring complex coacervation: for encapsulation of cells and colonic delivery (MORELLI; HOLDICH; DRAGOSAVAC, 2017) and production of oil droplets using fish gelatin and gum Arabic (PIACENTINI et al., 2013). However, the literature does not report the use of emulsions produced by metal membranes in complex coacervation by atomization.

For the first part of the study, Tween 20 solution (2% w/w) was used as continuous phase, considering that it is a model test system for studies comparing different membranes and emulsification conditions (HOLDICH et al., 2020; KOSVINTSEV et al., 2005). On the optimization studies of membrane emulsification, the goal was to determine the main parameters affecting membrane emulsification and to determine which membrane would be used for further emulsification assays. Two membranes were tested: membrane I (pore diameter $D_p$ = 28 μm; pore spacing $B_p$ = 102 μm) and membrane II (pore diameter $D_p$ = 24 μm; distance between pores $B_p$ = 250 μm). The pore size has direct influence on the dispersed phase flux through the membrane. The pores spacing interferes with the proper formation and separation of the emulsion droplet from the metal surface before it has contact with another droplet formed in a surrounding pore (MORELLI; HOLDICH; DRAGOSAVAC, 2017).

The objective of this work was to study the influence of metal membrane emulsification carried out using a dispersion cell, in complex coacervation by batch stirring and induced by a two-fluid nozzle. Optimization of membrane emulsification conditions was done using two membranes with different characteristics. Once the best conditions were delineated and the adequate membrane was chosen, gelatin/ginger oil emulsion was formed and used in complex coacervation assays. Finally, the morphology and size of the wet capsules and the encapsulation performance of the dried capsules were evaluated in function of the emulsification and complex coacervation conditions.

## 6.2. Material and methods

### *6.2.1 Materials*

Cold pressed ginger oil (Gran Oils, Brazil) was used as dispersed phase and microencapsulated core material. As a model test system for membrane emulsification was used Tween 20 (polyoxyethylene sorbitan monolaurate) (Fluka, United Kingdom). Type B gelatin, 240 bloom (Gelita, Mococa, Brazil) and gum Arabic (Dinâmica, Brazil) were used as wall

material. Glacial acetic acid (Dinâmica, Brazil) was used to pH adjustment. Hydrochloric acid 4 N (Dinâmica, Brazil) was used to digest the capsules to release the encapsulated oil. Hexane (Dinâmica, Brazil) was used as organic solvent for oil extraction.

*6.2.2 Membrane emulsification*

Two studies on membrane emulsification were carried out in this work. First, a broader study on the optimization of emulsification conditions varying the membrane morphology, the injection rate and the agitation/shear stress generated by the paddle stirrer was performed, using a dispersion cell (Micropore Technologies Ltd., United Kingdom) as presented in Figure 6.1. Tween 20 aqueous solution (2 % w/w) was used as continuous phase and ginger oil was used as dispersed phase. The stirrer driven by a motor powered by an AC 207-253 V power supply was used with voltage varying from 4 to 14 V, resulting in 540 to 2300 RPM or 56 to 240 rad/s, which corresponded to an applied shear stress of 7.3, 21.2, 46.1 and 68.1 Pa. The injection rate of ginger oil (dispersed phase) in the Tween 20 solution was of 1, 5 and 10 mL/min. Ginger oil was used at final concentration of 5 % (v/v) of the emulsion. Two nickel membranes (Micropore Technologies Ltd., United Kingdom) were tested during the optimization of the emulsification processes, membrane I (pore diameter $D_p$ = 28 μm; pores spacing $B_p$ = 102 μm) and membrane II ($D_p$ = 24 μm; $B_p$ = 250 μm), generating 24 emulsification conditions in total.

Based on the results of these assays, membrane II was chosen for further tests and the process conditions were narrowed down. A second set of membrane emulsification assays was carried out by dispersing ginger oil in aqueous gelatin solution for subsequent complex coacervation. Aqueous solutions of gelatin with concentrations of 4 and 10 % (w/w) were evaluated and the ratio of added ginger oil to gelatin concentration was 1:1 (gelatin:ginger oil) for all assays. Ginger oil was emulsified in the gelatin solution using the dispersion cell with membrane II. A stirrer driven by a motor powered by an AC 207-253 V power supply had voltage varying from 4 to 11 V, that corresponded to 540 to 1780 RPM or 56 to 186 rad/s, or applied shear stress of 13.0 to 97.4 Pa for emulsions with 4 % (w/w) of gelatin/ginger oil and 12.6 to 163.8 Pa for emulsions with 10 % (w/w) of gelatin/ginger oil. The injection rate of ginger oil (dispersed phase) in the continuous phase (gelatin solution 4 and 10 % (w/w)) was of 5 mL/min. Six different treatments were tested during membrane emulsification (Table 6.1). Initially, there is only the continuous phase (gelatin solution) inside the cylinder. By the end of the process the cylinder contains both dispersed (ginger oil) and continuous phase, forming a O/W emulsion.

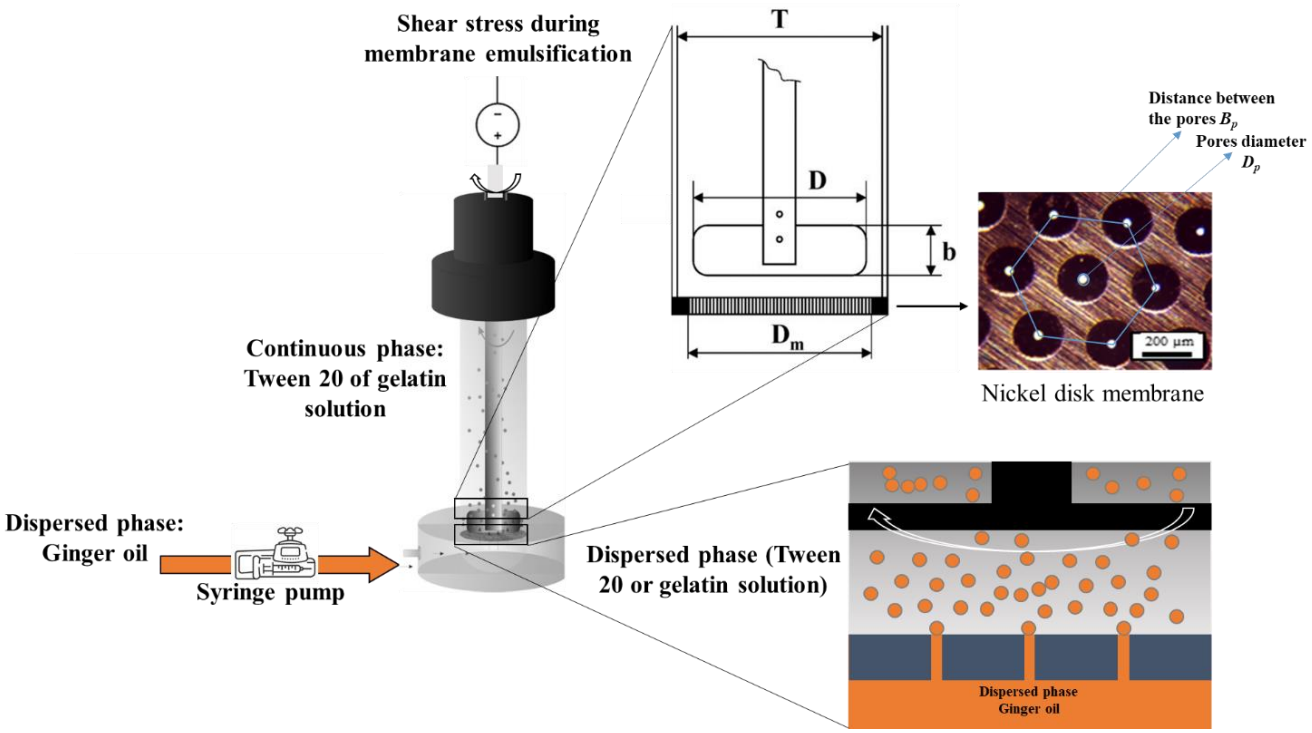


Figure 6.1. Experimental configuration and schematic diagram of dispersion cell (*DC*), used for emulsification of ginger oil in gelatin solution using metal membranes. *DC* with simple paddle stirrer above a nickel flat-disc membrane, in which T = 0.04, $D$ = 0.032 m, $D_m$ = 0.033 m and $b$ = 0.012 m.

Table 6.1. Operational parameters, size, size distribution of membrane emulsification and atomization, and encapsulation parameters.

| | | | Membrane emulsification | | | | Complex coacervation | | | | | |
|---|---|---|---|---|---|---|---|---|---|---|---|---|
| | | | | | | | Wet capsules | | | | Dry capsules | |
| Sample Code | Gelatin and ginger oil concentration (g/ 100 g of emulsion) | *Oh* | Agitation at DC (rpm) | Emulsification shear stress (Pa) | Emulsion droplet mean diameter[1] (um) | Emulsion's droplet VC (%) | Coacervation Shear Stress (Pa) | *We* | Capsule's mean diameter[2] (µm) | Capsule's VC (%) | EE[3] (%) | RO[3] (%) |
| 4GEM1BS | 4 | 0.03 | 540 | 13 | 128±35$^{a}$ | 28 | 0 | 0 | 151.3±15.2$^{a}$ | 10 | 12.9±2.2$^{hij}$ | 36.7±0.4$^{e}$ |
| 4GEM1AT1 | | | | | | | 23 | 87 | 47.8±5.3$^{kl}$ | 11 | N.A. | N.A. |
| 4GEM1AT2 | | | | | | | 48 | 242 | 57.7±7.9$^{gh}$ | 14 | N.A. | N.A. |
| 4GEM1AT3 | | | | | | | 77 | 475 | 46.4±8.8$^{lm}$ | 19 | N.A. | N.A. |
| 4GEM2BS | | | 1070 | 42 | 95±12$^{c}$ | 13 | 0 | 0 | 109.8±12.0$^{b}$ | 11 | 19.2±0.1$^{fghi}$ | 94.2±0.2$^{ab}$ |
| 4GEM2AT1 | | | | | | | 23 | 87 | 59.0±7.8$^{g}$ | 13 | 25.0±0.2$^{efgh}$ | 37.4±1.9$^{e}$ |
| 4GEM2AT2 | | | | | | | 48 | 242 | 41.7±3.8$^{p}$ | 9 | 27.2±1.0$^{defg}$ | 87.6±1.1$^{bc}$ |
| 4GEM2AT3 | | | | | | | 77 | 475 | 46.3±9.6$^{lmn}$ | 21 | 31.7±1.0$^{def}$ | 87.5±1.9$^{bc}$ |
| 4GEM3BS | | | 1780 | 97 | 67±8$^{d}$ | 12 | 0 | 0 | 76.8±8.7$^{f}$ | 11 | 5.4±0.1$^{j}$ | 99.7±0.0$^{a}$ |
| 4GEM3AT1 | | | | | | | 23 | 87 | 56.1±6.6$^{hi}$ | 12 | 9.3±0.1$^{ij}$ | 99.5±0.1$^{a}$ |
| 4GEM3AT2 | | | | | | | 48 | 242 | 44.1±4.7$^{no}$ | 11 | 34.0±1.0$^{de}$ | 99.0±0.5$^{a}$ |
| 4GEM3AT3 | | | | | | | 77 | 475 | 35.0±4.5$^{q}$ | 13 | 39.7±2.0$^{cd}$ | 99.6±0.0$^{a}$ |
| 10GEM1BS | 10 | 0.25 | 540 | 13 | 109±31$^{b}$ | 28 | 0 | 0 | 79.8±12.4$^{e}$ | 16 | 13.1±4.2$^{hij}$ | 71.3±0.5$^{d}$ |
| 10GEM1AT1 | | | | | | | 195 | 82 | 45.2±6.0$^{mno}$ | 13 | N.A. | N.A. |
| 10GEM1AT2 | | | | | | | 406 | 228 | 52.2±6.5$^{j}$ | 12 | N.A. | N.A. |
| 10GEM1AT3 | | | | | | | 657 | 447 | 43.3±6.3$^{op}$ | 15 | N.A. | N.A. |
| 10GEM2BS | | | 1070 | 57 | 32±8$^{e}$ | 24 | 0 | 0 | 100.8±14.2$^{c}$ | 14 | 17.4±0.6$^{ghij}$ | 99.0±0.9$^{a}$ |
| 10GEM2AT1 | | | | | | | 195 | 82 | 35.5±4.2$^{q}$ | 12 | 47.1±0.7$^{bc}$ | 99.6±0.2$^{a}$ |
| 10GEM2AT2 | | | | | | | 406 | 228 | 46.5±7.9$^{lm}$ | 17 | 64.7±3.3$^{a}$ | 77.6±0.1$^{d}$ |
| 10GEM2AT3 | | | | | | | 657 | 447 | 47.7±6.8$^{kl}$ | 14 | 49.8±2.1$^{bc}$ | 70.9±1.6$^{d}$ |
| 10GEM3BS | | | 1780 | 164 | 34±7$^{e}$ | 22 | 0 | 0 | 89.7±9.4$^{d}$ | 10 | 33.1±5.1$^{de}$ | 92.6±0.4$^{ab}$ |
| 10GEM3AT1 | | | | | | | 195 | 82 | 55.1±8.4$^{i}$ | 15 | 24.2±0.8$^{efgh}$ | 72.5±0.3$^{d}$ |
| 10GEM3AT2 | | | | | | | 406 | 228 | 52.6±6.1$^{j}$ | 12 | 56.2±4.0$^{ab}$ | 87.7±5.3$^{bc}$ |
| 10GEM3AT3 | | | | | | | 657 | 447 | 49.2±6.2$^{k}$ | 13 | 66.0±0.9$^{a}$ | 78.9±3.6$^{cd}$ |

[1]Mean values ± standard error (n = 300); [2]Mean values ± standard error (n = 600); [3]Mean values ± standard error (n = 3); N.A: Not applicable; *The number preceding "GE" indicate gelatin concentration, the number following "M" refers to membrane emulsification rpm/shear stress, the number following letters "AC" refers to atomization condition and "BS" stands for batch stirring. Different letters in superscript in each column indicate significant differences (Tukey test, $p < 0.05$)

*6.2.3 Mathematical description of the membrane emulsification process*

The emulsification process can be described in function of the shear stress applied during the membrane homogenisation. Equation (6.1) can be used to determine the boundary layer thickness (LANDAU; LIFSHITZ, 1966). Figure 6.1 presents the dimensions of the *DC*.

$$\delta = \sqrt{\frac{\mu}{\rho\omega}} \tag{6.1}$$

The radial distance at which the shear stress is maximum is called transitional radius and can be determined by equation (6.2):

$$r_{trans} = 1.23\frac{D}{2}\left(0.57 + \frac{D}{T}\right)\left(\frac{b}{T}\right)^{0.036} n^{0.016}\frac{Re_{me}}{1000+1.43Re_{me}} \tag{6.2}$$

in which D is the stirrer diameter, T is the dispersion cell diameter, *b* is the blade height, and *n* is the number of impeller blades. The Reynolds number during membrane emulsification ($Re_{me}$) can be defined by equation (6.3):

$$Re_{me} = \frac{\omega\rho D^2}{2\pi\mu} \tag{6.3}$$

in which ρ and μ are the continuous phase density and viscosity, respectively, and ω is the angular velocity in rad/s.

The maximum shear stress applied on the system by the stirrer paddler can be determined using equation (6.4).

$$\tau_{max} = \frac{0.825\mu\omega r_{trans}}{\delta} \tag{6.4}$$

Finally, using a simple force balance at the pore exit between the capillary ($F_{ca}=\pi d_p\gamma$) and drag force ($F_{drag}= 9\pi\tau d_p((d_d/2)^2-r_p^2)^{1/2}$), a model to predict the droplet diameter ($d_d$) can be determined. Assuming that in order to form droplets at the surface of the membrane $F_{ca} = F_{drag}$, where $r_p$ is the pore radius and γ is the interfacial tension and solving it for $d_d$ results in equation (6.5) (KOSVINTSEV et al., 2005).

$$d_d = \frac{\sqrt{18\tau^2 r_p{}^2 + 2\sqrt{81\tau^4 r_p{}^4 + 4\tau^2 r_p{}^2\gamma^2}}}{3\tau} \tag{6.5}$$

*6.2.4 Characterization of emulsion and biopolymer solutions*

The interfacial tension between the ginger oil/Tween 20 solution, ginger oil/gelatin solution and the surface tension measurements of the emulsion containing gelatin and ginger oil were measured in an DB2KS tensiometer (White Electric Instrument, United Kingdom) by the Du Noüy ring method using a platinum ring. The density of the gelatin solutions and gelatin/ginger oil emulsions were determined in a densimeter DMA ™ 4500 M (Anton Paar,

Austria) at 35 ºC. The rheological behaviour was evaluated in a rheometer AR100-N (TA Instruments, USA) at 35 ºC using a cone and plate geometry where the flow curves were determined. The parameters determined and used in the calculations of membrane emulsification and atomization are presented in Table 6.2. The emulsion droplet sizes and morphology were evaluated using an optical microscope GXML3201(GX microscopes, United Kingdom) coupled with a Retiga 6000 colour camera and the scanned images were analysed by Image Pro Plus 6.0 software (Media Cybernetics Inc., USA) for measurement of droplet diameters, reporting the average diameter of 300 droplets per sample.

*6.2.5 Complex coacervation in batch stirring*

Complex coacervation in batch stirring was done following the method described by Marfil et al. (2018), with modifications. Ginger oil/gelatin emulsions (4 and 10 % w/w) (106 g) (50 ± 1 °C) was added to the gum Arabic solution (1 % w/w) (890 and 1680 g) (50 ± 1 °C) in a 2 L beaker, and the mixture was kept under magnetic stirring (approximately 300 rpm). The pH (3.5 ± 0.1) was adjusted using pure glacial acetic acid and the system was immersed in an ice bath, maintaining agitation for slow cooling until 10 ± 1 °C. After 24 hours, the sedimented particles were transferred to aluminium trays and frozen at -20 °C. Drying was carried out by lyophilisation for 72 hours for further analyses.

Table 6.2. Physicochemical properties of gelatin and Tween 20 solutions used during membrane emulsification assays and ginger oil/gelatin emulsions used during complex coacervation.

| Continuous phase | Polymer concentration (g/100 g) | Ginger oil concentration (g/100 g) | Interfacial tension continuous phase/ginger oil[2] (mN/m) | Continuous phase viscosity (mPa·s) | Continuous phase density ($kg/m^3$) | Emulsion viscosity[1] (mPa·s) | Emulsion density[1] ($kg/m^3$) | Emulsion surface tension[2] (mN/m) |
|---|---|---|---|---|---|---|---|---|
| Gelatin | 4 | 4 | 9.3±0.1 | 5.2 | 1006.2±0.0 | 5.9 | 1002.4±0.1 | 49.9±0.4 |
| | 10 | 10 | 11.3±0.3 | 48.3 | 1025.3±0.0 | 48.1 | 1010.5±0.1 | 52.3±0.2 |
| Tween 20 | 2 | 5 | 5.1±0.2 | 1.02 | 999.5±0.0 | - | - | - |

[1]Mean values ± standard error (n = 3); [2]Mean values ± standard error (n = 10)

*6.2.6 Complex coacervation by atomization*

Complex coacervation by atomization was carried out as described by Ferreira and Nicoletti (2020) and Ferreira and Nicoletti (2021). Ginger oil/gelatin emulsions (4 and 10 % w/w) (106 g) were atomized over the aqueous solution of gum Arabic (1% w/w) (890 and 1680 g) using a two-fluid nozzle (0.7 mm diameter, Labmaq, Brazil), with controlled air and emulsion flowrates. The pH of the emulsion and of gum Arabic solution were adjusted to 3.5 before atomization. The atomization conditions and additional operational parameters are summarized in Table 6.3. The nozzle was positioned at a fixed height of 0.2 m above the vessel containing gum Arabic solution as described in Figure 6.2. Air flowrate was controlled using a rotameter FT074-02-CA-VN (Omega, USA). At the end of the coacervation process the system was immersed in an ice bath until reaching 10 ± 1 °C and then stored at 5 ± 1 °C in refrigerator.

Table 6.3. Physical properties of atomization air, dimensions of the atomization nozzle and operational parameters of atomization.

| **Characteristics of the two fluid nozzle** | |
|---|---|
| Diameter of emulsion outlet ($D_l$) - (mm) | 0.7 |
| Internal diameter of air outlet ($D_{int}$) - (mm) | 1.90 |
| External diameter of air outlet ($D_{ext}$) - (mm) | 2.80 |
| Emulsion outlet area - ($mm^2$) | 0.385 |
| Atomization air outlet area - ($mm^2$) | 3.32 |
| **Physical properties of the atomization air (25 ºC)** | |
| Density ($\rho_g$) - (kg $m^{-3}$) | 1.23 |
| Viscosity ($\mu_g$) - (µPa s) | 18 |
| **Atomization process parameters** | |
| Atomization air volumetric flow rate ($Q_g$) -$10^{-04}$ ($m^3$ $s^{-1}$) | 2.36 to 5.51 |
| Emulsion volumetric flow rate ($Q_l$) - $10^{-07}$ ($m^3$ $s^{-1}$) | 1.63 to 2.40 |
| Atomization air velocity ($V_g$) - (m $s^{-1}$) | 71.1 to 165.2 |
| Emulsion velocity ($V_l$) - (m $s^{-1}$) | 0.42 to 0.64 |

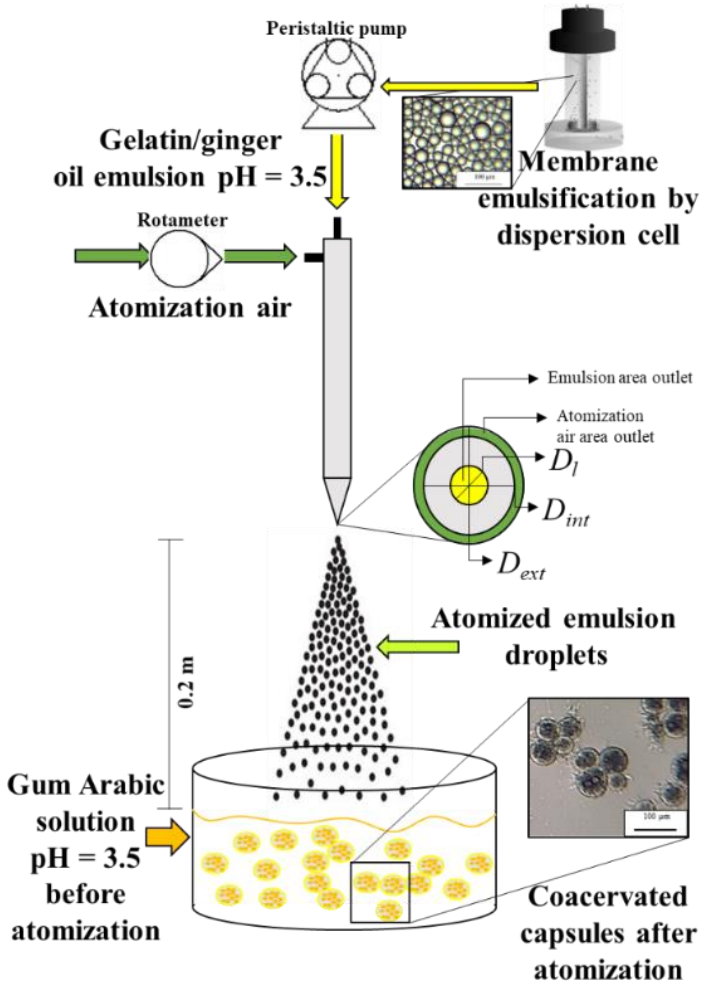


Figure 6.2. Schematic diagram of the complex coacervation process by atomization.

The complex coacervation by atomization process using a two-fluid nozzle was evaluated through the Weber (*We*, Equation 6.6) and Ohnesorge (*Oh*, Equation 6.7) numbers (FILKOVÁ; HUANG; MUJUMDAR, 2014). The shear stress during the atomization process was determined in function of the Weber number. Emulsions with 4 % (w/w) of gelatin/ginger oil behaved like a Newtonian fluid and Equation 6.8 was used to determine its shear stress during atomization. For emulsions with 10 % (w/w) of gelatin/ginger oil, which behaved as a Bingham fluid, Equation 6.9 was used (FERREIRA; NICOLETTI, 2020).

$$We = \frac{\rho_g (V_g - V_l)^2 D_l}{\sigma} \tag{6.6}$$

$$Oh = \frac{\mu_l}{\sqrt{\sigma D_l \rho_l}} \tag{6.7}$$

$$\tau_n = (25.3\, We + 2247.3)\, \mu_l \tag{6.8}$$

$$\tau_b = \tau_0 + \mu_l (25.3\, We + 2247.3) \tag{6.9}$$

In which $V_g$ is the atomizing air velocity; $V_l$ is the emulsion velocity; $\rho_g$ is the density of the atomizing air; $D_l$ is the diameter of the discharge orifice of the nozzle; σ is the emulsion surface tension; $\mu_l$ is the emulsion viscosity and $\rho_l$ the emulsion density.

*6.2.7 Characterization of wet microcapsules*

The microstructure of wet microcapsules was evaluated using an optical microscope GXML3201(GX microscopes, United Kingdom) coupled with a Retiga 6000 colour camera. The samples were conditioned on glass slides without dilution. The scanned images were analysed by Image Pro Plus 6.0 software (Media Cybernetics Inc., USA) for measurement of capsules diameters, reporting the average diameter of 600 capsules per sample.

*6.2.8 Characterization of dried microcapsules*

Encapsulation performance was determined as described by Tonon, Grosso and Hubinger (2011) and Wang, Adhikari and Barrow (2014), with modifications. Encapsulation performance was evaluated in terms of encapsulation efficiency (*EE*) that considers the total oil in the capsules (*OT*) and the capsule surface oil (*OS*), and encapsulation yield (*EY*) that considers the total oil on the initial emulsion (*OI*) versus the capsules total oil content after complex coacervation. After complex coacervation the capsules were freeze-dried and subjected to analysis as follows. To determine *OS*, 100 mg of microcapsules and 10 mL of hexane were shaken for one minute. The organic phase was filtered and the solvent was evaporated at 25 °C in a hood and then at 60 °C in drying oven until constant weight. *OT* was calculated mixing 100 mg of microcapsules in 20 mL of 4 N hydrochloric acid solution and kept under agitation for 1 hour at 35 °C for dissolution of the biopolymers. Then, 13 mL of hexane were added and again kept under agitation for 10 hours at 25 °C, forming a two-phase system. The two phases were separated by centrifugation (model Z 326 K, Hermle, Germany) at 10000×g for 30 minutes and the organic phase containing hexane and oil was transferred to Petri dishes. The solvent was evaporated at 25 °C in a hood and then at 60 °C in drying oven until constant weight. The *EE* and *EY* were calculated by Equations 6.10 and 6.11, respectively.

$$EE(\%) = \frac{OT - OS}{OT} \times 100 \quad (6.10)$$

$$EY(\%) = \frac{OT}{OI} \times 100 \quad (6.11)$$

*6.2.9 Statistical analysis*

All the assays were performed in triplicate. The results of the analytical determinations are expressed in arithmetic average submitted to analysis of variance (ANOVA) and comparison of means by Tukey test with probability level at 5% ($p \leq 0.05$), using statistical software Minitab 17 (MINITAB, USA). The uniformity of the data (size distribution) was presented in terms of the variation coefficient [VC=(SD/AV)*100], in which SD stands for standard deviation of the measurements.

## 6.3. Results and discussion

*6.3.1 Optimization of membrane emulsification parameters*

Figure 6.3 presents the results of average diameters and size distribution of the emulsion droplets formed using membranes I and II in function of the shear stress applied during membrane emulsification.

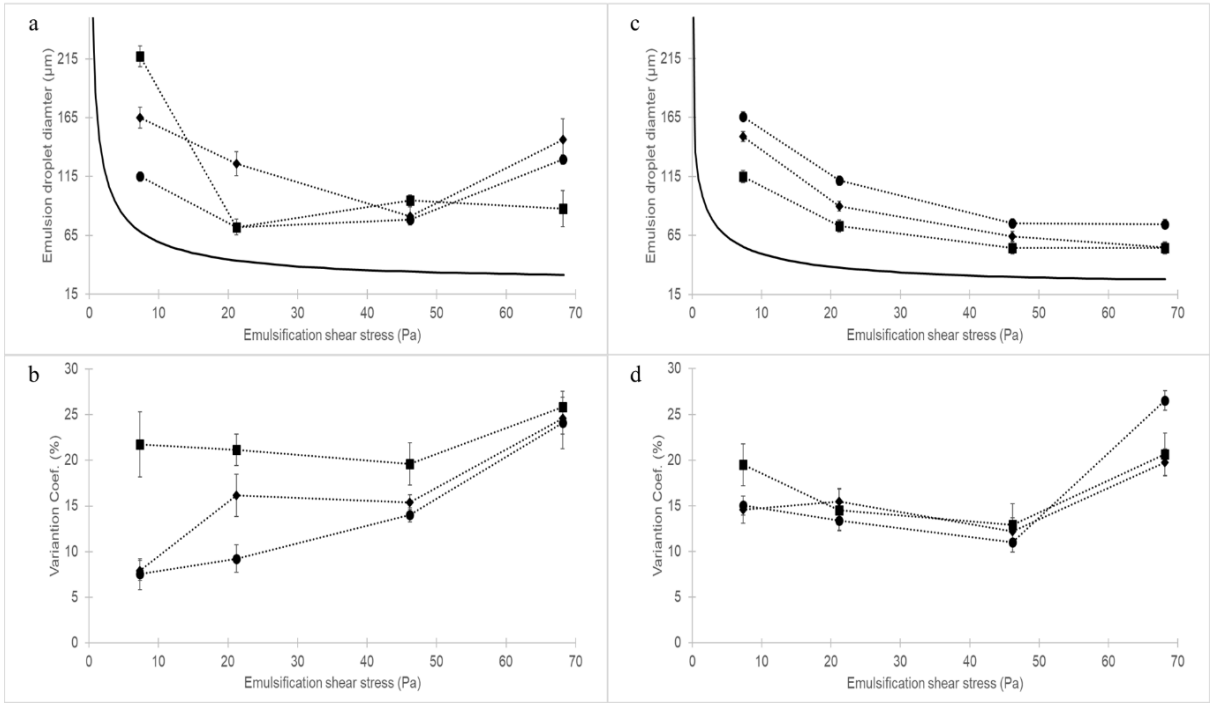


Figure 6.3. Size and size distribution of emulsion droplets in function of shear stress during membrane emulsification of ginger oil in Tween 20 solution for (a) average size for membrane I; (c) average size for membrane II; (b) variation coefficient for membrane I; (d) variation coefficient for membrane II. Symbols represent the injection rate: (■) 1 mL/min; (♦) 5 mL/min; (●) 10 mL/min; (▬) Equation 6.5.

For the emulsions produced using membrane I, the droplet diameters varied from 65 to 217 µm. In general, the experimental values did not follow the model (Equation 6.5) regarding the droplet diameters (Figure 6.3a), and no defined trend was observed when the

droplet diameter was plotted in function of the shear stress. Also, the increase in shear stress for the same oil injection rate, did not cause decreasing in the droplet diameter, with exception of samples subjected to shear stress of 7 Pa. Similar result was reported by Zhu and Barrow (2005), that varied the pore spacing from 20 to 100 μm using stationary and vibrating micro-machined membranes for emulsification and reported that the droplet size decreased with the increase of the injection rate, for smaller pore spacing. This may be related to the relationship between the transmembrane flux and the shear stress responsible to detach the droplets. An increase in the injection rate at constant shear stress, means an increase of the flux on each pore, and thus a possible increase on the speed of the detachment of the droplets. It is possible to say that 7 Pa could not be enough shear stress to detach the droplet from the membrane surface at lower injection rates and due to physical contact with neighbour droplets from neighbour pores the droplets presented an early coalescence. The early coalescence due to physical contact between the droplets ends up producing larger droplets with a wider size distribution for lower injection rates. It is possible to avoid early coalescence even for droplets that suffer physical contact before detachment, but higher concentrations of surfactant may be required (VLADISAVLJEVIĆ et al., 2007). For conditions where the physical contact between the droplet does not cause early coalescence, it is observed a “push off” effect, in which the contact between the droplets promotes the detachment from the membrane, leading to a more uniform size dispersion (DRAGOSAVAC et al., 2008; EGIDI et al., 2008; HOLDICH et al., 2020). Abrahamse et al. (2002), studying the droplet interaction in crossflow emulsification, found the droplets in neighbour pores may have physical contact among themselves generating early surface coalescence and the author attributed the growing of the droplets before detaching from the membrane to the steric interfere between the droplets. Studies on the literature regarding the kinetics of droplet formation may consider only the formation of one droplet in one pore, without consider the interaction between the droplets in neighbour pores (EGIDI et al., 2008; ZAWALA; SZCZEPANOWICZ; WARSZYNSKI, 2015). Zawala et al. (2015) reported the same result as reported at low shear stress, studying the experimental and theoretical behaviour of droplet detachment formed in a single pore, where a decrease on the droplet size with the increase of the dispersed phase injection rate was observed. However, it is important to note that this was observed in situations where the droplet size and the distance between the pores are of the same magnitude, and for lower detachment shear stress. The situation where the droplets detach from the membrane without the action of shear forces is called spontaneous transformation-based droplet formation, where the detachment is due to the geometry of the system membrane/droplet (EGIDI et al., 2008). The variation coefficient for emulsion droplets

formed using membrane I (Figures 6.3b) presented values under 30 %, with a trend to increase with the increase of emulsification shear stress. As can be seen in Figure 6.4b, emulsion droplets produced using membrane I have a wide size dispersion between the droplets. The pores distance of membrane I is $B_p$ = 102 µm and the average of the droplet diameter is greater than 65 µm, being more evidence of an early coalescence between the droplets due to physical contact. Considering that when the ginger oil is being pushed through the membrane and the droplet is being formed, if the space between two droplets in two nearby pores is not large enough, these droplets may coalesce before detach for the membrane surface, increasing the droplet size (DRAGOSAVAC et al., 2008).

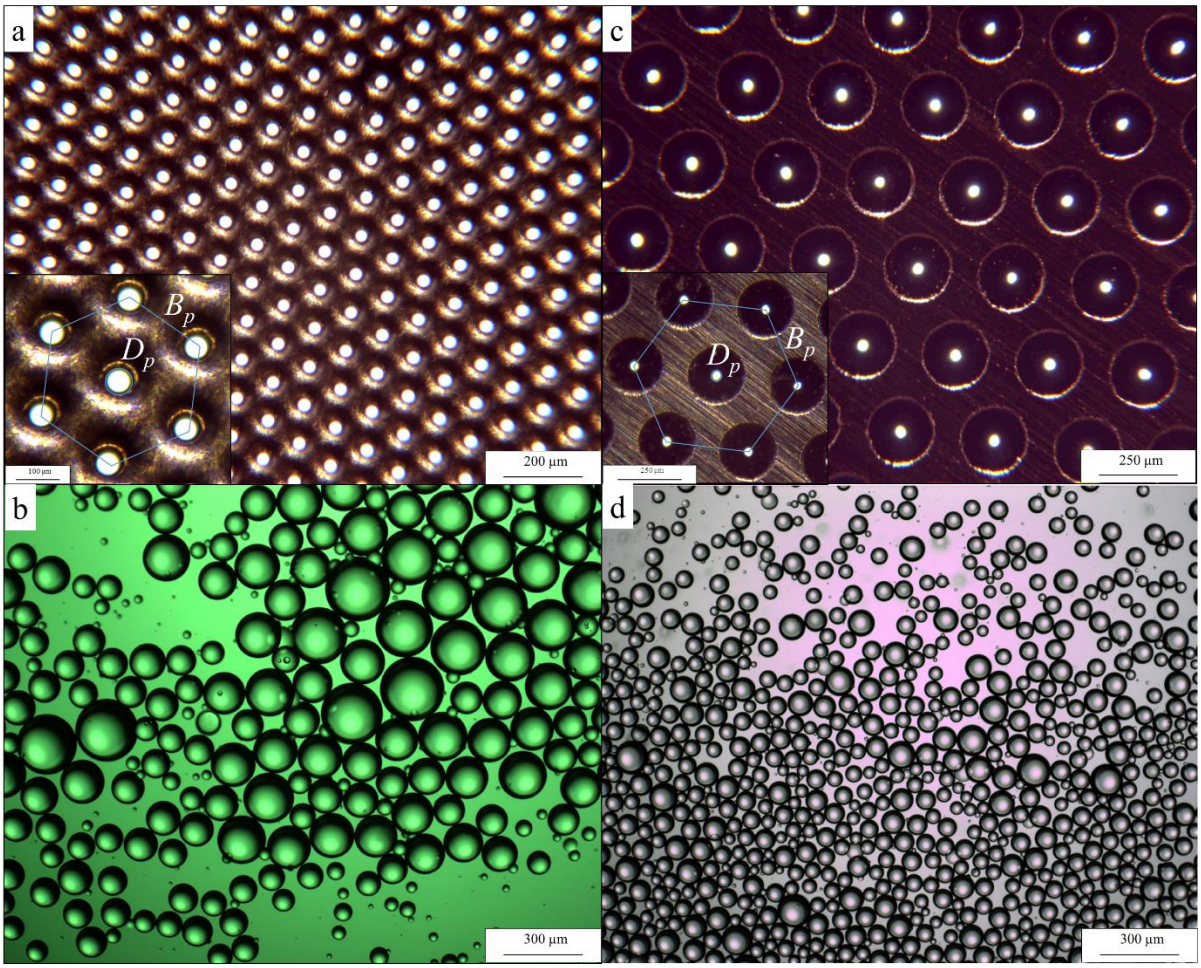


Figure 6.4. Morphology of metal membranes and Tween 20/ginger oil emulsion droplets. (a) Membrane I, $D_p$ = 28 µm and $B_p$ = 102 µm. (c) Membrane II, $D_p$ = 24 µm and $B_p$ = 250 µm. Emulsion droplets for (b) membrane I and (d) membrane II at 7 Pa of shear stress and 1 mL/min injection rate.

The droplets in the emulsion formed by membrane II had diameters varying from 54 to 165 µm (Figure 6.3c). Considering the model to predict the droplet diameter (Equation 6.5),

membrane II produced droplets that followed the trend predicted by the model, for all values of injection rate tested. The average diameter reported for emulsification shear stress of 46 and 68 Pa did not present statistical difference, indicating that the droplet sizes at 46 Pa would be the smallest possible to be obtained with a membrane with those characteristics, without affecting the size distribution. Differently from membrane I, the emulsion droplet diameter for the same shear stress increased with increasing oil injection rate, and no sign of early surface coalescence was observed, corroborating with the proposition of the influence of the pore spacing and final droplet size on the detachment process. In a recent study of membrane emulsification in crossflow using single annular pass, it was reported that for all shear stresses and injection rates tested there was a decrease of droplet diameter with the increase of shear stress, and an increase of droplet diameter with the increase of the injection rate (HOLDICH et al., 2020). The variation coefficient reached a minimum at 46 Pa increasing again after that, indicating that there is a limit of shear stress that can be applied on the system before it affects the size distribution (Figure 6.3d). The uniformity on the size of the capsules can be seen in Figure 6.4d where, in contrary of the observed for membrane II (Figure 6.4b), most of the capsules have similar diameter. Still, no treatment presented a VC higher than 30 %, indicating that the emulsification process is robust in replicating the droplet sizes on the conditions tested. The different profile of droplets that resulted from membranes I and II corroborates with the proposition of the influence of pore distance and droplet size on detachment process due to early sterical coalescence, if this distance is not large enough for low shear stress.

Considering that, for low or no shear stress, the detaching process of the droplet depends on the physical properties of the pores and droplets (EGIDI et al., 2008), evaluating the ratio between the droplet average diameter and the pores spacing ($R_{dB} = d_{av}/B_p$), and the ratio between pore diameter and pore spacing ($R_{pB} = D_d/B_p$), a membrane parameter, gives a good idea on the potential for physical contact and early coalescence between the droplets. At the lowest emulsification shear stress (7 Pa), increasing of injection rate resulted in $R_{dB}$ values of 2.13, 1.62, 1.13 for membrane I and 0.46, 0.60, 0.66 for membrane II. Moreover, membrane I had $R_{pB}$ = 0.27 and for membrane II $R_{pB}$ = 0.096. Smaller values of $R_{pB}$ means that the pore sizes are smaller, in comparison with the pore spacing, thus it is expected that smaller $R_{pB}$ decreases the probability of physical contact between the droplets prior to detach from the membrane, considering low values of shear stress. By the theoretical interpretation of $R_{dB}$, at lower or no shear, $R_{dB} < 1$ decrease the probability of physical contact between droplets in neighbour pores. Dragosavac *et al.* (2012) studying emulsification of pumpkin oil in Tween 20 solution for the production of multiple emulsions, reported that for shear stress of 1 Pa the

highest values of droplet size and size distribution ($1.5 < R_{dB} < 2.15$) was observed. In addition, the authors reported that for the same value of emulsification shear stress, when $R_{pB} = 0.1$ the droplet diameters varied from 150 to 200 μm and for $R_{pB} = 0.2$ the droplet size varied from 200 to 250 μm. Morelli et al. (2017) reported the highest values of droplet size ($R_{dB} = 1.7$) for shear stress of 1 Pa and the membrane used for emulsification for cell encapsulation and colonic delivery had $R_{pB} = 0.15$. The influence of emulsification shear stress was reported by Holdich *et al.* (2020): for shear stress of 0.8 Pa, $R_{dB}$ was 0.915, whereas for 6.0 Pa, $R_{dB}$ was 0.41 at the same surfactant concentration, using a membrane with $R_{pB} = 0.075$, in membrane emulsification by crossflow using a single annular pass. Egidi et al. (2008) reported that membrane with $R_{pB} = 0.25$ produced droplets considerable larger than a membrane with $R_{pB} = 0.1$, for low values of shear stress. In this sense, the authors propose that for emulsification conditions were is required to use low or no shear stress, the evidences show that is better to use a membrane with $R_{pB} \leq 0.1$, aiming to produce droplets in a region of $R_{dB} < 0.8$, thus avoiding the early coalescence between the droplets. The authors also recommend more studies focusing on droplet formation and detachment from the metal membrane, to further understand the kinect of this processes under low or no shear stress.

Based on the results presented in Figures 6.3 and 6.4, considering the droplet diameters and the respective size distribution, membrane II ($R_{pB} = 0.096$) was chosen for the next assays, taking into account that the experimental data showed a behaviour more compatible with the trend predicted by the theoretical model and presented a narrower and controlled *VC*, indicating a lower droplet size polydispersity. Therefore, the parameters on the dispersion cell to be applied in emulsification of ginger oil in gelatin solution was set to vary from 540 to 1780 RPM, which is 13 to 97 Pa for solution with 4 % (w/w) of gelatin, 13 to 164 Pa for gelatin solution with 10 % (w/w) of gelatin and injection rate of 5 mL/min.

### *6.3.2 Membrane emulsification of ginger oil in gelatin solution*

In order to obtain an efficient encapsulation process, the core and wall material must form a proper emulsion (FERREIRA et al., 2019; KAUSHIK et al., 2015). When using membrane emulsification (*ME*), parameters such as droplet mean diameter and size distribution will tell how stable the process is being carried, due to the minimization of Ostwald ripening or droplet coalescence (ZAWALA; SZCZEPANOWICZ; WARSZYNSKI, 2015). The results for membrane emulsification of ginger oil in gelatin solution of 4 and 10 % (w/w) are presented in Figure 6.5.

As can be seen in Figure 6.5a, the emulsion with 4 % of gelatin presented a significant linear decrease in droplet diameter with the increase in shear stress during membrane emulsification. The experimental droplet diameter did not match the diameter predicted by the model varying from 67 to 128 µm. The authors speculate that the model's value could be achieved in higher values of shear stress. Several studies reported that mainly for lower or mid values of shear stress, the experimental data does not match the predicted droplet size (HOLDICH et al., 2020; MORELLI; HOLDICH; DRAGOSAVAC, 2017; SANTOS et al., 2015). The *VC* for samples produced with 4 % (w/w) of gelatin presented a higher value (27%) for lower values of sheer stress. With the increase of shear stress there was a decrease of VC reaching below 15 % (Figure 6.5b), which indicates a production of emulsion droplets with low size distribution (MORELLI; HOLDICH; DRAGOSAVAC, 2017; STILLWELL et al., 2007).

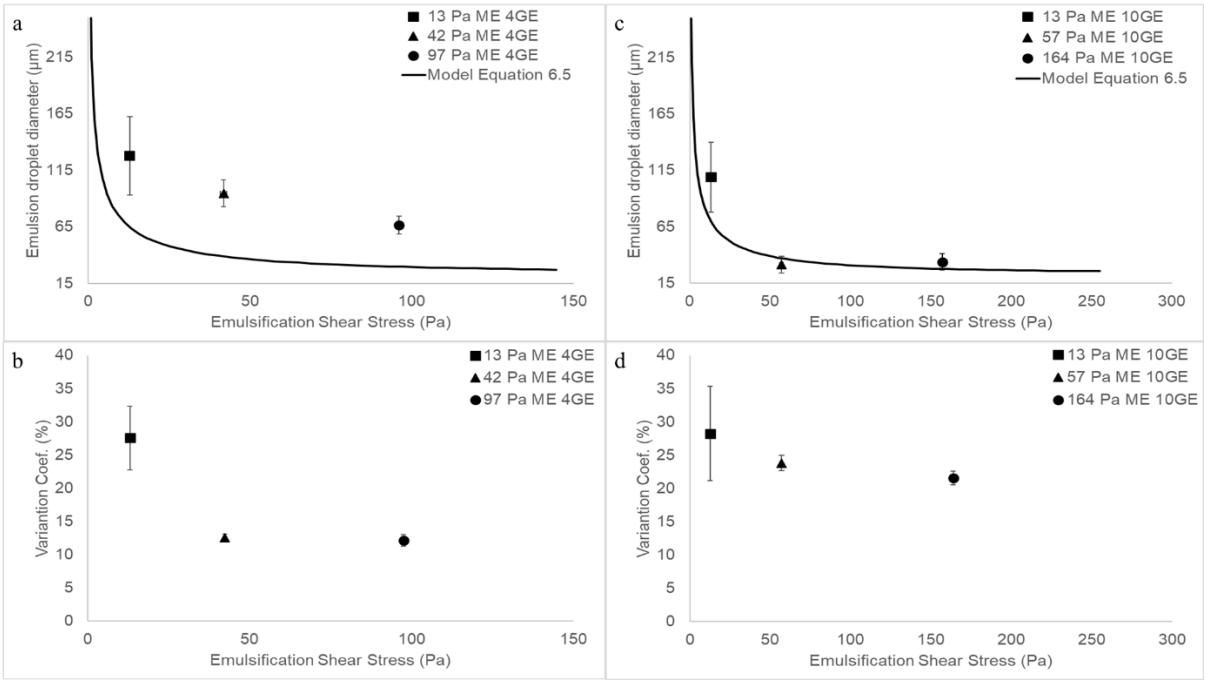


Figure 6.5. Size and size distribution in function of shear stress and injection rate of droplets produced by membrane emulsification of ginger oil in gelatin solution. (a) diameter of droplets with 4% of gelatin (experimental and model) in function of emulsification shear stress; (b) VC of the diameter of droplets with 4% of gelatin in function of emulsification shear stress; (c) diameter of droplets with 10% of gelatin (experimental and model) in function of emulsification shear stress; (d) VC of the diameter of droplets with 10% of gelatin in function of emulsification shear stress.

For emulsions produced with 10 % (w/w) of gelatin the experimental diameter and the values predicted by the model followed the same trend. In addition, the model (equation 6.5) predicted properly the experimental droplets diameters. The increase of shear stress caused a significant decrease in droplet diameters from 109 to 35 µm (Figure 6.5c). The same is

reported in the literature in several studies (DRAGOSAVAC et al., 2012; HOLDICH et al., 2010; PU; WOLF; DRAGOSAVAC, 2019; VLADISAVLJEVIĆ; SCHUBERT, 2003). On the other hand, the corresponding *VC* was slightly higher (21 - 28 %), decreasing with the increase in shear stress (Figure 6.5d).

By comparing the morphology of the emulsion droplets (Figure 6.6) it is clear the influence of the formulation on the size and size dispersion, corroborating with previous results. For Figure 6.6a and Figure 6.6d the droplets have the same size magnitude, however as the shear stress increases the emulsions with 10 % (w/w) of gelatin (Figures 6.6e and 6.6f) have a much larger decrease on droplet size than the emulsions with 4 % (w/w) of gelatin (Figure 6.6b and 6.6c). The reason why emulsions with higher gelatin concentration present higher size distribution is believed to be related to its higher viscosity. However, the same reason can be used to explain the fact that the model to predict the droplet size works better for more viscous emulsions. The model uses a balance force between capillary and drag forces to predict the size of the droplet after leaving the membrane pore (KOSVINTSEV et al., 2005; STILLWELL et al., 2007). Thus, having a viscous continuous phase with good emulsification properties may allow the oil droplet (dispersed phase) to keep its original size due to steric stabilization, in synergy with the shear stress applied on the system through agitation (TANAKA et al., 2020).

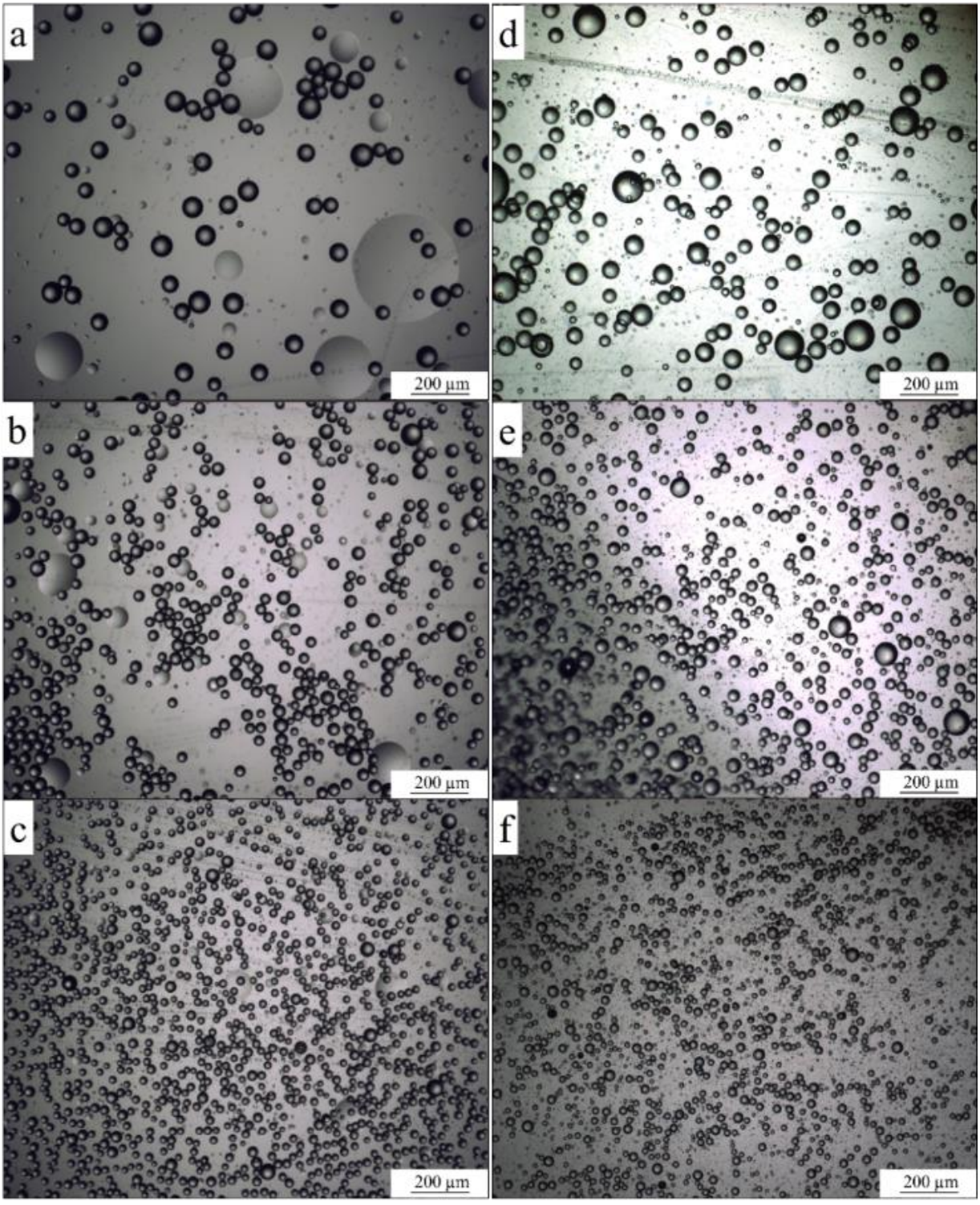


Figure 6.6. Morphology of gelatin/ginger oil emulsion droplets formed by membrane emulsification with 4 % of gelatin (a = 13 Pa, b = 42 Pa and c = 97 Pa) and 10 % of gelatin (c = 13 Pa, e = 57 Pa and f = 164 Pa) and 5 mL/min.

*6.3.3 Effect of complex coacervation by batch stirring and by atomization on wet capsules size and morphology*

In this section, the effects of complex coacervation conditions and methods (atomization or batch stirring) on capsules' size and morphology will be discussed. Complex coacervation was carried out departing from gelatin/ginger oil emulsions produced by metal membrane using the dispersion cell (*DC*). It is important to note that two kinds of shear stress will be taken into account: emulsification shear stress, which is related to the agitation applied on the system by the stirring paddle in the *DC*; and coacervation shear stress, which is related to the Weber number (*We*) during the atomization process of the gelatin/ginger oil emulsion over the Arabic gum solution (Figure 6.2).

Three atomization conditions (low, medium and high shear stress/*We*) were studied. It is possible to mathematically correlate *We* (Equation 6.6) and shear stress during coacervation for emulsions with 4 % (w/w) of gelatin (Equation 6.8) and 10 % (w/w) of gelatin (Equation 6.9). Figure 6.7 presents the relationship between size of the capsules produced under different conditions for complex coacervation (three conditions of atomization and one condition for batch stirring) in function of the shear stress during membrane emulsification.

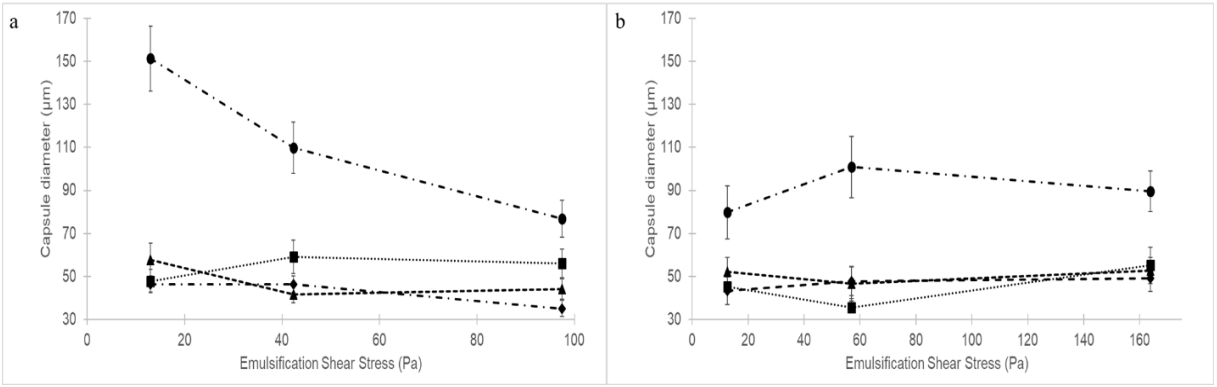


Figure 6.7. Capsule's mean diameter in function of emulsification shear stress for different complex coacervation conditions (where AT1 = (■), AT2 = (▲), AT3 = (♦) and BS = (●)) for formulations with 4% of gelatin (a) and with 10% of gelatin (b).

For the capsules formed using 4 % (w/w) of gelatin/ginger oil (Figure 6.7a) the diameter ranged from 35 to 151 µm. In addition, samples with 4 % (w/w) of gelatin/ginger oil produced by batch stirring presented a decrease of capsule size with the increase of membrane emulsification shear stress. The *VC* had values for samples with 4 %(w/w) of gelatin/ginger oil under 21 %, indicating a process with low size distribution (Table 6.1) (MORELLI; HOLDICH; DRAGOSAVAC, 2017). When using emulsions with 10 % (w/w) of gelatin the capsules'

diameter varied from 35 to 100 µm (Figure 6.7b). In addition, this formulation presented a narrower size distribution, with *VC* value below 17 % (Table 6.1). For both formulations tested, the capsules formed by batch stirring were significantly larger than those formed by atomization (Table 6.1). This is an indication that the method of complex coacervation together with thermodynamic factors has influence on the size of the capsules formed (FERREIRA; NICOLETTI, 2021). In batch complex coacervation for cell encapsulation preceded by membrane emulsification, Morelli et al. (2017) reported capsules size varying from 60 to 70 µm with *VC* varying from 19 to 23 %. In membrane emulsification carried out in continuous mode, followed by batch stirring complex coacervation of fish gelatin and gum Arabic, Piacentini et al. (2013) produced capsules size of 90 µm with shear stress varying from 1.3 to 13 Pa. It is possible to say that the use of shear stress by carrying out coacervation by atomization decreased significantly the capsule diameter when comparing with the samples produced by batch stirring. This result corroborates with previous results obtained where the complex coacervation induced by batch stirring and atomization for emulsions with the same formulation produced capsules with different size (FERREIRA; NICOLETTI, 2021).

Another way to analyse the data obtained is to consider the influence of atomization conditions (*We*) on the capsule diameter, for each membrane emulsification condition. For each emulsion with the same formulation and different emulsification parameters, the atomization conditions affected significantly the capsule's diameter. (Table 6.1). Moreover, for capsules produced under the same emulsification and coacervation condition but with different formulation, almost all have significant differences. Another important observation can be made for both emulsions produced with 97 Pa (4 % of gelatin) and 164 Pa (10 % of gelatin), in which the diameter of the capsules produced by atomization showed a significant linear decrease ($R^2$= 0.95) (graph not shown), with increase of *We*, not taking in consideration the capsules formed by batch stirring. The emulsions produced at higher shear stress (97 Pa and 164 Pa) during membrane emulsification resulted in smaller emulsion droplets (Figure 6.5), and for these emulsions, the increase of *We* during atomization generated a linear decrease of the capsules diameter. These effect could be attributed to the shear stress applied on the emulsion by the atomization air at the spray nozzle, that reduces even more the size of the droplets, thus creating smaller capsules.

Regarding the size distribution, for samples having 4 %(w/w) of gelatin, the increase of shear stress during coacervation caused an increase in VC (Table 6.1). However, for capsules formed with 10 % (w/w) of gelatin there was no apparent relationship between droplet diameter and increase of shear stress on the system. This may be due to the higher viscosity of the 10

%(w/w) emulsion, which makes the variability on the capsule size less susceptible to shear stress applied during the atomization process.

An important fact to be noted is that in some of the samples (4GEM1AT1, 4GEM1AT2, 4GEM1AT3, 4GEM2AT1, 4GEM2AT2, 4GEM2AT3, 4GEM3AT1, 4GEM3AT2, 4GEM3AT3, 10GEM1BS, 10GEM1AT1, 10GEM1AT2, and 10GEM1AT3) the initial emulsion droplets were larger than the final capsules, as presented in Table 6.1. This may indicate that in some point during the coacervation process, a secondary emulsification or droplet breakage during the emulsion atomization - due to shear stress applied to the emulsion at the atomization nozzle - must have happened in addition to the solvent repulsion present during the complex coacervation process. This can be seen when comparing the morphology of the capsules (Figure 6.8).

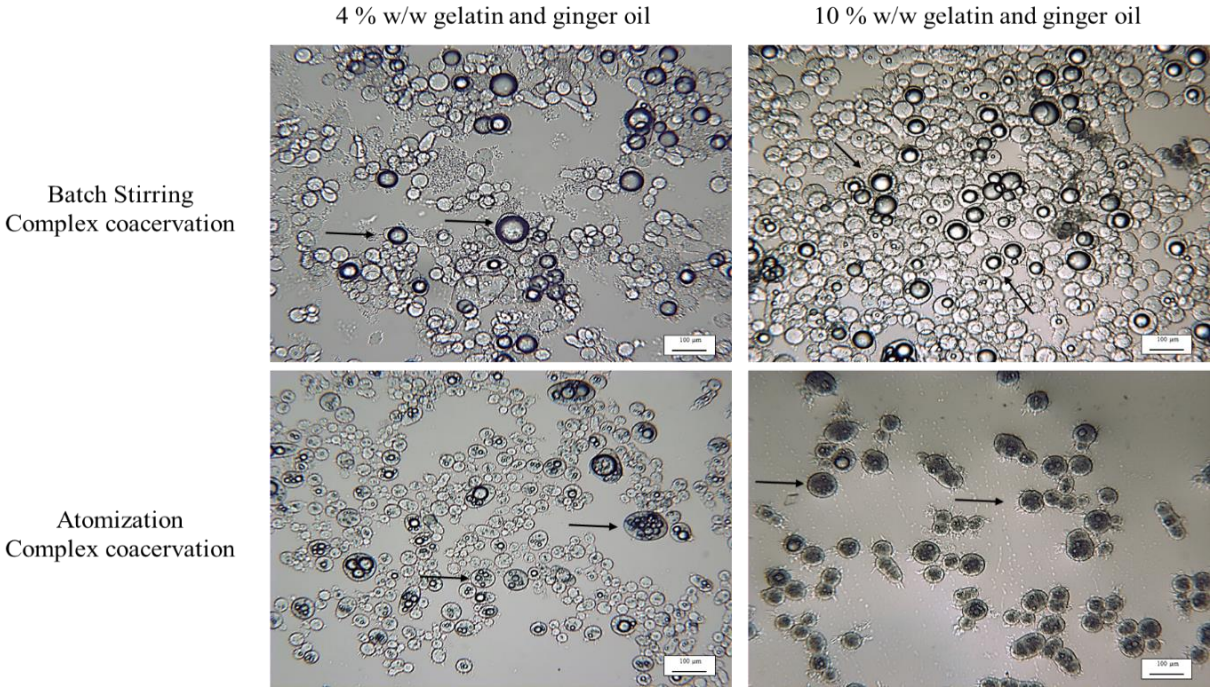


Figure 6.8. Morphology of the capsules produced by batch stirring and atomization, emulsified by membrane.

Concerning the morphology of the capsules formed, as presented in Figure 6.8, two main morphologies were observed: single core and multi core capsules. All samples coacervated by atomization presented multi core capsules, confirming the hypothesis that a secondary emulsification process happened at the atomization nozzle. The capsules formed by batch stirring presented a mononuclear core. This result is promising to produce capsules that must have a specific concentration of core material (e.g. drug delivery). Having capsules with a mononuclear core and controlled capsule size may promote an exact control over the amount of core per capsule (PIACENTINI et al., 2013). Recent study on effects of process conditions

on morphology and oxidative stability of capsules produced by complex coacervation, showed that in order to produce single core capsules is required agitation with 12600 < *Reynolds* < 18600 (MA et al., 2019). Thus, carrying out complex coacervation using emulsions produced by metal membranes presents a good alternative since some compounds cannot endure high values of Reynolds due to mechanical degradations, such as bacterial/yeast cells (MORELLI; HOLDICH; DRAGOSAVAC, 2017). Evaluating the morphology and size of capsules produced by complex coacervation during scale up, Lemetter et al. (2009) reported that to produce single core capsules with size varying from 10 to 25 µm, would be necessary a parental emulsion with droplet with size varying 5 to 10 µm with monomodal size distribution. In production of fish gelatin and gum Arabic capsules emulsified by metal membrane, Piacentini et al. (2013) produced single core capsules varying the polymer ratio, polymer concentration and agitation parameters.

The diameter of the capsules formed by batch stirring was smaller than its previous emulsion droplets. Considering that the shear stress during batch stirring complex coacervation was considerably low, the reason assumed for this fact resides on the solvent repulsion during phase separation, that decreases the volume fraction occupied by the liquid phase, thus decreasing the diameter of the final capsule formed (LI et al., 2018; LIU; CHAPEL; SCHATZ, 2017). The capsules produced with higher gelatin concentration, for both coacervation methods, seems to have a more uniform distribution of the core, what can be attributed to the smaller droplet size produced which generates a higher number of droplets for the same volume of ginger oil/gelatin emulsion. This may result in a higher value of encapsulation efficiency of the capsules with higher gelatin concentration. In general, capsules atomized with 10 % (w/w) of gelatin have the most heterogeneously distributed core on the capsules.

### *6.3.4 Effect of complex coacervation by batch stirring and by atomization on encapsulation efficiency*

The *EE* of the capsules produced ranged from 5 to 66 % considering both coacervation methods (Table 6.1). Traditionally complex coacervation is known to be a microencapsulation technique that provides capsules with high values of *EE* (ALEMZADEH et al., 2020; VEIS, 2011). However, a great number of studies of microencapsulation by complex coacervation uses crosslinkers to increase the interactions between the polymers (ALEMZADEH et al., 2020). This is true also for previous studies of emulsions formed by membrane technologies that went through complex coacervation (MORELLI; HOLDICH; DRAGOSAVAC, 2017; PIACENTINI et al., 2013). However, most of the crosslinking agents available are not food

grade, with a only few exceptions (ALVIM; GROSSO, 2010). Considering that the *EY* of the capsules ranged from 37 to 99 %, this indicates that the use of membrane emulsification to produce emulsions for complex coacervation is efficient in carry the ginger oil throughout the process. The use of a crosslinker agent may be of interest to increase the fraction of oil that stays inside the capsule increasing the *EE*, when considering future studies. In previous studies of complex coacervation carried out by atomization and emulsions formed by ultrasound homogenization, *EE* values ranged from 89 to 99 % (FERREIRA; NICOLETTI, 2021) and 9 to 78 % (FERREIRA; NICOLETTI, 2020), without the application of crosslinking agents. The values of *EE* in this study are lower than the values reported for complex coacervation carried out by batch stirring using gelatin and gum Arabic as wall materials with (ALVIM; GROSSO, 2010) and without (COMUNIAN et al., 2016; MARFIL et al., 2018; QV; ZENG; JIANG, 2011) crosslinking agents. This indicates that different conditions, such as emulsion formulation, emulsification method, coacervation method and use or not of crosslinker, may work alone or in synergy, in order to produce capsules with higher values of *EE*.

Emulsification is a crucial step to properly encapsulate a lipophilic compound (FERREIRA et al., 2016; KAUSHIK et al., 2015). Figure 6.9 presents the relationship of encapsulation parameters with emulsification conditions and capsules size for capsules produced by batch stirring. One way to understand how the emulsification parameters may interfere on encapsulation parameters is to see how the shear stress during membrane emulsification affects the *EY* and *EE* of the dried capsules (Figure 6.9a). Another approach is to correlate encapsulation parameters with the size of the capsule produced (Figure 6.9b). However, considering the hypothesis that a secondary emulsification may be happening at the atomization nozzle, presented in item 6.3.3 (Figure 6.8), only the encapsulation parameters of capsules produces by batch stirring are presented in Figure 6.9.

The increase of the emulsification shear stress increased the *EY*. The increase of *EY* was significant until 42 Pa, and the values of *EY* for batch stirred capsules varied from 37 to 99 % (Figure 6.9a). The same trend was not observed for *EE*, however the highest value of *EE* for batch stirring capsules (33 %) was found for the highest value of emulsification shear stress (164 Pa). Capsules with more than 150 µm presented the lowest *EY* (Figure 6.9b). A similar result was reported by Ferreira and Nicoletti (2021), where for complex coacervation by batch stirring the increase of capsule size and gelatin concentration decreased the *EY*. Comparing the use of gelatin, chitosan and gum Arabic for batch stirring complex coacervation, Gonçalves et al. (2018) obtained *EY* varying from 53 to 90 %, being the higher value from the combination

of gelatin and gum Arabic. The values of *EE* increased until the capsules size reached 90 µm, and after that decreased.

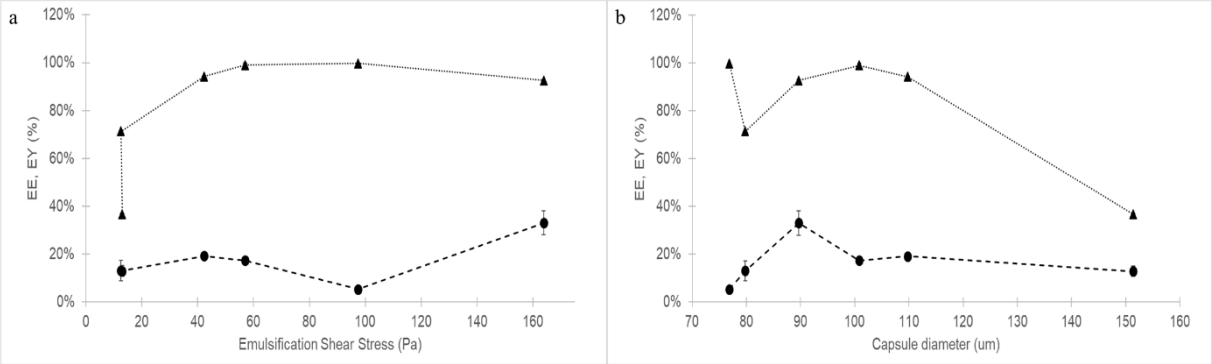


Figure 6.9. Encapsulation yield - *EY* (▲) and encapsulation efficiency - *EE* (●) in function of (a) membrane emulsification parameters and (b) capsule size of capsules formed by batch stirring complex coacervation.

Taking into account the influence of formulation on encapsulation parameters of capsules formed by batch stirring, emulsions with 4 % (w/w) of gelatin/ginger oil, presented a significant increase of *EY* from 36 to 94 % with an increase on emulsification shear stress from 13 to 42 Pa (Table 6.1). For emulsions with 10 % (w/w) of gelatin/ginger oil, the *EY* values significantly increased from 71 to 99 %, with the increase on the emulsification shear stress from 13 to 57 Pa. In other hand, the *EE* values for these emulsions increased from 17 to 33 %, highest value of *EE* among batch stirred capsules, with the increase on the emulsification shear stress from 57 to 164 Pa.

Finally, the influence of the complex coacervation method/parameters (batch stirring or atomization) on the encapsulation parameters was investigated, for emulsion produced under different shear stress during membrane emulsification (Figures 6.10 and 6.11 and Table 6.1).

The increase of *We* number from 87 to 242 increased significantly *EY* values from 37 to 88 %, however samples produced with *We* higher or equal than 242 (Figure 6.10a) had *EY* similar as the capsules by batch stirring (Table 6.1). This may be related to the lower energy input during the membrane emulsification step that is compensated by the shear stress during the atomization process. For emulsions formed with shear stress of 97 Pa (Figure 6.10b), the *EY* values did not change significantly in function of *We*. However, the increase of *We* number from 87 to 242 increased significantly the *EE* values from 9 to 34 %.

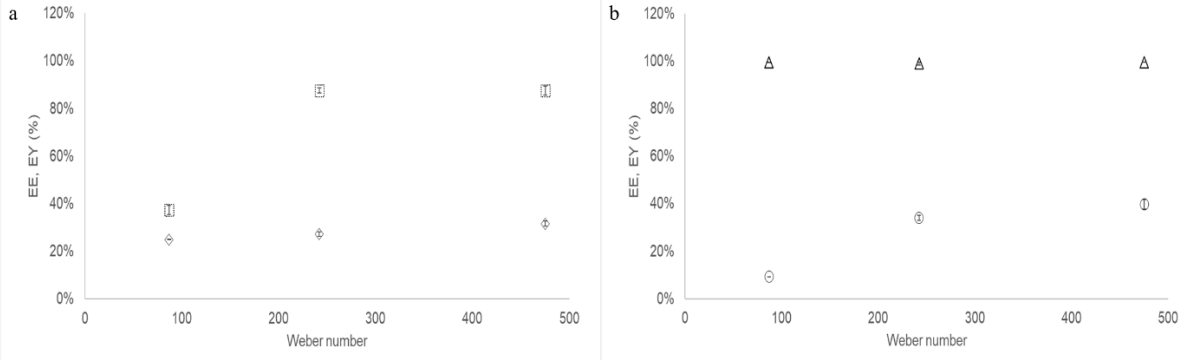


Figure 6.10. Encapsulation parameters in function of Weber number during complex coacervation for emulsions with 4% (w/w) of gelatin/ginger oil. Emulsification shear stress of 42 Pa represented in (a), where EY (□) and EE (◊). Emulsification shear stress of 97 Pa presented in (b), where EY (△) and EE (○).

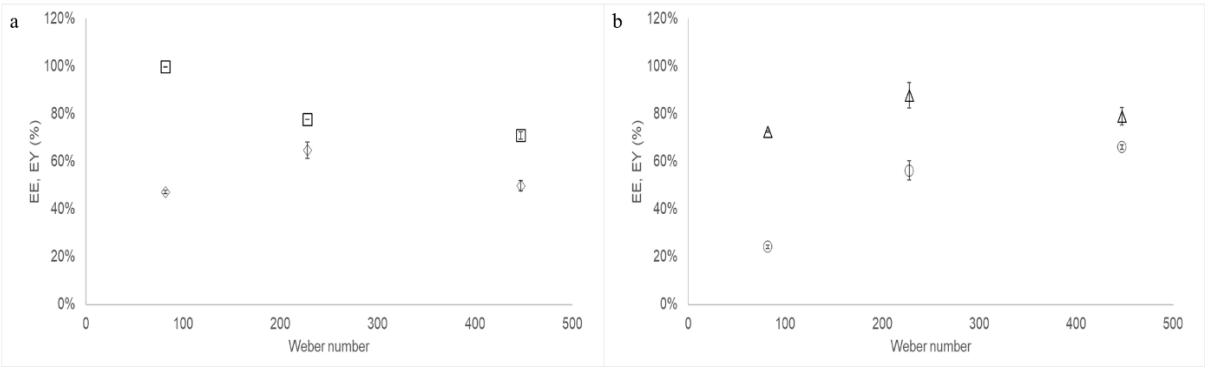


Figure 6.11. Encapsulation parameters in function of Weber number during complex coacervation for emulsions with 10% (w/w) of gelatin/ginger oil. Emulsification shear stress of 57 Pa represented in (a), where EY (□) and EE (◊). Emulsification shear stress of 164 Pa presented in (b), where EY (△) and EE (○).

For emulsions with 10 % (w/w) of gelatin/ginger oil and emulsified with shear stress of 57 Pa, the values of *EY* for batch stirring and lower value of *We* (82) were the same (Figure 6.11a). However, *EY* for $We > 82$ were significantly smaller than $We \leq 82$, which indicates that the energy input during emulsification must be not enough to form a stable emulsion to carry the oil. The peak of *EE* was reached at $We = 228$. The EE values for $We > 228$ were significantly smaller (Figure 6.11a). However, where the emulsions were formed with higher shear stress (164 Pa), the increase of *We* also increased the *EE* (Figure 6.11b). This is an indication that even though the emulsions formed with 57 and 164 Pa produced emulsions with similar droplet size, the coacervation process yielded different encapsulation properties. Studying the influence of dimensionless numbers on the atomization process during encapsulation of buriti oil by spray drying, Moser et al. (2019) for $We > 420$ reported *EE* of 81 to 92%.

The formulation of emulsions did not affect greatly the *EY* of the capsules (Figures 6.10 and 6.11), however there was influence on the *EE*. Emulsions with 4 % (w/w) produced

capsules with maximum *EE* of 40 % and emulsions with 10 % (w/w) of gelatin produced capsules with maximum *EE* of 66 %. A similar result was reported in previous study of complex coacervation by atomization, where emulsions with 2% (w/w) of gelatin had a decrease of *EE* with the increase of *We*, and the *EE* of emulsions with 6 % was not affected by *We*. Having a higher concentration of gelatin promotes a stronger emulsion structure, entrapping the oil droplet inside the capsules and increasing the *EE* (FERREIRA et al., 2016). These results corroborate with the result presented in section 6.3.3, where the morphology of the capsules indicated more core content inside the capsules with higher gelatin/ginger oil concentration, for both batch stirring and atomization complex coacervation.

## 6.4. Conclusions

The ratio of the membrane pore diameter and pore spacing had great influence on the droplet sizes, size distribution and prediction of droplet sizes, mainly for lower values of emulsification shear stress. Membrane with larger space between the pores produced smaller emulsion droplets with lower size distribution. Membrane emulsification produced proper emulsions for complex coacervation, with low size distribution. For emulsions with 10 % (w/w) of gelatin/ginger oil, it was possible to predict the size of the droplets. Indications of a second emulsification process was observed at the atomization nozzle, and this was observed more prominently for capsules atomized under higher Weber numbers. Capsules produced by batch stirring had a single core morphology and atomized capsules had a multi core morphology. The *EE* of the capsules ranged from 5 to 66 % and the *EY* varied from 37 to 99 % for both coacervation methods. The results of high values of *EY* and medium to low values of *EE* indicate that, even though the oil is being carried out throughout the encapsulation process, part of the oil is being encapsulated on the outer part of the capsules. For capsules produced by batch stirring the best condition found based on *EY* was emulsification shear stress of 164 Pa and 10 % (w/w) of gelatin/ginger oil emulsion.

## Acknowledgements

The authors thank: Micropore Technologies Ltd. for providing the dispersion cell/membranes for membrane emulsification and Adiella Abelseth for proof reading with a focus on the English language of the article.

This work was supported by the São Paulo Research Foundation - FAPESP (grant numbers 2015/23290-0 and 2018/16976-0) and National Council for Scientific and Technological Development - CNPq (grant number 305355/2016-3).

# CHAPTER 7 - COMPARISON OF TWO NOVEL METHODS TO INDUCE OIL MICROENCAPSULATION BY COMPLEX COACERVATION: METAL MEMBRANE AND ATOMIZATION

Sungil Ferreira[1]*, Vania Regina Nicoletti[1], Marijana Dragosavac[2].

[1]São Paulo State University (UNESP), Department of Food Engineering and Technology, São Jose do Rio Preto – SP, 15054-000, Brazil

[2]Department of Chemical Engineering, Loughborough University, S Building, Loughborough, LE11 3TU, United Kingdom

Abstract

This study introduces a novel method to induce complex coacervation by using metal membrane technology - which has been most used for drop-by-drop emulsification - to inject protein-stabilized oil droplets directly into a polysaccharide solution. Emulsions of gelatin (4 and 10 % w/w) and ginger oil (gelatin:ginger oil ratio of 1:1) were produced by high shear homogenization to further complex coacervation with gum Arabic at pH 3.5 using the proposed metal membrane methodology. The capsules produced by membrane coacervation had spherical shape with diameter varying from 53 to 72 μm, and encapsulation efficiency ranging between 61 – 93 %. The encapsulation yield varied from 15 to 90 % being significantly higher for emulsions with 4 % (w/w) of gelatin/ginger oil. Complex coacervation by metal membrane was compared with coacervation induced by atomization - another recent method developed in our group - and with complex coacervation by batch stirring. The results showed that the use of metal membranes are a promising new configuration to induce complex coacervation, with real possibilities for scale up of the process of complex coacervation.

Keywords: hydrocolloid matrix, dispersion cell, membranes, atomization, encapsulation, ginger oil, gelatin, gum Arabic.

## 7.1. Introduction

Microencapsulation is an effective way to physically protect lipophilic compounds from adverse conditions, in addition to provide conditions to controlled or targeted release, undesirable flavour masking, and change of physical state (ERATTE et al., 2015; JANISZEWSKA-TURAK et al., 2017; MA et al., 2019; RUTZ et al., 2017). Several methods for encapsulating a core material of interest can be applied, and the choice of encapsulation method and materials to be used lays on the application of the capsules, cost benefit, seasonality of core and wall material, trigger to core release and chemical nature of core (SHAHIDI; HAN, 1993; TIMILSENA et al., 2017b, 2019). Complex coacervation is featured by its simplicity, reproducibility, scalability and high encapsulation efficiency and yield (DRUSCH; REGIER; BRUHN, 2012; SPECOS et al., 2010; TIMILSENA et al., 2019).

Complex coacervation has been successfully used for microencapsulation of essential oils and flavours, which have extensive application in food, agricultural, textile and pharmaceutical industries. The technique is very versatile and is suitable for protection of these compounds against degradation, to prevent loss of volatiles, besides allowing modulated release and increased stability of the encapsulated material (ALEMZADEH et al., 2020; XIAO et al., 2014a, 2014b). Complex coacervation results mainly from the electrostatic interaction of oppositely charged polymers that, due to solvent repulsion, forms complexes that tends to precipitate. In addition, the presence of weaker interactions such as hydrophobic interactions and hydrogen bonding may contribute to coacervation (ACH et al., 2015; RUTZ et al., 2017). The complex coacervation process can be thermodynamically described in function of enthalpic forces, mainly long-range electrostatic interactions inter macroions, and entropic forces resulting from the loss of small ions (KAYITMAZER; KOKSAL; KILIC IYILIK, 2015). The influence of process conditions on batch stirring complex coacervation has received attention in previous works evaluating the influence of biopolymer concentration and ratio, core to biopolymer ratio (MARFIL et al., 2018), stirring speed and coacervation pH (LEMOS; MARIANO MARFIL; NICOLETTI, 2017; MA et al., 2019), influence of hydrodynamic conditions (DOBETTI; PANTALEO, 2002), and influence of drying method on particle properties (KAUSHIK et al., 2016).

The standard and well known pair of biopolymers used as a reference for new studies on complex coacervation are gelatin and gum Arabic. Gelatin is a well-known emulsifying polymer structured in the form of a triple helix, good emulsifying properties; being a protein, it has a net charge depending on the medium pH and its main three amino acids present are glycine, proline, and hydroxyproline (GILSENAN; ROSS-MURPHY, 2000; HECKERT

BASTOS et al., 2020). Gelatin has a clear flavour profile, which is very useful in microencapsulation (KARIM; BHAT, 2008). Gum Arabic is a carbohydrate vastly used in complex coacervation, presenting low viscosity, mild flavour, provides protection against volatile oxidation and has negative value of zeta potential (COMUNIAN et al., 2016; ZUANON; MALACRIDA; TELIS, 2013). It is composed by fractions with different chemical structures, about 70% of which consists of polysaccharide chains of a highly branched arrangement of galactose, arabinose, rhamnose, and glucuronic acid with little or no nitrogenous material between them (OSMAN et al., 1993; RAY et al., 1995). The use of gelatin and gum Arabic results in particles with higher encapsulation yield when compared with other hydrocolloid combinations and defined capsule morphology (GONÇALVES et al., 2018; MORELLI; HOLDICH; DRAGOSAVAC, 2017).

In an effort to present alternatives to the traditional method of inducing complex coacervation by batch stirring, few studies proposed different configurations to perform the process using three-fluid nozzles to combine coacervation and drying in a single step (JIANG et al., 2013; KAŠPAR; JAKUBEC; ŠTĚPÁNEK, 2013). Previous studies of our research group used a two-fluid nozzle to atomize gelatin emulsion over a gum Arabic solution to induce complex coacervation and proved the possibility of particle engineering (FERREIRA; NICOLETTI, 2020, FERREIRA; NICOLETTI, 2021). These studies evaluated the influence of process parameters on capsule size and morphology, showing that both process and thermodynamic conditions may play similar roles on capsule formation. In an attempt to offer additional possibilities of accomplishing microencapsulation by this technique, in the present study we evaluated the use of metal membranes as a new method to induce complex coacervation, using dispersion cells (*DC*), which are commonly applied for membrane emulsification (CONSOLI; HUBINGER; DRAGOSAVAC, 2020; KOSVINTSEV et al., 2005). The setup used for membrane emulsification and that was adapted for complex coacervation has received attention precisely because of its ability to produce particles or droplets with low size polydispersity and because it is a drop-by-drop technology (DRAGOSAVAC et al., 2008, 2012; KOSVINTSEV et al., 2005; PU; WOLF; DRAGOSAVAC, 2019). Moreover, there are in-place setups for membrane emulsification that could be used for membrane coacervation to be carried out in continuous process and in industrial scale (HANCOCKS; SPYROPOULOS; NORTON, 2016; HOLDICH *et al.*, 2018, 2020). In the dispersion cell configuration, a gelatin/oil emulsion, at the coacervation pH, is forced through a metal membrane, with cylindrical pores in hexagonal configuration, exiting in contact with the gum Arabic solution, also at the predetermined coacervation pH. In order to

detach the emulsion droplet from the membrane, a stirrer is used. Two main parameters are of particular significance for complex coacervation carried out by metal membranes: the emulsion injection rate and the shear stress generated by the stirrer (MORELLI; HOLDICH; DRAGOSAVAC, 2017; PIACENTINI et al., 2013).

This study aimed to investigate the possibility of applying dispersion cell to induce complex coacervation by metal membrane, which, to the best of our knowledge, has not been reported in the literature until now. The rheological behaviour of the emulsions was evaluated aiming to correlate their microstructure with the process performance. In addition, capsules produced by membrane coacervation were compared with those resulting from complex coacervation induced by atomization and batch stirring. The three methods were compared regarding wet capsules' size, size distribution and capsule morphology, as well as the dried capsules' encapsulation performance.

## 7.2. Material and Methods

### *7.2.1 Materials*

Cold pressed ginger oil (Gran Oils, São Paulo, Brazil) was used as encapsulated material. Gum Arabic (Dinâmica, Campinas, Brazil) and type B gelatin, 240 bloom (Gelita, Mococa, Brazil) were used as wall material to induce complex coacervation, and the pH was adjusted using glacial acetic acid (Dinâmica, Campinas, Brazil). The release of the encapsulated oil was induced by using hydrochloric acid 4 N (Dinâmica, Campinas, Brazil) and hexane (Dinâmica, Campinas, Brazil) was used as extraction solvent.

### *7.2.2 Methods*

7.2.2.1 Preparation of emulsions gelatin and ginger oil and gum Arabic solution

Gelatin was dispersed in deionized water at 60 °C at concentrations of 4 % (w/w) and 10 % (w/w) of the final emulsion. Ginger oil was added at the same concentrations as the gelatin (gelatin:ginger oil ratio of 1:1). Emulsions were homogenized using a rotor-stator high-shear homogenizer (Ultra Turrax, T-25, IKA, Germany) at 15000 rpm for 5 min. The solution of gum Arabic (1 g/100 g of solution) was prepared by adding it to deionized water (50 °C) under magnetic stirring until complete dissolution. For complex coacervation assisted by atomization and by membranes, the emulsion and gum Arabic solution had their pH adjusted to 3.5 prior to the coacervation process.

7.2.2.2 Characterization of emulsion and biopolymer solutions

The rheological behaviour of the gelatin/ginger oil emulsions and gum Arabic solution was determined in a rheometer AR2000ex (TA Instruments, USA) at 35 $^{o}$C. Non-oscillatory assays were carried out using cone and plate geometry. The interfacial tension between ginger oil and gelatin solution, and the surface tension measurements of the gelatin/ginger oil emulsion and gum Arabic solution were done in a DB2KS tensiometer (White Electric Instrument, United Kingdom) by the Du Noüy ring method. The density of the emulsions and gum Arabic solution was determined in a densimeter DMA ™ 4500 M (Anton Paar, Austria) at 35 $^{o}$C. The parameters are presented in Table 7.1 and for conciseness they will not be part of the discussion, since the values are only used to determine the shear stress during complex coacervation.

Table 7.1. Physicochemical properties of ginger oil/gelatin (35 $^{o}$C) emulsions and gum Arabic solution used during complex coacervation by metal membrane, atomization, and batch stirring.

| **Biopolymer** | **Biopolymer concentration (g/100 g)** | **Ginger oil concentration (g/100 g)** | **Surface tension[1] (mN/m)** | **Density[2] (kg/m$^3$)** | **Apparent viscosity (mPa·s)** | **Rheological model`s best fit/R$^2$** |
|---|---|---|---|---|---|---|
| Gelatin | 4 | 4 | 50.1±0.2 | 1002.4±0.1 | 6.2 | Newtonian/0.998 |
| | 10 | 10 | 51.9±0.3 | 1010.5±0.1 | 49.7 | Bingham/0.999 |
| Gum Arabic | 1 | - | 39.4±0.9 | 994.3±0.2 | 0.6 | Newtonian /0.999 |

[1]Mean values ± standard error (n = 10); [2]Mean values ± standard error (n = 3)

7.2.2.3 Effects of polymer ratio and pH on complex coacervation between gelatin and gum Arabic

The assays to study the influence of polymer ratio and pH on the coacervation were carried out following Lv et al. (2014), with minor modifications. Gum Arabic (GA) and gelatin (GE) aqueous solutions were prepared and the total biopolymer concentration of the final solution was 0.5% (w/w) varying the ratio of polymers as (GA:GE) 1:1; 2:1; 1:4; 0:1 and 1:0. Then the pH of the final solution was slowly adjusted ranging from 2.5 to 5.5, using acetic acid. The turbidity was measured at 600 nm in a spectrometer photometer lambda 35 UV/VIS (Perkin-Elmer, United Kingdom).

7.2.2.4 Complex coacervation in batch stirring

Complex coacervation in batch stirring was carried as described by Marfil et al. (2018). Ginger oil/gelatin emulsion (50 ± 1 °C) and gum Arabic solution (50 ± 1 °C) were mixed and kept under slow stirring. The pH was slowly adjusted to 3.5 using glacial acetic acid

(> 96%). Then the system was immersed in an ice bath for slow cooling until 10 ± 1°C. After 24 hours, part of the sedimented particles was analysed for size and morphology and part was transferred to aluminium trays and frozen at -20 °C. Drying was carried out by lyophilisation for 72 hours for further analyses.

7.2.2.5 Complex coacervation by metal membrane

The gelatin/ginger oil emulsion (35 ºC, pH 3.5) was forced through a metal membrane (24 µm pore diameter and 250 µm of distances between the pores) and dispersed in the gum Arabic solution (35 °C, pH 3.5) using a dispersion cell (Micropore Technologies Ltd., United Kingdom) (Figure 7.1). Emulsion injection rate varied from 3 to 10 mL/min. Agitation inside the dispersion cell varied from 540 to 1780 RPM (1 to 13 Pa). After all the emulsion was injected on the dispersion cell the mixture containing the capsules was cooled down to 10 °C in an ice bath. Freeze drying was performed as described in 2.2.4.

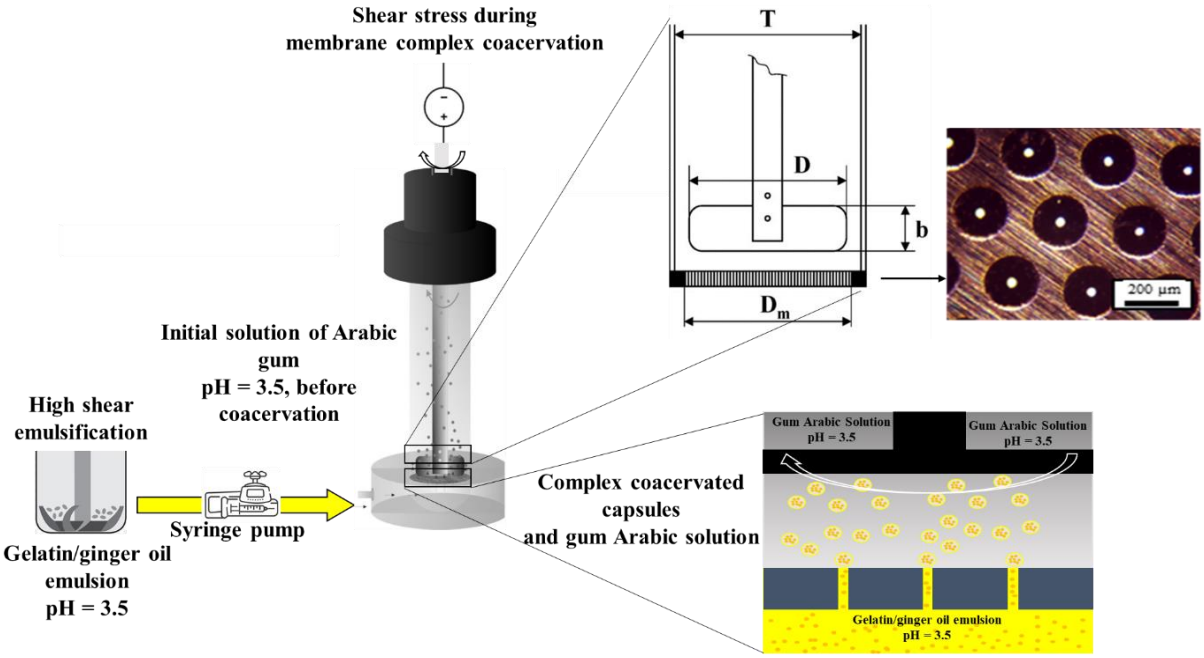


Figure 7.1. Schematic diagram of dispersion cell (*DC*) with simple paddle stirrer above a nickel flat-disc membrane, in which T = 0.04, *D* = 0.032 m, $D_m$ = 0.033 m and *b* = 0.012 m.

The membrane coacervation process can be described in function of the shear stress applied in the dispersion cell. Equation 7.1 can be used to determine the boundary layer thickness, $\delta$ (LANDAU; LIFSHITZ, 1966) .

$$\delta = \sqrt{\frac{\mu}{\rho\omega}} \qquad (7.1)$$

In Equation 7.1, $\rho$ and $\mu$ are the gum Arabic density and viscosity, respectively, and $\omega$ is the stirrer angular velocity in rad/s.

The radial distance at which the shear stress is maximum is called transitional radius, $r_{trans}$, and can be determined by Equation 7.2:

$$r_{trans} = 1.23\frac{D}{2}\left(0.57 + \frac{D}{T}\right)\left(\frac{b}{T}\right)^{0.036} n^{0.016}\frac{Re_{mcc}}{1000+1.43Re_{mcc}} \quad (7.2)$$

in which $D$ is the stirrer diameter, $T$ is the dispersion cell diameter, $b$ is the blade height, and $n$ is the number of impeller blades. The Reynolds number during membrane coacervation ($Re_{mcc}$) can be defined by Equation 7.3:

$$Re_{mcc} = \frac{\omega\rho D^2}{2\pi\mu} \quad (7.3)$$

The maximum shear stress applied in the system can be determined using Equation 7.4 and will be taken as the shear stress during membrane coacervation.

$$\tau_{mcc} = \frac{0.825\mu\omega r_{trans}}{\delta} \quad (7.4)$$

7.2.2.6 Complex coacervation by atomization

Complex coacervation by atomization was carried out as presented by Ferreira and Nicoletti (2020, 2021). Ginger oil/gelatin emulsions were sprayed over an aqueous solution of gum Arabic using a dual fluid atomizer nozzle (0.7 mm diameter, Labmaq, Brazil), with controlled air and emulsion flowrates (Figure 7.2). The atomization conditions and additional operational parameters are summarized in Table 7.2. The pH of the emulsion and of gum Arabic solution were adjusted to 3.5 using glacial acetic acid (> 96%), prior to atomization. Air flowrate was controlled using a rotameter FT074-02-CA-VN (Omega, USA). At the end of the coacervation process the system was immersed in an ice bath until reaching 10 ± 1 °C. Freeze drying of the capsules was performed was described in section 7.2.2.4.

The shear stress during the atomization process was determined in function of the Weber number (Equation 7.5). Since emulsions with 4 % (w/w) of gelatin/ginger oil behave like a Newtonian fluid (Table 7.2), Equation 7.6 was used to determine their shear stress during atomization. For emulsions with 10 % (w/w) of gelatin/ginger oil (Bingham fluid) Equation 7.7 was used, as described by Ferreira and Nicoletti (2020). The Reynolds number ($Re_{at}$) during atomization was calculated using Equation 7.8.

Table 7.2. Physical properties of atomization air, dimensions of the atomization nozzle and operational parameters of atomization.

| **Characteristics of the two fluid nozzle** | |
|---|---|
| Diameter of emulsion outlet ($D_l$) - (mm) | 0.7 |
| Internal diameter of air outlet ($D_{int}$) - (mm) | 1.90 |
| External diameter of air outlet ($D_{ext}$) - (mm) | 2.80 |
| Emulsion outlet area - ($mm^2$) | 0.385 |
| Atomization air outlet area - ($mm^2$) | 3.32 |
| **Physical properties of the atomization air (25 °C)** | |
| Density ($\rho_g$) - (kg $m^{-3}$) | 1.23 |
| Viscosity ($\mu_g$) - (µPa s) | 18 |
| **Atomization process parameters** | |
| Atomization air velocity ($V_g$) - (m $s^{-1}$) | 71.1 to 165.2 |
| Emulsion velocity ($V_l$) - (m $s^{-1}$) | 0.42 to 0.64 |

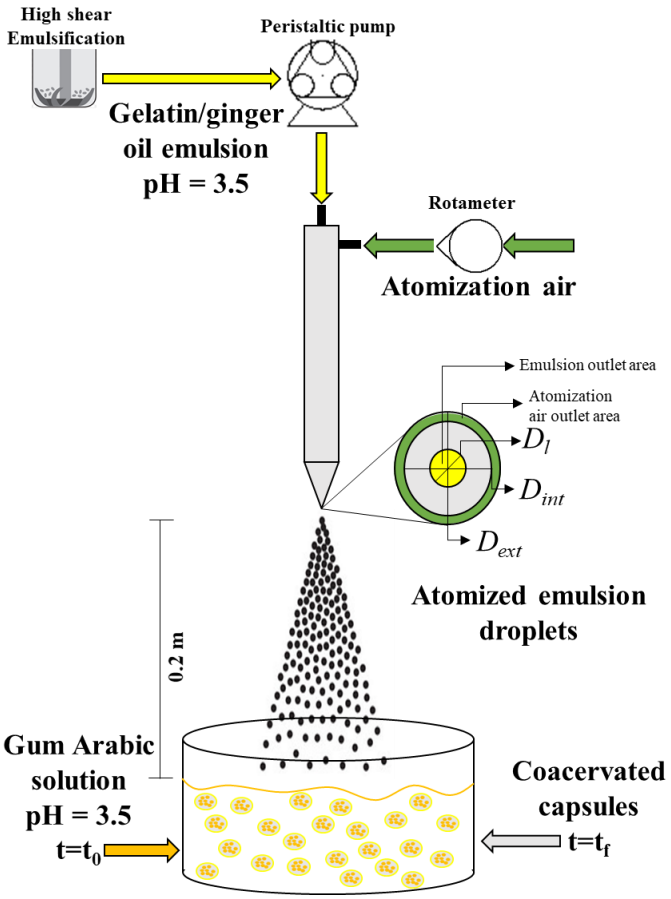


Figure 7.2. Schematic diagram of the complex coacervation process by atomization.

$$We = \frac{\rho_g (V_g - V_l)^2 D_l}{\sigma} \quad (7.5)$$

$$\tau_{new\ at} = (25.3\ We + 2247.3)\ \mu_l \quad (7.6)$$

$$\tau_{bing\ at} = \tau_0 + \mu_l (25.3\ We + 2247.3) \quad (7.7)$$

$$Re_{at} = \frac{\rho_g\ V_g\ b_g}{\mu_g} \quad (7.8)$$

7.2.2.7 Characterization of wet microcapsules

The microstructure of wet capsules was evaluated using a Retiga 6000 colour camera coupled to an optical microscope GXML3201(GX microscopes, UK). The scanned images were used to measure the capsule size using Image Pro Plus 6.0 software (Media Cybernetics Inc., USA), measuring the average diameter of 600 capsules per sample.

7.2.2.8 Characterization of dried microcapsules

Microencapsulation performance was determined following Tonon, Grosso and Hubinger (2011) and Wang, Adhikari and Barrow (2014) with modifications. After complex coacervation the microcapsules were freeze-dried and subjected to analysis as follows. Encapsulation efficiency (*EE*) and encapsulation yield (*EY*) were determined considering the oil content initially present in the gelatin/ginger oil emulsion (*OI*), the oil present on the surface of the dried capsules (*OS*) and the final total oil present in the capsules (*OT*). To determine *OS*, 100 mg of capsules and 10 mL of hexane were placed in a capped tube and agitated for one minute. The hexane carrying the surface oil was filtered, transferred to Petri dishes and evaporated at room temperature in a hood, and then at 60 °C until constant weight. To determine *OT*, 100 mg of capsules were dispersed in 20 mL of 4 N hydrochloric acid solution and shaken for 1 hour at 35 °C for digestion of the wall material. Then, 13 mL of hexane were added and agitated for 10 hours at 25 °C, forming a two-phase system. The non-organic and organic phases were separated by centrifugation at 10000×g for 30 minutes (model Z 326 K, Hermle, Germany) and the organic phase containing hexane and oil was transferred to Petri dishes. The solvent was evaporated at room temperature in a hood, and then in drying oven at 60 °C until constant weight. The *EE* and *EY* were calculated by Equations 7.9 and 7.10, respectively.

$$EE(\%) = \frac{OT - OS}{OT} \times 100 \quad (7.9)$$

$$EY(\%) = \frac{OT}{OI} \times 100 \quad (7.10)$$

7.2.2.9 Statistical analysis

Unless stated differently, the assays were done in triplicate. The results of the analytical determinations are expressed as arithmetic average (AV) submitted to analysis of variance (ANOVA) and comparison of means by Tukey test with probability level at 5% ($p \leq 0.05$), using statistical software Minitab 17 (MINITAB, State College - PA, USA). The size distribution of wet capsules is presented as variation coefficient [VC=(SD/AV)*100], in which SD stands for standard deviation.

## 7.3. Results and Discussion

*7.3.1 Effects of polymer ratio and pH on complex coacervation between gelatin and gum Arabic*

The appropriate combination of polymer ratio and pH to induce complex coacervation between gum Arabic and gelatin was defined based on the results of turbidity analysis (Figure 7.3). Three different combinations of polymer ratio/pH resulted in higher coacervation: for 1:1 and 1:4 (gum Arabic:gelatin) the optimum pH was 4.5, whereas for 2:1 (gum Arabic:gelatin) the optimum pH was 3.5. A similar result regarding polymer ratio and pH was reported in complex coacervation of fish gelatin and gum Arabic (LI et al., 2018). In a study of the influence of process conditions on complex coacervation, Ma et al. (2019) reported optimum ratio of 2:1 at pH 3.4, 1:1 at pH 4.1 and 3:1 at pH 5.4 (gum Arabic:gelatin). Ferreira and Nicoletti (2021) studying the influence of polymer ratio on complex coacervation induced by atomization, found that the optimum ratio ranged from 1.5:1 to 3:1 (gum Arabic:gelatin) at pH 3.5. In particular, using a polymer ratio with higher protein content would be of interest, considering that the oil is emulsified in the protein solution at 1:1 ratio, thus increasing the protein ratio over the carbohydrate means that it is possible to increase the oil content in the capsules.

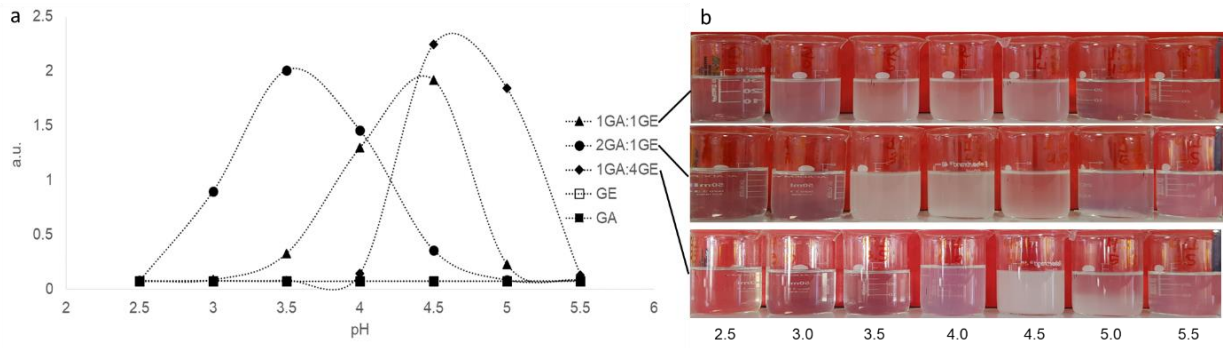


Figure 7.3. Absorbance (600 nm) in function of pH and polymer ratio complex coacervation between gelatin and gum Arabic.

The next step of our study aimed to perform complex coacervation using both gum Arabic:gelatin ratios (1:4 at pH = 4.5 and 2:1 at pH = 3.5) with emulsions formulated with two gelatin concentrations (4 and 10 w/w % of gelatin), to ensure that the ratios previously determined would form proper complex coacervated capsules. These assays were carried out by batch stirring, according to section 7.2.2.4.

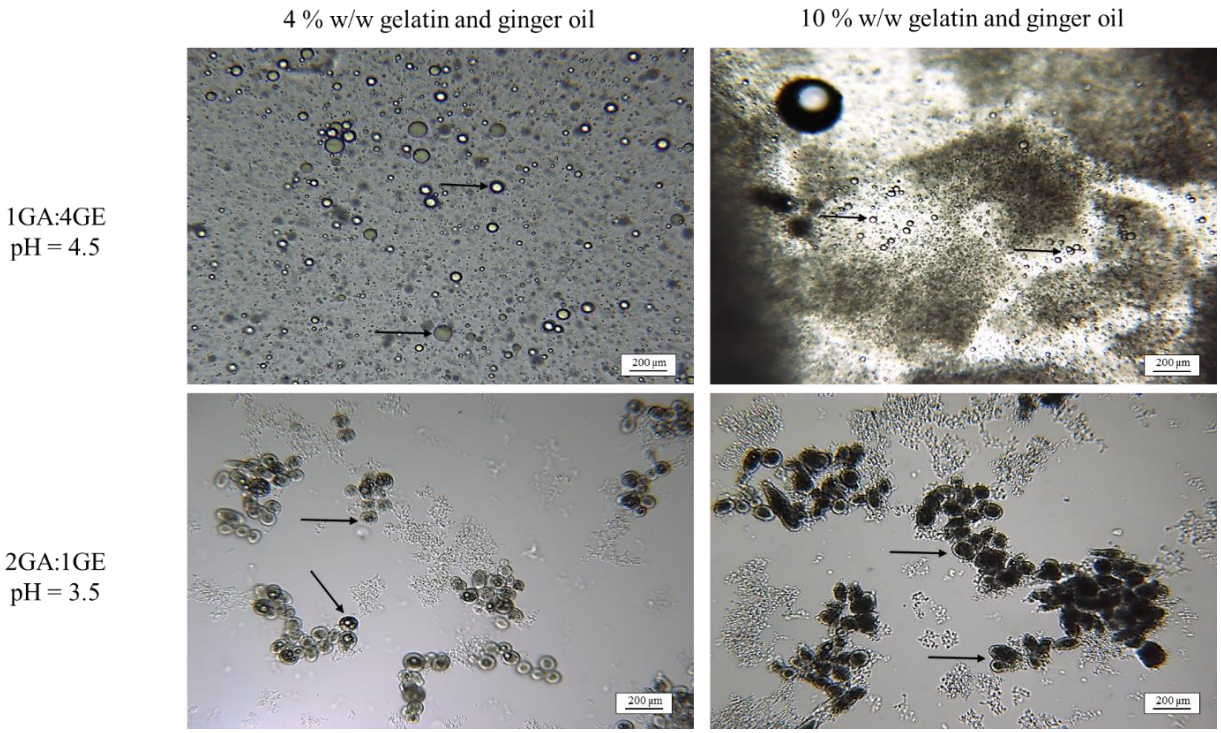


Figure 7.4. Complex coacervation assays at 10 ºC using gum Arabic:gelatin ratios of 1:4 (1GA:4GE) and 2:1 (2GA:1GE) at pH of 4.5 and 3.5, respectively, and different emulsion concentrations.

Optical micrographics of the systems (Figure 7.4) showed that the formulations 1GA:4GE (pH = 4.5) did not form capsules after cooling and hardening steps, independently of the gelatin concentration in the emulsion. It is important to mention that the data shown in Figure 7.3 was obtained right after the pH adjustment, before the systems being subjected to the hardening step. In this case, the gelatin was above its gelation temperature (approximately 25 ºC), keeping the coacervate's structure (DA SILVA et al., 2014). However, during the cooling step, the gelatin solution goes through a restructuring process, changing its triple helix conformation (GORNALL; TERENTJEV, 2008a, 2008b). Considering the fact that there are four times more protein than carbohydrates in the system, its volume fraction has greater effect on the matrix formation (DE KRUIF; WEINBRECK; DE VRIES, 2004; DE VRIES, 2004; GIRARD et al., 2004). As a result, instead of inducing phase separation due to solvent repulsion and polymer attraction, a gel-like network is formed, entrapping the oil droplets without

individual capsule formation, as can be seen in Figure 7.4 in formulation with 4 % (w/w) of gelatin/ginger oil. An example of the importance of protein chain organization during coacervation and cooling processes to guarantee the formation and morphology of the capsule is presented by Eratte et al. (2014), studying complex coacervation between whey protein isolate and gum Arabic: the authors produced individual capsules at a ratio of 1:3 (gum Arabic:whey protein isolate) and pH 3.75. The opposite results may be explained considering that whey protein does not form mechanically strong gels like gelatin, corroborating with the influence of the gel formation capacity of the polymer with its capacity to go through phase separation at higher gelatin concentration (BOYE et al., 1995; GOSAL; ROSS-MURPHY, 2000).

On the other hand, in the formulations using polymer ratio 2GA:1GE at pH = 3.5, the complex coacervated capsules formed as expected (Figure 7.4) independent of the emulsion concentration. A possible explanation is that, in the beginning of the coacervation process the gum Arabic adsorbs through electrostatic interaction around the gelatin/ginger oil emulsion droplets, leading to the formation of the capsules wall (ACH et al., 2015). Considering that the concentration of gum Arabic is twice the gelatin concentration, when the system is going to through the cooling process, the gelatin groups positively charged (lysine and arginine) are all or most of if interacting with the negative charged groups of gum Arabic (MOHANTY et al., 2005; WANG et al., 2015). Thus, the gel-like matrix is not formed, as the excess of gum Arabic stabilizes the coacervates both sterically and electrostatically. Another point to be considered is that the produced capsules are intended to target core release in intestine conditions, thus having to endure gastric conditions. Previous studies on the production of capsules for intestine-targeted delivery using o-carboxymethyl chitosan–gum Arabic coacervates showed that capsules produced using a lower pH endure better gastric conditions, and have a more efficient intestine delivery (HUANG et al., 2017a; HUANG et al., 2017b). Hence, using a formulation that calls for a lower pH during the coacervation is an important result considering gastric survival and intestine delivery, even though this formulation requires less gelatin, and as consequence, less ginger oil.

Taking into consideration the capsule formation assays, the conditions chose to carry out the complex coacervation were polymer ratio of 2:1 (gum Arabic:gelatin) at pH 3.5, for both emulsion formulations (4 and 10 % w/w of gelatin/ginger oil).

*7.3.2 Influence of complex coacervation methods on the size, size distribution and morphology of the capsules*

The knowledge of the capsules size and size distribution during a microencapsulation process, independently of the method used, is crucial to properly characterize the process performance (MOSER; FERREIRA; NICOLETTI, 2019; OZKAN et al., 2019). In addition, the overall size of the capsules can be directly correlated with their functionality, in particular with its total surface area, which is directly related to encapsulation efficiency and the core release kinetics (ZUANON et al., 2019). In the present work, the size and morphology of the capsules produced were investigated as affected by three different methods used to induce complex coacervation, i.e., metal membrane, atomization, and batch stirring, as well as varied operational conditions that defined different hydrodynamic regimens (Table 7.3).

All the samples produced with emulsions containing 4 % (w/w) of gelatin/ginger oil presented capsule sizes varying from 58 to 75 µm, whereas the samples produced from emulsions containing 10 % (w/w) of gelatin/ginger oil were significantly smaller, with sizes varying from 50 to 68 µm (Table 7.3). The exception was the coacervation assays G4-MC9 and G10-MC9, for which the average capsule sizes were not statistically different, and for MC5 and MC7 in which the capsules produced with 4% (w/w) of gelatin were significantly smaller. Similar results were reported by Rocha-Selmi, Favaro-Trindade and Grosso (2013) studying complex coacervation of lycopene, in which the increase on gelatin concentration from 2.5 to 7.5 % led to a decrease of capsule diameters from 144 to 61 µm. Marfil et al. (2018), investigating the production of capsules of gelatin and gum Arabic for the encapsulation of palm oil by complex coacervation in batch stirring, varied the wall material concentration from 0.8 to 9.21 % with the capsule diameters ranging from 97 to 690 µm, respectively. Jain et al. (2016) studied complex coacervation using casein and gum Tragacanth and reported that the increase on total polymer concentration from 0.375 to 0.5 % led to a decrease of capsule size at different protein to polysaccharide ratio. Investigating the influence of sodium dodecyl sulphate concentration and agitation rate in complex coacervation, Guo and Zhao (2008) reported that the increase on concentration from 0.005 to 0.015 % lead to a decrease of capsule diameter from 58 to 38 µm. In the present study, the final concentration of wall material (gelatin + Arabic Gum) was 1.3 % for samples with 4 % (w/w) of gelatin and 1.4 % to samples with 10 % (w/w) gelatin, considering the total wall material and the final mixture after coacervation. In complex coacervation of gelatin and gum Arabic for encapsulation of turmeric oleoresin, Zuanon, Malacrida and Telis (2013) reported capsules diameters of 46 µm for wall material concentration of 2.5 % and 53 µm to 5.0 % of wall material.

The variation coefficient (VC) of the capsules' average diameter is a good indicator of the size distribution of the capsules and how stable or under control is process (BROWN; BROWN, 1998). The VC for capsules with 4 % (w/w) of gelatin/ginger oil ranged from 16 to 25 %, whereas for capsules with 10 % (w/w) of gelatin the VC varied from 14 to 20 %. In addition, the capsules with 10 % (w/w) presented a smaller VC for all coacervation assays, with exception of conditions BS1 and MC3. In microencapsulation of *Saccharomyces cerevisiae* by complex coacervation assisted by membrane emulsification, Morelli, Holdich and Dragosavac (2017) reported VC as low as 17 %. The histograms in Figure 7.5a show that the sample produced by batch stirring (G4-BS1) presented the highest capsule diameter, and the sample G4-MC5 the smallest one among capsules with 4 % (w/w) gelatin ginger/oil. On the other hand, samples produced by atomization of a 10 % gelatin:ginger oil emulsion, mainly G10-AT11 and G10-AT13, presented the narrowest size distribution (Figure 7.5b) corroborated by the correspondent VC (Table 7.3). These results allow the conclusion that the use of a more concentrated emulsion generated capsules with narrower size distributions. Dragosavac et al. (2008), investigating the production of oil-in-water emulsions using a membrane setup similar to the one used in this study, presented similar results, in which more concentrated dispersed phase generated smaller emulsion droplets with narrower size distribution.

Table 7.3. Operational parameters, size, size distribution, encapsulation parameters of capsules produced by membrane and atomization complex coacervation

| Sample Code | Emulsion composition | Agitation at DC (rpm) | Emulsion injection flow rate (mL/min) | Atomization air flow rate $10^{-4}$ ($m^3$/s) | Complex coacervation shear stress (Pa) | Complex coacervation Reynolds number | Capsule's mean diameter[1] (um) | Capsule's size VC (%) | Encapsulation efficiency EE[2] (%) | Encapsulation yield EY[2] (%) |
|---|---|---|---|---|---|---|---|---|---|---|
| G4-BS1 | Gelatin:oil ratio 1:1 4 g gelatin/100 g | - | - | | - | - | $75.0^{a}$ | 15.9 | $90.9^{abc}$ | $78.8^{abc}$ |
| G4-MC2 | | 540 | 3 | | 1.1 | 5236 | $65.9^{def}$ | 19.5 | $61.9^{i}$ | $51.8^{de}$ |
| G4-MC3 | | 1070 | 3 | | 5.8 | 15257 | $64.9^{ef}$ | 17.6 | $72.2^{fghi}$ | $49.1^{def}$ |
| G4-MC4 | | 1780 | 3 | | 12.6 | 25278 | $72.2^{ab}$ | 21.8 | $74.8^{defghi}$ | $51.5^{de}$ |
| G4-MC5 | | 540 | 5 | | 1.1 | 5236 | $53.7^{j}$ | 19.1 | $69.9^{ghi}$ | $77.3^{abc}$ |
| G4-MC6 | | 1070 | 5 | | 5.8 | 15257 | $63.5^{fg}$ | 23.0 | $73.9^{efghi}$ | $67.6^{bcd}$ |
| G4-MC7 | | 1780 | 5 | | 12.6 | 25278 | $64.9^{ef}$ | 18.8 | $78.8^{cdefgh}$ | $79.5^{abc}$ |
| G4-MC8 | | 540 | 10 | | 1.1 | 5236 | $68.8^{cd}$ | 24.6 | $66.6^{hi}$ | $66.8^{cd}$ |
| G4-MC9 | | 1070 | 10 | | 5.8 | 15257 | $65.9^{def}$ | 21.1 | $69.3^{ghi}$ | $62.0^{cd}$ |
| G4-MC10 | | 1780 | 10 | | 12.6 | 25278 | $68.4^{cd}$ | 20.1 | $79.8^{cdefgh}$ | $90.8^{ab}$ |
| G4-AT11 | | - | 10 | 2.36 | 23 | 2176 | $71.0^{bc}$ | 23.1 | $83.5^{bcdef}$ | $61.0^{cd}$ |
| G4-AT12 | | - | 13 | 3.93 | 48 | 3627 | $68.3^{cd}$ | 18.2 | $86.4^{abcde}$ | $95.5^{a}$ |
| G4-AT13 | | - | 14 | 5.51 | 77 | 5078 | $58.7^{i}$ | 19.0 | $79.6^{cdefgh}$ | $84.1^{abc}$ |
| G10-BS1 | Gelatin:oil ratio 1:1 10 g gelatin/100 g | - | - | | - | - | $60.9^{ghi}$ | 16.4 | $98.1^{a}$ | $31.4^{efgh}$ |
| G10-MC2 | | 540 | 3 | | 1.1 | 5236 | $61.5^{ghi}$ | 19.2 | $93.5^{ab}$ | $50.8^{de}$ |
| G10-MC3 | | 1070 | 3 | | 5.8 | 15257 | $68.6^{cd}$ | 20.1 | $92.2^{abc}$ | $33.0^{efgh}$ |
| G10-MC4 | | 1780 | 3 | | 12.6 | 25278 | $62.9^{fgh}$ | 16.5 | $88.4^{abcd}$ | $31.3^{efgh}$ |
| G10-MC5 | | 540 | 5 | | 1.1 | 5236 | $63.9^{fg}$ | 18.6 | $72.9^{efghi}$ | $15.3^{h}$ |
| G10-MC6 | | 1070 | 5 | | 5.8 | 15257 | $66.0^{def}$ | 16.3 | $88.4^{abcd}$ | $26.6^{fgh}$ |
| G10-MC7 | | 1780 | 5 | | 12.6 | 25278 | $68.5^{cd}$ | 16.2 | $82.4^{bcdefg}$ | $22.7^{gh}$ |
| G10-MC8 | | 540 | 10 | | 1.1 | 5236 | $60.0^{hi}$ | 16.7 | $81.2^{bcdefg}$ | $25.0^{gh}$ |
| G10-MC9 | | 1070 | 10 | | 5.8 | 15257 | $67.2^{de}$ | 16.9 | $88.9^{abc}$ | $22.3^{h}$ |
| G10-MC10 | | 1780 | 10 | | 12.6 | 25278 | $64.7^{ef}$ | 15.7 | $90.9^{abc}$ | $35.0^{efgh}$ |
| G10-AT11 | | - | 10 | 2.36 | 195 | 2176 | $50.5^{k}$ | 14.6 | $92.1^{abc}$ | $45.9^{defg}$ |
| G10-AT12 | | - | 13 | 3.93 | 406 | 3627 | $52.^{jk}$ | 15.6 | $81.1^{bcdefg}$ | $17.2^{h}$ |
| G10-AT13 | | - | 14 | 5.51 | 657 | 5078 | $51.8^{jk}$ | 14.1 | $74.1^{efghi}$ | $11.7^{h}$ |

[1]Mean values ± standard error (n = 600); [2]Mean values ± standard error (n = 3); N.A: *The number after "GE" indicate gelatin concentration, the number following "MC" refers to membrane coacervation condition, the number following letters "AT" refers to atomization condition and "BS" stands for batch stirring.

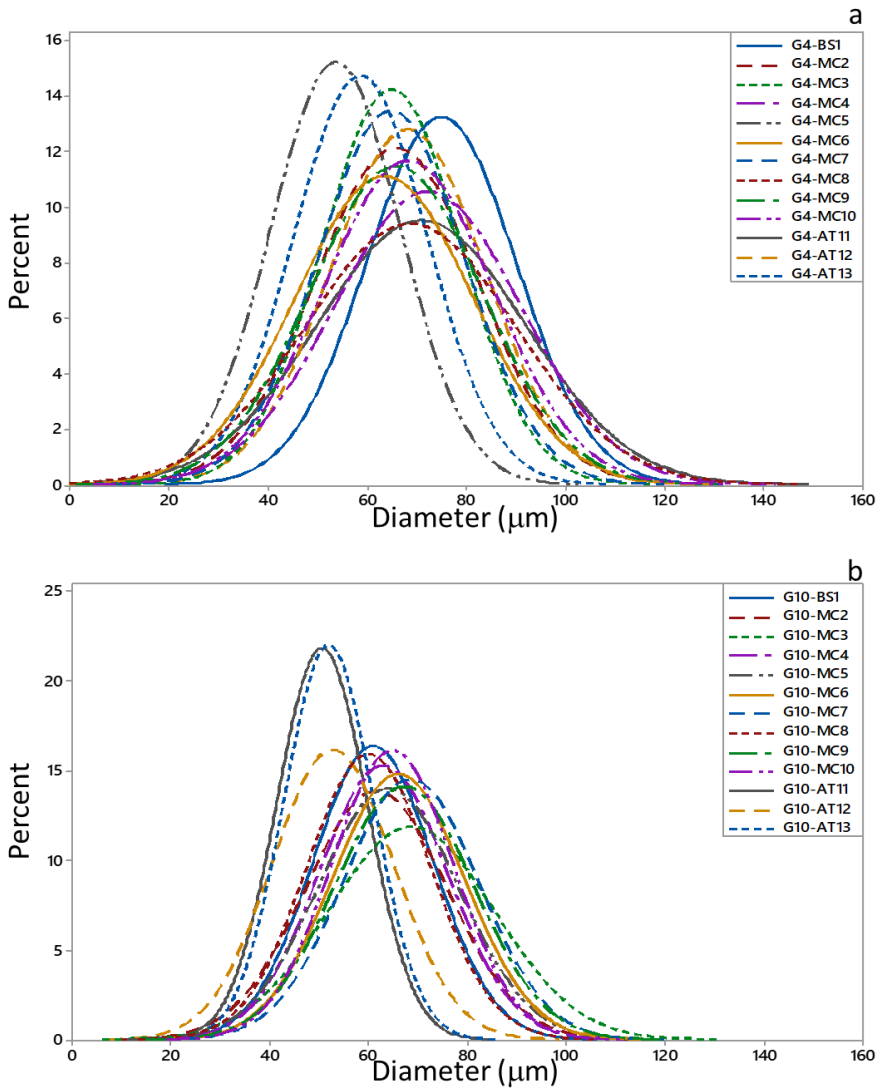


Figure 7.5. Size distribution of wet microcapsules produced with emulsions containing (a) 4% (w/w) of gelatin and (b) 10% (w/w) of gelatin.

To the best of our knowledge, the use of metal membrane technology as an alternative to carry out complex coacervation has not yet been reported in the literature. There is an increasing interest on using metal membranes to carry out emulsification, considering its ability to produce emulsions drop-by-drop, which generates emulsion droplets with low size distribution (DRAGOSAVAC et al., 2008; MORELLI; HOLDICH; DRAGOSAVAC, 2017; PU; WOLF; DRAGOSAVAC, 2019; SANTOS et al., 2015). In addition, the setup used for membrane emulsification using metal membranes has the technology in place to operate in both batch and continuous process, from laboratory to industrial scale (HOLDICH et al., 2020). In this context, the objective of this study is to set the primary process conditions for the promising idea of adapting the existent technology of metal membrane emulsification to induce complex coacervation.

Considering the process parameters for membrane complex coacervation, the shear stress varied from 1.1 to 12.6 Pa and the gelatin/ginger oil emulsion injection rate varied from 3 to 10 mL/mim (Figure 7.6).

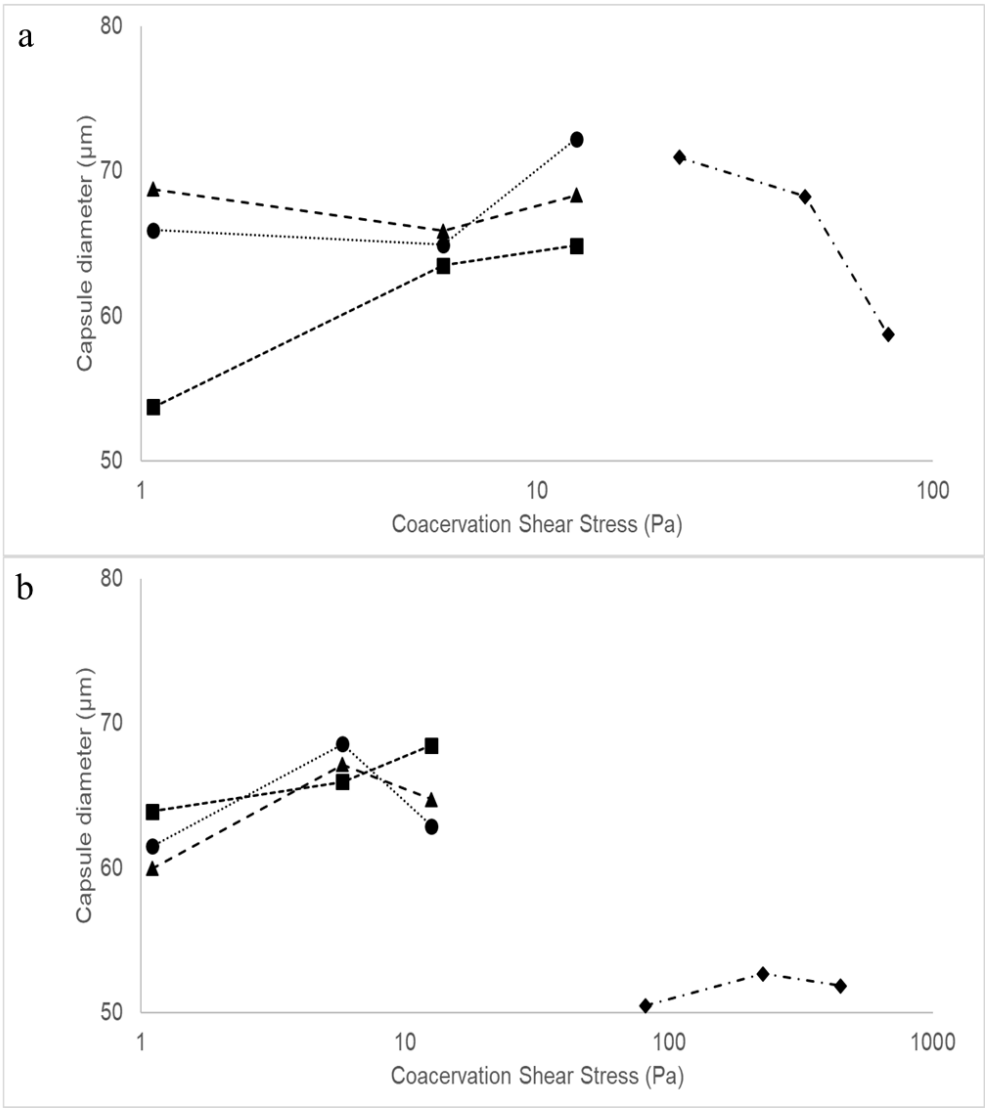


Figure 7.6. Capsule size in function of coacervation shear stress for emulsions with 4% (w/w) of gelatin (a) and emulsions with 10 % (w/w) of gelatin (b). The symbols represent: (●) 3 mL/min, (■) 5 mL/min and (▲) 10 mL/min by membrane complex coacervation and (♦) atomization complex coacervation. For clarity the error bars were not presented.

The coacervation shear stress caused during membrane coacervation is a function mainly of the agitation speed generated by the stirrer (DRAGOSAVAC et al., 2008). The capsule diameters obtained by membrane complex coacervation varied from 53 to 72 um for samples with 4 % (w/w) gelatin and from 60 to 69 um for formulations with 10 % (w/w) of gelatin/ginger oil. These capsule diameters are considered appropriate for application in foods products (OZKAN et al., 2019; PAULO; SANTOS, 2017; PEANPARKDEE; IWAMOTO; YAMAUCHI, 2016). The emulsion injection rate did not interfere significantly on the capsules' diameter for both formulations (Table 7.3). There is not a consensus in the literature about the

influence of the emulsion injection rate on emulsion droplet size. Dragosavac, Holdich, Vladisavljević and Sovilj (2012) investigating the production of multiple emulsions of pumpkin seed oil by membrane emulsification in disperse cells obtained results where the increase of the injection rate led to greater emulsion droplets. On the other hand, Holdich et al. (2020) obtained smaller droplets in higher injection rates of dispersed phase on membrane emulsification using an annular flow-crossflow membrane (continuous process).

When comparing the diameter of capsules produced by batch stirring and membrane, two different results were observed based on the formulation (Table 7.3). For capsules with 4 % (w/w) of gelatin/ginger oil the capsules produced by membrane were significantly smaller for all conditions applied comparing with batch stirring (75.0 µm), with the exception of the capsules produced with shear stress of 12.6 Pa and injection rate of 3 mL/min (Table 7.3). However, the capsules produced with 10 % (w/w) of gelatin/ginger oil by batch stirring (60.9 µm) were among the smallest capsules produced with this formulation, comparing with membrane complex coacervation. The different behaviours observed for both formulations may be attributed at least in part to the rheological parameters of the liquid medium during complex coacervation.

Considering the capsules formed by atomization, a decrease in the diameter with increasing shear stress for samples with 4 % (w/w) of gelatin/ginger oil was observed varying the size from 71.0 to 58.7 µm (Figure 7.6 and Table 7.3). For capsules with 10 % (w/w) the diameter ranged from 50.5 to 52.7 µm. Between 195 and 657 Pa the diameter of the three samples was significantly smaller than all other samples within this formulation. These conditions created the smallest capsules, except for the capsules produced with 1.1 Pa, 5 mL/min and 4 % (w/w) of gelatin/ginger oil. These results reinforce the conclusion that not only the method of complex coacervation (process conditions) has influence on the capsule size, but formulation (thermodynamic factors) also plays an important role (JAIN et al., 2016; JEGAT; TAVERDET, 2000; LEMETTER; MEEUSE; ZUIDAM, 2009; MA et al., 2019). Ferreira and Nicoletti (2020) investigating the influence of atomization parameters on complex coacervation induced by two-fluid nozzle ranged shear stress during the coacervation process from 6 to 170 Pa, producing capsules with size varying from 60 to 75 µm. Studying the application of a 4-fluid nozzle to produce particles of acetaminophen, chitosan, hydroxy propyl methylcellulose for sustained release, Chen et al. (2006) reported a wide particle size variation from 0.6 to 214.6 µm depending on the ratio and formulation used. For capsules produced by batch stirring, the literature presents a wide range of capsule sizes influenced by different process condition (e.g. formulation, pH, polymer ratio, agitation), such as 97 to 690 µm

(MARFIL et al., 2018), 60 to 70 µm (MORELLI; HOLDICH; DRAGOSAVAC, 2017), 132 to 490 µm (LEMOS; MARIANO MARFIL; NICOLETTI, 2017) and 61 to 144 µm (ROCHA-SELMI; FAVARO-TRINDADE; GROSSO, 2013).

The increase in the Reynolds number during the complex coacervation process affects the capsule size in different ways, with dependence on the formulation (Table 7.3). Regarding membrane coacervation, capsules produced with 4 % (w/w) had an increase in the diameter with increasing Reynolds number from 5236 to 25278 for injection rates of 3 and 5 mL/min. Similar behaviour was observed for capsules produced with 10 % (w/w) of gelatin/ginger oil for injection rate of 5 mL/min. In both formulations, injection flow rate of 5 mL/min produced the smallest capsules (Table 7.3). In complex coacervation by atomization however, the capsule size decreased with increasing Reynolds for the 4 % (w/w) samples, whereas 10 % (w/w) samples were not affected by this dimensionless number. The only data available in literature that allow some comparison are those obtained for complex coacervation by batch stirring. In that case, the rule seems to be that higher Reynolds number leads to smaller capsule sizes (JEGAT; TAVERDET, 2000; LEMETTER; MEEUSE; ZUIDAM, 2009; LEMOS; MARIANO MARFIL; NICOLETTI, 2017).

The morphology of the capsules produced in the different conditions did not show any remarkable distinct characteristic (Figure 7.7). In general, all coacervation methods, process parameters and formulations provided capsules with sizes of same order of magnitude and defined spherical shape, as expected for complex coacervation between gelatin and gum Arabic (MARFIL et al., 2018; PIACENTINI et al., 2013). The samples with 10 % (w/w) of gelatin seems darker, mainly the atomized ones, than those produced with 4 % (w/w). Taking into account that the emulsion produced with 10 % (w/w) have a higher density (Table 7.1), it is possible to infer that the samples with higher concentration of gelatin in the initial emulsion results in capsules with higher density. The same result was reported by Ferreira and Nicoletti (2021) for complex coacervation induced by atomization. Knowing the density of the capsule is an important parameter when considering the method of separation between the capsules and the non coacervated liquid. Typically, this separation underlays on gravity, thus denser capsules may facilitate this step (TOMAS, 2004).

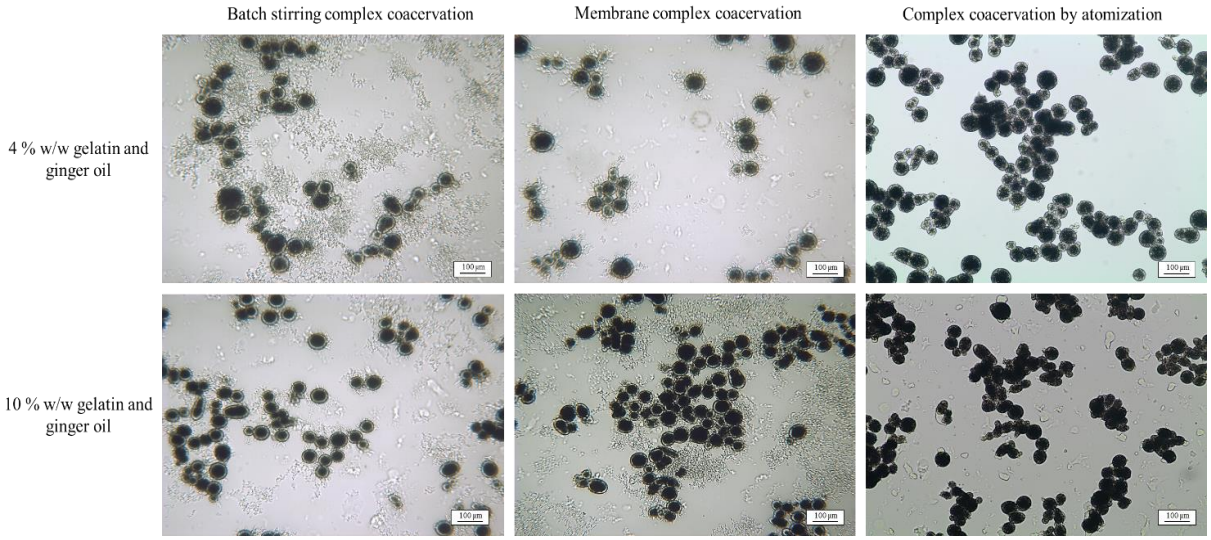


Figure 7.7. Morphology of capsules produced by different complex coacervation methods: batch stirring, membrane (MC6 – injection rate 5 mL/min and shear stress 13 Pa) and atomization (AT12 – shear stress of 48 (G4) and 406 (G10) Pa). Bar indicates 100 µm.

*7.3.3 Influence of complex coacervation methods on encapsulation efficiency and yield*

When proposing a new microencapsulation process the study of encapsulation parameters such as encapsulation efficiency *(EE*) and encapsulation yield (*EY*) provides a solid overview on the prospects of future application of this new technique, giving an idea for future improvements on its application. Complex coacervation is known to be a technique to provide high values of encapsulation efficiency, meaning that most of the core in encapsulated inside the capsule matrix (TIMILSENA et al., 2019).

The formulation and the method of complex coacervation had influence on encapsulation parameters studied (Table 7.3). For capsules with 4% (w/w) of gelatin/ginger oil the *EY* was 78.8 % for capsules produced by batch stirring, 49 to 91 % for membrane complex coacervation and 61 to 95 % to complex coacervation by atomization. The *EE* values for capsules with 4% (w/w) of gelatin/ginger oil was 91 % for batch stirring complex coacervation, and varied from 61 to 80 % for membrane coacervation and 83 to 86 % for coacervation by atomization. The *EY* for capsules with 10 % (w/w) gelatin/ginger oil was 31.4 % for batch stirring and the values varied from 15 to 50 % for membrane coacervation and 11 to 45 % for coacervation by atomization. The *EE* value for batch stirring was 98.1 % and ranged from 72 to 93 % for membrane coacervation and 74 to 92 to coacervation induced by atomization (Table 7.3). While *EY* decreased for the more concentrated emulsion, *EE* increased, although the differences were not so pronounced as in the case of *EY*. The fact that emulsions with 10 % (w/w) of gelatin presented a low OS and EY (Figure 7.8b and 7.8f) indicates that part of the ginger oil is being lost during the process but the oil that remains is trapped inside the capsule.

This can be attributed to the higher viscosity of the emulsion with 10 % (w/w) of gelatin, which promotes a sterical stability of the emulsion, but at the same time may difficult formation of a high amount of capsules. This effect may be illustrated by the high amount of polymer surrounding the microcapsules that appear in Figure 7.7, for membrane coacervation with 10 % (w/w) emulsion. Butstraen and Salaün (2014) studying the complex coacervation between gum Arabic and chitosan did not find relationship between *EY* and the increase of chitosan concentration, however the increase of chitosan increased *EE* up to 97 %. The influence of injection rate during membrane coacervation is presented in Figure 7.8. In general, injection rates of 5 am 10 mL/min resulted in higher *EE* and *EY* for capsules with 4% (w/w) of gelatin/ginger oil. On the other hand, for capsules with 10 % (w/w) of gelatin/ginger oil *EY* and *EE* decreased for values of injection rate above 3 mL/min (Figure 7.8b and 7.8d).

Figure 7.9 shows the influence of shear stress on encapsulation parameters for coacervation by membrane and by atomization. In membrane coacervation, for emulsions with 4 % (w/w) of gelatin/ginger/oil the increase in shear stress led to an increase in *EY* and *EE* (Figure 7.9a and 7.9c), whereas for complex coacervation by atomization, the higher values of *EY* and *EE* were observed at the intermediate value of shear stress (48 Pa). For capsules formulated with 10 % (w/w), *EE* and *EY* were favoured at the lower value of shear stress and injection rate of 3 mL/min for membrane coacervation and at the lower shear rate for atomization (Figure 7.9b and 7.9d). During atomization, the increase in shear stress increased the oil content in the surface of the capsules, what can be related to previous results indicating that there is a limit of shear forces that an emulsion is able to support during droplet formation before it starts to affect the encapsulation performance, and this limit can be directly correlated with the formulation of the system (FERREIRA; NICOLETTI, 2020). The curves shown in Figure 7.9 suggest that there is an interaction between shear stress, emulsion concentration, and formation of capsules with suitable values of *EE* and *EY* by membrane complex coacervation, and this interaction should be further investigated in order to optimize the encapsulation of oils by using metal membranes.

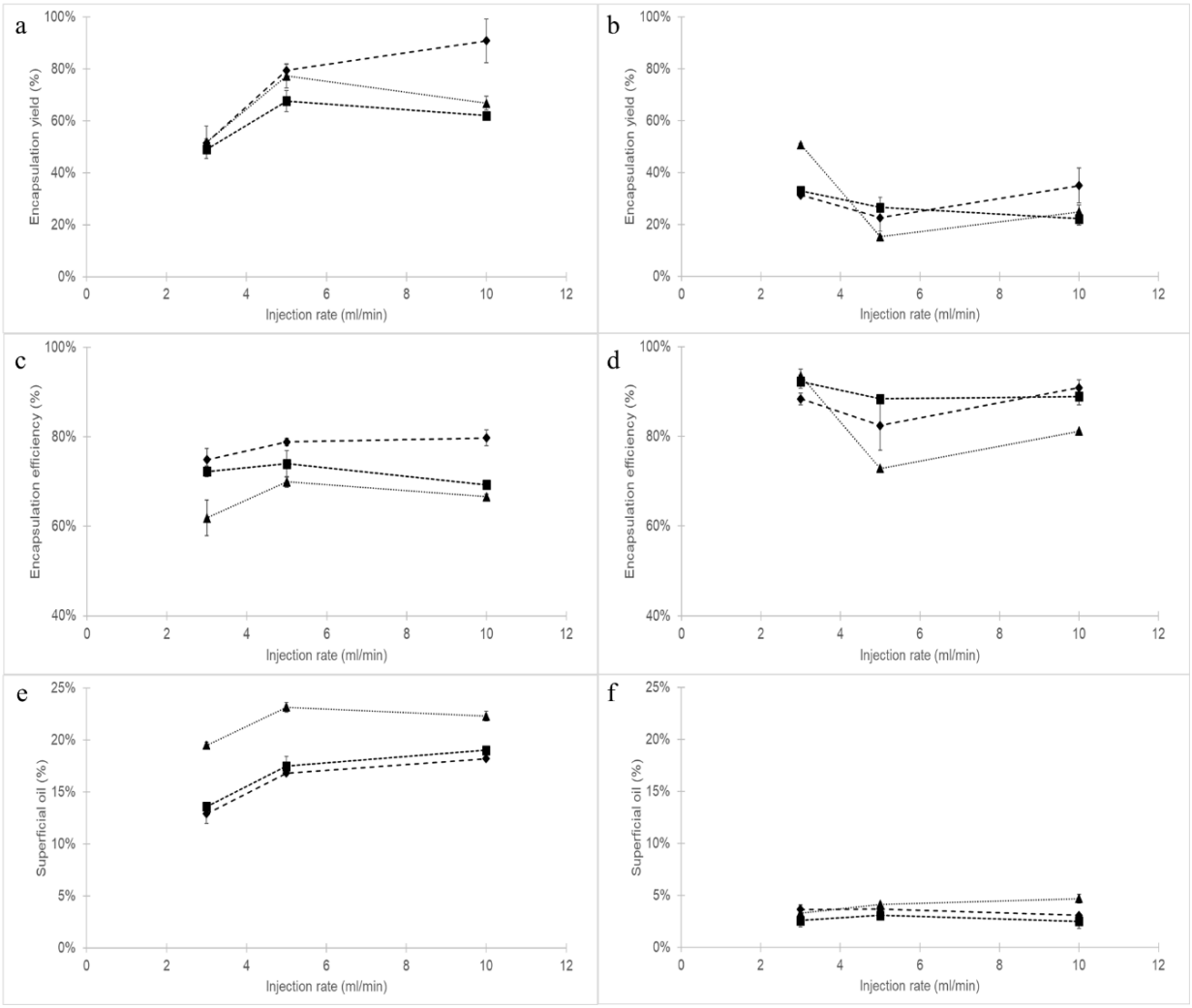


Figure 7.8. Encapsulation yield, encapsulation efficiency, and oil at the surface of microcapsules versus injection rate for capsules produced by membrane coacervation for emulsions with 4 % (w/w) gelatin (a, c, and e) and with 10 % (w/w) of gelatin (b, d, and f). The symbols represent coacervation shear stress of (●) 1.1 Pa, (■) 5.8 Pa, and (▲) 12.6 Pa.

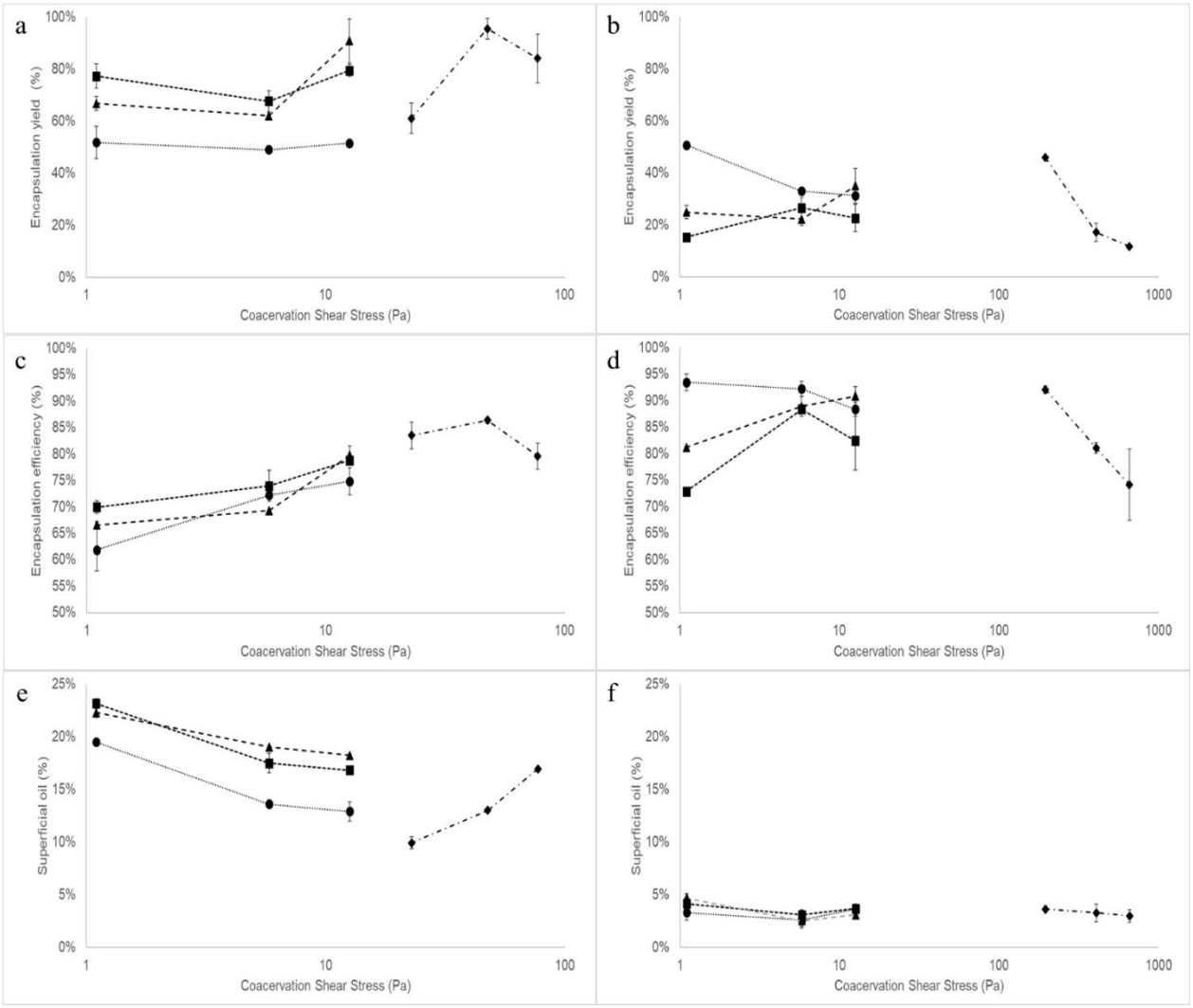


Figure 7.9. Encapsulation yield, encapsulation efficiency, and oil at the surface of microcapsules versus shear stress for capsules produced for emulsions with 4 % (w/w) gelatin (a, c, and e) and with 10 % (w/w) of gelatin (b, d, and f). The symbols represent injection rates of (●) 3 mL/min, (■) 5 mL/min, and (▲) 10 mL/min for membrane complex coacervation and (♦) atomization complex coacervation.

## 7.4. Conclusions

The two new setups proposed to induce complex coacervation (atomization and metal membrane) were successful in creating capsules comparable with the traditional technique of complex coacervation (batch stirring). The ratio of biopolymers and the pH affected the induction of complex coacervation. In addition, samples with lower ratio of gum Arabic:gelatin did not go successfully through the cooling process. The capsules produced by all methods were smaller than 100 μm, with a defined spherical shape and with a narrow size distribution, as expected for complex coacervation between gelatin and gum Arabic. Formulation played an important role in complex coacervation by membranes, in which emulsions with 4 % (w/w) of

gelatin/ginger oil generated capsules significantly smaller and with higher values of encapsulation efficiency and encapsulation yield. Emulsions containing 10 % (w/w) of gelatin/ginger oil were able to produce the smallest capsules, although the encapsulation yield was low. The shear stress applied during complex coacervation influenced differently the capsule production, depending on the formulation and method of complex coacervation. Capsules with 4 % (w/w) of gelatin/ginger oil had a better overall encapsulation performance considering coacervation by batch stirring, membrane and atomization. The best conditions for membrane complex coacervation was 12.6 Pa of shear stress and 10 mL/min of injection rate, and shear stress of 48 Pa for coacervation induced by atomization, departing from emulsions with 4 % (w/w) of gelatin/ginger oil for both methods. This study shows the potential of complex coacervation induced by metal membranes and atomization, both with potential to be carried out as continuous processes and in large scale.

**Acknowledgements**

The authors thank Micropore Technologies Ltd. for providing the dispersion cell/membranes for membrane coacervation, and Adiella E. Abelseth for proof reading with a focus on the English language of the article.

This work was supported by the São Paulo Research Foundation - FAPESP (grant numbers 2015/23290-0 and 2018/16976-0) and National Council for Scientific and Technological Development - CNPq (grant number 305355/2016-3).

## CHAPTER 8 – MAIN RESULTS AND DISCUSSION

Complex coacervation is a versatile microencapsulation technique capable of encapsulating and protecting hydrophobic and hydrophilic compounds. In addition, it is able to protect the encapsulated core from adverse conditions such as light, oxygen and low pH during digestion. Traditionally, complex coacervation is carried out in batch mode, which makes it more expensive and less desirable to be used in industrial scale. In complex coacervation, the polymeric solutions are mixed and their pH is adjusted to promote interaction between the polymers and subsequent coacervation. Once coacervation is achieved, the capsules may be cooled and cured. This process is done using a jacketed vessel in a slow cooling process. The curing of the capsules can be seen as one of the more significant bottlenecks of the process, since it demands time, sleeved tanks and large amounts of energy. Another point to be considered is that there are not many alternatives to predict the final size of the capsules based on their formulation or on the process conditions. In some applications, knowing the size of the capsule produced may be of interest, due to the amount of core to be delivery, sterical conditions, and others. The emulsification step is a crucial step during the coacervation process, since the emulsion stability and size of the droplets may play an important role on the final capsule parameters. Developing alternatives to produce stable emulsion droplets with controlled size and low size distribution is an efficient approach to produce proper coacervated capsules. Therefore, in this thesis, the application of atomization by a two-fluid nozzle and of flow through metal membranes to induce complex coacervation was studied aiming to pave the way to scale up the complex coacervation process. Both processes were described based on their specific process conditions and compared with the traditional batch stirring complex coacervation, regarding capsule size, size distribution, capsule morphology, encapsulation parameters and infrared spectra. Another attempt to scale up complex coacervation was made by evaluating the use of a tubular heat exchanger to cool and cure the capsules after the coacervation step. By doing so, the complex coacervation encapsulation process can be more reproducible, faster, cheaper (more efficient), scaled up and carried in a semi-continuous mode.

In the first part of this work (Chapter 3), coacervation by atomization was presented. The influence of formulation (polymers ratio and emulsion concentration) on particle formation, morphology, size and size distribution and encapsulation parameters was investigated, comparing it with capsules formed by batch stirring. Since capsules coacervated under lower pH values tend to be more resistant to gastric conditions, the pH value was set to 3.5. The optimum ratio obtained to be used throughout the thesis was 1.8:1 (later approximated to 2:1) of gum Arabic:gelatin. The gelatin concentration affected differently capsules formed

by atomization and batch stirring. The capsules produced by atomization were in general equal or better than those produced by batch stirring.

Knowing the influence of the formulation on complex coacervation by atomization, in Chapter 4 it was studied the influence of atomization conditions on complex coacervation. Using two formulations, one with 1 % (w/w) and one with 6 % (w/w) of gelatin, was evaluated the influence of atomization air flow rate and emulsion flow rate, on capsule size and encapsulation parameters. In addition, important advances were achieved mathematically describing the process in terms of its dimensionless numbers and presenting a model to predict the final size of the capsules after curing. This was accomplished by using as reference a hydrodynamic model that predicted the size of the emulsion droplets leaving the nozzle and applying it in a non-linear regression. The influence of atomization numbers Weber (*We*) and Ohnesorge (*Oh*), shear rate and shear stress on the encapsulation performance was analysed and a model able to predict the final size of the microcapsules produced at $We \geq 180$ and $Oh = 0.063$ was proposed.

Chapter 5 presented the effect of a tubular heat exchanger to promote the cure of the coacervated capsules, commonly done by a jacketed vessel. By using a heat exchanger, the curing of the capsules, that is a known bottle neck of the process, can be done faster, in a continuous mode, besides being easily scalable. Again, the coacervation step was done in batch stirring and atomization using formulation and atomization conditions previously determined. During the curing step the flow rate and the temperature were varied. The overall time of the curing step dropped drastically, to less than 10 minutes. A synergy between flow rate (shear forces) and the curing temperature was observed. Atomized capsules had their encapsulation parameters improved at higher curing flow rate. Also, the resistance of the capsules under gastric conditions was tested. Capsules cured using the tubular heat exchanger proved to have high resistance to simulated gastric conditions, which means that the core material was not released in gastric conditions. This is an important result, since the nutrient absorption occurs after the gastric phase. So, the use of a tubular heat exchanger to carry the curing step presents as a promising alternative.

The use of metal membranes to form emulsions to be then used complex coacervation process was evaluated in Chapter 6. The emulsification conditions and gelatin concentration had great influence on the emulsion droplet size. In coacervation by batch stirring, single core capsules were produced. When coacervation was induced by atomization, the capsules formed were smaller than the initial emulsion droplets formed my membrane emulsification. This indicated that the shear forces during the atomization process would promote a second

emulsification at the nozzle. The encapsulation parameters indicated that most of the oil was being transported throughout the coacervation process, but not inside the capsules. Hence, even though the previous chapters did not require the use of crosslinkers, for membrane emulsification followed by complex coacervation, this may be of necessity.

Chapter 7 presented complex coacervation assisted by metal membranes, in which the gelatin/ginger oil emulsion was forced through a metal membrane into the gum Arabic solution both polymers with their pH adjusted to 3.5, inducing the coacervation. In addition, a study evaluating both polymer and coacervation pH was done, confirming the results presented in Chapter 3, that for lower coacervation pH a higher polysaccharide:protein ratio was necessary. Since this part of the thesis and Chapter 6 were done in the United Kingdom, it was not possible to evaluate the use of the heat exchanger during the curing step. Even though the assays were carried in laboratory scale and in a dispersion cell (batch configuration), the technology of applying metal membranes is available in larger scale and in continuous process. Emulsion with lower gelatin concentration (4 %w/w) produced capsules with higher encapsulation properties. The use of metal membrane to assist coacervation proved to be possible. The process conditions described in this thesis can be used in future to carry out complex coacervation in continuous configuration. By using a heat exchanger to perform the cure of the capsules (as described in Chapter 5), the whole process of complex coacervation could be carried out in continuous process and in an industrial scale. Complex coacervation assisted by metal membranes proved to be possible to further applications and studies.

## CHAPTER 9 – GENERAL CONCLUSIONS

Complex coacervation assisted by a two-fluid nozzle was achieved and described. To induce proper complex coacervation the pH 3.5 and the polymer ratios of 2:1 or 1.8:1 (gum Arabic:gelatin), proved to be the best conditions. In general, capsules produced by atomization were comparable (size, encapsulation parameter and FTIR) to capsules produced by batch stirring, which opens new possibilities to carry out complex coacervation using a two-fluid nozzle.

Atomization conditions had great influence over capsules size and for $Oh > 0.01$ and $We > 180$ it was possible to model and to predict the size of the capsules based on these dimensionless numbers, paving the way to scaling up the process. Best encapsulation conditions were obtained for $We < 250$ and optimum conditions considering capsule size prediction and encapsulation parameter were for $180 < We < 250$.

The use of a tubular heat exchanger to cure the capsules has proven to be feasible and promising. The use of a continuous heat exchanger produced capsules ready to be freeze dried in less than 10 minutes. After freeze drying, the capsules presented high encapsulation parameters and gastric resistance. With this, the cure of capsules can be done faster, in larger scale, more efficiently and continuously. The process parameters used during the curing step of the capsules had great influence on capsules size, morphology and encapsulation parameters. Inducing complex coacervation at pH 3.5 proved to produce capsules resistant to gastric conditions.

The emulsions droplets produced by metal membrane technology had predictable size and low size distribution, which make it of interest for future applications in encapsulation. The use of metal membranes to produce capsules by complex coacervation proved to be feasible and are a promising alternative to achieve complex coacervation in continuous mode.

In conclusion, the alternative methods to induce oil encapsulation by complex coacervation proposed in this work showed to be feasible and represent potential and relevant advantages compared to the traditional batch stirring method.

## CHAPTER 10 – SUGESTIONS FOR FUTURE STUDIES

Evaluate the use of other polymeric pairs to carry out complex coacervation by atomization and metal membranes, cured using heat exchanger.

Study the influence of the increase of oil concentration on complex coacervation by atomization and metal membrane.

Perform a broader study varying atomization parameters and emulsion formulation to model prediction of capsules size.

Evaluate the stability of the capsules produced by atomization and metal membranes under different conditions.

Investigate complex coacervation by atomization and metal membranes of several encapsulated materials of different chemical natures, such as other oils, oleoresins, Hydrophilic and hydrophobic vitamin and other compounds, drug to controlled and targeted delivery and microorganisms.

Evaluate the application of the capsules produced by atomization and metal membrane and cured in a heat exchanger in products of different natures.

Scale up the curing process by using a larger heat exchanger and describe the process in function of non-dimensional numbers of heat and mass transfer.

Perform complex coacervation assisted by metal membranes coupled in a heat exchanger to achieve complex coacervation in continuous mode.

## REFERENCES

ABRAHAMSE, Anneke J.; VAN LIEROP, R.; VAN DER SMAN, R. G. M.; VAN DER PADT, A.; BOOM, R. M. Analysis of droplet formation and interactions during cross-flow membrane emulsification. **Journal of Membrane Science**, *[S. l.]*, 2002. DOI: 10.1016/S0376-7388(02)00028-5.

ACH, Delphine; BRIANÇON, Stéphanie; BROZE, Guy; PUEL, François; RIVOIRE, Alain; GALVAN, Jean Marc; CHEVALIER, Yves. Formation of microcapsules by complex coacervation. **Canadian Journal of Chemical Engineering**, *[S. l.]*, 2015. DOI: 10.1002/cjce.22086.

ALEMZADEH, I.; HAJIABBAS, M.; PAKZAD, H.; SAJADI DEHKORDI, S.; VOSSOUGHI, A. Encapsulation of food components and bioactive ingredients and targeted release. **International Journal of Engineering, Transactions A: Basics**, *[S. l.]*, 2020. DOI: 10.5829/ije.2020.33.01a.01.

ALISEDA, A.; HOPFINGER, E. J.; LASHERAS, J. C.; KREMER, D. M.; BERCHIELLI, A.; CONNOLLY, E. K. Atomization of viscous and non-newtonian liquids by a coaxial, high-speed gas jet. Experiments and droplet size modeling. **International Journal of Multiphase Flow**, *[S. l.]*, 2008. DOI: 10.1016/j.ijmultiphaseflow.2007.09.003.

ALVIM, Izabela Dutra; GROSSO, Carlos Raimundo Ferreira. Microparticles obtained by complex coacervation: influence of the type of reticulation and the drying process on the release of the core material. **Ciência e Tecnologia de Alimentos**, *[S. l.]*, v. 30, n. 4, p. 1069–1076, 2010. DOI: 10.1590/s0101-20612010000400036.

AMERI, Mahmoud; MAA, Yuh Fun. **Spray drying of biopharmaceuticals: Stability and process considerationsDrying Technology**, 2006. DOI: 10.1080/03602550600685275.

AN, Kejing; ZHAO, Dandan; WANG, Zhengfu; WU, Jijun; XU, Yujuan; XIAO, Gengsheng. Comparison of different drying methods on Chinese ginger (Zingiber officinale Roscoe): Changes in volatiles, chemical profile, antioxidant properties, and microstructure. **Food Chemistry**, *[S. l.]*, 2016. DOI: 10.1016/j.foodchem.2015.11.033.

ANTON, Nicolas; GAYET, Pascal; BENOIT, Jean Pierre; SAULNIER, Patrick. Nano-emulsions and nanocapsules by the PIT method: An investigation on the role of the temperature cycling on the emulsion phase inversion. **International Journal of Pharmaceutics**, *[S. l.]*, v. 344, n. 1–2, p. 44–52, 2007. DOI: 10.1016/j.ijpharm.2007.04.027.

ANVARI, Mohammad; CHUNG, Donghwa. Dynamic rheological and structural characterization of fish gelatin - Gum arabic coacervate gels cross-linked by tannic acid. **Food Hydrocolloids**, *[S. l.]*, 2016. DOI: 10.1016/j.foodhyd.2016.04.028.

ARSHADY, R. Microcapsules for food. **Journal of Microencapsulation**, *[S. l.]*, 1993. DOI: 10.3109/02652049309015320.

AUGUSTIN, Mary Ann; HEMAR, Yacine. Nano- and micro-structured assemblies for encapsulation of food ingredients. **Chemical Society Reviews**, *[S. l.]*, 2009. DOI: 10.1039/b801739p.

BAN, Zhaojun; ZHANG, Jinglin; LI, Li; LUO, Zisheng; WANG, Yongjiang; YUAN, Qiuping; ZHOU, Bin; LIU, Haidong. Ginger essential oil-based microencapsulation as an efficient delivery system for the improvement of Jujube (Ziziphus jujuba Mill.) fruit quality. **Food Chemistry**, *[S. l.]*, 2020. DOI: 10.1016/j.foodchem.2019.125628.

BASTOS, Lívia Pinto Heckert; DOS SANTOS, Carlos Henrique Corrêa; DE CARVALHO, Mario Geraldo; GARCIA-ROJAS, Edwin Elard. Encapsulation of the black pepper (Piper nigrum L.) essential oil by lactoferrin-sodium alginate complex coacervates: Structural characterization and simulated gastrointestinal conditions. **Food Chemistry**, *[S. l.]*, 2020. DOI: 10.1016/j.foodchem.2020.126345.

BAYVEL, L.; ORZECHOWSKI, Z.; BAYVEL, L.; ORZECHOWSKI, Z. Parameters of Atomized Liquid. *In*: **Liquid Atomization**. [s.l: s.n.]. DOI: 10.1201/9780203748787-3.

BAYVEL, L.; ORZECHOWSKI, Z.; BAYVEL, L.; ORZECHOWSKI, Z. Experimental Techniques and Measuring Devices. *In*: **Liquid Atomization**. [s.l: s.n.]. DOI: 10.1201/9780203748787-7.

BONDAREVA, N. V.; GRIGORIEV, A. L.; KOROVIN, T. G.; KOROTEEV, A. A.; SAFRONOV, A. A.; SKOROBOGATKO, T. D.; FILATOV, N. I.; KHLYNOV, A. V. Experimental study of the Ohnesorge number effect on the size of droplets formed as a result of the jet capillary breakup. **Thermophysics and Aeromechanics**, *[S. l.]*, 2019. DOI: 10.1134/S0869864319050093.

BOYE, Joyce I.; ALLI, Inteaz; ISMAIL, Ashraf A.; GIBBS, Bernard F.; KONISHI, Yasuo. Factors affecting molecular characteristics of whey protein gelation. **International Dairy Journal**, *[S. l.]*, 1995. DOI: 10.1016/0958-6946(94)00012-E.

BROWN, Charles E.; BROWN, Charles E. Coefficient of Variation. *In*: **Applied Multivariate Statistics in Geohydrology and Related Sciences**. [s.l: s.n.]. DOI: 10.1007/978-3-642-80328-4_13.

BUREY, P.; BHANDARI, B. R.; RUTGERS, R. P. G.; HALLEY, P. J.; TORLEY, P. J. Confectionery gels: A review on formulation, rheological and structural aspects. **International Journal of Food Properties**, *[S. l.]*, 2009. DOI: 10.1080/10942910802223404.

BURGESS, D. J.; PONSART, S. β-glucuronidase activity following complex coacervation and spray drying microencapsulation. **Journal of Microencapsulation**, *[S. l.]*, 1998. DOI: 10.3109/02652049809008241.

BUTSTRAEN, Chloé; SALAÜN, Fabien. Preparation of microcapsules by complex coacervation of gum Arabic and chitosan. **Carbohydrate Polymers**, *[S. l.]*, v. 99, p. 608–616, 2014. DOI: 10.1016/j.carbpol.2013.09.006.

CANAPLE, Laurence; REHOR, Annemie; HUNKELER, David. Improving cell encapsulation through size control. **Journal of Biomaterials Science, Polymer Edition**, *[S. l.]*, 2002. DOI: 10.1163/156856202760197410.

CANSELIER, J. P.; DELMAS, H.; WILHELM, A. M.; ABISMAÏL, B.; DELMAS, H.; WILHELM, A. M.; ULTRASOUND, B. Abismaïl. Ultrasound Emulsification — An Overview. **Journal of Dispersion Science and Technology**, *[S. l.]*, v. 23, n. February 2012, p. 333–349, 2002. DOI: 10.1080/01932690208984209.

CAO, Xian Kui; SUN, Zhi Gang; LI, Wei Feng; LIU, Hai Feng; YU, Zun Hong. A new breakup regime of liquid drops identified in a continuous and uniform air jet flow. **Physics of Fluids**, *[S. l.]*, 2007. DOI: 10.1063/1.2723154.

CARVALHO, I. T.; ESTEVINHO, B. N.; SANTOS, L. **Application of microencapsulated essential oils in cosmetic and personal healthcare products - A reviewInternational Journal of Cosmetic Science**, 2016. DOI: 10.1111/ics.12232.

CASANOVA, Francisca; SANTOS, Lúcia. **Encapsulation of cosmetic active ingredients for topical application-a reviewJournal of Microencapsulation**, 2016. DOI: 10.3109/02652048.2015.1115900.

CHAPEAU, Anne Laure; HAMON, Pascaline; ROUSSEAU, Florence; CROGUENNEC, Thomas; PONCELET, Denis; BOUHALLAB, Saïd. Scale-up production of vitamin loaded heteroprotein coacervates and their protective property. **Journal of Food Engineering**, *[S. l.]*, 2017. DOI: 10.1016/j.jfoodeng.2017.03.005.

CHEN, Richer; TAKAHASHI, Hirokazu; OKAMOTO, Hirokazu; DANJO, Kazumi. Particle design of three-component system for sustained release using a 4-fluid nozzle spray-drying technique. **Chemical and Pharmaceutical Bulletin**, *[S. l.]*, v. 54, n. 11, p. 1486–1490, 2006. DOI: 10.1248/cpb.54.1486.

COMUNIAN, Talita A.; GOMEZ-ESTACA, Joaquin; FERRO-FURTADO, Roselayne; CONCEIÇÃO, Gelson José Andrade; MORAES, Izabel Cristina Freitas; DE CASTRO, Inar Alves; FAVARO-TRINDADE, Carmen S. Effect of different polysaccharides and crosslinkers on echium oil microcapsules. **Carbohydrate Polymers**, *[S. l.]*, 2016. DOI: 10.1016/j.carbpol.2016.05.044.

COMUNIAN, Talita A.; NOGUEIRA, Marina; SCOLARO, Bianca; THOMAZINI, Marcelo; FERRO-FURTADO, Roselayne; DE CASTRO, Inar Alves; FAVARO-TRINDADE, Carmen S. Enhancing stability of echium seed oil and beta-sitosterol by their coencapsulation by complex coacervation using different combinations of wall materials and crosslinkers. **Food Chemistry**, *[S. l.]*, 2018. DOI: 10.1016/j.foodchem.2018.01.121.

COMUNIAN, Talita A.; THOMAZINI, Marcelo; ALVES, Ana Julia Gouvêa; DE MATOS JUNIOR, Fernando Eustáquio; DE CARVALHO BALIEIRO, Júlio C.; FAVARO-TRINDADE, Carmen S. Microencapsulation of ascorbic acid by complex coacervation: Protection and controlled release. **Food Research International**, *[S. l.]*, v. 52, n. 1, 2013. DOI: 10.1016/j.foodres.2013.03.028.

CONSOLI, Larissa; HUBINGER, Míriam Dupas; DRAGOSAVAC, Marijana M. Encapsulation of resveratrol using Maillard conjugates and membrane emulsification. **Food Research International**, *[S. l.]*, 2020. DOI: 10.1016/j.foodres.2020.109359.

CORRÊA-FILHO, Luiz C.; MOLDÃO-MARTINS, Margarida; ALVES, Vitor D. **Advances in the application of microcapsules as carriers of functional compounds for food productsApplied Sciences (Switzerland)**, 2019. DOI: 10.3390/app9030571.

COSTA, André M. M.; MORETTI, Leticia K.; SIMÕES, Grazieli; SILVA, Kelly A.; CALADO, Verônica; TONON, Renata V.; TORRES, Alexandre G. Microencapsulation of pomegranate (Punica granatum L.) seed oil by complex coacervation: Development of a potential functional ingredient for food application. **LWT**, *[S. l.]*, 2020. DOI: 10.1016/j.lwt.2020.109519.

DA SILVA, Marcelo A.; BODE, Franziska; DRAKE, Alex F.; GOLDONI, Silvia; STEVENS, Molly M.; DREISS, Cécile A. Enzymatically cross-linked gelatin/chitosan hydrogels: Tuning gel properties and cellular response. **Macromolecular Bioscience**, *[S. l.]*, 2014. DOI: 10.1002/mabi.201300472.

DA SILVA SOARES, Barbara; SIQUEIRA, Rodrigo Pinto; DE CARVALHO, Mario Geraldo; VICENTE, Juarez; GARCIA-ROJAS, Edwin Elard. Microencapsulation of sacha inchi oil (Plukenetia volubilis L.) using complex coacervation: Formation and structural characterization. **Food Chemistry**, *[S. l.]*, 2019. DOI: 10.1016/j.foodchem.2019.125045.

DE JONG BUNGENBERG, H. G.; KRUYT, H. R. Chemistry—Coacervation (Partial miscibility in colloid systems). **Proc. K. Ned. Akad. Wet.**, *[S. l.]*, 1929. DOI: 10.1016/0006-8993(92)91002-V.

DE KRUIF, Cornelus G.; WEINBRECK, Fanny; DE VRIES, Renko. Complex coacervation of proteins and anionic polysaccharides. **Current Opinion in Colloid and Interface Science**, *[S. l.]*, v. 9, n. 5, p. 340–349, 2004. DOI: 10.1016/j.cocis.2004.09.006.

DE VRIES, R. Monte Carlo simulations of flexible polyanions complexing with whey proteins at their isoelectric point. **Journal of Chemical Physics**, *[S. l.]*, 2004. DOI: 10.1063/1.1641003.

DESAI, Kashappa Goud H.; PARK, Hyun Jin. **Recent developments in microencapsulation of food ingredientsDrying Technology**, 2005. DOI: 10.1081/DRT-200063478.

DICKINSON, Eric. **Hydrocolloids at interfaces and the influence on the properties of dispersed systemsFood Hydrocolloids**, 2003. DOI: 10.1016/S0268-005X(01)00120-5.

DIVISION, Chemistry; ESTEVINHO, Berta Nogueiro; ROCHA, Fernando; SANTOS, Lúcia; ALVES, Arminda; DE AZEREDO, Henriette Monteiro Cordeiro. Drying Technology : An International Journal. **Trends in Food Science and Technology**, *[S. l.]*, v. 31, n. November 2012, p. 138–155, 2013. DOI: 10.1016/j.tifs.2013.04.001.

DO NASCIMENTO, Marília Alves; DA SILVA, Luana Carvalho; MENDES, Luana Guabiraba; FURTADO, Roselayne Ferro; DA COSTA, José Maria Correia; BISWAS, Atanu; CHENG, Huai N.; ALVES, Carlucio Roberto. Pequi oil microencapsulation by complex coacervation using gelatin-cashew gum. **International Journal of Food Studies**, *[S. l.]*, 2020. DOI: 10.7455/ijfs/9.SI.2020.a8.

DOBETTI, L.; PANTALEO, V. Application of a hydrodynamic model to microencapsulation by coacervation. **Journal of Microencapsulation**, *[S. l.]*, v. 19, n. 2, p. 139–151, 2002. DOI: 10.1080/02652040110055199.

DRAGOSAVAC, Marijana M.; HOLDICH, Richard G.; VLADISAVLJEVIĆ, Goran T.; SOVILJ, Milan N. Stirred cell membrane emulsification for multiple emulsions containing unrefined pumpkin seed oil with uniform droplet size. **Journal of Membrane Science**, *[S. l.]*, 2012. DOI: 10.1016/j.memsci.2011.12.009.

DRAGOSAVAC, Marijana M.; SOVILJ, Milan N.; KOSVINTSEV, Serguei R.; HOLDICH, Richard G.; VLADISAVLJEVIĆ, Goran T. Controlled production of oil-in-water emulsions containing unrefined pumpkin seed oil using stirred cell membrane emulsification. **Journal of Membrane Science**, *[S. l.]*, v. 322, n. 1, p. 178–188, 2008. DOI: 10.1016/j.memsci.2008.05.026.

DRUSCH, S.; REGIER, M.; BRUHN, M. Recent advances in the microencapsulation of oils high in polyunsaturated fatty acids. *In*: **Novel Technologies in Food Science: Their Impact on Products, Consumer Trends and the Environment**. [s.l: s.n.]. DOI: 10.1007/978-1-4419-7880-6_7.

DUBE, R. .. SPRAY ATOMIZATION AND DEPOSITION, by E.J. Lavernia and Y. Wu, 1996, Chichester, John Wiley, xii + 627 pp., hard bound, ISBN 0471 954772. **Journal of Materials Processing Technology**, *[S. l.]*, 2000. DOI: 10.1016/s0924-0136(99)00407-0.

DUGASANI, Swarnalatha; PICHIKA, Mallikarjuna Rao; NADARAJAH, Vishna Devi; BALIJEPALLI, Madhu Katyayani; TANDRA, Satyanarayana; KORLAKUNTA, Jayaveera Narsimha. Comparative antioxidant and anti-inflammatory effects of [6]-gingerol, [8]-gingerol, [10]-gingerol and [6]-shogaol. **Journal of Ethnopharmacology**, *[S. l.]*, v. 127, n. 2, p. 515–520, 2010. DOI: 10.1016/j.jep.2009.10.004.

DUPONT, Didier; LE FEUNTEUN, Steven; MARZE, Sébastien; SOUCHON, Isabelle. **Structuring food to control its disintegration in the gastrointestinal tract and optimize nutrient bioavailabilityInnovative Food Science and Emerging Technologies**, 2018. DOI: 10.1016/j.ifset.2017.10.005.

EGIDI, Emanuela; GASPARINI, Gilda; HOLDICH, Richard G.; VLADISAVLJEVIĆ, Goran T.; KOSVINTSEV, Serguei R. Membrane emulsification using membranes of regular pore spacing: Droplet size and uniformity in the presence of surface shear. **Journal of Membrane Science**, *[S. l.]*, v. 323, n. 2, p. 414–420, 2008. DOI: 10.1016/j.memsci.2008.06.047.

EL-GHORAB, Ahmed Hassan; NAUMAN, Muhammad; ANJUM, Faqir Muhammad; HUSSAIN, Shahzad; NADEEM, Muhammad. A Comparative study on chemical composition and antioxidant activity of ginger (Zingiber officinale) and cumin (Cuminum cyminum). **Journal of Agricultural and Food Chemistry**, *[S. l.]*, 2010. DOI: 10.1021/jf101202x.

ENDO, Érika; BORGES, Soraia Vilela; DAIUTO, Érica Regina; CEREDA, Marney Pascoli; AMORIM, Elizete. Avaliação da vida de prateleira do suco de maracujá (Passiflora edullis f. flavicarpa) desidratado. **Ciência e Tecnologia de Alimentos**, *[S. l.]*, v. 27, n. 2, p. 382–386, 2007. DOI: 10.1590/S0101-20612007000200029.

ERATTE, Divya; DOWLING, Kim; BARROW, Colin J.; ADHIKARI, Benu. **Recent advances in the microencapsulation of omega-3 oil and probiotic bacteria through complex coacervation: A reviewTrends in Food Science and Technology**, 2018. DOI: 10.1016/j.tifs.2017.10.014.

ERATTE, Divya; MCKNIGHT, Stafford; GENGENBACH, Thomas R.; DOWLING, Kim; BARROW, Colin J.; ADHIKARI, Benu P. Co-encapsulation and characterisation of omega-3 fatty acids and probiotic bacteria in whey protein isolate-gum Arabic complex coacervates. **Journal of Functional Foods**, *[S. l.]*, v. 19, 2015. DOI: 10.1016/j.jff.2015.01.037.

ERATTE, Divya; WANG, Bo; DOWLING, Kim; BARROW, Colin J.; ADHIKARI, Benu P. Complex coacervation with whey protein isolate and gum arabic for the microencapsulation of omega-3 rich tuna oil. **Food and Function**, *[S. l.]*, v. 5, n. 11, p. 2743–2750, 2014. DOI: 10.1039/c4fo00296b. Disponível em: http://dx.doi.org/10.1039/c4fo00296b.

FANG, Zhongxiang; BHANDARI, Bhesh. **Encapsulation of polyphenols - A reviewTrends in Food Science and Technology**, 2010. DOI: 10.1016/j.tifs.2010.08.003.

FAVARO-TRINDADE, Carmen Sílvia; PINHO, Samantha Cristina De. Revisão : Microencapsulação de ingredientes alimentícios. **Brazilian Journal of Food Technology**, *[S. l.]*, 2008.

FERNANDES, Regiane Vict??ria de Barros; BOTREL, Diego Alvarenga; SILVA, Eric Keven; BORGES, Soraia Vilela; OLIVEIRA, Cassiano Rodrigues De; YOSHIDA, Maria Irene; FEITOSA, Judith Pessoa de Andrade; DE PAULA, Regina C??lia Monteiro. Cashew gum and inulin: New alternative for ginger essential oil microencapsulation. **Carbohydrate Polymers**, *[S. l.]*, v. 153, 2016. a. DOI: 10.1016/j.carbpol.2016.07.096.

FERNANDES, Regiane Victória de Barros; BORGES, Soraia Vilela; SILVA, Eric Keven; DA SILVA, Yasmim Fernanda; DE SOUZA, Hugo Junior Barboza; DO CARMO, Eloá Lourenço; DE OLIVEIRA, Cassiano Rodrigues; YOSHIDA, Maria Irene; BOTREL, Diego Alvarenga. Study of ultrasound-assisted emulsions on microencapsulation of ginger essential oil by spray drying. **Industrial Crops and Products**, *[S. l.]*, 2016. b. DOI: 10.1016/j.indcrop.2016.09.010.

FERREIRA, S.; MALACRIDA, C. R.; TELIS, V. R. N. Influence of emulsification methods and use of colloidal silicon dioxide on the microencapsulation by spray drying of turmeric oleoresin in gelatin-starch matrices. **Canadian Journal of Chemical Engineering**, *[S. l.]*, v. 94, n. 11, 2016. DOI: 10.1002/cjce.22596.

FERREIRA, S.; NICOLETTI, V. R. Complex coacervation assisted by a two-fluid nozzle for microencapsulation of ginger oil: Effect of atomization parameters. **Food Research International**, *[S. l.]*, v. 138, 2020. DOI: 10.1016/j.foodres.2020.109828.

FERREIRA, S.; PIOVANNI, G. M. O.; MALACRIDA, C. R.; NICOLETTI, V. R. Influence of emulsification methods and spray drying parameters on the microencapsulation of turmeric oleoresin. **Emirates Journal of Food and Agriculture**, *[S. l.]*, 2019. DOI: 10.9755/ejfa.2019.v31.i7.1968.

FERREIRA, Sungil; MALACRIDA, C. R. Cassia R.; TELIS, Vania R. Influence of emulsification methods and use of colloidal silicon dioxide on the microencapsulation by spray drying of turmeric oleoresin in gelatin-starch matrices. **Canadian Journal of Chemical Engineering**, *[S. l.]*, v. 9999, n. 11, p. 1–9, 2016. DOI: 10.1002/cjce.22596. Disponível em: http://doi.wiley.com/10.1002/cjce.22596.

FERREIRA, Sungil; NICOLETTI, Vania Regina. Microencapsulation of ginger oil by complex coacervation using atomization: Effects of polymer ratio and wall material concentration. **Journal of Food Engineering**, *[S. l.]*, 2021. DOI: 10.1016/j.jfoodeng.2020.110214.

FILKOVÁ, Iva; HUANG, Li Xin; MUJUMDAR, Arun S. Industrial spray drying systems. *In*: **Handbook of Industrial Drying, Fourth Edition**. [s.l: s.n.]. DOI: 10.1201/b17208.

FINER, E. G.; FRANKS, F.; PHILLIPS, M. C.; SUGGETT, A. Gel formation from solutions of single-chain gelatin. **Biopolymers**, *[S. l.]*, 1975. DOI: 10.1002/bip.1975.360141002.

FRAJ, Jadranka; PETROVIĆ, Lidija; ĐEKIĆ, Ljiljana; BUDINČIĆ, Jelena Milinković; BUČKO, Sandra; KATONA, Jaroslav. Encapsulation and release of vitamin C in double W/O/W emulsions followed by complex coacervation in gelatin-sodium caseinate system. **Journal of Food Engineering**, *[S. l.]*, 2021. DOI: 10.1016/j.jfoodeng.2020.110353.

FUNAMI, Takahiro; ZHANG, Guoyan; HIROE, Mika; NODA, Sakie; NAKAUMA, Makoto; ASAI, Iwao; COWMAN, Mary K.; AL-ASSAF, Saphwan; PHILLIPS, Glyn O. Effects of the proteinaceous moiety on the emulsifying properties of sugar beet pectin. **Food Hydrocolloids**, *[S. l.]*, 2007. DOI: 10.1016/j.foodhyd.2006.10.009.

GAIKWAD, Shashank G.; PANDIT, Aniruddha B. Ultrasound emulsification: Effect of ultrasonic and physicochemical properties on dispersed phase volume and droplet size. **Ultrasonics Sonochemistry**, *[S. l.]*, v. 15, n. 4, p. 554–563, 2008. DOI: 10.1016/j.ultsonch.2007.06.011.

GARCÍA-SALDAÑA, Jesús S.; CAMPAS-BAYPOLI, Olga N.; LÓPEZ-CERVANTES, Jaime; SÁNCHEZ-MACHADO, Dalia I.; CANTÚ-SOTO, Ernesto U.; RODRÍGUEZ-RAMÍREZ, Roberto. Microencapsulation of sulforaphane from broccoli seed extracts by gelatin/gum Arabic and gelatin/pectin complexes. **Food Chemistry**, *[S. l.]*, 2016. DOI: 10.1016/j.foodchem.2016.01.087.

GIJSBERTSEN-ABRAHAMSE, A. J.; VAN DER PADT, A.; BOOM, R. M. Status of cross-flow membrane emulsification and outlook for industrial application. **Journal of Membrane Science**, *[S. l.]*, 2004. DOI: 10.1016/j.memsci.2003.11.006.

GILSENAN, P. M.; ROSS-MURPHY, S. B. Rheological characterisation of gelatins from mammalian and marine sources. **Food Hydrocolloids**, *[S. l.]*, v. 14, n. 3, p. 191–195, 2000. DOI: 10.1016/S0268-005X(99)00050-8.

GIRARD, Maude; SANCHEZ, Christian; LANEUVILLE, Sandra I.; TURGEON, Sylvie L.; GAUTHIER, Sylvie F. Associative phase separation of β-lactoglobulin/pectin solutions: A kinetic study by small angle static light scattering. **Colloids and Surfaces B: Biointerfaces**, *[S. l.]*, 2004. DOI: 10.1016/j.colsurfb.2004.02.002.

GOMEZ-ESTACA, J.; COMUNIAN, T. A.; MONTERO, P.; FERRO-FURTADO, R.; FAVARO-TRINDADE, C. S. Encapsulation of an astaxanthin-containing lipid extract from shrimp waste by complex coacervation using a novel gelatin-cashew gum complex. **Food Hydrocolloids**, *[S. l.]*, v. 61, 2016. DOI: 10.1016/j.foodhyd.2016.05.005.

GONÇALVES, Antónia; ESTEVINHO, Berta N.; ROCHA, Fernando. **Microencapsulation of vitamin A: A reviewTrends in Food Science and Technology**, 2016. DOI: 10.1016/j.tifs.2016.03.001.

GONÇALVES, Nathalia D.; GROSSO, Carlos R. F.; RABELO, Renata S.; HUBINGER, Miriam D.; PRATA, Ana S. Comparison of microparticles produced with combinations of gelatin, chitosan and gum Arabic. **Carbohydrate Polymers**, *[S. l.]*, 2018. DOI: 10.1016/j.carbpol.2018.05.027.

GORNALL, J. L.; TERENTJEV, E. M. Universal kinetics of helix-coil transition in gelatin. **Physical Review E - Statistical, Nonlinear, and Soft Matter Physics**, *[S. l.]*, 2008. a. DOI: 10.1103/PhysRevE.77.031908.

GORNALL, Joanne L.; TERENTJEV, Eugene M. Helix-coil transition of gelatin: Helical morphology and stability. **Soft Matter**, *[S. l.]*, 2008. b. DOI: 10.1039/b713075a.

GOSAL, Walraj S.; ROSS-MURPHY, Simon B. **Globular protein gelationCurrent Opinion in Colloid and Interface Science**, 2000. DOI: 10.1016/S1359-0294(00)00057-1.

GOUIN, Sébastien. Microencapsulation: Industrial appraisal of existing technologies and trends. *In*: TRENDS IN FOOD SCIENCE AND TECHNOLOGY 2004, **Anais** [...]. [s.l: s.n.] DOI: 10.1016/j.tifs.2003.10.005.

GRATTON, S.; LAWLESS, A. S.; NICHOLS, N. K. Approximate Gauss-newton methods for nonlinear least squares problems. **SIAM Journal on Optimization**, *[S. l.]*, 2007. DOI: 10.1137/050624935.

GREEN, Barrett K.; SCHLEICHER, Lowell. **Manifold record material** 1956.

GRZANNA, Reinhard; LINDMARK, Lars; FRONDOZA, Carmelita G. **Ginger - An herbal medicinal product with broad anti-inflammatory actionsJournal of Medicinal Food**, 2005. DOI: 10.1089/jmf.2005.8.125.

GUILDENBECHER, D. R.; LÓPEZ-RIVERA, C.; SOJKA, P. E. Secondary atomization. **Experiments in Fluids**, *[S. l.]*, 2009. DOI: 10.1007/s00348-008-0593-2.

GUO, Huilin; ZHAO, Xiaopeng. Preparation of microcapsules with narrow-size distribution by complex coacervation: Effect of sodium dodecyl sulphate concentration and agitation rate. **Journal of Microencapsulation**, *[S. l.]*, 2008. DOI: 10.1080/02652040701861828.

HANCOCKS, R. D.; SPYROPOULOS, F.; NORTON, I. T. The effects of membrane composition and morphology on the rotating membrane emulsification technique for food grade emulsions. **Journal of Membrane Science**, *[S. l.]*, 2016. DOI: 10.1016/j.memsci.2015.09.033.

HECKERT BASTOS, Lívia Pinto; VICENTE, Juarez; CORRÊA DOS SANTOS, Carlos Henrique; GERALDO DE CARVALHO, Mario; GARCIA-ROJAS, Edwin Elard. Encapsulation of black pepper (Piper nigrum L.) essential oil with gelatin and sodium alginate by complex coacervation. **Food Hydrocolloids**, *[S. l.]*, 2020. DOI: 10.1016/j.foodhyd.2019.105605.

HERNÁNDEZ-NAVA, Ruth; LÓPEZ-MALO, Aurelio; PALOU, Enrique; RAMÍREZ-CORONA, Nelly; JIMÉNEZ-MUNGUÍA, María Teresa. Encapsulation of oregano essential oil (Origanum vulgare) by complex coacervation between gelatin and chia mucilage and its properties after spray drying. **Food Hydrocolloids**, *[S. l.]*, 2020. DOI: 10.1016/j.foodhyd.2020.106077.

HERRERO-VANRELL, Rocío; BRAVO-OSUNA, Irene; ANDRÉS-GUERRERO, Vanessa; VICARIO-DE-LA-TORRE, Marta; MOLINA-MARTÍNEZ, Irene Teresa. **The potential of using biodegradable microspheres in retinal diseases and other intraocular pathologiesProgress in Retinal and Eye Research**, 2014. DOI: 10.1016/j.preteyeres.2014.04.002.

HOLDICH, Richard; DRAGOSAVAC, Marijana; WILLIAMS, Bruce; TROTTER, Samuel. High throughput membrane emulsification using a single-pass annular flow crossflow membrane. **AIChE Journal**, *[S. l.]*, 2020. DOI: 10.1002/aic.16958.

HOLDICH, Richard G.; DRAGOSAVAC, Marijana M.; VLADISAVLJEVIĆ, Goran T.; KOSVINTSEV, Serguei R. Membrane emulsification with oscillating and stationary membranes. **Industrial and Engineering Chemistry Research**, *[S. l.]*, 2010. DOI: 10.1021/ie900531n.

HOLDICH, Richard; SCHOU, Keith; DRAGOSAVAC, Marijana; KELLET, Simon; BANDULASENA, Hemaka. A comparison of azimuthal and axial oscillation microfiltration using surface and matrix types of microfilters with a cake-slurry shear plane exhibiting non-Newtonian behaviour. **Journal of Membrane Science**, *[S. l.]*, 2018. DOI: 10.1016/j.memsci.2017.12.079.

HUANG, Guo Qing; HAN, Xiao Na; XIAO, Jun Xia; CHENG, Ling Yun. Effects of coacervation acidity on the genipin crosslinking action and intestine-targeted delivery potency of the O-carboxymethyl chitosan–gum arabic coacervates. **International Journal of Polymeric Materials and Polymeric Biomaterials**, *[S. l.]*, 2017. a. DOI: 10.1080/00914037.2016.1190924.

HUANG, Guo Qing; LIU, Li Na; HAN, Xiao Na; XIAO, Jun Xia. Intestine-targeted delivery potency of the O-carboxymethyl chitosan–gum Arabic coacervate: Effects of coacervation acidity and possible mechanism. **Materials Science and Engineering C**, *[S. l.]*, 2017. b. DOI: 10.1016/j.msec.2017.05.074.

INCROPERA, Frank P.; DEWITT, David P.; BERGMAN, Theodore L.; LAVINE, Adrienne S. **Principles of heat and mass transfer**. [s.l: s.n.].

JACKSON, Lauren S.; LEE, Ken. **Microencapsulation and the food industryLWT - Food Science and Technology**, 1991.

JAFARI, Seid Mahdi; ASSADPOOR, Elham; HE, Yinghe; BHANDARI, Bhesh. Encapsulation Efficiency of Food Flavours and Oils during Spray Drying. **Drying Technology**, *[S. l.]*, v. 26, n. 7, p. 816–835, 2008. DOI: 10.1080/07373930802135972.

JAIN, Ashay; THAKUR, Deepika; GHOSHAL, Gargi; KATARE, O. P.; SHIVHARE, U. S. Characterization of microcapsulated β-carotene formed by complex coacervation using casein and gum tragacanth. **International Journal of Biological Macromolecules**, *[S. l.]*, 2016. DOI: 10.1016/j.ijbiomac.2016.01.117.

JANISZEWSKA-TURAK, Emilia; DELLAROSA, Nicolò; TYLEWICZ, Urszula; LAGHI, Luca; ROMANI, Santina; DALLA ROSA, Marco; WITROWA-RAJCHERT, Dorota. The influence of carrier material on some physical and structural properties of carrot juice microcapsules. **Food Chemistry**, *[S. l.]*, 2017. DOI: 10.1016/j.foodchem.2017.03.134.

JEGAT, C.; TAVERDET, J. L. Stirring speed influence study on the microencapsulation process and on the drug release from microcapsules. **Polymer Bulletin**, *[S. l.]*, v. 44, n. 3, p. 345–351, 2000. DOI: 10.1007/s002890050612.

JIANG, Hao; ZHANG, Min; MCKNIGHT, Stafford; ADHIKARI, Benu. Microencapsulation of α-Amylase by Carrying Out Complex Coacervation and Drying in a Single Step Using a Novel Three-Fluid Nozzle Spray Drying. **Drying Technology**, *[S. l.]*, v. 31, n. 16, p. 1901–1910, 2013. DOI: 10.1080/07373937.2013.771365.

JOHNSTON-BANKS, F. A. Gelatine. *In*: **Food Gels**. [s.l: s.n.]. DOI: 10.1007/978-94-009-0755-3_7.

JYOTHI, Nvn; VENKATA, N.; JYOTHI, Naga; PRASANNA, P. Muthu; NARAYAN SAKARKAR, Suhas; SURYA PRABHA, K.; RAMAIAH, P. Seetha; SRAWAN, G. Y. Microencapsulation Techniques, Factors Influencing Encapsulation Efficiency: A Review Microencapsulation techniques, factors influencing encapsulation efficiency. **Journal of Microencapsulation**, *[S. l.]*, 2010. DOI: 10.3109/02652040903131301.

KANDANSAMY, Kannan; SOMASUNDARAM, Priyenka Devi. **Microencapsulation of colors by spray drying-A reviewInternational Journal of Food Engineering**, 2012. DOI: 10.1515/1556-3758.2647.

KARIM, A. A.; BHAT, Rajeev. Gelatin alternatives for the food industry: recent developments, challenges and prospects. **Trends in Food Science and Technology**, *[S. l.]*, 2008. DOI: 10.1016/j.tifs.2008.08.001.

KASAPIS, Stefan; AL-MARHOOBI, Insaf M.; DESZCZYNSKI, Marcin; MITCHELL, John R.; ABEYSEKERA, Rukmal. Gelatin vs polysaccharide in mixture with sugar. **Biomacromolecules**, *[S. l.]*, 2003. DOI: 10.1021/bm0201237.

KAŠPAR, Ondřej; JAKUBEC, Martin; ŠTĚPÁNEK, František. Characterization of spray dried chitosan-TPP microparticles formed by two- and three-fluid nozzles. **Powder Technology**, *[S. l.]*, 2013. DOI: 10.1016/j.powtec.2012.07.010.

KAUSHIK, Pratibha; DOWLING, Kim; BARROW, Colin J.; ADHIKARI, Benu. Microencapsulation of omega-3 fatty acids: A review of microencapsulation and characterization methods. **Journal of Functional Foods**, *[S. l.]*, v. 19, p. 868–881, 2015. DOI: 10.1016/j.jff.2014.06.029.

KAUSHIK, Pratibha; DOWLING, Kim; MCKNIGHT, Stafford; BARROW, Colin J.; ADHIKARI, Benu. Microencapsulation of flaxseed oil in flaxseed protein and flaxseed gum complex coacervates. **Food Research International**, *[S. l.]*, 2016. DOI: 10.1016/j.foodres.2016.05.015.

KAYITMAZER, A. B.; KOKSAL, A. F.; KILIC IYILIK, E. Complex coacervation of hyaluronic acid and chitosan: Effects of pH, ionic strength, charge density, chain length and the charge ratio. **Soft Matter**, *[S. l.]*, 2015. DOI: 10.1039/c5sm01829c.

KAYITMAZER, A. Basak. Thermodynamics of complex coacervation. **Advances in Colloid and Interface Science**, *[S. l.]*, v. 239, p. 169–177, 2017. DOI: 10.1016/j.cis.2016.07.006.

KEMP, I. C.; HARTWIG, T.; HERDMAN, R.; HAMILTON, P.; BISTEN, A.; BERMINGHAM, S. Spray drying with a two-fluid nozzle to produce fine particles: Atomization, scale-up, and modeling. **Drying Technology**, *[S. l.]*, 2016. DOI: 10.1080/07373937.2015.1103748.

KEMP, Ian C.; WADLEY, Robert; HARTWIG, Thoralf; COCCHINI, Ugo; SEE-TOH, Yoong; GORRINGE, Lee; FORDHAM, Kim; RICARD, Francois. Experimental Study of Spray Drying and Atomization with a Two-Fluid Nozzle to Produce Inhalable Particles. **Drying Technology**, *[S. l.]*, 2013. DOI: 10.1080/07373937.2012.710693.

KHODE, Priya D.; KATRE, Tina B. Review of Micrencapsulation: A Review A Novel Approach in Drug Delivery. **Research Journal of Pharmaceutical Dosage Forms and Technology**, *[S. l.]*, 2019. DOI: 10.5958/0975-4377.2019.00034.x.

KOSVINTSEV, Serguei R.; GASPARINI, Gilda; HOLDICH, Richard G.; CUMMING, Iain W.; STILLWELL, Michael T. Liquid - Liquid membrane dispersion in a stirred cell with and without controlled shear. **Industrial and Engineering Chemistry Research**, *[S. l.]*, v. 44, n. 24, p. 9323–9330, 2005. DOI: 10.1021/ie0504699.

KRALOVEC, Jaroslav A.; ZHANG, Shuocheng; ZHANG, Wei; BARROW, Colin J. A review of the progress in enzymatic concentration and microencapsulation of omega-3 rich oil from fish and microbial sources. **Food Chemistry**, *[S. l.]*, 2012. DOI: 10.1016/j.foodchem.2011.08.085.

LACHMAN, L. LIEBERMAN, H. KANIG, J. **Teoria e Prática na Indústria FarmacêuticaTeoria e Prática na Indústria Farmacêutica**, 2001.

LAM, P. L.; GAMBARI, R. **Advanced progress of microencapsulation technologies: In vivo and in vitro models for studying oral and transdermal drug deliveriesJournal of Controlled Release**, 2014. DOI: 10.1016/j.jconrel.2013.12.028.

LAMPRECHT, A.; SCHÄFER, U. F.; LEHR, C. M. Characterization of microcapsules by confocal laser scanning microscopy: Structure, capsule wall composition and encapsulation rate. **European Journal of Pharmaceutics and Biopharmaceutics**, *[S. l.]*, v. 49, n. 1, p. 1–9, 2000. DOI: 10.1016/S0939-6411(99)00063-6.

LANDAU, L. D.; LIFSHITZ, E. M. **LandauLifshitz-FluidMechanics.pdf**. [s.l: s.n.].

LEE, YoungSoo; LEE, Soo-Yeun; DONOVAN, Joseph D. Stability Characterization and Sensory Testing in Food Products Containing Microencapsulants. *In*: **Microencapsulation in the Food Industry**. [s.l: s.n.]. DOI: 10.1016/b978-0-12-404568-2.00028-5.

LEMETTER, C. Y. G.; MEEUSE, F. M.; ZUIDAM, N. J. Control of the morphology and the size of complex coacervate microcapsules during scale-up. **AIChE Journal**, *[S. l.]*, 2009. DOI: 10.1002/aic.11816.

LEMOS, Yuri Pessoa; MARIANO MARFIL, Paulo Henrique; NICOLETTI, Vânia Regina. Particle size characteristics of buriti oil microcapsules produced by gelatin-sodium alginate complex coacervation: Effect of stirring speed. **International Journal of Food Properties**, *[S. l.]*, 2017. DOI: 10.1080/10942912.2017.1349139.

LI, Yong; ZHANG, Xiyue; ZHAO, Yu; DING, Jie; LIN, Songyi. Investigation on complex coacervation between fish skin gelatin from cold-water fish and gum arabic: Phase behavior, thermodynamic, and structural properties. **Food Research International**, *[S. l.]*, 2018. DOI: 10.1016/j.foodres.2018.02.053.

LIU, Xiaoqing; CHAPEL, Jean Paul; SCHATZ, Christophe. **Structure, thermodynamic and kinetic signatures of a synthetic polyelectrolyte coacervating systemAdvances in Colloid and Interface Science**, 2017. DOI: 10.1016/j.cis.2016.10.004.

LV, Yi; YANG, Fan; LI, Xueying; ZHANG, Xiaoming; ABBAS, Shabbar. Formation of heat-resistant nanocapsules of jasmine essential oil via gelatin/gum arabic based complex coacervation. **Food Hydrocolloids**, *[S. l.]*, 2014. DOI: 10.1016/j.foodhyd.2013.06.003.

MA, Tiezheng; ZHAO, Hongliang; WANG, Jing; SUN, Baoguo. Effect of processing conditions on the morphology and oxidative stability of lipid microcapsules during complex coacervation. **Food Hydrocolloids**, *[S. l.]*, 2019. DOI: 10.1016/j.foodhyd.2018.08.053.

MANSOUR, Adel; CHIGIER, Norman. Air-blast atomization of non-Newtonian liquids. **Journal of Non-Newtonian Fluid Mechanics**, *[S. l.]*, 1995. DOI: 10.1016/0377-0257(95)01356-Z.

MANSOURKHAKI, Ali; HAGHIRI, Majid; BERANGI, Mohamadjavad. A modified noise-prediction model for highways with significant motorcycle traffic. **Proceedings of the Institution of Civil Engineers - Transport**, *[S. l.]*, 2018. DOI: 10.1680/jtran.17.00117.

MARFIL, P. H. M.; PAULO, B. B.; ALVIM, I. D.; NICOLETTI, V. R. Production and characterization of palm oil microcapsules obtained by complex coacervation in gelatin/gum Arabic. **Journal of Food Process Engineering**, *[S. l.]*, 2018. DOI: 10.1111/jfpe.12673.

MARMOTTANT, Philippe; VILLERMAUX, Emmanuel. Atomisation primaire dans les jets coaxiaux. **Combustion**, *[S. l.]*, 2002.

MARTINS, Isabel M.; BARREIRO, Maria F.; COELHO, Manuel; RODRIGUES, Alírio E. Microencapsulation of essential oils with biodegradable polymeric carriers for cosmetic applications. **Chemical Engineering Journal**, *[S. l.]*, v. 245, p. 191–200, 2014. DOI: 10.1016/j.cej.2014.02.024.

MAULIDNA; WIRJOSENTONO, Basuki; TAMRIN; MARPAUNG, Lamek. Microencapsulation of ginger-based essential oil (Zingiber cassumunar roxb) with chitosan and oil palm trunk waste fiber prepared by spray-drying method. **Case Studies in Thermal Engineering**, *[S. l.]*, 2020. DOI: 10.1016/j.csite.2020.100606.

MCCLEMENTS, David Julian. **Food emulsions - principles, practices, and techniques**. [s.l: s.n.]. DOI: 10.1201/9781420029581.ch9.

MOHANTY, Biswaranjan; ASWAL, V. K.; KOHLBRECHER, J.; BOHIDAR, H. B. Synthesis of gelatin nanoparticles via simple coacervation. **Journal of Surface Science and Technology**, *[S. l.]*, 2005. DOI: 10.18311/jsst/2005/1995.

MOON, Sun Myung. **Exposition of the Divine Principle**. [s.l: s.n.].

MORELLI, S.; HOLDICH, R. G.; DRAGOSAVAC, M. M. Microparticles for cell encapsulation and colonic delivery produced by membrane emulsification. **Journal of Membrane Science**, *[S. l.]*, 2017. DOI: 10.1016/j.memsci.2016.11.058.

MOSER, Poliana; FERREIRA, Sungil; NICOLETTI, Vânia Regina. Buriti oil microencapsulation in chickpea protein-pectin matrix as affected by spray drying parameters. **Food and Bioproducts Processing**, *[S. l.]*, 2019. DOI: 10.1016/j.fbp.2019.07.009.

MÜLLER, R. H.; RADTKE, M.; WISSING, S. A. Nanostructured lipid matrices for improved microencapsulation of drugs. **International Journal of Pharmaceutics**, *[S. l.]*, 2002. DOI: 10.1016/S0378-5173(02)00180-1.

MUNSON, Bruce R.; OKIISHI, Theodore H.; HUEBSCH, Wade W.; ROTHMAYER; P, Alric. **Fundamentals of Fluid Mechanics Seventh Edition**. [s.l: s.n.].

MUYONGA, J. H.; COLE, C. G. B.; DUODU, K. G. Fourier transform infrared (FTIR) spectroscopic study of acid soluble collagen and gelatin from skins and bones of young and adult Nile perch (Lates niloticus). **Food Chemistry**, *[S. l.]*, 2004. DOI: 10.1016/j.foodchem.2003.09.038.

OMER, K.; ASHGRIZ, N. Spray Nozzles. *In*: **Handbook of Atomization and Sprays**. [s.l: s.n.]. DOI: 10.1007/978-1-4419-7264-4_24.

OSMAN, Mohamed E.; WILLIAMS, Peter A.; MENZIES, Alan R.; PHILLIPS, Glyn O. Characterization of Commercial Samples of Gum Arabic. **Journal of Agricultural and Food Chemistry**, *[S. l.]*, 1993. DOI: 10.1021/jf00025a016.

OZEKI, Tetsuya; BEPPU, Shuji; MIZOE, Takuto; TAKASHIMA, Yuuki; YUASA, Hiroshi; OKADA, Hiroaki. Preparation of two-drug composite microparticles to improve the dissolution of insoluble drug in water for use with a 4-fluid nozzle spray drier. **Journal of Controlled Release**, *[S. l.]*, 2005. DOI: 10.1016/j.jconrel.2005.06.012.

OZKAN, Gulay; FRANCO, Paola; DE MARCO, Iolanda; XIAO, Jianbo; CAPANOGLU, Esra. A review of microencapsulation methods for food antioxidants: Principles, advantages, drawbacks and applications. **Food Chemistry**, *[S. l.]*, 2019. DOI: 10.1016/j.foodchem.2018.07.205.

PAULO, Filipa; SANTOS, Lúcia. **Design of experiments for microencapsulation applications: A reviewMaterials Science and Engineering C**, 2017. DOI: 10.1016/j.msec.2017.03.219.

PAWAR, Nisha; BOHIDAR, H. B. Anisotropic domain growth and complex coacervation in nanoclay- polyelectrolyte solutions. **Advances in Colloid and Interface Science**, *[S. l.]*, 2011. DOI: 10.1016/j.cis.2011.06.007.

PEANPARKDEE, Methavee; IWAMOTO, Satoshi; YAMAUCHI, Ryo. MICROENCAPSULATION: A REVIEW OF APPLICATIONS IN THE FOOD AND PHARMACEUTICAL INDUSTRIES. **Reviews in Agricultural Science**, *[S. l.]*, 2016. DOI: 10.7831/ras.4.56.

PENG, S. J.; WILLIAMS, R. a. Part I : Droplet Formation from a Single Pore. **Trans IChemE**, *[S. l.]*, v. 76, n. November, p. 894–901, 1998. DOI: http://dx.doi.org/10.1205/026387698525694.

PERRECHIL, F. A.; CUNHA, R. L. Oil-in-water emulsions stabilized by sodium caseinate: Influence of pH, high-pressure homogenization and locust bean gum addition. **Journal of Food Engineering**, *[S. l.]*, v. 97, n. 4, p. 441–448, 2010. DOI: 10.1016/j.jfoodeng.2009.10.041. Disponível em: http://dx.doi.org/10.1016/j.jfoodeng.2009.10.041.

PIACENTINI, Emma; GIORNO, Lidietta; DRAGOSAVAC, Marijana M.; VLADISAVLJEVIĆ, Goran T.; HOLDICH, Richard G. Microencapsulation of oil droplets using cold water fish gelatine/gum arabic complex coacervation by membrane emulsification. **Food Research International**, *[S. l.]*, v. 53, n. 1, p. 362–372, 2013. DOI: 10.1016/j.foodres.2013.04.012.

PITT, A. R.; MORLEY, S. D.; BURBIDGE, N. J.; QUICKENDEN, E. L. The relationship between surfactant structure and limiting values of surface tension, in aqueous gelatin solution, with particular regard to multilayer coating. *In*: COLLOIDS AND SURFACES A: PHYSICOCHEMICAL AND ENGINEERING ASPECTS 1996, **Anais** [...]. [s.l: s.n.] DOI: 10.1016/0927-7757(96)03593-5.

PLATEL, K.; SRINIVASAN, K. Influence of dietary spices and their active principles on pancreatic digestive enzymes in albino rats. **Nahrung - Food**, *[S. l.]*, 2000. DOI: 10.1002/(SICI)1521-3803(20000101)44:1<42::AID-FOOD42>3.0.CO;2-D.

PRATA, Ana S.; ZANIN, Maria H. A. A.; RÉ, Maria I.; GROSSO, Carlos R. F. F. Release properties of chemical and enzymatic crosslinked gelatin-gum Arabic microparticles containing a fluorescent probe plus vetiver essential oil. **Colloids and Surfaces B: Biointerfaces**, *[S. l.]*, v. 67, n. 2, p. 171–178, 2008. DOI: 10.1016/j.colsurfb.2008.08.014.

PU, Xiaolu; WOLF, Bettina; DRAGOSAVAC, Marijana. Generation of magnesium enriched water-in-oil-in-water food emulsions by stirred cell membrane emulsification. **Journal of Food Engineering**, *[S. l.]*, 2019. DOI: 10.1016/j.jfoodeng.2018.11.022.

QV, Xiao Ying; ZENG, Zhi Ping; JIANG, Jian Guo. Preparation of lutein microencapsulation by complex coacervation method and its physicochemical properties and stability. **Food Hydrocolloids**, *[S. l.]*, v. 25, n. 6, p. 1596–1603, 2011. DOI: 10.1016/j.foodhyd.2011.01.006. Disponível em: http://dx.doi.org/10.1016/j.foodhyd.2011.01.006.

RAY, Apurba K.; BIRD, Philip B.; IACOBUCCI, Guillermo A.; CLARK, Benjamin C. Functionality of gum arabic. Fractionation, characterization and evaluation of gum fractions in citrus oil emulsions and model beverages. **Topics in Catalysis**, *[S. l.]*, 1995. DOI: 10.1016/S0268-005X(09)80274-9.

REBELLO, Flávia De Floriani Pozza. Microencapsulação de ingredientes alimentícios. **Revista Agrogeoambiental**, *[S. l.]*, 2009. DOI: 10.18406/2316-1817v1n32009223.

RIOS-MERA, Juan D.; SALDAÑA, Erick; RAMÍREZ, Yhosep; AUQUIÑIVÍN, Erick A.; ALVIM, Izabela D.; CONTRERAS-CASTILLO, Carmen J. Encapsulation optimization and pH- and temperature-stability of the complex coacervation between soy protein isolate and inulin entrapping fish oil. **LWT**, *[S. l.]*, 2019. DOI: 10.1016/j.lwt.2019.108555.

ROCHA-SELMI, Glaucia A.; FAVARO-TRINDADE, Carmen S.; GROSSO, Carlos R. F. Morphology, stability, and application of lycopene microcapsules produced by complex coacervation. **Journal of Chemistry**, *[S. l.]*, 2013. DOI: 10.1155/2013/982603.

RODRIGUES DA CRUZ, Michele Cristina; ANDREOTTI DAGOSTIN, João Luiz; PERUSSELLO, Camila Augusto; MASSON, Maria Lúcia. Assessment of physicochemical characteristics, thermal stability and release profile of ascorbic acid microcapsules obtained by complex coacervation. **Food Hydrocolloids**, *[S. l.]*, 2019. DOI: 10.1016/j.foodhyd.2018.07.043.

ROJAS-MORENO, Sandra; OSORIO-REVILLA, Guillermo; GALLARDO-VELÁZQUEZ, Tzayhrí; CÁRDENAS-BAILÓN, Fernando; MEZA-MÁRQUEZ, Gabriela. Effect of the cross-linking agent and drying method on encapsulation efficiency of orange essential oil by complex coacervation using whey protein isolate with different polysaccharides. **Journal of Microencapsulation**, *[S. l.]*, 2018. DOI: 10.1080/02652048.2018.1449910.

RUTZ, Josiane K.; BORGES, Caroline D.; ZAMBIAZI, Rui C.; CRIZEL-CARDOZO, Michele M.; KUCK, Luiza S.; NOREÑA, Caciano P. Z. Microencapsulation of palm oil by complex coacervation for application in food systems. **Food Chemistry**, *[S. l.]*, v. 220, p. 59–66, 2017. DOI: 10.1016/j.foodchem.2016.09.194.

SANCHEZ, Christian; MEKHLOUFI, Ghozlène; RENARD, Denis. Complex coacervation between β-lactoglobulin and Acacia gum: A nucleation and growth mechanism. **Journal of Colloid and Interface Science**, *[S. l.]*, 2006. DOI: 10.1016/j.jcis.2006.02.031.

SANTOS, Jenifer; VLADISAVLJEVIĆ, Goran T.; HOLDICH, Richard G.; DRAGOSAVAC, Marijana M.; MUÑOZ, José. Controlled production of eco-friendly emulsions using direct and premix membrane emulsification. **Chemical Engineering Research and Design**, *[S. l.]*, v. 98, p. 59–69, 2015. a. DOI: 10.1016/j.cherd.2015.04.009.

SANTOS, Milla G.; BOZZA, Fernanda T.; THOMAZINI, Marcelo; FAVARO-TRINDADE, Carmen S. Microencapsulation of xylitol by double emulsion followed by complex coacervation. **Food Chemistry**, *[S. l.]*, 2015. b. DOI: 10.1016/j.foodchem.2014.08.093.

SCHMITT, Christophe; SANCHEZ, Christian; DESOBRY-BANON, Sylvie; HARDY, Joël. **Structure and technofunctional properties of protein-polysaccharide complexes: A reviewCritical Reviews in Food Science and Nutrition**, 1998. DOI: 10.1080/10408699891274354.

SCHUBERT, Helmar; AX, Karin; BEHREND, Olaf. Product engineering of dispersed systems. **Trends in Food Science and Technology**, *[S. l.]*, 2003. DOI: 10.1016/S0924-2244(02)00245-5.

SCHWERTNER, Harvey A.; RIOS, Deborah C. High-performance liquid chromatographic analysis of 6-gingerol, 8-gingerol, 10-gingerol, and 6-shogaol in ginger-containing dietary supplements, spices, teas, and beverages. **Journal of Chromatography B: Analytical Technologies in the Biomedical and Life Sciences**, *[S. l.]*, v. 856, n. 1–2, p. 41–47, 2007. DOI: 10.1016/j.jchromb.2007.05.011.

SHADDEL, Rezvan; HESARI, Javad; AZADMARD-DAMIRCHI, Sodeif; HAMISHEHKAR, Hamed; FATHI-ACHACHLOUEI, Bahram; HUANG, Qingrong. Use of gelatin and gum Arabic for encapsulation of black raspberry anthocyanins by complex coacervation. **International Journal of Biological Macromolecules**, *[S. l.]*, 2018. DOI: 10.1016/j.ijbiomac.2017.10.044.

SHAHIDI, Fereidoon; HAN, Xiao Qing. Encapsulation of Food Ingredients. **Critical Reviews in Food Science and Nutrition**, *[S. l.]*, 1993. DOI: 10.1080/10408399309527645.

SHINDE, Ujwala; NAGARSENKER, Mangal. Microencapsulation of eugenol by gelatin-sodium alginate complex coacervation. **Indian Journal of Pharmaceutical Sciences**, *[S. l.]*, 2011. DOI: 10.4103/0250-474X.93524.

SHOJI, N.; IWASA, A.; TAKEMOTO, T.; ISHIDA, Y.; OHIZUMI, Y. Cardiotonic principles of ginger (Zingiber officinale Roscoe). **Journal of Pharmaceutical Sciences**, *[S. l.]*, 1982. DOI: 10.1002/jps.2600711025.

SHUKLA, Yogeshwer; SINGH, Madhulika. Cancer preventive properties of ginger: A brief review. **Food and Chemical Toxicology**, *[S. l.]*, v. 45, n. 5, p. 683–690, 2007. DOI: 10.1016/j.fct.2006.11.002.

SILVA, D. F.; FAVARO-TRINDADE, C. S.; ROCHA, G. A.; THOMAZINI, M. Microencapsulation of lycopene by gelatin-pectin complex coacervation. **Journal of Food Processing and Preservation**, *[S. l.]*, v. 36, n. 2, p. 185–190, 2012. DOI: 10.1111/j.1745-4549.2011.00575.x.

SOUZA, Clitor J. F.; COMUNIAN, Talita A.; KASEMODEL, Márcia G. C.; FAVARO-TRINDADE, Carmen S. Microencapsulation of lactase by W/O/W emulsion followed by complex coacervation: Effects of enzyme source, addition of potassium and core to shell ratio on encapsulation efficiency, stability and kinetics of release. **Food Research International**, *[S. l.]*, 2019. DOI: 10.1016/j.foodres.2018.12.053.

SPECOS, Miró M. M.; GARCÍA, J. J.; TORNESELLO, J.; MARINO, P.; VECCHIA, Della M.; TESORIERO, Defain M. V.; HERMIDA, L. G. Microencapsulated citronella oil for mosquito repellent finishing of cotton textiles. **Transactions of the Royal Society of Tropical Medicine and Hygiene**, *[S. l.]*, 2010. DOI: 10.1016/j.trstmh.2010.06.004.

STEFFE, James F.; PH, D.; PRESS, Freeman. **Rheological Methods in**. [s.l: s.n.]. v. 23 DOI: 10.1016/0260-8774(94)90090-6. Disponível em: http://linkinghub.elsevier.com/retrieve/pii/0260877494900906.

STEFFE, Jf; DAUBERT, Cr. **Bioprocessing pipelines: rheology and analysis**. [s.l: s.n.]. Disponível em: http://books.google.com/books?hl=en&lr=&id=msxXy_9q-8sC&oi=fnd&pg=PR5&dq=Bioprocessing+Pipelines+:+Rheology+and+Analysis&ots=QdpsqWEeTa&sig=55sKZulyZk0F3_0oSa4yc8TzqFk%5Cnhttp://books.google.com/books?hl=en&lr=&id=msxXy_9q-8sC&oi=fnd&pg=PR5&dq=Bioprocessing.

STILLWELL, Michael T.; HOLDICH, Richard G.; KOSVINTSEV, Serguei R.; GASPARINI, Gilda; CUMMING, Iain W. Stirred cell membrane emulsification and factors influencing dispersion drop size and uniformity. **Industrial and Engineering Chemistry Research**, *[S. l.]*, 2007. DOI: 10.1021/ie0611094.

STRAUSS, George; GIBSON, Suzanne M. Plant phenolics as cross-linkers of gelatin gels and gelatin-based coacervates for use as food ingredients. **Food Hydrocolloids**, *[S. l.]*, v. 18, n. 1, p. 81–89, 2004. DOI: 10.1016/S0268-005X(03)00045-6.

TANAKA, Toshihiro et al. Drug Release Property of Lipiodol Emulsion Formed by Glass Membrane Emulsification Device for Transarterial Chemoembolization. **CardioVascular and Interventional Radiology**, *[S. l.]*, 2020. DOI: 10.1007/s00270-019-02311-9.

TANG, Yuting; SCHER, Herbert B.; JEOH, Tina. Industrially scalable complex coacervation process to microencapsulate food ingredients. **Innovative Food Science and Emerging Technologies**, *[S. l.]*, 2020. DOI: 10.1016/j.ifset.2019.102257.

TAPSELL, Linda C. et al. **Health benefits of herbs and spices: the past, the present, the future.The Medical journal of Australia.**, 2006. DOI: 10.5694/j.1326-5377.2006.tb00548.x.

TAVARES, Loleny; NOREÑA, Caciano Pelayo Zapata. Encapsulation of Ginger Essential Oil Using Complex Coacervation Method: Coacervate Formation, Rheological Property, and Physicochemical Characterization. **Food and Bioprocess Technology**, *[S. l.]*, 2020. DOI: 10.1007/s11947-020-02480-3.

THAKUR, Deepika; JAIN, Ashay; GHOSHAL, Gargi; SHIVHARE, U. S.; KATARE, O. P. Microencapsulation of β-Carotene Based on Casein/Guar Gum Blend Using Zeta Potential-Yield Stress Phenomenon: an Approach to Enhance Photo-stability and Retention of Functionality. **AAPS PharmSciTech**, *[S. l.]*, 2017. DOI: 10.1208/s12249-017-0806-1.

THYBO, Pia; HOVGAARD, Lars; ANDERSEN, Sune Klint; LINDELØV, Jesper Sæderup. Droplet size measurements for spray dryer scale-up. **Pharmaceutical Development and Technology**, *[S. l.]*, 2008. DOI: 10.1080/10837450701830957.

TIMILSENA, Yakindra Prasad; ADHIKARI, Raju; BARROW, Colin J.; ADHIKARI, Benu. Digestion behaviour of chia seed oil encapsulated in chia seed protein-gum complex coacervates. **Food Hydrocolloids**, *[S. l.]*, 2017. a. DOI: 10.1016/j.foodhyd.2016.12.017.

TIMILSENA, Yakindra Prasad; AKANBI, Taiwo O.; KHALID, Nauman; ADHIKARI, Benu; BARROW, Colin J. **Complex coacervation: Principles, mechanisms and applications in microencapsulationInternational Journal of Biological Macromolecules**, 2019. DOI: 10.1016/j.ijbiomac.2018.10.144.

TIMILSENA, Yakindra Prasad; WANG, Bo; ADHIKARI, Raju; ADHIKARI, Benu. **Advances in microencapsulation of polyunsaturated fatty acids (PUFAs)-rich plant oils using complex coacervation: A reviewFood Hydrocolloids**, 2017. b. DOI: 10.1016/j.foodhyd.2017.03.007.

TOMAS, Jürgen. Gravity separation of particulate solids in turbulent fluid flow. *In*: PARTICULATE SCIENCE AND TECHNOLOGY 2004, **Anais** [...]. [s.l: s.n.] DOI: 10.1080/02726350490457222.

TONON, Renata V.; GROSSO, Carlos R. F.; HUBINGER, M??riam D. Influence of emulsion composition and inlet air temperature on the microencapsulation of flaxseed oil by spray drying. **Food Research International**, *[S. l.]*, v. 44, n. 1, p. 282–289, 2011. DOI: 10.1016/j.foodres.2010.10.018. Disponível em: http://dx.doi.org/10.1016/j.foodres.2010.10.018.

VARGA, C. M.; LASHERAS, J. C.; HOPFINGER, E. J. Initial breakup of a small-diameter liquid jet by a high-speed gas stream. **Journal of Fluid Mechanics**, *[S. l.]*, 2003. DOI: 10.1017/S0022112003006724.

VEIS, Arthur. **A review of the early development of the thermodynamics of the complex coacervation phase separationAdvances in Colloid and Interface Science**, 2011. DOI: 10.1016/j.cis.2011.01.007.

VLADISAVLJEVIĆ, Goran T. **Preparation of microemulsions and nanoemulsions by membrane emulsificationColloids and Surfaces A: Physicochemical and Engineering Aspects**, 2019. DOI: 10.1016/j.colsurfa.2019.123709.

VLADISAVLJEVIĆ, Goran T.; KOBAYASHI, Isao; NAKAJIMA, Mitsutoshi; WILLIAMS, Richard A.; SHIMIZU, Masataka; NAKASHIMA, Tadao. Shirasu Porous Glass membrane emulsification: Characterisation of membrane structure by high-resolution X-ray microtomography and microscopic observation of droplet formation in real time. **Journal of Membrane Science**, *[S. l.]*, 2007. DOI: 10.1016/j.memsci.2007.06.067.

VLADISAVLJEVIĆ, Goran T.; SCHUBERT, Helmar. Influence of process parameters on droplet size distribution in SPG membrane emulsification and stability of prepared emulsion droplets. **Journal of Membrane Science**, *[S. l.]*, 2003. DOI: 10.1016/S0376-7388(03)00212-6.

WANG, Bo; ADHIKARI, Benu; BARROW, Colin J. Optimisation of the microencapsulation of tuna oil in gelatin-sodium hexametaphosphate using complex coacervation. **Food Chemistry**, *[S. l.]*, 2014. DOI: 10.1016/j.foodchem.2014.02.135.

WANG, Bo; ADHIKARI, Benu; MATHESH, Motilal; YANG, Wenrong; BARROW, Colin J. Anchovy oil microcapsule powders prepared using two-step complex coacervation between gelatin and sodium hexametaphosphate followed by spray drying. **Powder Technology**, *[S. l.]*, 2019. DOI: 10.1016/j.powtec.2018.07.034.

WANG, Lixia; YANG, Shiwei; CAO, Jinli; ZHAO, Shaohua; WANG, Wuwei. Microencapsulation of ginger volatile oil based on gelatin/sodium alginate polyelectrolyte complex. **Chemical and Pharmaceutical Bulletin**, *[S. l.]*, 2016. DOI: 10.1248/cpb.c15-00571.

WANG, Lu; CAO, Yiping; ZHANG, Ke; FANG, Yapeng; NISHINARI, Katsuyoshi; PHILLIPS, Glyn O. Hydrogen bonding enhances the electrostatic complex coacervation between κ-carrageenan and gelatin. **Colloids and Surfaces A: Physicochemical and Engineering Aspects**, *[S. l.]*, 2015. DOI: 10.1016/j.colsurfa.2015.07.011.

WILLIAMS, P. A.; PHILLIPS, G. O. Introduction to food hydrocolloids. *In*: **Handbook of Hydrocolloids: Second Edition**. [s.l: s.n.]. DOI: 10.1533/9781845695873.1.

WOOD, J. V. Atomisation of melts for powder production and spray deposition. **International Materials Reviews**, *[S. l.]*, 1995. DOI: 10.1179/imr.1995.40.2.96.

WYNN, David; PARIKH, Nick. **( 12 ) United States Patent** 2013.

XIAO, Zuobing; LI, Wei; ZHU, Guangyong; ZHOU, Rujun; NIU, Yunwei. Study of production and the stability of styrallyl acetate nanocapsules using complex coacervation. **Flavour and Fragrance Journal**, *[S. l.]*, 2016. DOI: 10.1002/ffj.3306.

XIAO, Zuobing; LIU, Wanlong; ZHU, Guangyong; ZHOU, Rujun; NIU, Yunwei. A review of the preparation and application of flavour and essential oils microcapsules based on complex coacervation technology. **Journal of the Science of Food and Agriculture**, *[S. l.]*, v. 94, n. 8, p. 1482–1494, 2014. a. DOI: 10.1002/jsfa.6491.

XIAO, Zuobing; LIU, Wanlong; ZHU, Guangyong; ZHOU, Rujun; NIU, Yunwei. Production and characterization of multinuclear microcapsules encapsulating lavender oil by complex coacervation. **Flavour and Fragrance Journal**, *[S. l.]*, v. 29, n. 3, 2014. b. DOI: 10.1002/ffj.3192.

YOUSEFDOOST, S.; SAMADI, F.; JAFARI, S. M.; RAMEZANPOUR, S. S.; GANJI, F.; HASSANI, S. Evaluation of nano and microcapsules of silymarin in simulated gastrointestinal conditions for Animal Target Delivery. **Iranian Journal of Applied Animal Science**, *[S. l.]*, 2019.

ZAWALA, J.; SZCZEPANOWICZ, K.; WARSZYNSKI, P. Theoretical and experimental studies of drop size in membrane emulsification - Single pore studies of hydrodynamic detachment of droplets. **Colloids and Surfaces A: Physicochemical and Engineering Aspects**, *[S. l.]*, v. 470, p. 297–305, 2015. DOI: 10.1016/j.colsurfa.2015.01.030. Disponível em: http://dx.doi.org/10.1016/j.colsurfa.2015.01.030.

ZHANG, Zhi Qiang; PAN, Cheol Ho; CHUNG, Donghwa. Tannic acid cross-linked gelatin-gum arabic coacervate microspheres for sustained release of allyl isothiocyanate: Characterization and in vitro release study. **Food Research International**, *[S. l.]*, 2011. DOI: 10.1016/j.foodres.2011.02.044.

ZHAO, Meng; HUANG, Xue; ZHANG, Hui; ZHANG, Yanzhen; GÄNZLE, Michael; YANG, Nan; NISHINARI, Katsuyoshi; FANG, Yapeng. Probiotic encapsulation in water-in-water emulsion via heteroprotein complex coacervation of type-A gelatin/sodium caseinate. **Food Hydrocolloids**, *[S. l.]*, 2020. DOI: 10.1016/j.foodhyd.2020.105790.

ZHOU, Lili; SHI, Huihui; LI, Zibiao; HE, Chaobin. **Recent Advances in Complex Coacervation Design from Macromolecular Assemblies and Emerging ApplicationsMacromolecular Rapid Communications**, 2020. DOI: 10.1002/marc.202000149.

ZHU, Jie; BARROW, David. Analysis of droplet size during crossflow membrane emulsification using stationary and vibrating micromachined silicon nitride membranes. **Journal of Membrane Science**, *[S. l.]*, 2005. DOI: 10.1016/j.memsci.2005.02.038.

ZUANON, Larissa A. C.; FUZARI, Nathália C.; FERREIRA, Sungil; FREITAS, Mírian L. F.; MOSER, Poliana; NICOLETTI, Vânia R. Production and Storage Properties of Spray-Dried Red Beet Extract Using Polysaccharide-Based Carrier Systems. **International Journal of Food Engineering**, *[S. l.]*, 2019. DOI: 10.1515/ijfe-2018-0371.

ZUANON, Larissa Angélica Cirelli; MALACRIDA, Cassia Roberta; TELIS, Vania Regina Nicoletti. Production of turmeric oleoresin microcapsules by complex coacervation with gelatin-gum arabic. **Journal of Food Process Engineering**, *[S. l.]*, v. 36, n. 3, p. 364–373, 2013. DOI: 10.1111/jfpe.12003.

**TERMO DE REPRODUÇÃO XEROGRÁFICA**

Autorizo a reprodução xerográfica do presente Trabalho de Conclusão, na íntegra ou em partes, para fins de pesquisa.

São José do Rio Preto, 17 / 12 / 2020

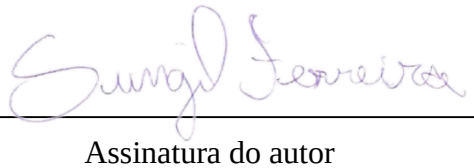

Assinatura do autor